nature genetics

SUPPLEMENTARY INFORMATION

https://doi.org/10.1038/s41588-019-0344-8

In the format provided by the authors and unedited.

Identification of common genetic risk variants for autism spectrum disorder

Jakob Grove[1,2,3,4], Stephan Ripke[5,6,7], Thomas D. Als[1,2,3], Manuel Mattheisen[1,2,3,8,9], Raymond K. Walters[5,6], Hyejung Won[10,11], Jonatan Pallesen[1,2,3], Esben Agerbo[1,12,13], Ole A. Andreassen[14,15], Richard Anney[16], Swapnil Awashti[7], Rich Belliveau[6], Francesco Bettella[14,15], Joseph D. Buxbaum[17,18,19,20], Jonas Bybjerg-Grauholm[1,21], Marie Bækvad-Hansen[1,21], Felecia Cerrato[6], Kimberly Chambert[6], Jane H. Christensen[1,2,3], Claire Churchhouse[5,6,22], Karin Dellenvall[23], Ditte Demontis[1,2,3], Silvia De Rubeis[17,18], Bernie Devlin[24], Srdjan Djurovic[14,25], Ashley L. Dumont[6], Jacqueline I. Goldstein[5,6,22], Christine S. Hansen[1,21,26], Mads Engel Hauberg[1,2,3], Mads V. Hollegaard[1,21], Sigrun Hope[14,27], Daniel P. Howrigan[5,6], Hailiang Huang[5,6], Christina M. Hultman[23], Lambertus Klei[24], Julian Maller[6,28,29], Joanna Martin[6,16,23], Alicia R. Martin[5,6,22], Jennifer L. Moran[6], Mette Nyegaard[1,2,3], Terje Nærland[14,30], Duncan S. Palmer[5,6], Aarno Palotie[5,6,22,31], Carsten Bøcker Pedersen[1,12,13], Marianne Giørtz Pedersen[1,12,13], Timothy dPoterba[5,6,22], Jesper Buchhave Poulsen[1,21], Beate St Pourcain[32,33,34], Per Qvist[1,2,3], Karola Rehnström[35], Abraham Reichenberg[17,18,19], Jennifer Reichert[17,18], Elise B. Robinson[5,6,36], Kathryn Roeder[37,38], Panos Roussos[18,39,40,41], Evald Saemundsen[42], Sven Sandin[17,18,23], F. Kyle Satterstrom[5,6,22], George Davey Smith[33,43], Hreinn Stefansson[44], Stacy Steinberg[44], Christine R. Stevens[6], Patrick F. Sullivan[10,23,45], Patrick Turley[5,6], G. Bragi Walters[44,46], Xinyi Xu[17,18], Autism Spectrum Disorder Working Group of the Psychiatric Genomics Consortium[47], BUPGEN[47], Major Depressive Disorder Working Group of the Psychiatric Genomics Consortium[48], 23andMe Research Team[48], Kari Stefansson[44,46], Daniel H. Geschwind[49,50,51], Merete Nordentoft[1,52], David M. Hougaard[1,21], Thomas Werge[1,26,53], Ole Mors[1,54], Preben Bo Mortensen[1,2,12,13], Benjamin M. Neale[5,6,22], Mark J. Daly[5,6,22,31*] and Anders D. Børglum[1,2,3*]

[1]The Lundbeck Foundation Initiative for Integrative Psychiatric Research, iPSYCH, Aarhus, Denmark. [2]Centre for Integrative Sequencing, iSEQ, Aarhus University, Aarhus, Denmark. [3]Department of Biomedicine–Human Genetics, Aarhus University, Aarhus, Denmark. [4]Bioinformatics Research Centre, Aarhus University, Aarhus, Denmark. [5]Analytic and Translational Genetics Unit, Department of Medicine, Massachusetts General Hospital and Harvard Medical School, Boston, MA, USA. [6]Stanley Center for Psychiatric Research, Broad Institute of Harvard and MIT, Cambridge, MA, USA. [7]Department of Psychiatry and Psychotherapy, Charité-Universitätsmedizin, Berlin, Germany. [8]Department of Psychiatry, Psychosomatics and Psychotherapy, University of Würzburg, Würzburg, Germany. [9]Centre for Psychiatry Research, Department of Clinical Neuroscience, Karolinska Institutet, Stockholm, Sweden. [10]Department of Genetics, University of North Carolina at Chapel Hill, Chapel Hill, NC, USA. [11]UNC Neuroscience Center, University of North Carolina at Chapel Hill, Chapel Hill, NC, USA. [12]National Centre for Register-Based Research, Aarhus University, Aarhus, Denmark. [13]Centre for Integrated Register-based Research, Aarhus University, Aarhus, Denmark. [14]NORMENT-KG Jebsen Centre for Psychosis Research, University of Oslo, Oslo, Norway. [15]Division of Mental Health and Addiction, Oslo University Hospital, Oslo, Norway. [16]MRC Centre for Neuropsychiatric Genetics and Genomics, Cardiff University, Cardiff, UK. [17]Seaver Autism Center for Research and Treatment, Icahn School of Medicine at Mount Sinai, New York, NY, USA. [18]Department of Psychiatry, Icahn School of Medicine at Mount Sinai, New York, NY, USA. [19]Friedman Brain Institute, Icahn School of Medicine at Mount Sinai, New York, NY, USA. [20]Mindich Child Health and Development Institute, Icahn School of Medicine at Mount Sinai, New York, NY, USA. [21]Center for Neonatal Screening, Department for Congenital Disorders, Statens Serum Institut, Copenhagen, Denmark. [22]Program in Medical and Population Genetics, Broad Institute of Harvard and MIT, Cambridge, MA, USA. [23]Department of Medical Epidemiology and Biostatistics, Karolinska Institutet, Stockholm, Sweden. [24]Department of Psychiatry, University of Pittsburgh School of Medicine, Pittsburgh, PA, USA. [25]Department of Medical Genetics, Oslo University Hospital, Oslo, Norway. [26]Institute of Biological Psychiatry, MHC SctHans, Mental Health Services, Copenhagen, Denmark. [27]Department of Neurohabilitation, Oslo University Hospital, Oslo, Norway. [28]Genomics plc, Oxford, UK. [29]Vertex Pharmaceuticals, Abingdon, UK. [30]NevSom, Department of Rare Disorders and Disabilities, , Oslo University Hospital, Oslo, Norway. [31]Institute for Molecular Medicine Finland, University of Helsinki, Helsinki, Finland. [32]Language and Genetics Department, Max Planck Institute for Psycholinguistics, Nijmegen, the Netherlands. [33]MRC Integrative Epidemiology Unit, University of Bristol, Bristol, UK. [34]Donders Institute for Brain, Cognition and Behaviour, Radboud University, Nijmegen, the Netherlands. [35]Wellcome Trust Sanger Institute, Hinxton, Cambridge, UK. [36]Department of Epidemiology, Harvard T.H. Chan School of Public Health, Boston, MA, USA. [37]Computational Biology Department,

Carnegie Mellon University, Pittsburgh, PA, USA. [38]Department of Statistics and Data Science, Carnegie Mellon University, Pittsburgh, PA, USA. [39]Institute for Genomics and Multiscale Biology, Department of Genetics and Genomic Sciences, Icahn School of Medicine at Mount Sinai, New York, NY, USA. [40]Friedman Brain Institute, Department of Neuroscience, Icahn School of Medicine at Mount Sinai, New York, NY, USA. [41]Mental Illness Research Education and Clinical Center (MIRECC), James J. Peters VA Medical Center, Bronx, NY, USA. [42]The State Diagnostic and Counselling Centre, Kópavogur, Iceland. [43]Population Health Sciences, Bristol Medical School, University of Bristol, Bristol, UK. [44]deCODE genetics/Amgen, Reykjavík, Iceland. [45]Department of Psychiatry, University of North Carolina at Chapel Hill, Chapel Hill, NC, USA. [46]Faculty of Medicine, University of Iceland, Reykjavik, Iceland. [47]A list of members and affiliations appears in the Supplementary Note. [48]A list of members and affiliations appears at the end of the paper. [49]Program in Neurogenetics, Department of Neurology, David Geffen School of Medicine, University of California, Los Angeles, Los Angeles, CA, USA. [50]Center for Autism Research and Treatment and Center for Neurobehavioral Genetics, Semel Institute for Neuroscience and Human Behavior, University of California, Los Angeles, Los Angeles, CA, USA. [51]Department of Human Genetics, David Geffen School of Medicine, University of California, Los Angeles, Los Angeles, CA, USA. [52]Mental Health Services in the Capital Region of Denmark, Mental Health Center Copenhagen, University of Copenhagen, Copenhagen, Denmark. [53]Department of Clinical Medicine, University of Copenhagen, Copenhagen, Denmark. [54]Psychosis Research Unit, Aarhus University Hospital, Risskov, Denmark. *e-mail: mjdaly@atgu.mgh.harvard.edu; anders@biomed.au.dk

Contents

Part I

Supplementary Notes

Sample description and data processing

1.1 The iPSYCH ASD sample

1.1.1 The iPSYCH sample

The iPSYCH ASD sample is a population based case-cohort sample extracted from a baseline cohort consisting of all children born in Denmark between May 1st 1981 and December 31st 2005[1]. Eligible were singletons born to a known mother and resident in Denmark on their one-year birthday. Cases were identified from the Danish Psychiatric Central Research Register (DPCRR)[2], which includes data on all individuals treated in Denmark at psychiatric hospitals (from 1969 onwards) as well as at outpatient psychiatric clinics (from 1995 onwards). Cases were identified with schizophrenia, bipolar affective disorder, affective disorder, ASD and ADHD up until 2012. The controls constitute a random sample from the set of eligible subjects.

1.1.2 The iPSYCH ASD GWAS sample

The ASD GWAS is based on a register update. Cases were selected from the iPSYCH sample as those diagnosed with ASD in 2013 or earlier by a psychiatrist according to ICD10, including diagnoses of childhood autism (ICD10 code F84.0), atypical autism (F84.1), Asperger's syndrome (F84.5), other pervasive developmental disorders (F84.8), and pervasive developmental disorder, unspecified (F84.9). As controls we selected from the random iPSYCH control cohort children that did not have an ASD diagnosis by 2013.

For descriptive statistics and numbers describing the data flow for the steps described below see Table 1.

1.1.3 Genotyping and calling

The samples were linked using the unique personal identification number to the Danish Newborn Screening Biobank (DNSB) at Statens Serum Institute (SSI), where DNA was extracted from Guthrie cards and whole genome amplified in triplicates as described previously[3, 4]. Genotyping was performed at the Broad Institute of Harvard and MIT (Cambridge, MA, USA) using the PsychChip array from Illumina (CA, San Diego, USA) according to the instructions of the manufacturer. Genotyping was carried out on the full iPSYCH sample in 23 waves and so was the subsequent data processing.

Genotype calling of markers with minor allele frequency (MAF) > 0.01 was performed by merging callsets from GenCall[5] and Birdseed[6] while less frequent variants were called with zCall[7]. Details on the merging procedure for variants with MAF > 0.01 are described elsewhere (`https://sites.google.com/a/broadinstitute.org/ricopili/utilities/merge-calling-algorithms` and [1]). Prior to the subsequent QC and imputation SNPs where excluded when they were on either of two lists: a) a global blacklist comprising SNPs for which genotyping failed in 4 cohorts genotyped at the Broad as part of the PsychChip project (Psychiatric Genomics Consortium) with Illumina's PsychChip and/or b) a local blacklist of SNPs for which the MAF in the GenCall and Birdseed callsets where substantially different ($\Delta_{\text{MAF}} > 5\%$) prior to the merging of variants.

1.1.4 QC and Imputation

Ricopili[8], the pipeline developed by the Psychiatric Genomics Consortium (PGC) Statistical Analysis Group was used for quality control, imputation, principle component analysis (PCA) and primary association analysis. The data was processed separately in the 23 genotyping batches. Details for ricopili are described elsewhere (https://sites.google.com/a/broadinstitute.org/ricopili/home). In brief, the quality control (QC) step included manipulations of the data ensuring proper subsequent processing as well as filtering of SNPs and samples using a broad variety of different measures. Before subsequent imputation the data was (strand) aligned with the respective reference sample. Phasing was achieved using SHAPEIT v2[9] and imputation done by IMPUTE2[10, 11] with haplotypes from the 1000 Genomes Project, phase 3[12, 13] (1kGP3) as reference. Post imputation filtering of SNPs was carried out using measures for accuracy of imputation (INFO scores > 0.1) and MAF (> 0.5%).

1.1.5 PCA

After excluding regions of high LD[15], the genotypes were pruned down to a set of roughly 30k markers by pruning in a sliding window fashion using PLINK 1.9[16, 17]. This was done with an r^2 limit of 0.075, window size 1000 and step size 100. Using PLINK's identity by state analysis pairs of subjects were identified with $\hat{\pi} > 0.2$ and one subject of each such pair excluded at random (with a preference for keeping cases). PCA was carried out using smartPCA[18, 19]. A sub-sample of European ancestry was selected as an ellipsoid in the space of PC1-3 centred and scaled using the mean and 8 standard deviation of the sub-sample consisting of those whose parents and grandparents were all known from the registries to have been born in Denmark (n=31 500).

Principal component (PC) one and two of the initial PCA are shown in Figure 1 annotated by parental origin.

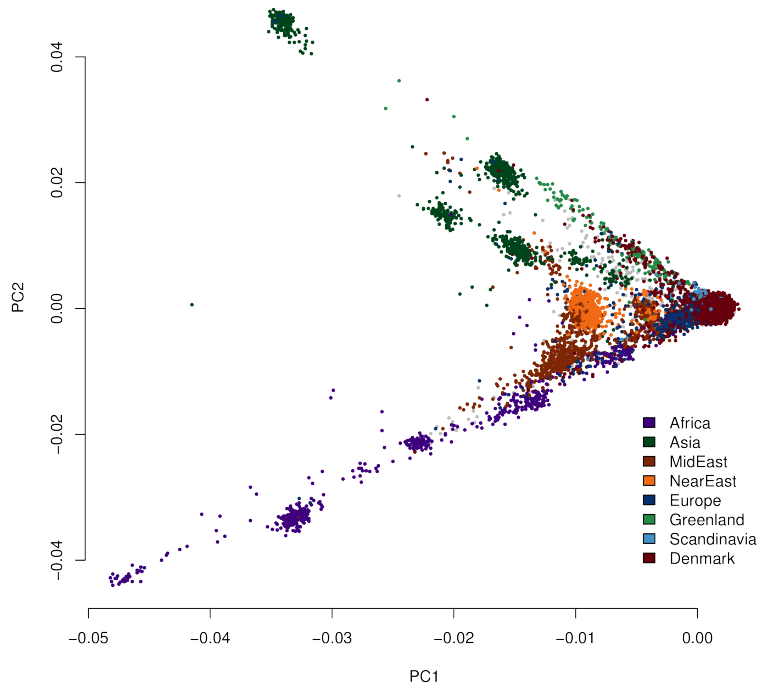

Supplementary Note, Figure 1: PCA plot showing the first to principal components of the initial PCA on the 39 542 unrelated individuals coloured by parental origin (if at least one parent was born outside of Europe that dictates the colour, red indicates all parents and grandparents were born in Denmark.)

A secondary PCA was run to provide covariates for the association analysis. These covariates were tested for association to the outcome (adjusting for index variables for the waves). In the association analysis we included PC1–4 plus any PC above that which was nominally significantly associated to the outcome.

1.2 The PGC ASD sample

In brief, five cohorts provided genotypes to the sample (n denoting the number of trios for which genotypes were available): The Geschwind Autism Center of Excellence (ACE; n = 391), the Autism Genome Project[20] (AGP; n = 2272), the Autism Genetic Resource Exchange[21, 22] (AGRE; n = 974), the NIMH Repository https://www.nimhgenetics.org/available_data/autism/, the Montreal[23]/Boston Collection (MONBOS; n = 1396, and the Simons Simplex Collection (SSC; n = 2231). The trios were analysed as cases and pseudo controls. A detailed description of the sample is available on the PGC web site: https://www.med.unc.edu/pgc/files/resultfiles/PGCASDEuro_Mar2015.readme.pdf and even more details are provided in[24].

The contributing samples were all processed for quality control, imputation, principle component analysis (PCA) and association analysis in the Ricopili pipeline[8]. In particular SHAPEIT[9] was used for phasing and imputation was done by IMPUTE2[10, 11] employing the 1000 Genomes Project, phase 3[13, 14] (1kGP3) as reference. Trio samples were imputed as a case-pseudo-controls design.

The CEU subset was chosen using a Euclidean distance measure weighted by the variance explain for each of the first 3 PCs. Individuals more distant than 10 standard deviations from the combined CEU and TSI HapMap reference populations were excluded.

1.3 The follow-up samples

1.3.1 deCODE

The Icelandic sample has been described previously[25]. Briefly, patients were ascertained through the State Diagnostic Counselling Center and the Department of Child and Adolescent Psychiatry, and were diagnosed based on ICD-10 criteria. Controls were recruited through ongoing projects at deCODE. Chip-typing, long-range phasing, imputation and association analysis were carried out as described previously[26].

Patients and controls from Georgia, Serbia and Ukraine were recruited by mental health clinics in their respective countries. Patients were diagnosed using ICD-10 criteria[27]. Samples were genotyped using Illumina arrays, phased with EAGLE v2, and imputed using IMPUTE v2 based on the 1000-genomes Phase3 reference data set.

All studies were approved by relevant ethics and data protection agencies, and written, informed consent was obtained from individuals providing blood samples.

1.3.2 Finnish autism case-control study

The families for the Finnish autism dataset were recruited via Finnish university and central hospitals, mainly Helsinki University Hospital, Jyväskylä Central Hospital and Kuopio University Hospital. The control samples originate from Finnish population cohorts[28]. Two groups of families were included 1) families with at least one child diagnosed with autism, including families with additional siblings diagnosed with other ASDs or 2) families with no individuals diagnosed with strict autism but at least two individuals with a diagnosis of Asperger Syndrome[29–32].

Diagnostic evaluations were made by a multidisciplinary group of clinicians at the neurological department of hospitals. Data were collected from extensive diagnostic examinations including neurological examinations, assessment of developmental history as well as psychological and neuropsychological examinations. Final diagnoses were based on ICD-10 and DSM-IV diagnostic nomenclatures. Families with known associated medical conditions or chromosomal abnormalities such as fragile X syndrome were excluded from the study. All families were Finnish except for one family where the father was of Turkish origin. Subsequently, the ADI-R was administered to autism families willing to continue to participate in the study. In a subset of the Finnish autism families a 96% concordance rate was observed between ICD-10 and ADI-R diagnosis of autism[33] making the Finnish autism families clinically comparable to international family sets used for genetic studies.

One individual was included from each family in the case-control datasets, choosing the most severely affected individual (i.e. autism before Asperger Syndrome). If several individuals in the family had the same diagnosis, the individual with highest genotyping success rate was included. Genotyping was performed in multiple stages

using Illumina HumanHap300/550, HumanHapCNV370 and Human610 arrays. All genotypes were called using Illumina BeadStudio.

1.3.3 PAGES

Data for this project were available from three sources, controls obtained from the Swedish Schizophrenia study and limited to the samples used in the Gaugler et al.[34]; ASD cases and controls genotyped at MSSM; and controls genotyped at MSSM. These samples were genotyped on different platforms and at different times. For details see Table 1. Genotypes for autosomal SNP were imputed up to the 1000G Phase 3 v5 reference panel using the Michigan Imputation Server in a separate job for each of the three sources.

Supplementary Note, Table 1: Available data from each of the three sources (207,822 SNP were genotyped on all three platforms.

Source	Cases	Controls	SNPs
Gaugler study (G)		2580	491,543
Nov 2016 (N)	1075	235	678,539
Jan 2017 (J)		1365	884,875
All	1075	4180	1,279,969

Removing controls appearing in more than one sample retaining index cases in a handful of full-sib pairs and parent-offspring resulted in 2477, 235, and 1355 controls from G, N, and J, respectively. In addition 1069 cases remained from N.

Genetic ancestry was determined using dacGem in GemTools[35, 36] based on 11,402 SNPs. These SNPs were selected from the set of 207,822 SNP with the conditions that they are autosomal, have a minor allele frequency > 0.05, and pass pruning using `-indep-pairwise` with settings window=50, overlap=5, and $r^2 < 0.01$. The settings for dacGem were to use 500 random individuals in the base and to no longer sub-divide clusters after the initial round. dacGem identified 2 significant dimensions of ancestry and broke the data into 5 clusters.

For the replication we limited ourselves to the 622 and 3841 Swedish ancestry cases and controls, respectively. This reflects the exclusion of 304 PAGES samples that potentially were included in the combined iPSYCH-PGC-Aut analysis. Data were analysed using a model including the 2 significant eigenvectors obtained from GemTools.

1.3.4 BUPGEN

The study was part of the national Norwegian BUPGEN network, recruiting patients from Norwegian health services specializing in assessment of ASD and other neurodevelopmental disorders. The current sample comprised 102 children with ASD recruited between 2013 and May 2016 and assessed at age 6-18 years, with childhood autism (28%), atypical autism (8%), Asperger syndrome (37%) and unspecified pervasive developmental disorder(27%). 656 Controls were collected from the population of South-East Norway.

The children were assessed by a team of experienced clinicians (clinical psychologists and child psychiatrist). Diagnostic conclusions were best-estimate clinical diagnoses derived from tests, interview results and observations. All diagnoses were based on the International Statistical Classification of Diseases and Related Health Problems 10th Revision (ICD-10) (27). Criteria and autistic symptoms were evaluated using Autism Diagnostic Interview-Revised (ADI-R) (28) and/or Autism Diagnostic Observation Schedule (ADOS) (29). In addition, the assessment included a full medical and developmental history, physical examination, and IQ assessment.

Samples were genome-wide genotyped with Human Omni Express-24 v.1.1 at deCODE Genetics (Iceland). Quality control of genotypes, imputation, principal component analysis and primary association analyses were performed using the bioinformatics pipeline Ricopili[8] applying standard settings except where noted. Subjects and SNPs were included in the analyses based on the standard quality control settings in the Ricopili pipeline, with one adjustment: The SNP call rate filter was set to 0.96 instead of 0.98, as a stringent SNP call rate filter would exclude a large number of SNPs. Imputation was performed using the standard settings of the Ricopili pipeline, using haplotypes from the 1000 Genomes Project, phase 3 (1KGP3)[13, 14]. The data set included samples from three

separate batches; one of the batches contained only 2 cases and was excluded from the analysis after the imputation was performed. After these quality control steps, the study contained 194 cases and 3802 controls.

Prior to performing principal component analysis, a set of regions with high LD[15] was removed, and the number of controls was randomly reduced to four times the number of cases. The analysis was performed using Ricopili with the following settings: `ldsubgr 8000` (using all individuals), `nwind 1000` (the number of SNPs in window for pruning), `stepw 100` (window step size), `r2 0.075` (limit for LD pruning), `noproject` (perform smartpca on complete dataset). Removal of genetic outliers based on the principal components was performed in two steps. In both steps outliers were defined as samples that were outside of a 4-dimensional ellipsoid with center based on the first 4 principal components of the samples, and size based on the variance in the first 4 principal components among the samples. In the first step, an external set of homogenous Danish samples from the iPSYCH data set was included in the analysis. This set of homogenous Danish samples was assigned as defining the center and variance of the ellipsoid, and samples with a distance larger than 8 standard deviations in from the center in the 4-dimensional space were removed. This step excluded samples that were highly genetically heterogenous from Scandinavians. The second step was performed with the remaining samples, and without including the set of homogenous Danish samples. Genetic outliers were defined as having a distance larger than 4 standard deviations from the center. After removal of genetic outliers, the study contained 164 cases and 3449 controls. A final PCA was performed with these samples and the PCs used in the subsequent association analysis.

Association analysis was performed using standard Ricopili settings. The number of controls was randomly reduced to four times the number of cases. As the criterion for which principal components to include, we included the first four plus any of principal components 5–20 which had a significant correlation with case/control status. This resulted in principal components 1–4 and 8 being used as covariates in the association analysis.

Statistical Analyses

2.1 GWAS

2.1.1 SNP-wise analysis

Association analyses were done by applying PLINK 1.9 to the imputed dosage data (the sum of imputation probabilities P(A1A2) + 2P(A1A1)) including the first four principal components (PCs) as covariates as well as any PC beyond that, which were significantly associated with ASD in the sample. Combined results for iPSYCH and for iPSYCH with the PGC was achieved by meta analysing batch-wise and study-wise results using METAL[37] (July 2010 version) employing an inverse variance weighted fixed effect model[38]. Subsequently we applied a quality filter allowing only markers with an imputation info score ≥ 0.7, MAF ≥ 0.01 and an effective sample size of at least 70% of the maximum. The effective sample size tells what the number of cases would be if a balanced design were to give equivalent statistical power. It was estimated from the number of cases, N_{ca}, and controls, N_{co}, contributing to the individual regression as $2N_{ca}N_{co}/(N_{ca} + N_{co})$.

The degree to which the deviation in the test statistics can be ascribed to cryptic relatedness and population stratification rather than to polygenicity was estimated from the intercept in LD score regression[39] (LDSC) as the ratio

$$\frac{\text{intercept} - 1}{\text{mean}(\chi^2) - 1}.$$

2.1.2 Gene-based association and gene-set analyses

MAGMA 1.06[40] was applied to the summary statistics to test for gene-based association. Using NCBI 37.3 gene definitions and restricting the analysis to SNPs located within the transcribed region (i.e. no padding was applied), mean SNP association was tested with the sum of -log(SNP p-value) as test statistic. The resulting gene-based p-values were further used in gene-set enrichment analyses in MAGMA. We used the default settings where the regression is adjusted fro gene size, gene density, sample size, the reciprocal of the minimal allele count, and the logarithm of all these.

One hypothesis driven analysis explored the candidate sets M13, M16 and M17 from Parikshak et al. 2013[41] as well as constrained genes[42, 43] determined from data of the Exome Aggregation Consortium (ExAC)[43]. The probability of being loss-of-function (LoF) intolerant (pLI) has been estimated based on the observed and expected protein-truncating variant (PTV) counts within each gene in the full ExAC data and are publicly available at `ftp://ftp.broadinstitute.org/pub/ExAC_release/release0.3.1/functional_gene_constraint`. Genes were defined as constrained if the had pLI ≥ 0.9. Moreover, we added two small gene sets selected specifically for their association to ASD: the 65 genes identified at an FDR< 0.1 in [234], and the highly curated list of ASD genes(`https://spark-sf.s3.amazonaws.com/SPARK_gene_list.pdf`) from SPARK[235]. Another gene-set analysis was an hypothesis free analysis of the Gene Ontology[44, 45] sets 'molecular function' from MsigDB 6.0[46]. In general we analysed only genes outside the broad MHC region (hg19:chr6:25–35M) and included only gene sets with 10–1000 genes. However, the Sanders and the SPARK sets has no more than 1 gene in the MHC region and that was left in. All gene sets with significant enrichment were inspected to ensure that the signal was not generated by one or a few associated loci, where in reality only one of N genes in tight LD might truly be

associated.

2.1.3 MTAG analyses

MTAG[47] was run with standard settings pairing up the iPSYCH-PGC meta-analysis summary statistics with the summary statistics for major depression[48] (including the results from 23andMe[49], but excluding the Danish samples, 111 902 cases, 312 113 controls, and mean $\chi^2 = 1.477$), schizophrenia[8] (without the Danish samples, 34 129 cases, 45 512 controls, and mean $\chi^2 = 1.804$) and educational attainment[50] (328 917 samples and mean $\chi^2 = 1.648$) respectively. These samples are much better powered than the ASD sample with 18 381 cases, 27 969 controls and mean $\chi^2 = 1.201$. This poses the risk of generating signals that only have basis in the secondary phenotype. This however is countered by a more modest genetic correlation in the order or 0.2–0.4, which means that the weight given to the secondary phenotypes are equally modest ranging from 0.11 for educational attainment to 0.27 for schizophrenia with major depression slightly lower at 0.24. Hence, in general it will take a relatively strong ASD signal to generate a significant MTAG signal, and the rare cases where an exceptionally strong signal in the secondary phenotype is sufficient to drive home a significant MTAG signal will be easy to spot. This reasoning might not hold if analyzing more than two phenotypes simultaneously, where the interplay between the phenotypes gets more convoluted. Therefore, we ran the MTAG analyses pairwise rather than all together to minimize the risk of false positives.

The results were clumped and we highlighted loci of interest by selecting those that were significant at $5 \cdot 10^{-8}$ in the iPSYCH-PGC meta-analysis or the meta-analysis with the replication sample or were significant at $1.67 \cdot 10^{-8}$ in any of the three MTAG analyses. The composite GWAS consisting of the minimal p-values at each marker over these five analyses was used as a background when creating Manhattan plots for the different analyses. This way we are able to show both what is maximally achieved, where it comes from, and what the individual analysis contributes.

Moreover, we estimated max FDR — the FDR in the worst case. Briefly, the maxFDR estimation is done in the following way: For two traits, each locus will be associated with both, neither, or only one of the traits (the four states TT, FF, FT, and TF). If we knew the fraction of each type of SNP along with the distribution of effect sizes for true associations, it would be possible to estimate MTAG's FDR. These fractions are unknown, however, so we instead search through a fine grid in the space of possible fractions and calculate FDR for each point. The maximum achieved it the estimate maxFDR. To estimate FDR given the four fraction, we first assume that, conditional on a SNP being associated with one or both traits, the effect sizes are drawn from a normal or bivariate normal distribution. This implies that the unconditional distribution of effect sizes is a generalization of a spike-and-slab distribution (i.e., a mixture of normal distributions) which is a class of distributions that approximates many thick-tailed distributions. Distributions such as non-infinitesimal models where some fraction of SNPs are null for a subset of traits. For details see the supplementary note of Turley, P et al.[47]

As recommended in [47] we conducted the FDR analysis under the assumption that at least 10% of SNPs from the ASD summary statistics are tagging causal SNPs. For the secondary phenotype we allowed this to drop to 3% to accomodate a potentially much fewer causal SNPs for ASD. This resulted in estimated max FDR of 0.021 for educational attainment, 0.019 for schizophrenia and 0.012 for major dression giving a conservative estimate of max FDR for the combined analysis of 0.021. I comparison the analogous estimate for the ASD scan alone was 0.020.

2.1.4 Reviews

We compiled reviews of the loci in Table 4. Information on gene function, expression and association to disease was retrieved by targeted searches in the UniProtKB protein knowledgebase (http://www.uniprot.org/uniprot/), the GTEx Portal (https://www.gtexportal.org/home/), Pubmed (https://www.ncbi.nlm.nih.gov/pubmed) and SFARI Gene (https://gene.sfari.org/). Independent signals of association were identified for each locus using the NHGRI-EBI Catalog of published genome-wide association studies available at: www.ebi.ac.uk/gwas[51] (accessed October 10th, 2017). Each locus was defined as the $r^2 = 0.1$ clump around the index SNP (LD region from the Ricopilli output file), adding additionally 0.5 Mb to each side. The coordinates in hg19 were then liftet to hg38 using the Lift Genome Annotations function in the UCSC Genome Browser available at: https://genome.ucsc.edu/[52]. The hg38 coordinates were used to query the GWAS catalog, and studies filtered using the p-value threshold of $5 \cdot 10^{-8}$. All studies of mental, neurological, educational and brain related traits, having one or more SNPs within the locus reaching genome wide significance (p=5x10-8) are listed.

2.2 SNP heritability

SNP heritability was estimated using LDSC[39] for the full sample and GCTA[53–55] for sub-samples too small for LDSC.

LDSC

For LDSC we used precomputed LD scores based on the European ancestry samples of the 1000 Genomes Project[14] restricted to HapMap3[56] SNPs (downloaded from the https://github.com/bulik/ldsc). The summary stats with standard LDSC filtering were regressed onto these scores. For liability scale estimates, we used a population prevalence for Denmark of 1.22%[57]. Lacking proper prevalence estimates for subtypes and sex specific analyses, we scaled the full spectrum prevalence based on the composition of the case sample.

GCTA

For sub-samples too small for LDSC, the GREML approach of GCTA was used. On best guess genotypes (genotype probability > 0.8, missing rate < 0.01 and MAF > 0.05) with INDELs removed, a genetic relatedness matrix (GRM) was fitted for the association sample (i.e. the subjects of European ancestry with $\hat{\pi} \leq 0.2$) providing a relatedness estimate for all pairwise combinations of individuals. Estimation of the phenotypic variance explained by the SNPs (REML) was performed including PC 1–4 as continuous covariates together with any other PC that was nominally significantly associated to the phenotype as well as batches as categorical indicator covariates. To test for statistical significanse of differences in SNP heritabilies across subtypes, we conducted permutation test shuffling the different case labels while keeping the controls. I.e. for the subtypes childhood autism, atypical autism, Asperger's and pervasive disorders, each permutation resultet in a different split of the cases into four parts of sizes equal to the original suptypes, which subsequently processed by GCTA together with the full control group. Thousand permutations were run for each analysis.

Partitioned heritability

Following Finucane et al.[58], we conducted an enrichment analysis of the heritability for SNPs for functional annotation and for SNPs located in cell-type-specific regulatory elements. Using first the same 24 overlapping functional annotations (stripped down from 53) as in Finucane et al., we regressed the χ^2 from the summary statistics on to the cell-type specific LD scores download from the site mentioned above with baseline scores, regression weights and allele frequencies based on European ancestry 1000 Genome Project data. The enrichment of a category was defined as the proportion of SNP heritability in the category divided by the proportion of SNPs in that category. Still following Finucane et al., we did a similar analysis using 220 cell type–specific annotations divided into 10 overlapping groups. In addition to this, we conducted an analysis based on annotation derived from data on H3K4Me1 imputed gapped peaks data from the Roadmap Epigenomics Mapping Consortium[59, 60]; more specifically information excluding the broad MHC-region (chr6:25–35MB). In line with Finucane et al. we truncate out of bounds estimates to the unit interval and does likewise for confidence intervals.

2.3 Genetic correlation and prediction

For the main samples, genetic correlations were estimated using LDSC[39] and for the analysis of ASD subtypes and subgroups where the sample size were generally small, we used GCTA[53–55]. In both cases, we followed the same procedures as explained above. The summary statistics were also uploaded to LD hub[61] for comparison to all together 219 phenotypes.

2.3.1 Polygenic risk scores

For the polygenic risk scores (PRS) we filtered and clumped the summary stats applying slight adaptations to the standard Ricopili process and parameters: We filtered at a MAF limit of 0.05, info score at 0.9 when present, and

we removed the broad MHC-region (chr6:25–35MB). When using external summary stats not processed Ricopili or imputed using different imputation references, we excluded all ambiguous markers to avoid potential strand conflicts. To improve performance of the scores and aviod including artefacts from batch effects, we restricted the summary stats to include only SNPs known to be present in the iPSYCH data at a reasonable quality (info score ≥ 0.6 and MAF ≥ 0.01) throughout all 23 sample waves. This step also checked for allele flips. Clumping was done on the filtered summary stats employing PLINK and the flags `--clump-p1 1`, `--clump-p2 1`, `--clump-r2 0.1` and `--clump-kb 500`.

PRS were generated by Ricopili (as interface to PLINK) at the default p-value thresholds ($5 \cdot 10^{-8}$, 10^{-6}, 10^{-4}, 0.001, 0.01, 0.05, 0.1, 0.2, 0.5 and 1) as a weighted sum of the allele dosages: Summing over the markers abiding by the p-value threshold in the training set and weighing by the additive scale effect measure of the marker (log(OR) or β) as estimated in the training set. Scores were normalized prior to analysis.

We evaluated the predictive power using Nagelkerke's R^2 and plots of odds ratios and confidence intervals over score deciles. Both R^2 and odds ratios were estimated in regression analyses including the relevant PCs and indicator variable for genotyping waves.

Subtype analyses

The ASD subtypes are overlapping in the sense that one individual may have multiple of these sub-diagnoses. To analyse ASD subtypes in relation PRS we needed a disjoint set of individuals representing to a high degree subjects with the diagnoses in question. While lumping together 'other pervasive developmental disorder'(ICD10 F84.8) and 'pervasive developmental disorder, unspecified' (ICD10 F84.9) into one, 'pervasive disorder, mixed' (PDM), we created a set of non-overlapping hierarchical subtypes presented in Table 13 and whose counts can be seen in the last line if Table 1.

We are interested in whether the PRS for different phenotypes have different distribution or loading on ASD subtypes. In order to investigate that while taking into account both batch effect from the genotyping waves as well as PCs, we fit a multivariate regression

$$\mathbf{Y} = \mathbf{XB} + \mathbf{E},$$

where $\mathbf{Y}$ is a matrix of n observations on m response variables, the normalized PRS, $\mathbf{X}$ is a model matrix with k columns for regressors, $\mathbf{B}$ is the matrix of regression coefficients (one column for each response variable), and $\mathbf{E}$ is an error matrix. The first column of $\mathbf{X}$ consists of 1s for the regression constant and corresponds in $\mathbf{B}$ to the intercept, which is the first row. The next few columns, say k_0, of $\mathbf{X}$ holds the subtype variables of interest while the subsequent ones are the wave dummy variables and PCs. This means that only the first rows of $\mathbf{B}$ are really of interest to us, and we take for the ith phenotype the vector $(\beta_{1i}, \ldots, \beta_{k_0 i})$ as a profile for how the score is loading across subtypes (β_{0i} being the intercept).

The advantage of the multivariate regression is that not only does it handle the correlation that may exist among the PRS, but most importantly it allows us to test a great number of hypotheses of interest. Eg. if the loading profile of one phenotype is different from that of another.

We test any linear null hypothesis by specifying a matrix equation:

$$H_0: \quad \mathbf{LBP} = \mathbf{C},$$

where $\mathbf{C}$ is usually the zero matrix, $\mathbf{L}$ has k columns and selects and relates the subtypes βs within each score, and the matrix $\mathbf{P}$ with m rows selects and relates the scores to use. For instance to test any hypothesis on the ith score we set

$$\mathbf{P} = (0, \ldots, 0, 1, 0, \ldots, 0)^T,$$

with 1 on the ith position. To select the k_0 element profile vector for testing, we specify the $(k_0 \times k)$ matrix

$$\mathbf{L} = \begin{pmatrix} 0 & 1 & 0 & \cdots & 0 & 0 & \cdots & 0 \\ \vdots & \ddots & \ddots & \ddots & \vdots & \vdots & & \vdots \\ 0 & \cdots & 0 & 1 & 0 & 0 & \cdots & 0 \end{pmatrix}.$$

Say we want to test the 0-hypothesis that the profile for phenotype i is identical to that of phenotype j, we use the $\mathbf{L}$-matrix just above and

$$\mathbf{P} = (0, \ldots, 0, 1, 0, \ldots, 0, -1, 0, \ldots, 0)^T,$$

where the 1 and the -1 are at the ith and jth position. This will be sensitive also an overall difference in loading, so if we want to attempt at a scale free version of the hypothesis testing just of the directions are the same (that the normalized vectors are identical), we can put

$$\mathbf{P} = (0, \ldots, 0, \tfrac{1}{\nu_i}, 0, \ldots, 0, -\tfrac{1}{\nu_j}, 0, \ldots, 0)^T,$$

where $\nu_i = |(\beta_{1i}, \ldots, \beta_{k_0 i})|$. This will approximately be the correct test for a scale free hypothesis.

Internally trained PRS

Lacking a large ASD sample outside of iPSYCH and PGC, we trained a set of PRS for ASD internally in the following way. We divided the sample in five sub-samples of roughly equal size respecting the division into batches; see Table 2. We then ran five GWAS leaving out each group in turn from the training set and meta analysed these with the PGC results. This produced a set of PRS For each of the five sub-samples trained on their complement. Prior to analyses, each score was normalized on the group where it was defined. We evaluated the predictive power in each group and on the whole sample combined.

Supplementary Note, Table 2: Make-up of wave group for internal scoring. The table show the waves that compose the groups as well as case control counts in the groups and the complement of each group in the iPSYCH ASD GWAS plus the PGC ASD GWAS.

		Group		Compl+PGC	
Group	Waves	N cases	N ctrls	N cases	N ctrls
1	1, 3, 11 and 20	2 624	3 694	10 452	18 970
2	2, 8, 10 and 22	2 622	5 432	10 454	17 232
3	4, 9, 12, 19 and 21	2 611	4 666	10 465	17 998
4	5, 7, 13, 15 and 16	2 583	4 360	10 493	18 304
5	6, 14, 17, 18 and 23	2 636	4 512	10 440	18 152

Leveraging the power of polygenic overlap

As a simple way of exploiting the genetic overlap with other phenotype to help improve prediction of the PRS, we added PRS from a number of phenotypes in a weighted sum with the internally trained ASD score. The phenotypes we included were subjective well being[62], schizophrenia[8], depressive symptoms[62], educational attainment[50], chronotype[63], ADHD[64], MDD[65], Openess[66], Extraversion[66], Agreeableness[66] and Childhood intelligence[67]. For each phenotype we chose the one score of the ten with the highest Nagelkerke's R^2 for ASD. The weights assigned could be any measure of 'importance' in context of ASD and we chose here to use the log(OR) for the logistic regression of ASD status on each score as a continuous factor adjusting for relevant PCs and wave indicators. One at a time, starting with the phenotype with highest abs(log(OR)) and ending with the lowest, we added a PRS weighted by its log(OR) and then standardized. This way we ended up with a sequence of scores starting with $S_0 = S_{ASD}$ and continuing with:

$$S_k = \frac{S_{ASD} + \sum_{i=1}^{k} \log(OR_{P_i}) S_{P_i} - \mu\left(S_{ASD} + \sum_{i=1}^{k} \log(OR_{P_i}) S_{P_i}\right)}{\sigma\left(S_{ASD} + \sum_{i=1}^{k} \log(OR_{P_i}) S_{P_i}\right)},$$

where S_{ASD} is the ASD score, S_{P_i} the score for phenotype P_i, OR_{P_i} the odds ratio from the logistic regression of ASD status on S_{P_i} as a continuous factor adjusting for relevant PCs and wave indicators, and μ is the mean and σ the standard deviation. In Figure 93 we show Nagelkerke's R^2 and in Figure 94 the decile plots over wave groups and on the full sample.

2.4 Hi-C analysis

The Hi-C data was generated from two major cortical laminae: the germinal zone (GZ), containing primarily mitotically active neural progenitors, and the cortical and subcortical plate (CP), consisting primarily of post-

mitotic neurons[68]. We first selected the top ranking loci from the ASD scan. Balancing the bumber of loci to work with and the depth in the p-value, we chose the top 30 loci, and of these 28 were represented in the reference set used in the Hi-C pipeline. The result was a list of 28 loci from which we derived a set of credible SNPs (putative causal SNPs) using CAVIAR[69]. To test whether credible SNPs are enriched in active marks in the fetal brain[60], we employed GREAT as previously described[68, 70]. Credible SNPs were, sub-grouped into those without known function (unannotated) and functionally annotated SNPs (SNPs in the gene promoters and SNPs that cause nonsynonymous variants) (Figure 98). Then we integrated unannotated credible SNPs with chromatin contact profiles during fetal corticogenesis[68], defining genes physically interacting with intergenic or intronic SNPs (Figure 98).

Spatiotemporal transcriptomic atlas of human brain was obtained from Kang et al[71]. We used transcriptomic profiles of multiple brain regions with developmental epochs that span prenatal (6–37 post-conception week, PCW) and postnatal (4 months-42 years) periods. Expression values were log-transformed and centered to the mean expression level for each sample using a scale(center=T, scale=F)+1 function in R. ASD candidate genes identified by Hi-C analyses (Figure 98) were selected for each sample and their average centered expression values were calculated and plotted.

Consortia Membership

Autism Spectrum Disorder Working Group of the Psychiatric Genomics Consortium

Richard JL Anney[1,2],
Stephan Ripke[3,4,5,6],
Verneri Anttila[3,4,5],
Peter Holmans[1],
Hailiang Huang[3,4,5],
Lambertus Klei[7],
Phil H Lee[3,4,5,8],
Sarah E Medland[9],
Benjamin Neale[3,4,5],
Elise Robinson[3,4,5],
Lauren A Weiss[10,11],
Joana Almeida[12],
Thomas D Als[13,14,15],
David Amaral[16,17,18],
Evdokia Anagnostou[19],
Elena Bacchelli[20],
Joel S Bader[21],
Marie Baekvad-Hansen[22],
Anthony J Bailey[23,24],
Gillian Baird[25],
Vanessa H Bal[10],
Agatino Battaglia[26],
Arthur L Beaudet[27],
Raphael Bernier[28],
Catalina Betancur[29,30,31],
Nadia Bolshakova[2],
Sven Bölte[32,33,34],
Patrick F Bolton[35,36],
Anders D Børglum[13,14,15],
Thomas Bourgeron[37,38,39,40],
Sean Brennan[2],
Cátia Café[12],
Rita M Cantor[41,42],
Jillian Casey[43,44],
Patrícia BS Celestino-Soper[27,45],
Andreas G Chiocchetti[32],
Ines C Conceição[46,47],
Judith Conroy[43,44],
Catarina T Correia[46,47],
Michael L Cuccaro[48],
Geraldine Dawson[49,50],
Maretha V De Jonge[51],
Silvia De Rubeis[52,53],
Richard Delorme[37,38,39,54],
Ditte Demontis[13,14,15],
Eftichia Duketis[32],
Frederico Duque[12,55],
Sean Ennis[44,56],
A. Gulhan Ercan-Sencicek[57],
M. Daniele Fallin[58],
Bridget Fernandez[59],
Susan E Folstein[60],
Eric Fombonne[61],
Christine M Freitag[32],
Louise Gallagher[2],
John Gilbert[48],
Christopher Gillberg[62],
Arthur P Goldberg[52,53],
Jonas Grauholm[22],
Andrew Green[44,56],
Jonathan M Green[63,64],
Dorothy E Grice[53],
Jakob Grove[13,14,15,65],
Stephen J Guter[66],
Jonathan L Haines[67],
Christine S Hansen[22],
Thomas F Hansen[14,68],
Robert Hendren[10],
Irva Hertz-Picciotto[16,69],
Mads V Hollegaard[22],
David M Hougaard[22],
Christina M Hultman[70],
Bozenna Iliadou[70],
Suma Jacob[66,71],
Sabine M Klauck[72,73],
Alexander Kolevzon[52,53,74,75],
Christine Ladd-Acosta[76],
Ann S Le Couteur[77,78],
Marion Leboyer[37,79,80,81],
David H Ledbetter[82],
Francesco Lescai[13,14,15],
Christa Lese Martin[83],
Pat Levitt[84],
Catherine Lord[85],

Jennifer K Lowe[86,87,88], Elena Maestrini[20], Tiago Magalhaes[44,89], Pall Magnusson[90], Shrikant M Mane[91], Donna M Martin[92], Igor Martsenkovsky[93], Manuel Mattheisen[13,14,15], Susan G McGrew[94], William M McMahon[95], Alison Merikangas[2], Nancy Minshew[7], Anthony P Monaco[96,97], Daniel Moreno-De-Luca[98], Eric M Morrow[99], Ole Mors[14,100], Preben B Mortensen[13,14,101], Susana Mouga[12,55], Michael T Murtha[57], Merete Nordentoft[14,102], Bent Norgaard-Pedersen[22], John I Nurnberger[45,103], Guiomar Oliveira[12,55], Alistair T Pagnamenta[96], Jeremy R Parr[77,78], Andrew D Paterson[104,105,106], Milica Pejovic Milovancevic[107], Margaret A Pericak-Vance[48], Dalila Pinto[52,53,74,75,108,109], Joseph Piven[110], Jesper Poulsen[22], Christopher S Poultney[52,53], Fritz Poustka[32], Regina Regan[44,89], Karola Rehnström[111], Abraham Reichenberg[52,53], Jennifer Reichert[52,53], Wendy Roberts[112], Kathryn Roeder[113,114], Bernadette Rogé[115], Guy A Rouleau[116], Evald Saemundsen[117], Stephan J Sanders[10], Sven Sandin[70], Gerard D Schellenberg[118], Stephen W Scherer[104,105,119], Teimuraz Silagadze[120], Latha Soorya[52,53,121], Matthew W State[10], Hreinn Stefansson[122], Kari Stefansson[122], Stacy Steinberg[122], Oscar Svantesson[70], Peter Szatmari[123], Ann P Thompson[124], Kathryn Tsang[10,11], Herman van Engeland[51], Astrid M Vicente[46,47], Veronica J Vieland[125], Jacob AS Vorstman[51], Simon Wallace[23], Christopher A Walsh[126,127,128,129,130], Regina Waltes[32], Thomas H Wassink[131], Thomas Werge[68,132], Ellen M Wijsman[133,134], A. Jeremy Willsey[10], Kerstin Wittemeyer[135], Timothy W Yu[126], Lonnie Zwaigenbaum[136], Joseph D Buxbaum[52,53,74,75,108,137], Aravinda Chakravarti[21], Edwin H Cook[66], Hilary Coon[95], Daniel H Geschwind[42,86,87,88], Michael Gill[2], Hakon Hakonarson[138,139], Joachim Hallmayer[140], Aarno Palotie[111], Susan Santangelo[141], James S Sutcliffe[67,142], Dan E Arking[21], Bernie Devlin[7], and Mark J Daly[3,4,5]

1. MRC Centre for Neuropsychiatric Genetics & Genomics, Cardiff University, Cardiff, UK
2. Department of Psychiatry, Trinity College Dublin, Dublin, Ireland
3. Analytic and Translational Genetics Unit, Department of Medicine, Massachusetts General Hospital and Harvard Medical School, Boston, MA, USA
4. Stanley Center for Psychiatric Research, Broad Institute of Harvard and MIT, Cambridge, MA, USA
5. Program in Medical and Population Genetics, Broad Institute of Harvard and MIT, Cambridge, MA, USA
6. Department of Psychiatry and Psychotherapy, Charité Universitätsmedizin Berlin, CCM, Berlin, Germany
7. Department of Psychiatry, University of Pittsburgh School of Medicine, Pittsburgh, PA, USA
8. Department of Psychiatry, Harvard Medical School, Boston, MA, USA
9. Queensland Institute of Medical Research, Brisbane, QLD, Australia
10. Department of Psychiatry, University of California San Francisco, San Francisco, CA, USA
11. Inst. Human Genetics, University of California San Francisco, San Francisco, CA, USA
12. Unidade de Neurodesenvolvimento e Autismo do Serviço do Centro de Desenvolvimento da Criança and Centro de Investigação e Formação Clinica, Pediatric Hospital, Centro Hospitalar e Universitário de Coimbra, Coimbra, Portugal
13. Department of Biomedicine and Human Genetics, Aarhus University, Aarhus, Denmark

14. Lundbeck Foundation Initiative for Integrative Psychiatric Research (iPSYCH), Copenhagen, Denmark
15. Centre for Integrative Sequencing (iSEQ), Aarhus University, Aarhus, Denmark
16. The MIND Institute, School of Medicine, University of California Davis, Davis, CA, USA
17. Department of Psychiatry, School of Medicine, University of California Davis, Davis, CA, USA
18. Department of Behavioural Sciences, School of Medicine, University of California Davis, Davis, CA, USA
19. Bloorview Research Institute, University of Toronto, Toronto, ON, Canada
20. Department of Pharmacy and Biotechnology, University of Bologna, Bologna, Italy
21. McKusick-Nathans Institute of Genetic Medicine, Johns Hopkins University, Baltimore, MD, USA
22. Department for Congenital Disorders, Center for Neonatal Screening, Statens Serum Institut, Copenhagen, Denmark
23. Department of Psychiatry, University of Oxford and Warneford Hospital, Oxford, UK
24. Mental Health and Addictions Research Unit, University of British Colombia, Vancouver, BC, Canada
25. Paediatric Neurodisability, King's Health Partners, Kings College London, London, UK
26. Stella Maris Institute for Child and Adolescent Neuropsychiatr, Pisa, Italy
27. Department of Molecular and Human Genetics, Baylor College of Medicine, Houston, TX, USA
28. Department of Psychiatry and Behavioral Sciences, University of Washington, Seattle, WA, USA
29. INSERM U1130, Paris, France
30. CNRS UMR 8246, Paris, France
31. Sorbonne Universités, UPMC Univ Paris 6, Neuroscience Paris Seine, Paris, France
32. Department of Child and Adolescent Psychiatry, Psychosomatics and Psychotherapy, JW Goethe University Frankfurt, Frankfurt am Main, Germany
33. Department of Women's and Children's Health, Center of Neurodevelopmental Disorders, Karolinska Institutet, Stockholm, Sweden
34. Child and Adolescent Psychiatry, Center for Psychiatry Research, Stockholm County Council, Stockholm, Sweden
35. Institute of Psychiatry, Kings College London, London, UK
36. South London & Maudsley Biomedical Research Centre for Mental Health, London, UK
37. FondaMental Foundation, Créteil, France
38. Human Genetics and Cognitive Functions Unit, Institut Pasteur, Paris, France
39. Centre National de la Recherche Scientifique URA 2182 Institut Pasteur, Paris, France
40. University Paris Diderot, Sorbonne Paris Cité, Paris, France
41. Department of Psychiatry, David Geffen School of Medicine at University of California Los Angeles, Los Angeles, CA, USA
42. Department of Human Genetics, David Geffen School of Medicine at University of California Los Angeles, Los Angeles, CA, USA
43. Temple Street Children's University Hospital, Dublin, Ireland
44. Academic Centre on Rare Diseases, University College Dublin, Dublin, Ireland
45. Department of Medical and Molecular Genetics and Program in Medical Neuroscience, Indiana University School of Medicine, Indianapolis, IN, USA
46. Instituto Nacional de Saúde Dr. Ricardo Jorge, Lisboa, Portugal
47. Center for Biodiversity, Functional and Integrative Genomics, Campus da FCUL, Lisboa, Portugal
48. The John P. Hussman Institute for Human Genomics, University of Miami, Miami, FL, USA
49. Duke Center for Autism and Brain Developments, Duke University School of Medicine, Durham, NC, USA
50. Duke Institute for Brain Sciences, Duke University School of Medicine, Durham, NC, USA
51. Department of Psychiatry, Brain Center Rudolf Magnus, University Medical Center Utrecht, Utrecht, CG, The Netherlands
52. Seaver Autism Center for Research and Treatment, Icahn School of Medicine at Mount Sinai, New York, NY, USA
53. Department of Psychiatry, Icahn School of Medicine at Mount Sinai, New York, NY, USA
54. Department of Child and Adolescent Psychiatry, Robert Debré Hospital, Assistance Publique – Hôpitaux de Paris, Paris, France
55. University Clinic of Pediatrics and Institute for Biomedical Imaging and Life Science, Faculty of Medicine, University of Coimbra, Coimbra, Portugal
56. Centre for Medical Genetics, Our Lady's Hospital Crumlin, Dublin, Ireland
57. Programs on Neurogenetics, Yale University School of Medicine, New Haven, CT, USA
58. Department of Mental Health, Johns Hopkins Bloomberg School of Public Health, Baltimore, MD, USA

59. Memorial University of Newfoundland, St. John's, NL, Canada
60. Division of Child and Adolescent Psychiatry, Department of Psychiatry, Miller School of Medicine, University of Miami, Miami, FL, USA
61. Department of Psychiatry, Institute for Development and Disability, Oregon Health & Science University, Portland, OR, USA
62. Gillberg Neuropsychiatry Centre, University of Gothenburg, Gothenburg, Sweden
63. Manchester Academic Health Sciences Centre, Manchester, UK
64. Institute of Brain, Behaviour, and Mental Health, University of Manchester, Manchester, UK
65. Bioinformatics Research Centre,
66. Institute for Juvenile Research, Department of Psychiatry, University of Illinois at Chicago, Chicago, IL, USA
67. Department of Molecular Physiology & Biophysics, Vanderbilt University, Nashville, TN, USA
68. Institute of Biological Psychiatry, Mental Health Center, Mental Health Services Copenhagen, Copenhagen, Denmark
69. Department of Public Health Sciences, School of Medicine, University of California Davis, Davis, CA, USA
70. Karolinska Institutet, Solna, Sweden
71. Institute of Translational Neuroscience and Department of Psychiatry, University of Minnesota, Minneapolis, MN, USA
72. Division of Molecular Genome Analysis, Deutsches Krebsforschungszentrum, Heidelberg, Germany
73. Working Group Cancer Genome Research, Deutsches Krebsforschungszentrum, Heidelberg, Germany
74. Friedman Brain Institute, Icahn School of Medicine at Mount Sinai, New York, NY, USA
75. The Mindich Child Health and Development Institute, Icahn School of Medicine at Mount Sinai, New York, NY, USA
76. Department of Epidemiology, Johns Hopkins Bloomberg School of Public Health, Baltimore, MD, USA
77. Institute of Neuroscience, Newcastle University, Newcastle Upon Tyne, UK
78. Institue of Health and Science, Newcastle University, Newcastle Upon Tyne, UK
79. INSERM U955, Paris, France
80. Faculté de Médecine, Université Paris Est, Créteil, France
81. Department of Psychiatry, Henri Mondor-Albert Chenevier Hospital, Assistance Publique – Hôpitaux de Paris, Créteil, France
82. Chief Scientific Officer, Geisinger Health System, Danville, PA, USA
83. Autism & Developmental Medicine Institute, Geisinger Health System, Danville, PA, USA
84. Department of Pediatrics, Keck School of Medicine, University of Southern California, Los Angeles, CA, USA
85. Department of Psychiatry, Weill Cornell Medical College, Cornell University, New York, NY, USA
86. Center for Autism Research and Treatment, Semel Institute, David Geffen School of Medicine at University of California Los Angeles, Los Angeles, CA, USA
87. Program in Neurogenetics, Department of Neurology, David Geffen School of Medicine, University of California, Los Angeles, Los Angeles, CA, USA
88. Center for Neurobehavioral Genetics, Semel Institute, David Geffen School of Medicine, University of California, Los Angeles, Los Angeles, CA, USA
89. National Childrens Research Centre, Our Lady's Hospital Crumlin, Dublin, Ireland
90. Department of Child and Adolescent Psychiatry, National University Hospital, Reykjavik, Iceland
91. Yale Center for Genomic Analysis, Yale University School of Medicine, New Haven, CT, USA
92. Department of Pediatrics and Human Genetics, University of Michigan, Ann Arbor, MI, USA
93. Department of Child, Adolescent Psychiatry and Medical-Social Rehabilitation, Ukrainian Research Institute of Social Forensic Psychiatry and Drug Abuse, Kyiv, Ukraine
94. Department of Pediatrics, Vanderbilt University, Nashville, TN, USA
95. Department of Psychiatry, University of Utah, Salt Lake City, UT, USA
96. Wellcome Trust Centre for Human Genetics, Oxford University, Oxford, UK
97. Tufts University, Boston, MA, USA
98. Department of Psychiatry, Yale University School of Medicine, New Haven, CT, USA
99. Department of Psychiatry and Human Behaviour, Brown University, Providence, RI, USA
100. Aarhus University Hospital, Risskov, Denmark
101. National Centre for Register-based Research, University
102. Mental Health Services in the Capital Region of Denmark, Mental Health Center, Mental Health Services Copenhagen, Copenhagen, Denmark
103. Institute of Psychiatric Research, Department of Psychiatry, Indiana University School of Medicine, Indianapo-

lis, IN, USA
104. Department of Molecular Genetics, University of Toronto, Toronto, ON, Canada
105. The Centre for Applied Genomics, The Hospital for Sick Children, Toronto, ON, Canada
106. Dalla Lana School of Public Health, Toronto, ON, Canada
107. Institute of Mental Health and Medical Faculty, University of Belgrade, Belgrade, Serbia
108. Department of Genetics and Genomic Sciences, Icahn School of Medicine at Mount Sinai, New York, NY, USA
109. The Icahn Institute for Genomics and Multiscale Biology, Icahn School of Medicine at Mount Sinai, New York, NY, USA
110. University of North Carolina, Chapel Hill, NC, USA
111. Sanger Institute, Hinxton, UK
112. Autism Research Unit, The Hospital for Sick Children, Toronto, ON, Canada
113. Department of Computational Biology, Carnegie Mellon University, Pittsburgh, PA, USA
114. Department of Statistics, Carnegie Mellon University, Pittsburgh, PA, USA
115. Centre d'Etudes et de Recherches en Psychopathologie, Toulouse University, Toulouse, France
116. Montreal Neurological Institute, Departmentof Neurology and Neurosurgery, McGill University, Montreal, QC, Canada
117. State Diagnostic and Counseling Centre, Kopavogur, Iceland
118. Department of Pathology and Laboratory Medicine, University of Pennsylvania, Philadelphia, PA, USA
119. McLaughlin Centre, University of Toronto, Toronto, ON, Canada
120. Department of Psychiatry and Drug Addiction, Tbilisi State Medical University, Tbilisi, Georgia
121. Department of Psychiatry, Rush University Medical Center, Chicago, IL, USA
122. deCODE Genetics, Reykjavik, Iceland
123. Department of Psychiatry, University of Toronto, ON, Canada
124. Department of Psychiatry and Behavioral Neurosciences, McMaster University, Hamilton, ON, Canada
125. Battelle Center for Mathematical Medicine, The Research Institute at Nationwide Children's Hospital, Columbus, OH, USA
126. Division of Genetics, Children's Hospital Boston, Harvard Medical School, Boston, MA, USA
127. Program in Genetics and Genomics, Harvard Medical School, Boston, MA, USA
128. Howard Hughes Medical Institute, Harvard Medical School, Boston, MA, USA
129. Department of Pediatrics, Harvard Medical School, Boston, MA, USA
130. Department of Neurology, Harvard Medical School, Boston, MA, USA
131. Department of Psychiatry, Carver College of Medicine, Iowa City, IA, USA
132. Department of Clinical Medicine, University of Copenhagen, Copenhagen, Denmark
133. Department of Medicine, University of Washington, Seattle, WA, USA
134. Department of Biostatistics, University of Washington, Seattle, WA, USA
135. School of Education, University of Birmingham, Birmingham, UK
136. Department of Pediatrics, University of Alberta, Edmonton, AB, Canada
137. Department of Neuroscience, Icahn School of Medicine at Mount Sinai, New York, NY, USA
138. The Center for Applied Genomics and Division of Human Genetics, Children's Hospital of Philadelphia, University of Pennsylvania School of Medicine, Philadelphia, PA, USA
139. Departmentof Pediatrics, University of Pennsylvania, Philadelphia, PA, USA
140. Department of Psychiatry, Stanford University, Stanford, CA, USA
141. Maine Medical Center Research Institute, Portland, ME, USA
142. Center for Human Genetics Research, Vanderbilt University, Nashville, TN, USA

BUPGEN

Ole A Andreassen[1,2]

Terje Nærland[1,2,3]

Srdjan Djurovic[1,2]

Sigrun Hope[4]

Berhard Weidle[5]

Anne Lise Høiland[6]

Siv Kvernmo[7]

Jarle Johannessen[8]

Eva Malt[9]

Irene Bircow Elgen[10]

Merete Glenne Øie[11,12]

Tonje Torske[13]

Anett Kaale[14]

Berit Hjelde Hansen[9]

Geir Øgrim[15]

Magnar Mathisen[15] Nina Stenberg[18] Elen Gjevik[18]
Vera Lonning[1,16] Thomas Bjella[1,2] Torstein Øverland[19]
Lise Reindal[17] Francesco Bettella[1,2] Krister Fjermestad[20]

1. NORMENT, KG Jebsen Centre for Psychosis Research, Institute of Clinical Medicine, University of Oslo, Oslo, Norway
2. Oslo University Hospital, Oslo, Norway
3. NevSom, Department of rare disorders Oslo University hospital, Oslo, Norway
4. Department of Neuro Habilitation, Oslo University Hospital Ullevål, Oslo, Norway
5. Department of Psychiatry, St. Olavs Hospital, Trondheim University Hospital, Trondheim, Norway
6. Department of Pediatrics, St. Olavs Hospital, Trondheim University Hospital, Trondheim, Norway
7. University Hospital of North Norway, Tromsø, Norway
8. Autism Society of Norway, Oslo, Norway
9. Division of Mental Health, Akershus University Hospital, Lørenskog, Norway
10. Haukeland University Hospital, Bergen, Norway
11. Institute of Psychology, University of Oslo, Oslo, Norway
12. Innlandet Hospital, Lillehammer, Norway
13. Vestre Viken Health Trust, Drammen, Norway
14. Institute of Special education, University of Oslo, Oslo, Norway
15. Department of Psychiatry, Hospital of Østfold, Kalnes, Norway
16. Diakonhjemmet Hospital, Oslo, Norway
17. Møre og Romsdal Health trust, Volda, Norway
18. Department of Child and adolescent Psychiatry, Oslo University Hospital, Oslo, Norway
19. Department of pediatrics, Oslo University Hospital Oslo, Norway
20. Frambu centre of rare disorders, Frambu, Norway

Major Depressive Disorder Working Group of the Psychiatric Genomics Consortium

The list of members of the Major Depressive Disorder Working Group of the PGC are also listed in main manuscript, but people occuring in the list of named authors were removed. Here we bring the complete list.

Naomi R Wray*[1,2], Douglas HR Blackwood[11], Franziska Degenhardt[35,36],
Stephan Ripke*[3,4,5], Julien Bryois[22], Eske M Derks[28],
Manuel Mattheisen*[6,7,8,9], Henriette N Buttenschøn[8,9,23], Nese Direk[37,38],
Maciej Trzaskowski*[1], Jonas Bybjerg-Grauholm[9,18], Conor V Dolan[10],
Enda M Byrne[1], Na Cai[24,25], Erin C Dunn[39,40,41],
Abdel Abdellaoui[10], Enrique Castelao[26], Thalia C Eley[27],
Mark J Adams[11], Jane H Christensen[7,8,9], Valentina Escott-Price[42],
Esben Agerbo[9,12,13], Toni-Kim Clarke[11], Farnush Farhadi Hassan Kiadeh[43],
Tracy M Air[14], Jonathan RI Coleman[27], Hilary K Finucane[44,45],
Till FM Andlauer[15,16], Lucía Colodro-Conde[28], Andreas J Forstner[35,36,46,47],
Silviu-Alin Bacanu[17], Baptiste Couvy-Duchesne[29,30], Josef Frank[48],
Marie Bækvad-Hansen[9,18], Nick Craddock[31], Héléna A Gaspar[27],
Aartjan TF Beekman[19], Gregory E Crawford[32,33], Michael Gill[49],
Tim B Bigdeli[17,20], Gail Davies[34], Fernando S Goes[50],
Elisabeth B Binder[15,21], Ian J Deary[34], Scott D Gordon[28],

Jakob Grove[7,8,9,51],
Lynsey S Hall[11,52],
Christine S Hansen[9,18],
Thomas F Hansen[53,54,55],
Stefan Herms[35,36,47],
Ian B Hickie[56],
Per Hoffmann[35,36,47],
Georg Homuth[57],
Carsten Horn[58],
Jouke-Jan Hottenga[10],
David M Hougaard[9,18],
Marcus Ising[59],
Rick Jansen[19,19],
Eric Jorgenson[60],
James A Knowles[61],
Isaac S Kohane[62,63,64],
Julia Kraft[4],
Warren W Kretzschmar[65],
Jesper Krogh[66],
Zoltán Kutalik[67,68],
Yihan Li[65],
Penelope A Lind[28],
Donald J MacIntyre[69,70],
Dean F MacKinnon[50],
Robert M Maier[2],
Wolfgang Maier[71],
Jonathan Marchini[72],
Hamdi Mbarek[10],
Patrick McGrath[73],
Peter McGuffin[27],
Sarah E Medland[28],
Divya Mehta[2,74],
Christel M Middeldorp[10,75,76],
Evelin Mihailov[77],
Yuri Milaneschi[19,19],
Lili Milani[77],
Francis M Mondimore[50],
Grant W Montgomery[1],
Sara Mostafavi[78,79],
Niamh Mullins[27],
Matthias Nauck[80,81],
Bernard Ng[79],
Michel G Nivard[10],
Dale R Nyholt[82],
Paul F O'Reilly[27],
Hogni Oskarsson[83],
Michael J Owen[84],
Jodie N Painter[28],
Carsten Bøcker Pedersen[9,12,13],
Marianne Giørtz Pedersen[9,12,13],
Roseann E Peterson[17,85],
Erik Pettersson[22],
Wouter J Peyrot[19],
Giorgio Pistis[26],
Danielle Posthuma[86,87],
Jorge A Quiroz[88],
Per Qvist[7,8,9],
John P Rice[89],
Brien P Riley[17],
Margarita Rivera[27,90],
Saira Saeed Mirza[37],
Robert Schoevers[91],
Eva C Schulte[92,93],
Ling Shen[60],
Jianxin Shi[94],
Stanley I Shyn[95],
Engilbert Sigurdsson[96],
Grant CB Sinnamon[97],
Johannes H Smit[19],
Daniel J Smith[98],
Hreinn Stefansson[99],
Stacy Steinberg[99],
Fabian Streit[48],
Jana Strohmaier[48],
Katherine E Tansey[100],
Henning Teismann[101],
Alexander Teumer[102],
Wesley Thompson[9,54,103,104,105],
Pippa A Thomson[106],
Thorgeir E Thorgeirsson[99],
Matthew Traylor[107],
Jens Treutlein[48],
Vassily Trubetskoy[4],
André G Uitterlinden[108],
Daniel Umbricht[109],
Sandra Van der Auwera[110],
Albert M van Hemert[111],
Alexander Viktorin[22],
Peter M Visscher[1,2],
Yunpeng Wang[9,54,104,105],
Bradley T Webb[85],
Shantel Marie Weinsheimer[9,54],
Jürgen Wellmann[101],
Gonneke Willemsen[10],
Stephanie H Witt[48],
Yang Wu[1],
Hualin S Xi[112],
Jian Yang[2,113],
Futao Zhang[1],
Volker Arolt[114],
Bernhard T Baune[14],
Klaus Berger[101],
Dorret I Boomsma[10],
Sven Cichon[35,47,115,116],
Udo Dannlowski[114],
EJC de Geus[10,117],
J Raymond DePaulo[50],
Enrico Domenici[118],
Katharina Domschke[119],
Tõnu Esko[5,77],
Hans J Grabe[110],
Steven P Hamilton[120],
Caroline Hayward[121],
Andrew C Heath[89],
Kenneth S Kendler[17],
Stefan Kloiber[59,122,123],
Glyn Lewis[124],
Qingqin S Li[125],
Susanne Lucae[59],
Pamela AF Madden[89],

Patrik K Magnusson[22],
Nicholas G Martin[28],
Andrew M McIntosh[11,34],
Andres Metspalu[77,126],
Ole Mors[9,127],
Preben Bo Mortensen[8,9,12,13],
Bertram Müller-Myhsok[15,16,128],
Merete Nordentoft[9,129],
Markus M Nöthen[35,36],
Michael C O'Donovan[84],
Sara A Paciga[130],
Nancy L Pedersen[22],
Brenda WJH Penninx[19],
Roy H Perlis[39,131],
David J Porteous[106],
James B Potash[132],
Martin Preisig[26],
Marcella Rietschel[48],
Catherine Schaefer[60],
Thomas G Schulze[48,50,93,133,134],
Jordan W Smoller[39,40,41],
Kari Stefansson[99,135],
Henning Tiemeier[37,136,137],
Rudolf Uher[138],
Henry Völzke[102],
Myrna M Weissman[73,139],
Thomas Werge[9,54,140],
Cathryn M Lewis[*27,141],
Douglas F Levinson[*142],
Gerome Breen[*27,143],
Anders D Børglum[*7,8,9], and
Patrick F Sullivan[*22,144,145]

1. Institute for Molecular Bioscience, The University of Queensland, Brisbane, QLD, Australia
2. Queensland Brain Institute, The University of Queensland, Brisbane, QLD, Australia
3. Analytic and Translational Genetics Unit, Massachusetts General Hospital, Boston, MA, USA
4. Department of Psychiatry and Psychotherapy, Universitätsmedizin Berlin Campus Charité Mitte, Berlin, Germany
5. Program in Medical and Population Genetics, Broad Institute of Harvard and MIT, Cambridge, MA, USA
6. Centre for Psychiatry Research, Department of Clinical Neuroscience, Karolinska Institutet, Stockholm, Sweden
7. Department of Biomedicine, Aarhus University, Aarhus, Denmark
8. Centre for Integrative Sequencing, iSEQ, Aarhus University, Aarhus, Denmark
9. The Lundbeck Foundation Initiative for Integrative Psychiatric Research, iPSYCH, Denmark
10. Departmentof Biological Psychology & EMGO+ Institute for Health and Care Research, Vrije Universiteit, Amsterdam, Amsterdam, Netherlands
11. Division of Psychiatry, University of Edinburgh, Edinburgh, UK
12. Centre for Integrated Register-based Research, Aarhus University, Aarhus, Denmark
13. National Centre for Register-Based Research, Aarhus University, Aarhus, Denmark
14. Discipline of Psychiatry, University of Adelaide, Adelaide, SA, Australia
15. Department of Translational Research in Psychiatry, Max Planck Institute of Psychiatry, Munich, Germany
16. Munich Cluster for Systems Neurology (SyNergy), Munich, Germany
17. Department of Psychiatry, Virginia Commonwealth University, Richmond, VA, USA
18. Center for Neonatal Screening, Department for Congenital Disorders, Statens Serum Institut, Copenhagen, Denmark
19. Department of Psychiatry, Vrije Universiteit Medical Center and GGZ inGeest, Amsterdam, Netherlands
20. Virginia Institute for Psychiatric and Behavior Genetics, Richmond, VA, USA
21. Department of Psychiatry and Behavioral Sciences, Emory University School of Medicine, Atlanta, GA, USA
22. Department of Medical Epidemiology and Biostatistics, Karolinska Institutet, Stockholm, Sweden
23. Department of Clinical Medicine, Translational Neuropsychiatry Unit, Aarhus University, Aarhus, Denmark
24. Human Genetics, Wellcome Trust Sanger Institute, Cambridge, UK
25. Statistical genomics and systems genetics, European Bioinformatics Institute (EMBL-EBI), Cambridge, UK
26. Department of Psychiatry, University Hospital of Lausanne, Prilly, Vaud, Switzerland
27. MRC Social Genetic and Developmental Psychiatry Centre, King's College London, London, UK
28. Genetics and Computational Biology, QIMR Berghofer Medical Research Institute, Brisbane, QLD, Australia
29. Centre for Advanced Imaging, The University of Queensland, Saint Lucia, QLD, Australia
30. Queensland Brain Institute, The University of Queensland, Saint Lucia, QLD, Australia
31. Psychological Medicine, Cardiff University, Cardiff, UK
32. Center for Genomic and Computational Biology, Duke University, Durham, NC, USA
33. Department of Pediatrics, Division of Medical Genetics, Duke University, Durham, NC, USA
34. Centre for Cognitive Ageing and Cognitive Epidemiology, University of Edinburgh, Edinburgh, UK
35. Institute of Human Genetics, University of Bonn, Bonn, Germany
36. Life&Brain Center, Department of Genomics, University of Bonn, Bonn, Germany
37. Epidemiology, Erasmus MC, Rotterdam, Zuid-Holland, Netherlands

38. Psychiatry, Dokuz Eylul University School Of Medicine, Izmir, Turkey
39. Department of Psychiatry, Massachusetts General Hospital, Boston, MA, USA
40. Psychiatric and Neurodevelopmental Genetics Unit (PNGU), Massachusetts General Hospital, Boston, MA, USA
41. Stanley Center for Psychiatric Research, Broad Institute of Harvard and MIT, Cambridge, MA, USA
42. Neuroscience and Mental Health, Cardiff University, Cardiff, UK
43. Bioinformatics, University of British Columbia, Vancouver, BC, Canada
44. Department of Epidemiology, Harvard T.H. Chan School of Public Health, Boston, MA, USA
45. Department of Mathematics, Massachusetts Institute of Technology, Cambridge, MA, USA
46. Department of Psychiatry (UPK), University of Basel, Basel, Switzerland
47. Human Genomics Research Group, Department of Biomedicine, University of Basel, Basel, Switzerland
48. Department of Genetic Epidemiology in Psychiatry, Central Institute of Mental Health, Medical Faculty, Mannheim, Heidelberg University, Mannheim, Baden-Württemberg, Germany
49. Department of Psychiatry, Trinity College Dublin, Dublin, Ireland
50. Department of Psychiatry and Behavioral Sciences, Johns Hopkins University, Baltimore, MD, USA
51. Bioinformatics Research Centre, Aarhus University, Aarhus, Denmark
52. Institute of Genetic Medicine, Newcastle University, Newcastle upon Tyne, UK
53. Danish Headache Centre, Department of Neurology, Rigshospitalet, Glostrup, Denmark
54. Institute of Biological Psychiatry, Mental Health Center Sct. Hans, Mental Health Services Capital Region of Denmark, Copenhagen, Denmark
55. iPSYCH, The Lundbeck Foundation Initiative for Psychiatric Research, Copenhagen, Denmark
56. Brain and Mind Centre, University of Sydney, Sydney, NSW, Australia
57. Interfaculty Institute for Genetics and Functional Genomics, Department of Functional Genomics, University Medicine and Ernst Moritz Arndt University Greifswald, Greifswald, Mecklenburg-Vorpommern, Germany
58. Roche Pharmaceutical Research and Early Development, Pharmaceutical Sciences, Roche Innovation Center Basel, F. Hoffmann-La Roche Ltd, Basel, Switzerland
59. Max Planck Institute of Psychiatry, Munich, Germany
60. Division of Research, Kaiser Permanente Northern California, Oakland, CA, USA
61. Psychiatry & The Behavioral Sciences, University of Southern California, Los Angeles, CA, USA
62. Department of Biomedical Informatics, Harvard Medical School, Boston, MA, USA
63. Department of Medicine, Brigham and Women's Hospital, Boston, MA, USA
64. Informatics Program, Boston Children's Hospital, Boston, MA, USA
65. Wellcome Trust Centre for Human Genetics, University of Oxford, Oxford, UK
66. Department of Endocrinology at Herlev University Hospital, University of Copenhagen, Copenhagen, Denmark
67. Institute of Social and Preventive Medicine (IUMSP), University Hospital of Lausanne, Lausanne, VD, Switzerland
68. Swiss Institute of Bioinformatics, Lausanne, VD, Switzerland
69. Division of Psychiatry, Centre for Clinical Brain Sciences, University of Edinburgh, Edinburgh, UK
70. Mental Health, NHS 24, Glasgow, UK
71. Department of Psychiatry and Psychotherapy, University of Bonn, Bonn, Germany
72. Statistics, University of Oxford, Oxford, UK
73. Psychiatry, Columbia University College of Physicians and Surgeons, New York, NY, USA
74. School of Psychology and Counseling, Queensland University of Technology, Brisbane, QLD, Australia
75. Child and Youth Mental Health Service, Children's Health Queensland Hospital and Health Service, South Brisbane, QLD, Australia
76. Child Health Research Centre, University of Queensland, Brisbane, QLD, Australia
77. Estonian Genome Center, University of Tartu, Tartu, Estonia
78. Medical Genetics, University of British Columbia, Vancouver, BC, Canada
79. Statistics, University of British Columbia, Vancouver, BC, Canada
80. DZHK (German Centre for Cardiovascular Research), Partner Site Greifswald, University Medicine, University Medicine Greifswald, Greifswald, Mecklenburg-Vorpommern, Germany
81. Institute of Clinical Chemistry and Laboratory Medicine, University Medicine Greifswald, Greifswald, Mecklenburg-Vorpommern, Germany
82. Institute of Health and Biomedical Innovation, Queensland University of Technology, Brisbane, QLD, Australia
83. Humus, Reykjavik, Iceland
84. MRC Centre for Neuropsychiatric Genetics and Genomics, Cardiff University, Cardiff, UK

85. Virginia Institute for Psychiatric & Behavioral Genetics, Virginia Commonwealth University, Richmond, VA, USA
86. Clinical Genetics, Vrije Universiteit Medical Center, Amsterdam, Netherlands
87. Complex Trait Genetics, Vrije Universiteit Amsterdam, Amsterdam, Netherlands
88. Solid Biosciences, Boston, MA, USA
89. Department of Psychiatry, Washington University in Saint Louis School of Medicine, Saint Louis, MO, USA
90. Department of Biochemistry and Molecular Biology II, Institute of Neurosciences, Center for Biomedical Research, University of Granada, Granada, Spain
91. Department of Psychiatry, University of Groningen, University Medical Center Groningen, Groningen, Netherlands
92. Department of Psychiatry and Psychotherapy, Medical Center of the University of Munich, Campus Innenstadt, Munich, Germany
93. Institute of Psychiatric Phenomics and Genomics (IPPG), Medical Center of the University of Munich, Campus Innenstadt, Munich, Germany
94. Division of Cancer Epidemiology and Genetics, National Cancer Institute, Bethesda, MD, USA
95. Behavioral Health Services, Kaiser Permanente Washington, Seattle, WA, USA
96. Faculty of Medicine, Department of Psychiatry, University of Iceland, Reykjavik, Iceland
97. School of Medicine and Dentistry, James Cook University, Townsville, QLD, Australia
98. Institute of Health and Wellbeing, University of Glasgow, Glasgow, UK
99. deCODE Genetics / Amgen, Reykjavik, Iceland
100. College of Biomedical and Life Sciences, Cardiff University, Cardiff, UK
101. Institute of Epidemiology and Social Medicine, University of Münster, Münster, Nordrhein-Westfalen, Germany
102. Institute for Community Medicine, University Medicine Greifswald, Greifswald, Mecklenburg-Vorpommern, Germany
103. Department of Psychiatry, University of California, San Diego, San Diego, CA, USA
104. NORMENT - KG Jebsen Centre for Psychosis Research, University of Oslo, Oslo, Norway
105. Division of Mental Health and Addiction, Oslo University Hospital, Oslo, Norway
106. Medical Genetics Section, CGEM, IGMM, University of Edinburgh, Edinburgh, UK
107. Clinical Neurosciences, University of Cambridge, Cambridge, UK
108. Internal Medicine, Erasmus MC, Rotterdam, Zuid-Holland, Netherlands
109. Roche Pharmaceutical Research and Early Development, Neuroscience, Ophthalmology and Rare Diseases Discovery & Translational Medicine Area, Roche Innovation Center Basel, F. Hoffmann-La Roche Ltd, Basel, Switzerland
110. Department of Psychiatry and Psychotherapy, University Medicine Greifswald, Greifswald, Mecklenburg-Vorpommern, Germany
111. Department of Psychiatry, Leiden University Medical Center, Leiden, Netherlands
112. Computational Sciences Center of Emphasis, Pfizer Global Research and Development, Cambridge, MA, USA
113. Institute for Molecular Bioscience, Queensland Brain Institute, The University of Queensland, Brisbane, QLD, Australia
114. Department of Psychiatry, University of Münster, Münster, Nordrhein-Westfalen, Germany
115. Institute of Medical Genetics and Pathology, University Hospital Basel, University of Basel, Basel, Switzerland
116. Institute of Neuroscience and Medicine (INM-1), Research Center Juelich, Juelich, Germany
117. Amsterdam Public Health Institute, Vrije Universiteit Medical Center, Amsterdam, Netherlands
118. Centre for Integrative Biology, Università degli Studi di Trento, Trento, Trentino-Alto Adige, Italy
119. Department of Psychiatry and Psychotherapy, Medical Center, University of Freiburg, Faculty of Medicine, University of Freiburg, Freiburg, Germany
120. Psychiatry, Kaiser Permanente Northern California, San Francisco, CA, USA
121. Medical Research Council Human Genetics Unit, Institute of Genetics and Molecular Medicine, University of Edinburgh, Edinburgh, UK
122. Department of Psychiatry, University of Toronto, Toronto, ON, Canada
123. Centre for Addiction and Mental Health, Toronto, ON, Canada
124. Division of Psychiatry, University College London, London, UK
125. Neuroscience Therapeutic Area, Janssen Research and Development, LLC, Titusville, NJ, USA
126. Institute of Molecular and Cell Biology, University of Tartu, Tartu, Estonia
127. Psychosis Research Unit, Aarhus University Hospital, Risskov, Aarhus, Denmark

128. University of Liverpool, Liverpool, UK
129. Mental Health Center Copenhagen, Copenhagen University Hospital, Copenhagen, Denmark
130. Human Genetics and Computational Biomedicine, Pfizer Global Research and Development, Groton, CT, USA
131. Psychiatry, Harvard Medical School, Boston, MA, USA
132. Psychiatry, University of Iowa, Iowa City, IA, USA
133. Department of Psychiatry and Psychotherapy, University Medical Center Göttingen, Goettingen, Niedersachsen, Germany
134. Human Genetics Branch, NIMH Division of Intramural Research Programs, Bethesda, MD, USA
135. Faculty of Medicine, University of Iceland, Reykjavik, Iceland
136. Child and Adolescent Psychiatry, Erasmus MC, Rotterdam, Zuid-Holland, Netherlands
137. Psychiatry, Erasmus MC, Rotterdam, Zuid-Holland, Netherlands
138. Psychiatry, Dalhousie University, Halifax, NS, Canada
139. Division of Epidemiology, New York State Psychiatric Institute, New York, NY, USA
140. Department of Clinical Medicine, University of Copenhagen, Copenhagen, Denmark
141. Department of Medical & Molecular Genetics, King's College London, London, UK
142. Psychiatry & Behavioral Sciences, Stanford University, Stanford, CA, USA
143. NIHR BRC for Mental Health, King's College London, London, UK
144. Genetics, University of North Carolina at Chapel Hill, Chapel Hill, NC, USA
145. Psychiatry, University of North Carolina at Chapel Hill, Chapel Hill, NC, USA

Bibliography

[1] Pedersen, C. B. et al. "The iPSYCH2012 case-cohort sample: new directions for unravelling the genetic and environmental architecture of severe mental disorders". *Molecular Psychiatry* (Sept. 19, 2017). DOI: 10.1038/mp.2017.196. PMID: 28924187. (Visited on 09/19/2017).

[2] Mors, O., Perto, G. P., and Mortensen, P. B. "The Danish Psychiatric Central Research Register." *Scandinavian journal of public health* **39**, (7 Suppl July 2011), pp. 54–57. ISSN: 1651-1905. DOI: 10.1177/1403494810395825. PMID: 21775352.

[3] Børglum, A. D. et al. "Genome-wide study of association and interaction with maternal cytomegalovirus infection identifies new schizophrenia loci". *Molecular Psychiatry* **19**, (2014). published online 29 January 2013, pp. 325–333. DOI: 10.1038/mp.2013.2. PMID: 23358160.

[4] Hollegaard, M. et al. "Robustness of genome-wide scanning using archived dried blood spot samples as a DNA source". *BMC Genet* **12**,1 (2011), p. 58. ISSN: 1471-2156. DOI: 10.1186/1471-2156-12-58. PMID: 21726430.

[5] *Illumina GenCall Data Analysis Software*. Tech. rep. Illumina, Inc., 2005. URL: http://www.illumina.com/downloads/GenCallTechSpotlight.pdf.

[6] Korn, J. M. et al. "Integrated genotype calling and association analysis of SNPs, common copy number polymorphisms and rare CNVs." *Nature genetics* **40**, (10 Oct. 2008), pp. 1253–1260. ISSN: 1546-1718. DOI: 10.1038/ng.237. PMID: 18776909.

[7] Goldstein, J. I. et al. "zCall: a rare variant caller for array-based genotyping: genetics and population analysis." *Bioinformatics (Oxford, England)* **28**, (19 Oct. 2012), pp. 2543–2545. ISSN: 1367-4811. DOI: 10.1093/bioinformatics/bts479. PMID: 22843986.

[8] Schizophrenia Working Group of the Psychiatric Genomics Consortium. "Biological insights from 108 schizophrenia-associated genetic loci." eng. *Nature* **511**,7510 (July 2014), pp. 421–427. DOI: 10.1038/nature13595. PMID: 25056061.

[9] Delaneau, O., Marchini, J., and Zagury, J.-F. "A linear complexity phasing method for thousands of genomes." *Nature methods* **9**, (2 Dec. 2011), pp. 179–181. ISSN: 1548-7105. DOI: 10.1038/nmeth.1785. PMID: 22138821.

[10] Howie, B. et al. "Fast and accurate genotype imputation in genome-wide association studies through pre-phasing." eng. *Nat Genet* **44**,8 (Aug. 2012), pp. 955–959. DOI: 10.1038/ng.2354. PMID: 22820512.

[11] Howie, B. N., Donnelly, P., and Marchini, J. "A flexible and accurate genotype imputation method for the next generation of genome-wide association studies." eng. *PLoS Genet* **5**,6 (June 2009), e1000529. DOI: 10.1371/journal.pgen.1000529. PMID: 19543373.

[12] Consortium, 1. G. P. et al. "A global reference for human genetic variation." *Nature* **526**, (7571 Oct. 2015), pp. 68–74. ISSN: 1476-4687. DOI: 10.1038/nature15393. PMID: 26432245.

[13] Sudmant, P. H. et al. "An integrated map of structural variation in 2,504 human genomes." *Nature* **526**, (7571 Oct. 2015), pp. 75–81. ISSN: 1476-4687. DOI: 10.1038/nature15394. PMID: 26432246.

[14] 1000 Genomes Project Consortium et al. "An integrated map of genetic variation from 1,092 human genomes." eng. *Nature* **491**,7422 (Nov. 2012), pp. 56–65. DOI: 10.1038/nature11632. PMID: 23128226.

[15] Price, A. L. et al. "Long-range LD can confound genome scans in admixed populations." eng. *Am J Hum Genet* **83**,1 (July 2008), pp. 132–5, 132–5. DOI: 10.1016/j.ajhg.2008.06.005. PMID: 18606306.

[16] Purcell, S. and Chang, C. *PLINK verion 1.9*. 2015. URL: https://www.cog-genomics.org/plink2.

[17] Chang, C. C. et al. "Second-generation PLINK: rising to the challenge of larger and richer datasets." *GigaScience* **4**, (2015). Original DateCompleted: 20150227, p. 7. ISSN: 2047-217X. DOI: 10.1186/s13742-015-0047-8. PMID: 25722852.

[18] Price, A. L. et al. "Principal components analysis corrects for stratification in genome-wide association studies." eng. *Nat Genet* **38**,8 (Aug. 2006), pp. 904–909. DOI: 10.1038/ng1847. PMID: 16862161.

[19] Patterson, N., Price, A. L., and Reich, D. "Population structure and eigenanalysis." eng. *PLoS Genet* **2**,12 (Dec. 2006), e190. DOI: 10.1371/journal.pgen.0020190. PMID: 17194218.

[20] Anney, R. et al. "A genome-wide scan for common alleles affecting risk for autism." eng. *Hum Mol Genet* **19**,20 (Oct. 2010), pp. 4072–4082. DOI: 10.1093/hmg/ddq307. PMID: 20663923.

[21] Lajonchere, C. M. and Consortium, A. "Changing the landscape of autism research: the autism genetic resource exchange." *Neuron* **68**, (2 Oct. 2010), pp. 187–191. ISSN: 1097-4199. DOI: 10.1016/j.neuron.2010.10.009. PMID: 20955925.

[22] Geschwind, D. H. et al. "The autism genetic resource exchange: a resource for the study of autism and related neuropsychiatric conditions." *American journal of human genetics* **69**, (2 Aug. 2001), pp. 463–466. ISSN: 0002-9297. DOI: 10.1086/321292. PMID: 11452364.

[23] Gauthier, J. et al. "Autism spectrum disorders associated with X chromosome markers in French-Canadian males." *Molecular psychiatry* **11**, (2 Feb. 2006), pp. 206–213. ISSN: 1359-4184. DOI: 10.1038/sj.mp.4001756. PMID: 16261168.

[24] Anney, R. J. L. et al. "Meta-analysis of GWAS of over 16,000 individuals with autism spectrum disorder highlights a novel locus at 10q24.32 and a significant overlap with schizophrenia". *Molecular Autism* **8**,1 (2017), p. 21. ISSN: 2040-2392. DOI: 10.1186/s13229-017-0137-9. PMID: 28540026.

[25] Weiss, L. A. et al. "Association between microdeletion and microduplication at 16p11.2 and autism." *The New England journal of medicine* **358**, (7 Feb. 2008), pp. 667–675. ISSN: 1533-4406. DOI: 10.1056/NEJMoa075974. PMID: 18184952.

[26] Gudbjartsson, D. F. et al. "Large-scale whole-genome sequencing of the Icelandic population." *Nature genetics* **47**, (5 May 2015), pp. 435–444. ISSN: 1546-1718. DOI: 10.1038/ng.3247. PMID: 25807286.

[27] Steinberg, S. et al. "Common variant at 16p11.2 conferring risk of psychosis." *Molecular psychiatry* **19**, (1 Jan. 2014), pp. 108–114. ISSN: 1476-5578. DOI: 10.1038/mp.2012.157. PMID: 23164818.

[28] Teslovich, T. M. et al. "Biological, clinical and population relevance of 95 loci for blood lipids." *Nature* **466**, (7307 Aug. 2010), pp. 707–713. ISSN: 1476-4687. DOI: 10.1038/nature09270. PMID: 20686565.

[29] Auranen, M. et al. "A genomewide screen for autism-spectrum disorders: evidence for a major susceptibility locus on chromosome 3q25-27." *American journal of human genetics* **71**, (4 Oct. 2002), pp. 777–790. ISSN: 0002-9297. DOI: 10.1086/342720. PMID: 12192642.

[30] Ylisaukko-oja, T. et al. "Genome-wide scan for loci of Asperger syndrome." *Molecular psychiatry* **9**, (2 Feb. 2004), pp. 161–168. ISSN: 1359-4184. DOI: 10.1038/sj.mp.4001385. PMID: 14966474.

[31] Rehnström, K. et al. "Independent replication and initial fine mapping of 3p21-24 in Asperger syndrome." *Journal of medical genetics* **43**, (2 Feb. 2006), e6. ISSN: 1468-6244. DOI: 10.1136/jmg.2005.033621. PMID: 16467216.

[32] Kilpinen, H. et al. "Linkage and linkage disequilibrium scan for autism loci in an extended pedigree from Finland." *Human molecular genetics* **18**, (15 Aug. 2009), pp. 2912–2921. ISSN: 1460-2083. DOI: 10.1093/hmg/ddp229. PMID: 19454485.

[33] Lampi, K. M. et al. "Brief report: validity of Finnish registry-based diagnoses of autism with the ADI-R." *Acta paediatrica (Oslo, Norway : 1992)* **99**, (9 Sept. 2010), pp. 1425–1428. ISSN: 1651-2227. DOI: 10.1111/j.1651-2227.2010.01835.x. PMID: 20412100.

[34] Gaugler, T. et al. "Most genetic risk for autism resides with common variation." eng. *Nat Genet* (July 2014). DOI: 10.1038/ng.3039. PMID: 25038753.

[35] Klei, L. et al. "GemTools: A fast and efficient approach to estimating genetic ancestry" (Apr. 6, 2011). arXiv: 1104.1162v1 [stat.AP].

[36] Lee, A. B., Luca, D., and Roeder, K. "A Spectral Graph Approach to Discovering Genetic Ancestry". *Annals of Applied Statistics, 4(1), 179-201, 2010* (Aug. 17, 2009). arXiv: 0908.2409v1 [stat.AP].

[37] Willer, C. J., Li, Y., and Abecasis, G. R. "METAL: fast and efficient meta-analysis of genomewide association scans." *Bioinformatics (Oxford, England)* **26**, (17 Sept. 2010), pp. 2190–2191. ISSN: 1367-4811. DOI: 10.1093/bioinformatics/btq340. PMID: 20616382.

[38] Begum, F., Ghosh, D., Tseng, G. C., and Feingold, E. "Comprehensive literature review and statistical considerations for GWAS meta-analysis." *Nucleic acids research* **40**, (9 May 2012), pp. 3777–3784. ISSN: 1362-4962. DOI: 10.1093/nar/gkr1255. PMID: 22241776.

[39] Bulik-Sullivan, B. K. et al. "LD Score regression distinguishes confounding from polygenicity in genome-wide association studies." eng. *Nat Genet* **47**,3 (Mar. 2015), pp. 291–295. DOI: 10.1038/ng.3211. PMID: 25642630.

[40] de Leeuw, C. A., Mooij, J. M., Heskes, T., and Posthuma, D. "MAGMA: generalized gene-set analysis of GWAS data." eng. *PLoS Comput Biol* **11**,4 (Apr. 2015), e1004219. DOI: 10.1371/journal.pcbi.1004219. PMID: 25885710.

[41] Parikshak, N. N. et al. "Integrative functional genomic analyses implicate specific molecular pathways and circuits in autism." *Cell* **155**, (5 Nov. 2013), pp. 1008–1021. ISSN: 1097-4172. DOI: 10.1016/j.cell.2013.10.031. PMID: 24267887.

[42] Samocha, K. E. et al. "A framework for the interpretation of de novo mutation in human disease." eng. *Nat Genet* **46**,9 (Sept. 2014), pp. 944–950. DOI: 10.1038/ng.3050. PMID: 25086666.

[43] Lek, M. et al. "Analysis of protein-coding genetic variation in 60,706 humans." *Nature* **536**, (7616 Aug. 2016), pp. 285–291. ISSN: 1476-4687. DOI: 10.1038/nature19057. PMID: 27535533.

[44] Ashburner, M. et al. "Gene ontology: tool for the unification of biology. The Gene Ontology Consortium." *Nature genetics* **25**, (1 May 2000), pp. 25–29. ISSN: 1061-4036. DOI: 10.1038/75556. PMID: 10802651.

[45] Consortium, G. O. "Gene Ontology Consortium: going forward." *Nucleic acids research* **43**, (Database issue Jan. 2015), pp. D1049–D1056. ISSN: 1362-4962. DOI: 10.1093/nar/gku1179. PMID: 25428369.

[46] Subramanian, A. et al. "Gene set enrichment analysis: a knowledge-based approach for interpreting genome-wide expression profiles." *Proceedings of the National Academy of Sciences of the United States of America* **102**, (43 Oct. 2005), pp. 15545–15550. ISSN: 0027-8424. DOI: 10.1073/pnas.0506580102. PMID: 16199517.

[47] Turley, P. et al. "Multi-trait analysis of genome-wide association summary statistics using MTAG". *Nature Genetics* **50**, (2018), pp. 229–237. DOI: 10.1038/s41588-017-0009-4. PMID: 29292387.

[48] Wray, N. R. et al. "Genome-wide association analyses identify 44 risk variants and refine the genetic architecture of major depressive disorder". *Nature Genetics* (2018). DOI: 10.1038/s41588-018-0090-3. PMID: 29700475. eprint: https://www.nature.com/articles/s41588-018-0090-3.

[49] Hyde, C. L. et al. "Identification of 15 genetic loci associated with risk of major depression in individuals of European descent." *Nature genetics* **48**, (9 Sept. 2016), pp. 1031–1036. ISSN: 1546-1718. DOI: 10.1038/ng.3623. PMID: 27479909.

[50] Okbay, A. et al. "Genome-wide association study identifies 74 loci associated with educational attainment." *Nature* **533**, (7604 May 2016), pp. 539–542. ISSN: 1476-4687. DOI: 10.1038/nature17671. PMID: 27225129.

[51] MacArthur, J. et al. "The new NHGRI-EBI Catalog of published genome-wide association studies (GWAS Catalog)." *Nucleic acids research* **45**, (D1 Jan. 2017), pp. D896–D901. ISSN: 1362-4962. DOI: 10.1093/nar/gkw1133. PMID: 27899670.

[52] Kent, W. J. et al. "The human genome browser at UCSC." *Genome research* **12**, (6 June 2002), pp. 996–1006. ISSN: 1088-9051. DOI: 10.1101/gr.229102.Articlepublishedonlinebeforeprintin May2002. PMID: 12045153.

[53] Lee, S. H., Wray, N. R., Goddard, M. E., and Visscher, P. M. "Estimating missing heritability for disease from genome-wide association studies." eng. *Am J Hum Genet* **88**,3 (Mar. 2011), pp. 294–305. DOI: 10.1016/j.ajhg.2011.02.002. PMID: 21376301.

[54] Yang, J. et al. "Common SNPs explain a large proportion of the heritability for human height." eng. *Nat Genet* **42**,7 (July 2010), pp. 565–569. DOI: 10.1038/ng.608. PMID: 20562875.

[55] Yang, J., Lee, S. H., Goddard, M. E., and Visscher, P. M. "GCTA: a tool for genome-wide complex trait analysis." eng. *Am J Hum Genet* **88**,1 (Jan. 2011), pp. 76–82. DOI: 10.1016/j.ajhg.2010.11.011. PMID: 21167468.

[56] Consortium, I. H. 3. et al. "Integrating common and rare genetic variation in diverse human populations." *Nature* **467**, (7311 Sept. 2010), pp. 52–58. ISSN: 1476-4687. DOI: 10.1038/nature09298. PMID: 20811451.

[57] Hansen, S. N., Overgaard, M., Andersen, P. K., and Parner, E. T. "Estimating a population cumulative incidence under calendar time trends." *BMC medical research methodology* **17**, (1 Jan. 2017), p. 7. ISSN: 1471-2288. DOI: 10.1186/s12874-016-0280-6. PMID: 28077076.

[58] Finucane, H. K. et al. "Partitioning heritability by functional annotation using genome-wide association summary statistics". *Nature Genetics* **47**, (2015), pp. 1228–1235. DOI: 10.1038/ng.3404. PMID: 26414678.

[59] Ernst, J. and Kellis, M. "Large-scale imputation of epigenomic datasets for systematic annotation of diverse human tissues." *Nature biotechnology* **33**, (4 Apr. 2015), pp. 364–376. ISSN: 1546-1696. DOI: 10.1038/nbt.3157. PMID: 25690853.

[60] Consortium, R. E. et al. "Integrative analysis of 111 reference human epigenomes." *Nature* **518**, (7539 Feb. 2015), pp. 317–330. ISSN: 1476-4687. DOI: 10.1038/nature14248. PMID: 25693563.

[61] Zheng, J. et al. "LD Hub: a centralized database and web interface to perform LD score regression that maximizes the potential of summary level GWAS data for SNP heritability and genetic correlation analysis." *Bioinformatics* **33**, (2 Jan. 2017), pp. 272–279. ISSN: 1367-4811. DOI: 10.1093/bioinformatics/btw613. PMID: 27663502.

[62] Okbay, A. et al. "Genetic variants associated with subjective well-being, depressive symptoms, and neuroticism identified through genome-wide analyses." *Nature genetics* **48**, (6 June 2016), pp. 624–633. ISSN: 1546-1718. DOI: 10.1038/ng.3552. PMID: 27089181.

[63] Jones, S. E. et al. "Genome-Wide Association Analyses in 128,266 Individuals Identifies New Morningness and Sleep Duration Loci." *PLoS genetics* **12**, (8 Aug. 2016), e1006125. ISSN: 1553-7404. DOI: 10.1371/journal.pgen.1006125. PMID: 27494321.

[64] Neale, B. M. et al. "Meta-analysis of genome-wide association studies of attention-deficit/hyperactivity disorder." *Journal of the American Academy of Child and Adolescent Psychiatry* **49**, (9 Sept. 2010), pp. 884–897. ISSN: 1527-5418. DOI: 10.1016/j.jaac.2010.06.008. PMID: 20732625.

[65] Major Depressive Disorder Working Group of the Psychiatric GWAS Consortium et al. "A mega-analysis of genome-wide association studies for major depressive disorder." *Molecular psychiatry* **18**, (4 Apr. 2013), pp. 497–511. ISSN: 1476-5578. DOI: 10.1038/mp.2012.21. PMID: 22472876.

[66] Moor, M. H. M. de et al. "Meta-analysis of genome-wide association studies for personality." *Molecular psychiatry* **17**, (3 Mar. 2012), pp. 337–349. ISSN: 1476-5578. DOI: 10.1038/mp.2010.128. PMID: 21173776.

[67] Rietveld, C. A. et al. "Common genetic variants associated with cognitive performance identified using the proxy-phenotype method." eng. *PNAS* **111**,38 (Sept. 2014), pp. 13790–13794. DOI: 10.1073/pnas.1404623111. PMID: 25201988.

[68] Won, H. et al. "Chromosome conformation elucidates regulatory relationships in developing human brain." *Nature* **538**, (7626 Oct. 2016), pp. 523–527. ISSN: 1476-4687. DOI: 10.1038/nature19847. PMID: 27760116.

[69] Hormozdiari, F. et al. "Identifying causal variants at loci with multiple signals of association." *Genetics* **198**, (2 Oct. 2014), pp. 497–508. ISSN: 1943-2631. DOI: 10.1534/genetics.114.167908. PMID: 25104515.

[70] McLean, C. Y. et al. "GREAT improves functional interpretation of cis-regulatory regions." *Nature biotechnology* **28**, (5 May 2010), pp. 495–501. ISSN: 1546-1696. DOI: 10.1038/nbt.1630. PMID: 20436461.

[71] Kang, H. J. et al. "Spatio-temporal transcriptome of the human brain." *Nature* **478**, (7370 Oct. 2011), pp. 483–489. ISSN: 1476-4687. DOI: 10.1038/nature10523. PMID: 22031440.

[72] Funatsu, N. et al. "Characterization of a novel rat brain glycosylphosphatidylinositol-anchored protein (Kilon), a member of the IgLON cell adhesion molecule family." *The Journal of biological chemistry* **274**, (12 Mar. 1999), pp. 8224–8230. ISSN: 0021-9258. PMID: 10075727.

[73] Marg, A. et al. "Neurotractin, a novel neurite outgrowth-promoting Ig-like protein that interacts with CEPU-1 and LAMP." *The Journal of cell biology* **145**, (4 May 1999), pp. 865–876. ISSN: 0021-9525. PMID: 10330412.

[74] Pischedda, F. et al. "A cell surface biotinylation assay to reveal membrane-associated neuronal cues: Negr1 regulates dendritic arborization." *Molecular & cellular proteomics : MCP* **13**, (3 Mar. 2014), pp. 733–748. ISSN: 1535-9484. DOI: 10.1074/mcp.M113.031716. PMID: 24382801.

[75] Hashimoto, T. et al. "IgLON cell adhesion molecule Kilon is a crucial modulator for synapse number in hippocampal neurons." *Brain research* **1224**, (Aug. 2008), pp. 1–11. ISSN: 0006-8993. DOI: 10.1016/j.brainres.2008.05.069. PMID: 18602091.

[76] Boender, A. J., Rozen, A. J. van, and Adan, R. A. H. "Nutritional state affects the expression of the obesity-associated genes Etv5, Faim2, Fto, and Negr1." *Obesity (Silver Spring, Md.)* **20**, (12 Dec. 2012), pp. 2420–2425. ISSN: 1930-739X. DOI: 10.1038/oby.2012.128. PMID: 22627920.

[77] Kim, H. et al. "The new obesity-associated protein, neuronal growth regulator 1 (NEGR1), is implicated in Niemann-Pick disease Type C (NPC2)-mediated cholesterol trafficking." *Biochemical and biophysical research communications* **482**, (4 Jan. 2017), pp. 1367–1374. ISSN: 1090-2104. DOI: 10.1016/j.bbrc.2016.12.043. PMID: 27940359.

[78] Miyata, S. et al. "Biochemical and ultrastructural analyses of IgLON cell adhesion molecules, Kilon and OBCAM in the rat brain." *Neuroscience* **117**, (3 2003), pp. 645–658. ISSN: 0306-4522. PMID: 12617969.

[79] Schäfer, M. et al. "Neurotractin/kilon promotes neurite outgrowth and is expressed on reactive astrocytes after entorhinal cortex lesion." *Molecular and cellular neurosciences* **29**, (4 Aug. 2005), pp. 580–590. ISSN: 1044-7431. DOI: 10.1016/j.mcn.2005.04.010. PMID: 15946856.

[80] Lee, A. W. S. et al. "Functional inactivation of the genome-wide association study obesity gene neuronal growth regulator 1 in mice causes a body mass phenotype." *PloS one* **7**, (7 2012), e41537. ISSN: 1932-6203. DOI: 10.1371/journal.pone.0041537. PMID: 22844493.

[81] Genovese, A., Cox, D. M., and Butler, M. G. "Partial Deletion of Chromosome 1p31.1 Including only the Neuronal Growth Regulator 1 Gene in Two Siblings." *Journal of pediatric genetics* **4**, (1 Mar. 2015), pp. 23–28. ISSN: 2146-4596. DOI: 10.1055/s-0035-1554977. PMID: 27617112.

[82] Goes, F. S. et al. "Genome-wide association study of schizophrenia in Ashkenazi Jews." *American journal of medical genetics. Part B* **168**, (8 Dec. 2015), pp. 649–659. ISSN: 1552-485X. DOI: 10.1002/ajmg.b.32349. PMID: 26198764.

[83] Sniekers, S. et al. "Genome-wide association meta-analysis of 78,308 individuals identifies new loci and genes influencing human intelligence." *Nature genetics* **49**, (May 2017), pp. 1546–1718. DOI: 10.1038/ng.3869. PMID: 28530673. (Visited on 05/22/2017).

[84] Vuong, J. K. et al. "PTBP1 and PTBP2 Serve Both Specific and Redundant Functions in Neuronal Pre-mRNA Splicing." *Cell reports* **17**, (10 Dec. 2016), pp. 2766–2775. ISSN: 2211-1247. DOI: 10.1016/j.celrep.2016.11.034. PMID: 27926877.

[85] Boutz, P. L. et al. "A post-transcriptional regulatory switch in polypyrimidine tract-binding proteins reprograms alternative splicing in developing neurons." *Genes & development* **21**, (13 July 2007), pp. 1636–1652. ISSN: 0890-9369. DOI: 10.1101/gad.1558107. PMID: 17606642.

[86] Makeyev, E. V., Zhang, J., Carrasco, M. A., and Maniatis, T. "The MicroRNA miR-124 promotes neuronal differentiation by triggering brain-specific alternative pre-mRNA splicing." *Molecular cell* **27**, (3 Aug. 2007), pp. 435–448. ISSN: 1097-2765. DOI: 10.1016/j.molcel.2007.07.015. PMID: 17679093.

[87] Spellman, R., Llorian, M., and Smith, C. W. J. "Crossregulation and functional redundancy between the splicing regulator PTB and its paralogs nPTB and ROD1." *Molecular cell* **27**, (3 Aug. 2007), pp. 420–434. ISSN: 1097-2765. DOI: 10.1016/j.molcel.2007.06.016. PMID: 17679092.

[88] Zheng, S. et al. "PSD-95 is post-transcriptionally repressed during early neural development by PTBP1 and PTBP2." *Nature neuroscience* **15**, (3 Jan. 2012), 381–8, S1. ISSN: 1546-1726. DOI: 10.1038/nn.3026. PMID: 22246437.

[89] Polydorides, A. D. et al. "A brain-enriched polypyrimidine tract-binding protein antagonizes the ability of Nova to regulate neuron-specific alternative splicing." *Proceedings of the National Academy of Sciences of the United States of America* **97**, (12 June 2000), pp. 6350–6355. ISSN: 0027-8424. DOI: 10.1073/pnas.110128397. PMID: 10829067.

[90] Romanelli, M. G., Lorenzi, P., and Morandi, C. "Identification and analysis of the human neural polypyrimidine tract binding protein (nPTB) gene promoter region." *Gene* **356**, (Aug. 2005), pp. 11–18. ISSN: 0378-1119. DOI: 10.1016/j.gene.2005.04.031. PMID: 16002244.

[91] Rahman, L., Bliskovski, V., Reinhold, W., and Zajac-Kaye, M. "Alternative splicing of brain-specific PTB defines a tissue-specific isoform pattern that predicts distinct functional roles." *Genomics* **80**, (3 Sept. 2002), pp. 245–249. ISSN: 0888-7543. PMID: 12213192.

[92] Ni, J. Z. et al. "Ultraconserved elements are associated with homeostatic control of splicing regulators by alternative splicing and nonsense-mediated decay." *Genes & development* **21**, (6 Mar. 2007), pp. 708–718. ISSN: 0890-9369. DOI: 10.1101/gad.1525507. PMID: 17369403.

[93] Wollerton, M. C. et al. "Autoregulation of polypyrimidine tract binding protein by alternative splicing leading to nonsense-mediated decay." *Molecular cell* **13**, (1 Jan. 2004), pp. 91–100. ISSN: 1097-2765. PMID: 14731397.

[94] Carter, M. T. et al. "Hemizygous deletions on chromosome 1p21.3 involving the DPYD gene in individuals with autism spectrum disorder." *Clinical genetics* **80**, (5 Nov. 2011), pp. 435–443. ISSN: 1399-0004. DOI: 10.1111/j.1399-0004.2010.01578.x. PMID: 21114665.

[95] Willemsen, M. H. et al. "Chromosome 1p21.3 microdeletions comprising DPYD and MIR137 are associated with intellectual disability." *Journal of medical genetics* **48**, (12 Dec. 2011), pp. 810–818. ISSN: 1468-6244. DOI: 10.1136/jmedgenet-2011-100294. PMID: 22003227.

[96] Doan, R. N. et al. "Mutations in Human Accelerated Regions Disrupt Cognition and Social Behavior." *Cell* **167**, (2 Oct. 2016), 341–354.e12. ISSN: 1097-4172. DOI: 10.1016/j.cell.2016.08.071. PMID: 27667684.

[97] De Rubeis, S. et al. "Synaptic, transcriptional and chromatin genes disrupted in autism." *Nature* **515**, (7526 Nov. 2014), pp. 209–215. ISSN: 1476-4687. DOI: 10.1038/nature13772. PMID: 25363760.

[98] Iossifov, I. et al. "The contribution of de novo coding mutations to autism spectrum disorder." eng. *Nature* **515**,7526 (Nov. 2014), pp. 216–221. DOI: 10.1038/nature13908. PMID: 25363768.

[99] Petrie, M. et al. "The Vesicle Priming Factor CAPS Functions as a Homodimer via C2 Domain Interactions to Promote Regulated Vesicle Exocytosis." *The Journal of biological chemistry* **291**, (40 Sept. 2016), pp. 21257–21270. ISSN: 1083-351X. DOI: 10.1074/jbc.M116.728097. PMID: 27528604.

[100] Wassenberg, J. J. and Martin, T. F. J. "Role of CAPS in dense-core vesicle exocytosis." *Annals of the New York Academy of Sciences* **971**, (Oct. 2002), pp. 201–209. ISSN: 0077-8923. PMID: 12438120.

[101] Hoz, A. B. de la et al. "3p14 De Novo Interstitial Microdeletion in a Patient with Intellectual Disability and Autistic Features with Language Impairment: A Comparison with Similar Cases." *Case reports in genetics* **2015**, (2015), p. 876348. ISSN: 2090-6544. DOI: 10.1155/2015/876348. PMID: 26075115.

[102] Sadakata, T. et al. "Autistic-like phenotypes in Cadps2-knockout mice and aberrant CADPS2 splicing in autistic patients." *The Journal of clinical investigation* **117**, (4 Apr. 2007), pp. 931–943. ISSN: 0021-9738. DOI: 10.1172/JCI29031. PMID: 17380209.

[103] Li, Q. S. et al. "Variations in the FRA10AC1 Fragile Site and 15q21 Are Associated with Cerebrospinal Fluid Aβ1-42 Level." *PloS one* **10**, (8 2015), e0134000. ISSN: 1932-6203. DOI: 10.1371/journal.pone.0134000. PMID: 26252872.

[104] Levkowitz, G. et al. "Zinc finger protein too few controls the development of monoaminergic neurons." *Nature neuroscience* **6**, (1 Jan. 2003), pp. 28–33. ISSN: 1097-6256. DOI: 10.1038/nn979. PMID: 12469125.

[105] Yang, N., Dong, Z., and Guo, S. "Fezf2 regulates multilineage neuronal differentiation through activating basic helix-loop-helix and homeodomain genes in the zebrafish ventral forebrain." *The Journal of neuroscience : the official journal of the Society for Neuroscience* **32**, (32 Aug. 2012), pp. 10940–10948. ISSN: 1529-2401. DOI: 10.1523/JNEUROSCI.2216-12.2012. PMID: 22875928.

[106] Chen, B., Schaevitz, L. R., and McConnell, S. K. "Fezl regulates the differentiation and axon targeting of layer 5 subcortical projection neurons in cerebral cortex." *Proceedings of the National Academy of Sciences of the United States of America* **102**, (47 Nov. 2005), pp. 17184–17189. ISSN: 0027-8424. DOI: 10.1073/pnas.0508732102. PMID: 16284245.

[107] Takaba, H. et al. "Fezf2 Orchestrates a Thymic Program of Self-Antigen Expression for Immune Tolerance." *Cell* **163**, (4 Nov. 2015), pp. 975–987. ISSN: 1097-4172. DOI: 10.1016/j.cell.2015.10.013. PMID: 26544942.

[108] Inoue, K., Terashima, T., Nishikawa, T., and Takumi, T. "Fez1 is layer-specifically expressed in the adult mouse neocortex." *The European journal of neuroscience* **20**, (11 Dec. 2004), pp. 2909–2916. ISSN: 0953-816X. DOI: 10.1111/j.1460-9568.2004.03763.x. PMID: 15579145.

[109] Wang, K. et al. "Common genetic variants on 5p14.1 associate with autism spectrum disorders." eng. *Nature* **459**,7246 (May 2009), pp. 528–533. DOI: 10.1038/nature07999. PMID: 19404256.

[110] Sanders, S. J. et al. "De novo mutations revealed by whole-exome sequencing are strongly associated with autism." *Nature* **485**, (7397 Apr. 2012), pp. 237–241. ISSN: 1476-4687. DOI: 10.1038/nature10945. PMID: 22495306.

[111] Chen, L. et al. "Genomic selection identifies vertebrate transcription factor Fezf2 binding sites and target genes." *The Journal of biological chemistry* **286**, (21 May 2011), pp. 18641–18649. ISSN: 1083-351X. DOI: 10.1074/jbc.M111.236471. PMID: 21471212.

[112] Baala, L. et al. "Homozygous silencing of T-box transcription factor EOMES leads to microcephaly with polymicrogyria and corpus callosum agenesis." *Nature genetics* **39**, (4 Apr. 2007), pp. 454–456. ISSN: 1061-4036. DOI: 10.1038/ng1993. PMID: 17353897.

[113] Seth, A. et al. "belladonna/(Ihx2) is required for neural patterning and midline axon guidance in the zebrafish forebrain." *Development (Cambridge, England)* **133**, (4 Feb. 2006), pp. 725–735. ISSN: 0950-1991. DOI: 10.1242/dev.02244. PMID: 16436624.

[114] Shim, S. et al. "Cis-regulatory control of corticospinal system development and evolution." *Nature* **486**, (7401 May 2012), pp. 74–79. ISSN: 1476-4687. DOI: 10.1038/nature11094. PMID: 22678282.

[115] Kwan, K. Y. "Transcriptional dysregulation of neocortical circuit assembly in ASD." *International review of neurobiology* **113**, (2013), pp. 167–205. ISSN: 2162-5514. DOI: 10.1016/B978-0-12-418700-9.00006-X. PMID: 24290386.

[116] Urade, T. et al. "Identification and characterization of TMEM33 as a reticulon-binding protein." *The Kobe journal of medical sciences* **60**, (3 Nov. 2014), E57–E65. ISSN: 1883-0498. PMID: 25612671.

[117] Sakabe, I. et al. "TMEM33: a new stress-inducible endoplasmic reticulum transmembrane protein and modulator of the unfolded protein response signaling." *Breast cancer research and treatment* **153**, (2 Sept. 2015), pp. 285–297. ISSN: 1573-7217. DOI: 10.1007/s10549-015-3536-7. PMID: 26268696.

[118] Chapman, D. C., Stocki, P., and Williams, D. B. "Cyclophilin C Participates in the US2-Mediated Degradation of Major Histocompatibility Complex Class I Molecules." *PloS one* **10**, (12 2015), e0145458. ISSN: 1932-6203. DOI: 10.1371/journal.pone.0145458. PMID: 26691022.

[119] Ma, D. et al. "Whole exome sequencing identified genetic variations in Chinese hemangioblastoma patients." *American journal of medical genetics. Part A* **173**, (10 Oct. 2017), pp. 2605–2613. ISSN: 1552-4833. DOI: 10.1002/ajmg.a.38350. PMID: 28742274.

[120] Chen, Y.-H., Kim, J. H., and Stallcup, M. R. "GAC63, a GRIP1-dependent nuclear receptor coactivator." *Molecular and cellular biology* **25**, (14 July 2005), pp. 5965–5972. ISSN: 0270-7306. DOI: 10.1128/MCB.25.14.5965-5972.2005. PMID: 15988012.

[121] Chen, Y.-H. et al. "Role of GAC63 in transcriptional activation mediated by beta-catenin." *Nucleic acids research* **35**, (6 2007), pp. 2084–2092. ISSN: 1362-4962. DOI: 10.1093/nar/gkm095. PMID: 17344318.

[122] Perez, Y. et al. "SLC30A9 mutation affecting intracellular zinc homeostasis causes a novel cerebro-renal syndrome." *Brain : a journal of neurology* **140**, (4 Apr. 2017), pp. 928–939. ISSN: 1460-2156. DOI: 10.1093/brain/awx013. PMID: 28334855.

[123] Arora, M. et al. "Fetal and postnatal metal dysregulation in autism." *Nature communications* **8**, (June 2017), p. 15493. ISSN: 2041-1723. DOI: 10.1038/ncomms15493. PMID: 28569757.

[124] Sanders, S. J. et al. "Multiple recurrent de novo CNVs, including duplications of the 7q11.23 Williams syndrome region, are strongly associated with autism." *Neuron* **70**, (5 June 2011), pp. 863–885. ISSN: 1097-4199. DOI: 10.1016/j.neuron.2011.05.002. PMID: 21658581.

[125] Abdelraheim, S. R., Spiller, D. G., and McLennan, A. G. "Mammalian NADH diphosphatases of the Nudix family: cloning and characterization of the human peroxisomal NUDT12 protein." *The Biochemical journal* **374**, (Pt 2 Sept. 2003), pp. 329–335. ISSN: 1470-8728. DOI: 10.1042/BJ20030441. PMID: 12790796.

[126] Lin, M. T. et al. "SK2 channel plasticity contributes to LTP at Schaffer collateral-CA1 synapses." *Nature neuroscience* **11**, (2 Feb. 2008), pp. 170–177. ISSN: 1097-6256. DOI: 10.1038/nn2041. PMID: 18204442.

[127] Hammond, R. S. et al. "Small-conductance Ca2+-activated K+ channel type 2 (SK2) modulates hippocampal learning, memory, and synaptic plasticity." *The Journal of neuroscience : the official journal of the Society for Neuroscience* **26**, (6 Feb. 2006), pp. 1844–1853. ISSN: 1529-2401. DOI: 10.1523/JNEUROSCI.4106-05.2006. PMID: 16467533.

[128] Murthy, S. R. K. et al. "Small-conductance Ca2+-activated potassium type 2 channels regulate the formation of contextual fear memory." *PloS one* **10**, (5 2015), e0127264. ISSN: 1932-6203. DOI: 10.1371/journal.pone.0127264. PMID: 25938421.

[129] Fakira, A. K. et al. "Increased small conductance calcium-activated potassium type 2 channel-mediated negative feedback on N-methyl-D-aspartate receptors impairs synaptic plasticity following context-dependent sensitization to morphine." *Biological psychiatry* **75**, (2 Jan. 2014), pp. 105–114. ISSN: 1873-2402. DOI: 10.1016/j.biopsych.2013.04.026. PMID: 23735878.

[130] Sun, J. et al. "UBE3A Regulates Synaptic Plasticity and Learning and Memory by Controlling SK2 Channel Endocytosis." *Cell reports* **12**, (3 July 2015), pp. 449–461. ISSN: 2211-1247. DOI: 10.1016/j.celrep.2015.06.023. PMID: 26166566.

[131] Willis, M. et al. "Small-conductance calcium-activated potassium type 2 channels (SK2, KCa2.2) in human brain." *Brain structure & function* **222**, (2 Mar. 2017), pp. 973–979. ISSN: 1863-2661. DOI: 10.1007/s00429-016-1258-1. PMID: 27357310.

[132] Duro, E. et al. "Identification of the MMS22L-TONSL complex that promotes homologous recombination." *Molecular cell* **40**, (4 Nov. 2010), pp. 632–644. ISSN: 1097-4164. DOI: 10.1016/j.molcel.2010.10.023. PMID: 21055984.

[133] O'Donnell, L. et al. "The MMS22L-TONSL complex mediates recovery from replication stress and homologous recombination." *Molecular cell* **40**, (4 Nov. 2010), pp. 619–631. ISSN: 1097-4164. DOI: 10.1016/j.molcel.2010.10.024. PMID: 21055983.

[134] Campos, E. I. et al. "Analysis of the Histone H3.1 Interactome: A Suitable Chaperone for the Right Event." *Molecular cell* **60**, (4 Nov. 2015), pp. 697–709. ISSN: 1097-4164. DOI: 10.1016/j.molcel.2015.08.005. PMID: 26527279.

[135] Saredi, G. et al. "H4K20me0 marks post-replicative chromatin and recruits the TONSL–MMS22L DNA repair complex." *Nature* **534**, (7609 June 2016), pp. 714–718. ISSN: 1476-4687. DOI: 10.1038/nature18312. PMID: 27338793.

[136] Piwko, W. et al. "The MMS22L-TONSL heterodimer directly promotes RAD51-dependent recombination upon replication stress." *The EMBO journal* **35**, (23 Dec. 2016), pp. 2584–2601. ISSN: 1460-2075. DOI: 10.15252/embj.201593132. PMID: 27797818.

[137] Nguyen, M.-H., Ueda, K., Nakamura, Y., and Daigo, Y. "Identification of a novel oncogene, MMS22L, involved in lung and esophageal carcinogenesis." *International journal of oncology* **41**, (4 Oct. 2012), pp. 1285–1296. ISSN: 1791-2423. DOI: 10.3892/ijo.2012.1589. PMID: 22895565.

[138] Savci-Heijink, C. D., Halfwerk, H., Koster, J., and Vijver, M. J. van de. "A novel gene expression signature for bone metastasis in breast carcinomas." *Breast cancer research and treatment* **156**, (2 Apr. 2016), pp. 249–259. ISSN: 1573-7217. DOI: 10.1007/s10549-016-3741-z. PMID: 26965286.

[139] Mühleisen, T. W. et al. "Genome-wide association study reveals two new risk loci for bipolar disorder." *Nature communications* **5**, (Mar. 2014), p. 3339. ISSN: 2041-1723. DOI: 10.1038/ncomms4339. PMID: 24618891.

[140] Hou, L. et al. "Genome-wide association study of 40,000 individuals identifies two novel loci associated with bipolar disorder." *Human molecular genetics* **25**, (15 Aug. 2016), pp. 3383–3394. ISSN: 1460-2083. DOI: 10.1093/hmg/ddw181. PMID: 27329760.

[141] Davies, G. et al. "Genetic contributions to variation in general cognitive function: a meta-analysis of genome-wide association studies in the CHARGE consortium (N=53949)." *Molecular psychiatry* **20**, (2 Feb. 2015), pp. 183–192. ISSN: 1476-5578. DOI: 10.1038/mp.2014.188. PMID: 25644384.

[142] Rietveld, C. A. et al. "GWAS of 126,559 individuals identifies genetic variants associated with educational attainment." *Science (New York, N.Y.)* **340**, (6139 June 2013), pp. 1467–1471. ISSN: 1095-9203. DOI: 10.1126/science.1235488. PMID: 23722424.

[143] Davies, G. et al. "Genome-wide association study of cognitive functions and educational attainment in UK Biobank (N=112,151)." *Molecular psychiatry* **21**, (6 June 2016), pp. 758–767. ISSN: 1476-5578. DOI: 10.1038/mp.2016.45. PMID: 27046643.

[144] Zhao, F.-Q. "Octamer-binding transcription factors: genomics and functions." *Frontiers in bioscience (Landmark edition)* **18**, (June 2013), pp. 1051–1071. ISSN: 1093-4715. PMID: 23747866.

[145] Nakai, S. et al. "The POU domain transcription factor Brn-2 is required for the determination of specific neuronal lineages in the hypothalamus of the mouse." *Genes & development* **9**, (24 Dec. 1995), pp. 3109–3121. ISSN: 0890-9369. PMID: 8543155.

[146] McEvilly, R. J. et al. "Transcriptional regulation of cortical neuron migration by POU domain factors." *Science (New York, N.Y.)* **295**, (5559 Feb. 2002), pp. 1528–1532. ISSN: 1095-9203. DOI: 10.1126/science.1067132. PMID: 11859196.

[147] Sugitani, Y. et al. "Brn-1 and Brn-2 share crucial roles in the production and positioning of mouse neocortical neurons." *Genes & development* **16**, (14 July 2002), pp. 1760–1765. ISSN: 0890-9369. DOI: 10.1101/gad.978002. PMID: 12130536.

[148] Kasher, P. R. et al. "Small 6q16.1 Deletions Encompassing POU3F2 Cause Susceptibility to Obesity and Variable Developmental Delay with Intellectual Disability." *American journal of human genetics* **98**, (2 Feb. 2016), pp. 363–372. ISSN: 1537-6605. DOI: 10.1016/j.ajhg.2015.12.014. PMID: 26833329.

[149] He, X. et al. "Expression of a large family of POU-domain regulatory genes in mammalian brain development." *Nature* **340**, (6228 July 1989), pp. 35–41. ISSN: 0028-0836. DOI: 10.1038/340035a0. PMID: 2739723.

[150] Strunk, D., Weber, P., Röthlisberger, B., and Filges, I. "Autism and intellectual disability in a patient with two microdeletions in 6q16: a contiguous gene deletion syndrome?" *Molecular cytogenetics* **9**, (2016), p. 88. ISSN: 1755-8166. DOI: 10.1186/s13039-016-0299-8. PMID: 27980676.

[151] Belinson, H. et al. "Prenatal β-catenin/Brn2/Tbr2 transcriptional cascade regulates adult social and stereotypic behaviors." *Molecular psychiatry* **21**, (10 Oct. 2016), pp. 1417–1433. ISSN: 1476-5578. DOI: 10.1038/mp.2015.207. PMID: 26830142.

[152] Nasu, M. et al. "Mammalian-specific sequences in pou3f2 contribute to maternal behavior." *Genome biology and evolution* **6**, (5 Apr. 2014), pp. 1145–1156. ISSN: 1759-6653. DOI: 10.1093/gbe/evu072. PMID: 24709564.

[153] Hashizume, K., Yamanaka, M., and Ueda, S. "POU3F2 participates in cognitive function and adult hippocampal neurogenesis via mammalian-characteristic amino acid repeats." *Genes, brain, and behavior* (Aug. 2017). ISSN: 1601-183X. DOI: 10.1111/gbb.12408. PMID: 28782255.

[154] Simmons, J. L., Pierce, C. J., Al-Ejeh, F., and Boyle, G. M. "MITF and BRN2 contribute to metastatic growth after dissemination of melanoma." *Scientific reports* **7**, (1 Sept. 2017), p. 10909. ISSN: 2045-2322. DOI: 10.1038/s41598-017-11366-y. PMID: 28883623.

[155] Mas-Y-Mas, S. et al. "The Human Mixed Lineage Leukemia 5 (MLL5), a Sequentially and Structurally Divergent SET Domain-Containing Protein with No Intrinsic Catalytic Activity." *PloS one* **11**, (11 2016), e0165139. ISSN: 1932-6203. DOI: 10.1371/journal.pone.0165139. PMID: 27812132.

[156] Sun, X.-J. et al. "Genome-wide survey and developmental expression mapping of zebrafish SET domain-containing genes." *PloS one* **3**, (1 Jan. 2008), e1499. ISSN: 1932-6203. DOI: 10.1371/journal.pone.0001499. PMID: 18231586.

[157] Ali, M. et al. "Molecular basis for chromatin binding and regulation of MLL5." *Proceedings of the National Academy of Sciences of the United States of America* **110**, (28 July 2013), pp. 11296–11301. ISSN: 1091-6490. DOI: 10.1073/pnas.1310156110. PMID: 23798402.

[158] Lemak, A. et al. "Solution NMR structure and histone binding of the PHD domain of human MLL5." *PloS one* **8**, (10 2013), e77020. ISSN: 1932-6203. DOI: 10.1371/journal.pone.0077020. PMID: 24130829.

[159] Zhang, X., Novera, W., Zhang, Y., and Deng, L.-W. "MLL5 (KMT2E): structure, function, and clinical relevance." *Cellular and molecular life sciences : CMLS* **74**, (13 July 2017), pp. 2333–2344. ISSN: 1420-9071. DOI: 10.1007/s00018-017-2470-8. PMID: 28188343.

[160] Wang, T. et al. "De novo genic mutations among a Chinese autism spectrum disorder cohort." *Nature communications* **7**, (Nov. 2016), p. 13316. ISSN: 2041-1723. DOI: 10.1038/ncomms13316. PMID: 27824329.

[161] Iossifov, I. et al. "De novo gene disruptions in children on the autistic spectrum." *Neuron* **74**, (2 Apr. 2012), pp. 285–299. ISSN: 1097-4199. DOI: 10.1016/j.neuron.2012.04.009. PMID: 22542183.

[162] Dong, S. et al. "De novo insertions and deletions of predominantly paternal origin are associated with autism spectrum disorder." *Cell reports* **9**, (1 Oct. 2014), pp. 16–23. ISSN: 2211-1247. DOI: 10.1016/j.celrep.2014.08.068. PMID: 25284784.

[163] Gui, J. F., Lane, W. S., and Fu, X. D. "A serine kinase regulates intracellular localization of splicing factors in the cell cycle." *Nature* **369**, (6482 June 1994), pp. 678–682. ISSN: 0028-0836. DOI: 10.1038/369678a0. PMID: 8208298.

[164] Wang, H. Y. et al. "SRPK2: a differentially expressed SR protein-specific kinase involved in mediating the interaction and localization of pre-mRNA splicing factors in mammalian cells." *The Journal of cell biology* **140**, (4 Feb. 1998), pp. 737–750. ISSN: 0021-9525. PMID: 9472028.

[165] Hong, Y. et al. "SRPK2 phosphorylates tau and mediates the cognitive defects in Alzheimerś disease." *The Journal of neuroscience : the official journal of the Society for Neuroscience* **32**, (48 Nov. 2012), pp. 17262–17272. ISSN: 1529-2401. DOI: 10.1523/JNEUROSCI.3300-12.2012. PMID: 23197718.

[166] Jang, S.-W. et al. "Interaction of Akt-phosphorylated SRPK2 with 14-3-3 mediates cell cycle and cell death in neurons." *The Journal of biological chemistry* **284**, (36 Sept. 2009), pp. 24512–24525. ISSN: 0021-9258. DOI: 10.1074/jbc.M109.026237. PMID: 19592491.

[167] Lo, M.-T. et al. "Genome-wide analyses for personality traits identify six genomic loci and show correlations with psychiatric disorders." *Nature genetics* **49**, (1 Jan. 2017), pp. 152–156. ISSN: 1546-1718. DOI: 10.1038/ng.3736. PMID: 27918536.

[168] Takash, W. et al. "SOX7 transcription factor: sequence, chromosomal localisation, expression, transactivation and interference with Wnt signalling." *Nucleic acids research* **29**, (21 Nov. 2001), pp. 4274–4283. ISSN: 1362-4962. PMID: 11691915.

[169] Wat, J. J. and Wat, M. J. "Sox7 in vascular development: review, insights and potential mechanisms." *The International journal of developmental biology* **58**, (1 2014), pp. 1–8. ISSN: 1696-3547. DOI: 10.1387/ijdb.130323mw. PMID: 24860989.

[170] Artus, J., Piliszek, A., and Hadjantonakis, A.-K. "The primitive endoderm lineage of the mouse blastocyst: sequential transcription factor activation and regulation of differentiation by Sox17." *Developmental biology* **350**, (2 Feb. 2011), pp. 393–404. ISSN: 1095-564X. DOI: 10.1016/j.ydbio.2010.12.007. PMID: 21146513.

[171] Kinoshita, M., Shimosato, D., Yamane, M., and Niwa, H. "Sox7 is dispensable for primitive endoderm differentiation from mouse ES cells." *BMC developmental biology* **15**, (Oct. 2015), p. 37. ISSN: 1471-213X. DOI: 10.1186/s12861-015-0079-4. PMID: 26475439.

[172] Cuvertino, S., Lacaud, G., and Kouskoff, V. "SOX7-enforced expression promotes the expansion of adult blood progenitors and blocks B-cell development." *Open biology* **6**, (7 July 2016). ISSN: 2046-2441. DOI: 10.1098/rsob.160070. PMID: 27411892.

[173] Stovall, D. B., Cao, P., and Sui, G. "SOX7: from a developmental regulator to an emerging tumor suppressor." *Histology and histopathology* **29**, (4 Apr. 2014), pp. 439–445. ISSN: 1699-5848. DOI: 10.14670/HH-29.10.439. PMID: 24288056.

[174] Li, N. et al. "PinX1 is recruited to the mitotic chromosome periphery by Nucleolin and facilitates chromosome congression." *Biochemical and biophysical research communications* **384**, (1 June 2009), pp. 76–81. ISSN: 1090-2104. DOI: 10.1016/j.bbrc.2009.04.077. PMID: 19393617.

[175] Yuan, K. et al. "PinX1 is a novel microtubule-binding protein essential for accurate chromosome segregation." *The Journal of biological chemistry* **284**, (34 Aug. 2009), pp. 23072–23082. ISSN: 1083-351X. DOI: 10.1074/jbc.M109.001990. PMID: 19553660.

[176] Yoo, J. E., Oh, B.-K., and Park, Y. N. "Human PinX1 mediates TRF1 accumulation in nucleolus and enhances TRF1 binding to telomeres." *Journal of molecular biology* **388**, (5 May 2009), pp. 928–940. ISSN: 1089-8638. DOI: 10.1016/j.jmb.2009.02.051. PMID: 19265708.

[177] Zuo, J. et al. "Expression and mechanism of PinX1 and telomerase activity in the carcinogenesis of esophageal epithelial cells." *Oncology reports* **30**, (4 Oct. 2013), pp. 1823–1831. ISSN: 1791-2431. DOI: 10.3892/or.2013.2649. PMID: 23912465.

[178] Liao, C. et al. "Over-expression of LPTS-L in hepatocellular carcinoma cell line SMMC-7721 induces crisis." *World journal of gastroenterology* **8**, (6 Dec. 2002), pp. 1050–1052. ISSN: 1007-9327. PMID: 12439923.

[179] Zhou, X. Z. et al. "The telomerase inhibitor PinX1 is a major haploinsufficient tumor suppressor essential for chromosome stability in mice." *The Journal of clinical investigation* **121**, (4 Apr. 2011), pp. 1266–1282. ISSN: 1558-8238. DOI: 10.1172/JCI43452. PMID: 21436583.

[180] Liao, C. et al. "Identification of the gene for a novel liver-related putative tumor suppressor at a high-frequency loss of heterozygosity region of chromosome 8p23 in human hepatocellular carcinoma." *Hepatology (Baltimore, Md.)* **32**, (4 Pt 1 Oct. 2000), pp. 721–727. ISSN: 0270-9139. DOI: 10.1053/jhep.2000.17967. PMID: 11003615.

[181] Zhou, X. Z. and Lu, K. P. "The Pin2/TRF1-interacting protein PinX1 is a potent telomerase inhibitor." *Cell* **107**, (3 Nov. 2001), pp. 347–359. ISSN: 0092-8674. PMID: 11701125.

[182] Li, H.-L. et al. "PinX1: structure, regulation and its functions in cancer." *Oncotarget* **7**, (40 Oct. 2016), pp. 66267–66275. ISSN: 1949-2553. DOI: 10.18632/oncotarget.11411. PMID: 27556185.

[183] Pinto, D. et al. "Functional impact of global rare copy number variation in autism spectrum disorders." *Nature* **466**, (7304 July 2010), pp. 368–372. ISSN: 1476-4687. DOI: 10.1038/nature09146. PMID: 20531469.

[184] Lennerz, J. K. et al. "Loss of Par-1a/MARK3/C-TAK1 kinase leads to reduced adiposity, resistance to hepatic steatosis, and defective gluconeogenesis." *Molecular and cellular biology* **30**, (21 Nov. 2010), pp. 5043–5056. ISSN: 1098-5549. DOI: 10.1128/MCB.01472-09. PMID: 20733003.

[185] Kwan, J. et al. "DLG5 connects cell polarity and Hippo signaling protein networks by linking PAR-1 with MST1/2." *Genes & development* **30**, (24 Dec. 2016), pp. 2696–2709. ISSN: 1549-5477. DOI: 10.1101/gad.284539.116. PMID: 28087714.

[186] Wang, C. et al. "Upregulation of Mark3 and Rpgrip1 mRNA expression by jujuboside A in mouse hippocampus." *Acta pharmacologica Sinica* **28**, (3 Mar. 2007), pp. 334–338. ISSN: 1671-4083. DOI: 10.1111/j.1745-7254.2007.00497.x. PMID: 17302994.

[187] Saadat, I. et al. "Helicobacter pylori CagA targets PAR1/MARK kinase to disrupt epithelial cell polarity." *Nature* **447**, (7142 May 2007), pp. 330–333. ISSN: 1476-4687. DOI: 10.1038/nature05765. PMID: 17507984.

[188] Styrkarsdottir, U. et al. "New sequence variants associated with bone mineral density." *Nature genetics* **41**, (1 Jan. 2009), pp. 15–17. ISSN: 1546-1718. DOI: 10.1038/ng.284. PMID: 19079262.

[189] Calabrese, G. M. et al. "Integrating GWAS and Co-expression Network Data Identifies Bone Mineral Density Genes SPTBN1 and MARK3 and an Osteoblast Functional Module." *Cell systems* **4**, (1 Jan. 2017), 46–59.e4. ISSN: 2405-4712. DOI: 10.1016/j.cels.2016.10.014. PMID: 27866947.

[190] Maussion, G. et al. "Convergent evidence identifying MAP/microtubule affinity-regulating kinase 1 (MARK1) as a susceptibility gene for autism." *Human molecular genetics* **17**, (16 Aug. 2008), pp. 2541–2551. ISSN: 1460-2083. DOI: 10.1093/hmg/ddn154. PMID: 18492799.

[191] Wallimann, T. et al. "Intracellular compartmentation, structure and function of creatine kinase isoenzymes in tissues with high and fluctuating energy demands: the phosphocreatine circuit for cellular energy homeostasis." *The Biochemical journal* **281 (Pt 1)**, (Jan. 1992), pp. 21–40. ISSN: 0264-6021. PMID: 1731757.

[192] Wallimann, T. et al. "Some new aspects of creatine kinase (CK): compartmentation, structure, function and regulation for cellular and mitochondrial bioenergetics and physiology." *BioFactors (Oxford, England)* **8**, (3-4 1998), pp. 229–234. ISSN: 0951-6433. PMID: 9914824.

[193] Inoue, K., Yamada, J., Ueno, S., and Fukuda, A. "Brain-type creatine kinase activates neuron-specific K+-Cl- co-transporter KCC2." *Journal of neurochemistry* **96**, (2 Jan. 2006), pp. 598–608. ISSN: 0022-3042. DOI: 10.1111/j.1471-4159.2005.03560.x. PMID: 16336223.

[194] Fons, C. and Campistol, J. "Creatine Defects and Central Nervous System." *Seminars in pediatric neurology* **23**, (4 Nov. 2016), pp. 285–289. ISSN: 1558-0776. DOI: 10.1016/j.spen.2016.11.003. PMID: 28284390.

[195] Lv, M.-N. et al. "The neonatal levels of TSB, NSE and CK-BB in autism spectrum disorder from Southern China." *Translational neuroscience* **7**, (1 2016), pp. 6–11. ISSN: 2081-3856. DOI: 10.1515/tnsci-2016-0002. PMID: 28123815.

[196] Lin, Y.-S. et al. "Enhancement of brain-type creatine kinase activity ameliorates neuronal deficits in Huntingtoń disease." *Biochimica et biophysica acta* **1832**, (6 June 2013), pp. 742–753. ISSN: 0006-3002. DOI: 10.1016/j.bbadis.2013.02.006. PMID: 23416527.

[197] Martins-de-Souza, D. et al. "Prefrontal cortex shotgun proteome analysis reveals altered calcium homeostasis and immune system imbalance in schizophrenia." *European archives of psychiatry and clinical neuroscience* **259**, (3 Apr. 2009), pp. 151–163. ISSN: 1433-8491. DOI: 10.1007/s00406-008-0847-2. PMID: 19165527.

[198] Kim, H.-J. et al. "Roles of interferon-gamma and its target genes in schizophrenia: Proteomics-based reverse genetics from mouse to human." *Proteomics* **12**, (11 June 2012), pp. 1815–1829. ISSN: 1615-9861. DOI: 10.1002/pmic.201100184. PMID: 22623148.

[199] Miyake, K. et al. "Comparison of Genomic and Epigenomic Expression in Monozygotic Twins Discordant for Rett Syndrome." *PloS one* **8**, (6 2013), e66729. ISSN: 1932-6203. DOI: 10.1371/journal.pone.0066729. PMID: 23805272.

[200] Chujo, T. and Suzuki, T. "Trmt61B is a methyltransferase responsible for 1-methyladenosine at position 58 of human mitochondrial tRNAs." *RNA (New York, N.Y.)* **18**, (12 Dec. 2012), pp. 2269–2276. ISSN: 1469-9001. DOI: 10.1261/rna.035600.112. PMID: 23097428.

[201] Briknarová, K. et al. "BAG4/SODD protein contains a short BAG domain." *The Journal of biological chemistry* **277**, (34 Aug. 2002), pp. 31172–31178. ISSN: 0021-9258. DOI: 10.1074/jbc.M202792200. PMID: 12058034.

[202] Arakawa, A. et al. "The C-terminal BAG domain of BAG5 induces conformational changes of the Hsp70 nucleotide-binding domain for ADP-ATP exchange." *Structure (London, England : 1993)* **18**, (3 Mar. 2010), pp. 309–319. ISSN: 1878-4186. DOI: 10.1016/j.str.2010.01.004. PMID: 20223214.

[203] Gupta, M. K. et al. "GRP78 Interacting Partner Bag5 Responds to ER Stress and Protects Cardiomyocytes From ER Stress-Induced Apoptosis." *Journal of cellular biochemistry* **117**, (8 Aug. 2016), pp. 1813–1821. ISSN: 1097-4644. DOI: 10.1002/jcb.25481. PMID: 26729625.

[204] Kalia, S. K. et al. "BAG5 inhibits parkin and enhances dopaminergic neuron degeneration." *Neuron* **44**, (6 Dec. 2004), pp. 931–945. ISSN: 0896-6273. DOI: 10.1016/j.neuron.2004.11.026. PMID: 15603737.

[205] Wang, X. et al. "[Direct interaction between BAG5 protein and Parkin protein]." *Zhong nan da xue xue bao. Yi xue ban = Journal of Central South University. Medical sciences* **35**, (11 Nov. 2010), pp. 1156–1161. ISSN: 1672-7347. DOI: 10.3969/j.issn.1672-7347.2010.11.007. PMID: 21131737.

[206] Qin, L.-X. et al. "BAG5 Interacts with DJ-1 and Inhibits the Neuroprotective Effects of DJ-1 to Combat Mitochondrial Oxidative Damage." *Oxidative medicine and cellular longevity* **2017**, (2017), p. 5094934. ISSN: 1942-0994. DOI: 10.1155/2017/5094934. PMID: 28348719.

[207] Wang, X. et al. "BAG5 protects against mitochondrial oxidative damage through regulating PINK1 degradation." *PloS one* **9**, (1 2014), e86276. ISSN: 1932-6203. DOI: 10.1371/journal.pone.0086276. PMID: 24475098.

[208] Guo, K. et al. "Bag5 protects neuronal cells from amyloid β-induced cell death." *Journal of molecular neuroscience : MN* **55**, (4 Apr. 2015), pp. 815–820. ISSN: 1559-1166. DOI: 10.1007/s12031-014-0433-1. PMID: 25367796.

[209] Che, X.-Q. et al. "The BAG2 and BAG5 proteins inhibit the ubiquitination of pathogenic ataxin3-80Q." *The International journal of neuroscience* **125**, (5 May 2015), pp. 390–394. ISSN: 1563-5279. DOI: 10.3109/00207454.2014.940585. PMID: 25006867.

[210] Melchionda, L. et al. "Mutations in APOPT1, encoding a mitochondrial protein, cause cavitating leukoencephalopathy with cytochrome c oxidase deficiency." *American journal of human genetics* **95**, (3 Sept. 2014), pp. 315–325. ISSN: 1537-6605. DOI: 10.1016/j.ajhg.2014.08.003. PMID: 25175347.

[211] Takata, A., Matsumoto, N., and Kato, T. "Genome-wide identification of splicing QTLs in the human brain and their enrichment among schizophrenia-associated loci." *Nature communications* **8**, (Feb. 2017), p. 14519. ISSN: 2041-1723. DOI: 10.1038/ncomms14519. PMID: 28240266.

[212] Pernigo, S., Lamprecht, A., Steiner, R. A., and Dodding, M. P. "Structural basis for kinesin-1:cargo recognition." *Science (New York, N.Y.)* **340**, (6130 Apr. 2013), pp. 356–359. ISSN: 1095-9203. DOI: 10.1126/science.1234264. PMID: 23519214.

[213] Fu, M.-m. and Holzbaur, E. L. F. "Integrated regulation of motor-driven organelle transport by scaffolding proteins." *Trends in cell biology* **24**, (10 Oct. 2014), pp. 564–574. ISSN: 1879-3088. DOI: 10.1016/j.tcb.2014.05.002. PMID: 24953741.

[214] Traina, G., Federighi, G., and Brunelli, M. "Up-regulation of kinesin light-chain 1 gene expression by acetyl-L-carnitine: therapeutic possibility in Alzheimer's disease." *Neurochemistry international* **53**, (6-8 Dec. 2008), pp. 244–247. ISSN: 0197-0186. DOI: 10.1016/j.neuint.2008.08.001. PMID: 18761385.

[215] Sisodia, S. S. "Biomedicine. A cargo receptor mystery APParently solved?" *Science (New York, N.Y.)* **295**, (5556 Feb. 2002), pp. 805–807. ISSN: 1095-9203. DOI: 10.1126/science.1069661. PMID: 11823626.

[216] Jiang, M. et al. "Microtubule motors transport phagosomes in the RPE, and lack of KLC1 leads to AMD-like pathogenesis." *The Journal of cell biology* **210**, (4 Aug. 2015), pp. 595–611. ISSN: 1540-8140. DOI: 10.1083/jcb.201410112. PMID: 26261180.

[217] Wu, M. et al. "The link between apolipoprotein E, presenilin 1, and kinesin light chain 1 gene polymorphisms and age-related cortical cataracts in the Chinese population." *Molecular vision* **21**, (2015), pp. 412–416. ISSN: 1090-0535. PMID: 25883527.

[218] Liu, N. et al. "XRCC2 and XRCC3, new human Rad51-family members, promote chromosome stability and protect against DNA cross-links and other damages." *Molecular cell* **1**, (6 May 1998), pp. 783–793. ISSN: 1097-2765. PMID: 9660962.

[219] Masson, J. Y. et al. "Identification and purification of two distinct complexes containing the five RAD51 paralogs." *Genes & development* **15**, (24 Dec. 2001), pp. 3296–3307. ISSN: 0890-9369. DOI: 10.1101/gad.947001. PMID: 11751635.

[220] Pierce, A. J., Johnson, R. D., Thompson, L. H., and Jasin, M. "XRCC3 promotes homology-directed repair of DNA damage in mammalian cells." *Genes & development* **13**, (20 Oct. 1999), pp. 2633–2638. ISSN: 0890-9369. PMID: 10541549.

[221] Brenneman, M. A. et al. "XRCC3 controls the fidelity of homologous recombination: roles for XRCC3 in late stages of recombination." *Molecular cell* **10**, (2 Aug. 2002), pp. 387–395. ISSN: 1097-2765. PMID: 12191483.

[222] Wang, Z. and Zhang, W. "Association between XRCC3 Thr241Met polymorphism and colorectal cancer risk." *Tumour biology : the journal of the International Society for Oncodevelopmental Biology and Medicine* **34**, (3 June 2013), pp. 1421–1429. ISSN: 1423-0380. DOI: 10.1007/s13277-012-0639-1. PMID: 23504553.

[223] Feijs, K. L. H., Forst, A. H., Verheugd, P., and Lüscher, B. "Macrodomain-containing proteins: regulating new intracellular functions of mono(ADP-ribosyl)ation." *Nature reviews. Molecular cell biology* **14**, (7 July 2013), pp. 443–451. ISSN: 1471-0080. DOI: 10.1038/nrm3601. PMID: 23736681.

[224] Maas, N. M. C. et al. "The C20orf133 gene is disrupted in a patient with Kabuki syndrome." *Journal of medical genetics* **44**, (9 Sept. 2007), pp. 562–569. ISSN: 1468-6244. DOI: 10.1136/jmg.2007.049510. PMID: 17586838.

[225] Vermeesch, J. R. et al. "The causality of de novo copy number variants is overestimated." *European journal of human genetics : EJHG* **19**, (11 Nov. 2011), pp. 1112–1113. ISSN: 1476-5438. DOI: 10.1038/ejhg.2011.83. PMID: 21587321.

[226] West, S., Gromak, N., and Proudfoot, N. J. "Human 5'–> 3' exonuclease Xrn2 promotes transcription termination at co-transcriptional cleavage sites." *Nature* **432**, (7016 Nov. 2004), pp. 522–525. ISSN: 1476-4687. DOI: 10.1038/nature03035. PMID: 15565158.

[227] Kinjo, E. R. et al. "A possible new mechanism for the control of miRNA expression in neurons." *Experimental neurology* **248**, (Oct. 2013), pp. 546–558. ISSN: 1090-2430. DOI: 10.1016/j.expneurol.2013.07.022. PMID: 23933240.

[228] Oshimori, N., Ohsugi, M., and Yamamoto, T. "The Plk1 target Kizuna stabilizes mitotic centrosomes to ensure spindle bipolarity." *Nature cell biology* **8**, (10 Oct. 2006), pp. 1095–1101. ISSN: 1465-7392. DOI: 10.1038/ncb1474. PMID: 16980960.

[229] Manoli, M. and Driever, W. "nkx2.1 and nkx2.4 genes function partially redundant during development of the zebrafish hypothalamus, preoptic region, and pallidum." *Frontiers in neuroanatomy* **8**, (2014), p. 145. ISSN: 1662-5129. DOI: 10.3389/fnana.2014.00145. PMID: 25520628.

[230] Kale, T., Patil, R., and Pandit, R. "A Newborn with Panhypopituitarism and Seizures." *Case reports in genetics* **2017**, (2017), p. 4364216. ISSN: 2090-6544. DOI: 10.1155/2017/4364216. PMID: 28255477.

[231] Daughters, K., Manstead, A. S. R., and Rees, D. A. "Hypopituitarism is associated with lower oxytocin concentrations and reduced empathic ability." *Endocrine* **57**, (1 July 2017), pp. 166–174. ISSN: 1559-0100. DOI: 10.1007/s12020-017-1332-3. PMID: 28597171.

[232] Briscoe, J. et al. "Homeobox gene Nkx2.2 and specification of neuronal identity by graded Sonic hedgehog signalling." *Nature* **398**, (6728 Apr. 1999), pp. 622–627. ISSN: 0028-0836. DOI: 10.1038/19315. PMID: 10217145.

[233] Prakash, N. et al. "A Wnt1-regulated genetic network controls the identity and fate of midbrain-dopaminergic progenitors in vivo." *Development (Cambridge, England)* **133**, (1 Jan. 2006), pp. 89–98. ISSN: 0950-1991. DOI: 10.1242/dev.02181. PMID: 16339193.

[234] Sanders, S. J. et al. "Insights into Autism Spectrum Disorder Genomic Architecture and Biology from 71 Risk Loci". *Neuron* **87**,6 (2015), pp. 1215–1233. DOI: 10.1016/j.neuron.2015.09.016. PMID: 26402605.

[235] SPARK Consortium. "SPARK: A US Cohort of 50,000 Families to Accelerate Autism Research." *Neuron* **97**, (3 Feb. 2018), pp. 488–493. ISSN: 1097-4199. DOI: 10.1016/j.neuron.2018.01.015. PMID: 29420931.

[236] Locke, A. E. et al. "Genetic studies of body mass index yield new insights for obesity biology." eng. *Nature* **518**,7538 (Feb. 2015), pp. 197–206. DOI: 10.1038/nature14177. PMID: 25673413.

Part II

Supplementary Information

Supplementary tables

List of Supplementary Tables

3.1 Sample description

Supplementary Table 1: Descriptive statistics of key characteristics for the iPSYCH ASD GWAS sample. Top part shows the data flow from ascertainment in the registers, identification in the biobank and extraction and amplification of DNA, exclusion of related individuals to the final study sample consisting of individuals of European ancestry. Percents are relative to the register sample for the column. Everything below the line in the middle relates to the study sample of European ancestry.
† Median and IQR.
§ The last of the hierarchical subtypes consists of those with a diagnosis of 'other pervasive devopmental disorder' or 'pervasive developmental disorder, unspecified' without any of the preceding subtype diagnoses. See table 13 for the definitions of the hierarchical subtypes.

Characteristics	Ctrl		ASD		CHA		ATA		Asp		OPDD		PDDU	
Register sample	29659		17763		4892		2276		5910		2660		5097	
Ident and WGAed	28316	(95.5%)	15744	(88.6%)	4324	(88.4%)	1995	(87.7%)	5270	(89.2%)	2394	(90.0%)	4522	(88.7%)
Gtyped and QCed	26005	(87.7%)	14970	(84.3%)	4060	(83.0%)	1889	(83.0%)	5049	(85.4%)	2286	(85.9%)	4306	(84.5%)
$\hat{\pi} \leq 0.2$	25205	(85.0%)	14337	(80.7%)	3850	(78.7%)	1800	(79.1%)	4848	(82.0%)	2194	(82.5%)	4141	(81.2%)
Eur ancestry	22664	(76.4%)	13076	(73.6%)	3310	(67.7%)	1607	(70.6%)	4622	(78.2%)	2042	(76.8%)	3753	(73.6%)
Birth years														
1981–1985	3782	(16.7%)	725	(5.5%)	97	(2.9%)	70	(4.4%)	382	(8.3%)	132	(6.5%)	158	(4.2%)
1986–1990	4775	(21.1%)	1764	(13.5%)	241	(7.3%)	194	(12.1%)	865	(18.7%)	321	(15.7%)	430	(11.5%)
1991–1995	5199	(22.9%)	3714	(28.4%)	762	(23.0%)	507	(31.5%)	1464	(31.7%)	640	(31.3%)	983	(26.2%)
1996–2000	5090	(22.5%)	4278	(32.7%)	1169	(35.3%)	544	(33.9%)	1367	(29.6%)	648	(31.7%)	1289	(34.3%)
2001–2005	3818	(16.8%)	2595	(19.8%)	1041	(31.5%)	292	(18.2%)	544	(11.8%)	301	(14.7%)	893	(23.8%)
Females	11168	(49.3%)	2820	(21.6%)	630	(19.0%)	407	(25.3%)	924	(20.0%)	463	(22.7%)	869	(23.2%)
ID (IQ<70)	109	(0.5%)	1873	(14.3%)	955	(28.9%)	460	(28.6%)	101	(2.2%)	180	(8.8%)	625	(16.7%)
Age at 1st diag†			10	(7 – 14)	7	(5 – 12)	11	(7 – 14)	12	(9 – 15)	11	(8 – 14)	10	(6 – 14)
ASD subtypes:														
Childhod autism			3310	(25.3%)			113	(7.0%)	147	(3.2%)	71	(3.5%)	598	(15.9%)
Atypical autism			1607	(12.3%)	113	(3.4%)			64	(1.4%)	51	(2.5%)	294	(7.8%)
Asperger			4622	(35.3%)	147	(4.4%)	64	(4.0%)			166	(8.1%)	554	(14.8%)
Other pervasive DD			2042	(15.6%)	71	(2.1%)	51	(3.2%)	166	(3.6%)			335	(8.9%)
Pervasive DD, unspec			3753	(28.7%)	598	(18.1%)	294	(18.3%)	554	(12.0%)	335	(16.4%)		
Hierar subtypes§					3310	(100.0%)	1494	(93.0%)	4417	(95.6%)		3855	(70.6%)	

Supplementary Table 2: Key numbers for the follow-up study. First three data rows show sample sizes, and the bottom rows show SNP counts. The numbers for the iPSYCH-PGC meta analysis and the numbers of SNPs (index SNPs, proxy SNPs and total) are displayed in the first data column. The subsequent columns provide the numbers SNPs that could be matched to index SNPS and to proxies when matching failed for index SNPs. Total SNPs for the replication samples is the total number of SNPs contributing to the analysis directly through index SNPs or via proxies when necessary.

Name	iPSYCH+PGC	BUPGEN	PAGES	Finland	deCODE Iceland	deCODE East Eur	In All Reps
Cases	18,381	164	926	159	574	296	2,119
Controls	27,969	656	3,841	526	136,968	388	142,379
Total	46,350	820	4,767	685	137,542	684	144,498
Index SNPs	88	88	61	82	71	85	45
Proxy SNPs	364	0	0	0	5	0	
Total SNPs	456	88	61	82	76	85	49

3.2 GWAS

3.2.1 The ASD GWAS and follow-up

Supplementary Table 3: Summary of the top 88 ASD associations from the iPSYCH-PGC meta analysis together with follow-up results and results of the combined analysis with the follow-up samples. The columns are a part from the basic identity and location of the loci, the p-values and ORs from the iPSYCH-PGC meta analysis, direction of effect for each follow-up sample (BUPGEN, PAGES, Finland, deCODE Iceland, deCODE East Eur; + for same direction as iPSYCH-PGC, 0 for opposite and ? for not present), p-values and ORs for follow-up together and the combined meta analysis of iPSYCH-PGC and the follow-up samples. All meta-analyses are inverse variance weighted and the p-values derived from z-scores. Loci identified by the MTAG analysis (Table 6) are marked by * (but 3 of the MTAG loci had ASD p-values below the threshold of 10^{-5}).

SNP	CHR	BP	A1A2	MAFCa	MAFCo	P	OR	Dir	P-fup	OR-fup	P-comb	OR-comb
rs910805	20	21,248,116	A/G	0.745	0.760	$2{\cdot}10^{-9}$	0.909	>+00+0<	0.312	1.039	$3{\cdot}10^{-7}$	0.927
rs10099100	8	10,576,775	C/G	0.348	0.331	$1{\cdot}10^{-8}$	1.088	>++++0<	0.310	1.036	$1{\cdot}10^{-8}$	1.080
rs71190156	20	14,836,243	GTTTTTTT/G	0.460	0.481	$3{\cdot}10^{-8}$	0.925	>+++00<	0.362	0.969	$4{\cdot}10^{-8}$	0.931
rs6047270	20	21,122,212	T/C	0.335	0.319	$8{\cdot}10^{-8}$	1.084	>+00+0<	0.983	0.999	$8{\cdot}10^{-7}$	1.071
rs111931861	7	104,744,219	A/G	0.960	0.966	$1{\cdot}10^{-7}$	0.805	>++?++<	0.087	0.802	$3{\cdot}10^{-8}$	0.805
rs2391769	1	96,978,961	A/G	0.348	0.369	$1{\cdot}10^{-7}$	0.926	>+0+++<	0.687	0.986	$5{\cdot}10^{-7}$	0.935
rs138867053	19	37,439,641	A/G	0.021	0.017	$1{\cdot}10^{-7}$	1.331	>0+?+0<	0.652	1.059	$4{\cdot}10^{-7}$	1.285
rs183563276m	8	48,036,474	A/G	0.987	0.989	$2{\cdot}10^{-7}$	0.658	>?0?00<	0.133	1.524	$4{\cdot}10^{-6}$	0.701
rs1452075*	3	62,481,063	T/C	0.738	0.721	$2{\cdot}10^{-7}$	1.084	>0++00<	0.565	1.021	$6{\cdot}10^{-7}$	1.074
rs1222063	1	96,602,440	A/G	0.349	0.332	$3{\cdot}10^{-7}$	1.084	>++0+0<	0.315	1.035	$3{\cdot}10^{-7}$	1.075
rs142920272	17	44,301,840	T/C	0.798	0.813	$3{\cdot}10^{-7}$	0.913	>+0?00<	0.982	1.001	$9{\cdot}10^{-7}$	0.919
rs55962189	20	21,242,161	A/T	0.690	0.706	$3{\cdot}10^{-7}$	0.926	>+00+0<	0.602	1.019	$6{\cdot}10^{-6}$	0.939
rs112635299	14	94,838,142	T/G	0.030	0.025	$3{\cdot}10^{-7}$	1.247	>+0?++<	0.327	1.208	$2{\cdot}10^{-7}$	1.245
rs6701243	1	99,092,784	A/C	0.626	0.609	$3{\cdot}10^{-7}$	1.076	>+++00<	0.644	1.016	$1{\cdot}10^{-6}$	1.067
rs4595836	10	16,691,399	T/C	0.078	0.067	$3{\cdot}10^{-7}$	1.149	>00+++<	0.898	0.991	$3{\cdot}10^{-6}$	1.126
rs325485*	5	103,995,368	A/G	0.396	0.378	$3{\cdot}10^{-7}$	1.076	>0+++0<	0.891	1.005	$2{\cdot}10^{-6}$	1.066
rs201910565	1	96,561,801	A/AT	0.672	0.689	$3{\cdot}10^{-7}$	0.927	>+++00<	0.039	0.930	$4{\cdot}10^{-8}$	0.927
rs210894m	6	11,731,999	T/TA	0.566	0.548	$5{\cdot}10^{-7}$	1.073	>0++0+<	0.251	1.039	$4{\cdot}10^{-7}$	1.068
rs72934503*	6	98,583,488	A/G	0.523	0.537	$6{\cdot}10^{-7}$	0.932	>+?+++<	0.152	0.942	$2{\cdot}10^{-7}$	0.933
rs11185408	1	104,792,257	A/G	0.503	0.523	$7{\cdot}10^{-7}$	0.934	>+?++0<	0.756	0.987	$1{\cdot}10^{-6}$	0.939
rs141455452	17	44,019,083	T/G	0.542	0.525	$9{\cdot}10^{-7}$	1.082	>0+?+0<	0.320	1.048	$6{\cdot}10^{-7}$	1.078
rs78827416	10	72,749,037	A/G	0.093	0.086	$9{\cdot}10^{-7}$	1.139	>++0++<	0.799	0.986	$2{\cdot}10^{-5}$	1.108
rs59566011	2	159,385,181	GA/G	0.586	0.569	$9{\cdot}10^{-7}$	1.073	>0?0++<	0.515	1.028	$1{\cdot}10^{-6}$	1.068
rs10666089m	8	53,341,258	C/CAA	0.733	0.745	$1{\cdot}10^{-6}$	0.919	>+?00+<	0.167	1.062	$5{\cdot}10^{-5}$	0.937
rs147317628	17	44,277,476	CTTTAG/C	0.212	0.195	$1{\cdot}10^{-6}$	1.087	>++?+0<	0.991	0.999	$3{\cdot}10^{-6}$	1.079
rs292441	18	55,872,558	A/G	0.660	0.676	$1{\cdot}10^{-6}$	0.930	>+0+00<	0.616	0.982	$3{\cdot}10^{-6}$	0.937
chr5:168173526	5	168,173,526	A/G	0.020	0.016	$1{\cdot}10^{-6}$	1.342	>++?0+<	0.065	1.286	$2{\cdot}10^{-7}$	1.332
rs4750990	10	130,488,026	T/C	0.591	0.603	$1{\cdot}10^{-6}$	0.934	>00000<	0.168	1.048	$9{\cdot}10^{-5}$	0.950
rs117603308m	11	106,827,977	T/C	0.030	0.026	$1{\cdot}10^{-6}$	1.270	>+0?0?<	0.901	0.984	$9{\cdot}10^{-6}$	1.229
rs34938366	16	72,097,255	C/CA	0.179	0.168	$2{\cdot}10^{-6}$	1.109	>0+0+0<	0.717	1.014	$1{\cdot}10^{-5}$	1.086
rs35404050	12	73,196,902	T/C	0.210	0.195	$2{\cdot}10^{-6}$	1.088	>++000<	0.902	0.995	$1{\cdot}10^{-5}$	1.073
rs11480060	20	54,230,218	C/CA	0.712	0.727	$2{\cdot}10^{-6}$	0.927	>+?000<	0.489	1.032	$2{\cdot}10^{-5}$	0.937
rs740883	6	29,575,405	A/T	0.902	0.912	$2{\cdot}10^{-6}$	0.893	>0+?++<	0.386	0.937	$1{\cdot}10^{-6}$	0.896
rs16879023	6	16,753,147	A/G	0.136	0.148	$2{\cdot}10^{-6}$	0.909	>+0+0+<	0.900	1.006	$2{\cdot}10^{-5}$	0.923
rs141319505	10	65,421,442	A/G	0.983	0.980	$2{\cdot}10^{-6}$	1.337	>0+?++<	0.937	1.016	$4{\cdot}10^{-6}$	1.308
rs77691144	13	66,970,212	T/C	0.969	0.975	$2{\cdot}10^{-6}$	0.813	>++?+?<	0.152	0.795	$6{\cdot}10^{-7}$	0.811
rs4916723	5	87,854,395	A/C	0.560	0.572	$2{\cdot}10^{-6}$	0.935	>0+++++<	0.506	0.978	$3{\cdot}10^{-6}$	0.941
rs2635182	5	92,255,166	T/C	0.485	0.466	$2{\cdot}10^{-6}$	1.069	>++++++<	0.102	1.057	$5{\cdot}10^{-7}$	1.067
rs10110094	8	131,472,047	A/G	0.171	0.163	$2{\cdot}10^{-6}$	1.095	>0++0+<	0.154	1.068	$8{\cdot}10^{-7}$	1.091
rs12942300	17	43,859,405	A/T	0.158	0.171	$2{\cdot}10^{-6}$	0.915	>++?++<	0.478	0.958	$2{\cdot}10^{-6}$	0.918
rs78058104	15	93,953,737	A/G	0.035	0.030	$2{\cdot}10^{-6}$	1.207	>00?0+<	0.106	0.790	$3{\cdot}10^{-5}$	1.172
chr7:105064665	7	105,064,665	T/TCCCTCCCTCTCT+6	0.263	0.250	$2{\cdot}10^{-6}$	1.081	>??0++<	0.590	1.028	$3{\cdot}10^{-6}$	1.076
rs28729902	9	76,179,384	A/G	0.803	0.814	$2{\cdot}10^{-6}$	0.920	>++000<	0.242	1.048	$1{\cdot}10^{-4}$	0.940
rs144911765	21	37,255,329	T/C	0.966	0.971	$2{\cdot}10^{-6}$	0.827	>+0?+0<	0.729	1.044	$1{\cdot}10^{-5}$	0.845
rs11787216*	8	142,615,222	T/C	0.347	0.364	$3{\cdot}10^{-6}$	0.933	>00+++<	0.482	0.976	$4{\cdot}10^{-6}$	0.940
rs33966416	4	171,206,603	C/CA	0.456	0.470	$3{\cdot}10^{-6}$	0.937	>0?00+<	0.197	1.058	$5{\cdot}10^{-5}$	0.947
rs200332011	3	158,001,670	CT/C	0.219	0.231	$3{\cdot}10^{-6}$	0.922	>0?+00<	0.715	0.982	$6{\cdot}10^{-6}$	0.928
rs7000276	8	10,804,843	A/G	0.408	0.392	$3{\cdot}10^{-6}$	1.068	>+00+0<	0.726	0.989	$3{\cdot}10^{-5}$	1.055
rs13188074	5	113,801,423	A/G	0.408	0.391	$3{\cdot}10^{-6}$	1.068	>++++++<	0.246	1.041	$2{\cdot}10^{-6}$	1.064
rs9389208	6	135,035,609	T/C	0.374	0.359	$3{\cdot}10^{-6}$	1.070	>+00+0<	0.323	0.967	$9{\cdot}10^{-5}$	1.053
rs6692705	1	193,502,609	A/G	0.413	0.400	$3{\cdot}10^{-6}$	1.068	>++0+++<	0.118	1.053	$1{\cdot}10^{-6}$	1.066
rs76397219	8	60,390,318	A/G	0.926	0.933	$4{\cdot}10^{-6}$	0.869	>0+?00<	0.859	1.017	$1{\cdot}10^{-5}$	0.882
chr11:102751102	11	102,751,102	C/<CN0>	0.955	0.963	$4{\cdot}10^{-6}$	0.851	>+??00<	0.823	1.036	$8{\cdot}10^{-6}$	0.859
chr7:71618506	7	71,618,506	T/TA	0.365	0.381	$4{\cdot}10^{-6}$	0.934	>0?00+<	0.751	1.014	$2{\cdot}10^{-5}$	0.942
rs79940520	3	191,838,169	A/G	0.847	0.859	$4{\cdot}10^{-6}$	0.909	>+0+00<	0.664	0.977	$9{\cdot}10^{-6}$	0.918
rs201369005m	14	76,835,623	G/GT	0.057	0.051	$4{\cdot}10^{-6}$	1.169	>0?+0+<	0.913	1.012	$9{\cdot}10^{-6}$	1.155
rs78653484	1	147,183,927	T/C	0.032	0.039	$5{\cdot}10^{-6}$	0.838	>++?+0<	0.807	0.974	$1{\cdot}10^{-5}$	0.853
rs12203328	6	23,767,038	C/G	0.291	0.278	$5{\cdot}10^{-6}$	1.072	>+++0+<	0.170	1.052	$2{\cdot}10^{-6}$	1.069
rs116977567	20	54,184,200	T/G	0.970	0.974	$5{\cdot}10^{-6}$	0.822	>00?00<	0.029	1.334	$3{\cdot}10^{-4}$	0.861
rs529507	11	131,773,383	A/G	0.840	0.848	$6{\cdot}10^{-6}$	0.913	>+0+++<	0.826	0.990	$2{\cdot}10^{-5}$	0.925
rs77810738	19	37,392,818	A/G	0.963	0.968	$6{\cdot}10^{-6}$	0.842	>++?++<	0.289	0.898	$4{\cdot}10^{-6}$	0.849
rs113003385	12	113,568,531	A/G	0.075	0.071	$6{\cdot}10^{-6}$	1.142	>+0+0+<	0.640	1.032	$1{\cdot}10^{-5}$	1.124
rs12449792	17	43,302,259	T/C	0.471	0.459	$6{\cdot}10^{-6}$	1.066	>000+0<	0.111	0.948	$4{\cdot}10^{-4}$	1.047
rs6430841	2	140,318,199	A/G	0.815	0.801	$6{\cdot}10^{-6}$	1.083	>+0++0<	0.537	1.025	$1{\cdot}10^{-5}$	1.073
rs13201465	6	134,234,093	A/G	0.984	0.987	$6{\cdot}10^{-6}$	0.755	>++?0+<	0.897	0.977	$2{\cdot}10^{-5}$	0.775
rs7578456	2	202,235,348	A/G	0.417	0.401	$7{\cdot}10^{-6}$	1.066	>0++00<	0.726	0.988	$6{\cdot}10^{-5}$	1.053
rs34739626	6	23,870,775	T/TA	0.630	0.617	$7{\cdot}10^{-6}$	1.073	>0?++0<	0.515	1.027	$8{\cdot}10^{-6}$	1.067
rs6082289	20	21,019,305	T/C	0.218	0.207	$7{\cdot}10^{-6}$	1.079	>+0000<	0.189	0.948	$3{\cdot}10^{-4}$	1.058

Continues on the next page

Supplementary Table 3 – continued from previous page

SNP	CHR	BP	A1A2	MAFCa	MAFCo	P	OR	Dir	P-fup	OR-fup	P-comb	OR-comb
rs597040	20	3,663,913	C/G	0.019	0.016	$7{\cdot}10^{-6}$	1.294	>++?+0<	0.857	1.029	$2{\cdot}10^{-5}$	1.259
rs148587110	3	20,641,966	T/C	0.986	0.989	$7{\cdot}10^{-6}$	0.719	>0+?0?<	0.062	0.715	$1{\cdot}10^{-6}$	0.718
chr6:96509180	6	96,509,180	D/I	0.657	0.641	$7{\cdot}10^{-6}$	1.078	>+?+0+<	0.446	1.034	$8{\cdot}10^{-6}$	1.072
rs6256326	3	70,608,317	A/G	0.263	0.252	$7{\cdot}10^{-6}$	1.074	>+0++0<	0.528	1.024	$1{\cdot}10^{-5}$	1.066
rs116346488	4	132,217,275	A/G	0.054	0.048	$8{\cdot}10^{-6}$	1.154	>+0?00<	0.890	0.987	$3{\cdot}10^{-5}$	1.136
rs507059	6	23,909,381	A/G	0.170	0.182	$8{\cdot}10^{-6}$	0.917	>00++0<	0.993	1.000	$5{\cdot}10^{-5}$	0.931
rs2282828	6	15,392,310	T/C	0.406	0.419	$8{\cdot}10^{-6}$	0.933	>0?00+<	0.373	1.039	$1{\cdot}10^{-4}$	0.945
rs143609523	18	33,265,230	A/G	0.986	0.988	$8{\cdot}10^{-6}$	0.745	>?+?+?<	0.069	0.692	$1{\cdot}10^{-6}$	0.740
rs56054767m	4	84,621,317	C/CA	0.124	0.113	$9{\cdot}10^{-6}$	1.113	>0?+++<	0.202	1.089	$4{\cdot}10^{-6}$	1.110
rs41363353	2	63,072,403	C/G	0.835	0.848	$9{\cdot}10^{-6}$	0.919	>0+00+<	0.841	0.991	$3{\cdot}10^{-5}$	0.930
rs115833252	1	61,879,203	T/C	0.024	0.019	$9{\cdot}10^{-6}$	1.262	>+0?0?<	0.421	0.860	$5{\cdot}10^{-5}$	1.228
rs78298487	7	132,177,702	T/G	0.980	0.984	$9{\cdot}10^{-6}$	0.775	>+0?0?<	0.837	1.047	$2{\cdot}10^{-5}$	0.789
rs4609618	11	128,818,792	A/C	0.370	0.389	$9{\cdot}10^{-6}$	0.938	>++000<	0.645	1.016	$9{\cdot}10^{-5}$	0.949
rs16933101	12	28,765,600	A/G	0.044	0.051	$9{\cdot}10^{-6}$	0.858	>+0+00<	0.873	0.989	$5{\cdot}10^{-5}$	0.883
rs113764414	10	64,649,396	A/G	0.683	0.672	$9{\cdot}10^{-6}$	1.076	>0++++<	0.016	1.090	$5{\cdot}10^{-7}$	1.078
rs17517971	13	110,828,119	A/G	0.068	0.063	$1{\cdot}10^{-5}$	1.152	>00000<	0.392	0.947	$4{\cdot}10^{-4}$	1.107
rs684502	6	89,896,927	T/G	0.554	0.566	$1{\cdot}10^{-5}$	0.939	>00+00<	0.554	1.020	$1{\cdot}10^{-4}$	0.951
rs34509057	5	153,601,262	A/G	0.238	0.226	$1{\cdot}10^{-5}$	1.076	>++++++<	0.255	1.045	$6{\cdot}10^{-6}$	1.071
rs201179706	10	30,995,488	T/C	0.494	0.508	$1{\cdot}10^{-5}$	0.934	>0?+0+<	0.945	1.003	$3{\cdot}10^{-5}$	0.941
rs71868489	2	171,338,669	C/CT	0.827	0.817	$1{\cdot}10^{-5}$	1.090	>+?0+0<	0.879	1.009	$2{\cdot}10^{-5}$	1.081

Supplementary Table 4: Review of the top loci identified in the single SNP analysis with and without follow-up sample, the three MTAG analyses, and the gene-wise MAGMA analysis (see also main Table 1, Table 3, 10 and Box 1 for further details and explanations of significance tests). Loci are $r^2 = 0.1$ clumps and the genes listed are the protein coding genes in the locus except marked with * (see below) or on chromosome 8 where the locus around rs10099100 was restricted to a $r^2 = 0.6$ clump plus 50kb flanks. See section 2.1.4 for details.
* Nearest protein coding gene within ±1 Mb from locus.
** Results based on samples overlapping the present ASD sample, hence not independent.
† Previous GWS hits for brain disorders in locus.

Chr	Gene	Index SNP (BP)	Analysis P-value	Function	Tissue specificity	Disease	Previous GWS hits in locus†
1	*NEGR1*	rs1620977 (72729142)	MTAG MD: $6.7 \cdot 10^{-9}$	*NEGR1* encodes the Neuronal growth regulator 1, a GPI-anchored IgLON protein belonging to the immunoglobulin superfamily of cell adhesion molecules. *NEGR1* has been identified as a raft-associated component of the brain that is involved in neurite outgrowth[72–74] and neurodevelopmental determination of synapse number in the hippocampus[75]. *NEGR1* expression levels are affected by nutritional state in brain areas relevant to feeding[76] and *NEGR1* may also serve a role in intracellular cholesterol trafficking[77].	NEGR1 is localized at postsynaptic sites of dendritic and somatic synapses[78] and is expressed at high levels during postnatal development in cerebral cortex, hippocampus, cerebellum, and hypothalamus[78–80].	A 1p31.1 deletion including a part of *NEGR1* (and no other genes) has been identified in two siblings with a history of neuropsychiatric and behavioral problems, learning difficulties, hypotonia, mild aortic root dilatation, hypermobility and scoliosis[81].	Meta-analysis of autism spectrum disorder and schizophrenia[24]**, Schizophrenia[82], Educational attainment[50], Depressive symptoms[62], Major depression[48], Intelligence[83]
1	*PTBP2**	rs201910565 (96561801)	Comb: $2.5 \cdot 10^{-8}$	*PTBP2* encodes Polypyrimidine tract-binding protein 2. PTBP2 is a PTBP1 (Polypyrimidine tract-binding protein 1) paralog and is also known as nPTB (neuronal PTB) or brPTB (brain PTB). PTBP1 and PTBP2 binds to intronic polypyrimidine clusters in pre-mRNA molecules and each target large sets of exons to coordinate programs of splicing events during development[84]. During neuronal development and differentiation, several switches in the expression of *PTBP1* and *PTBP2* activates networks of new spliced isoforms[85–88].	*PTBP2* is expressed at high levels in adult brain, testis, myoblasts and lymphocytes[89, 90]. Different isoforms generated by alternative splicing of *PTBP2* are expressed in a tissue specific manner[90, 91]. In neuronal cells, *PTBP2* acts by autoregulating its own exon 10 inclusion, leading to an increased expression level of the PTBP2 protein[92]. PTBP1 promotes the exon 10 exclusion from *PTBP2* transcripts, leading to NMD of *PTBP2* transcripts[93].	Hemizygous deletion of varying genomic regions containing *PTBP2*, *DPYD* and *MIR137* have been reported in cases with ASD, severe speech delay and intellectual disability[94, 95]. Two brothers with ASD and intellectual disability born to consanguineous parents were found to be homozygous for a novel 5 bp indel variant located in a human accelerated region (HAR) between *DPYD* and *PTBP2*[96]. This intergenic indel variant was suggested to affect the PTBP2-directed enhancer activity of the region and that this effect was relatively specific to neurons[96]. Further evidence pointing to *PTBP2* as a ASD risk gene include identification of a *de novo PTBP2* potentially damaging missense variant in an ASD proband[97] as well as identification of a *de novo PTBP2* intronic insertion in a ASD proband from a simplex family[98].	Educational attainment[50]

continues on the next page...

Supplementary Table 4 — continued from the previous page

Chr	Gene	Index SNP (BP)	Analysis P-value	Function	Tissue specificity	Disease	Previous GWS hits in locus[†]
3	*CADPS*	rs1452075 (62481063)	MTAG Edu: $3.2 \cdot 10^{-9}$	*CADPS* encodes the Calcium-dependent secretion activator 1 (CAPS-1). CAPS-1 serves an essential role in the docking and priming of dense core vesicles and synaptic vesicles in endocrine and neural cells, [99] and references herein.	In line with *CADPS* mRNA being mainly expressed in brain and pituitary (https://www.gtexportal.org), immunoreactive CAPS-1 is localized in neural and various endocrine tissues[100].	A *de novo* microdeletion including *CADPS* (and five other genes) has been described in a case with intellectual disability and autistic features with language impairment[101]. The *CADPS2* gene, encoding a CAPS-1 isoform (CAPS-2) of almost identical function is located in the 7q autism susceptibility locus, *AUTS1*. *CADPS2* knockout mice show phenotypes with translational relevance to autism and an aberrant *CADPS2* splice variant have been identified in patients with autism[102].	Cognitive decline rate in late mild cognitive impairment[103]
3	*FEZF2*		Hi-C interaction with *CADPS* locus	*FEZF2* encodes the Fez family zinc finger protein 2 (also known as known as *FEZL* and ZFP312/ZNF312). *FEZF2* is a transcriptional repressor containing 6 highly conserved C2H2 zinc-finger repeats[104]. *FEZF2* is crucial in multilineage differentiation of neurons in zebra fish[104, 105] and it regulates the differentiation of layer-5 subcortical projection neurons in mice[106]. *FEZF2* also play a role in medullary thymic epithelial cells to ensure immunologic tolerance against certain tissue antigens and suppress development of autoimmunity[107].	*FEZF2* seems to be almost exclusively expressed in amygdala, hippocampus and cortex (https://www.gtexportal.org). This is consistent with mouse Fezf2 being selectively expressed in layer V and VI subcortical projection pyramidal neurons and their progenitor cells[108].	*FEZF2* has been associated with ASD in two cohorts of European ancestry[109] and a *FEZF2 de novo* missense variant has been identified in ASD[110]. Eomesa/tbr2 and lhx2b has been identified as target genes of Fezf2[111]. Mutations in *EOMES/TBR2* cause microcephaly in humans[112] and lhx2b is a critical regulator of cell fate and axonal targeting in the developing forebrain[113]. *FEZF2* is regulated by a non-exonic cis-regulatory element (E4) located 7.3 kb downstream of the Fezf2 transcription start site[114]. The potential role of *FEZF2* (and related transcription factors) in autism has is discussed in detail in[115].	
4	*TMEM33*	rs16854048 (42123728)	MTAG MD: $1.3 \cdot 10^{-8}$	*TMEM33* encodes Transmembrane protein 33. TMEM33 is a three transmembrane domain reticulon binding protein localized in the ER membrane[116]. It is likely involved in regulating the ER tubule polygonal network[116]. *TMEM33* is ER stress-inducible in cancer cells and regulates positively two main drivers of the unfolded protein response: PERK and IRE1α[117].	*TMEM33* mRNA is ubiquitously expressed (https://www.gtexportal.org).	*TMEM33* (along with malectin and PDIA6) enhances human cytomegalovirus US2-mediated degradation of Major Histocompatibility Complex Class I molecules[118].	
4	*DCAF4L1*	rs16854048 (42123728)	MTAG MD: $1.3 \cdot 10^{-8}$	*DCAF4L1* encodes the DDB1- and CUL4-associated factor 4-like protein 1. *DCAF4L1* interactions with ubiquitin conjugation pathway proteins CUL4A, COPS5 and COPS6 have been demonstrated experimentally (IntAct database). Otherwise, DCAF4L1is largely uncharacterized.	*DCAF4L1* seems to be exclusively expressed in testis (https://www.gtexportal.org).	Variants in *DCAF4L1* may be involved in hemangioblastomas[119].	

continues on the next page...

Supplementary Table 4 — continued from the previous page

Chr	Gene	Index SNP (BP)	Analysis P-value	Function	Tissue specificity	Disease	Previous GWS hits in locus[†]
4	*SLC30A9*	rs16854048 (42123728)	MTAG MD: $1.3 \cdot 10^{-8}$	*SLC30A9* encodes Zinc transporter 9. *SLC30A9* has been identified as a nuclear receptor coactivator involved in Wnt signaling[120, 121]. A later paper found that SLC30A9 is involved in zinc transport in neuronal cells[122].	*SLC30A9* mRNA is ubiquitously expressed with high levels in fetal brain, cerebellum, skeletal muscle and kidney[122].	A single amino acid deletion (Ala350del) in *SLC30A9* has been associated with early-onset autosomal recessive cerebro-renal syndrome comprising different combinations of profound intellectual disability (very low social and verbal skills), muscle weakness, oculomotor apraxia and early onset nephropathy[122]. In neuronal cell lines, the mutation seems to affect zinc transport and thus, intracellular zinc homeostasis rather than Wnt signaling[122]. It has been shown that autism cases show developmental dysregulation in zinc uptake[123].	
4	*BEND4*	rs16854048 (42123728)	MTAG MD: $1.3 \cdot 10^{-8}$	*BEND4* encodes BEN domain-containing protein 4. *BEND4* is largely uncharacterized.	*BEND4* transcript is mainly expressed in EBV-transformed lymphocytes and testis (https://www.gtexportal.org).	Microduplications in 7q11.23 have been associated with autism in a simplex cohort with a frequency of 0.09% in 3816 ASD probands[124]. Notably, *BEND4* has been identified as a target gene of the key 7q11.23 gene, *GTF2I*[124] and is proposed as one among three genes responsible for mediating the molecular pathogenesis of both 7q-microduplication syndrome and Williams-Beuren syndrome that also comprise ASD features[124]. The evidence has mainly been obtained from patient-derived induced pluripotent stem cells and include BEND4 sensitivity to the dosage of *GTF2I* and its LSD1-mediated repressive activity but also that *BEND4* expression is inversely correlated with the expression of *GTF2I* in human brain[124].	
5	*NUDT12*[*]	rs325506 (104012303)	MTAG MD: $3.3 \cdot 10^{-11}$	*NUDT12* encodes Peroxisomal NADH pyrophosphatase *NUDT12*, a peroxisomal enzymes that hydrolyses NAD(P)H to NMNH and AMP (2',5'-ADP), and diadenosine diphosphate to AMP[125]. *NUDT12* may act to regulate the concentration of peroxisomal nicotinamide nucleotide cofactors required for oxidative metabolism[125]. Besides, *NUDT12* may possess mRNA decapping activity thereby regulating RNA stability and degradation[125].	*NUDT12* is expressed in many tissues with highest levels in adrenal gland, bladder, spinal chord, transformed fibroblasts, tibial nerve and thyroid (https://www.gtexportal.org).		Educational attainment[50]

continues on the next page...

Supplementary Table 4 — continued from the previous page

Chr	Gene	Index SNP (BP)	Analysis P-value	Function	Tissue specificity	Disease	Previous GWS hits in locus[†]
5	*KCNN2*		MAGMA: $1.0 \cdot 10^{-9}$	*KCNN2* encodes Small conductance calcium-activated potassium channel protein 2. *KCNN2* (alternatively SK or KCa2.2) is a voltage-independent Ca2+-activated K+ channel that responds to changes in intracellular calcium concentration and couples calcium metabolism to potassium flux and membrane excitability. In CNS neurons, activation of *KCNN2* modulates neuronal excitability by causing membrane hyperpolarization[126]. Hippocampal *KCNN2* play an important role in the formation of new memory[127], in encoding and consolidation of contextual fear[128] and in drug-induced plasticity[129].	Synaptic levels of *KCNN2* are regulated by the E3 ubiquitin ligase UBE3A[130], whose deficiency results in Angelman syndrome and overexpression in increased risk of ASD, respectively. At least four different isoforms of *KCNN2* are expressed in human brain including the hippocampal formation, amygdala and neocortex[131].		Educational attainment[50].
6	*MMS22L*[*]	rs2388334 (98591622)	MTAG Edu: $3.3 \cdot 10^{-12}$	*MMS22L* encodes Protein MMS22-like. *MMS22L* is part of the TONSL–MMS22L complex implicated in homologous recombination, replication fork recovery, and reading of replication-dependent histone marks[132–136].	*MMS22L* mRNA levels are low in most tissues with highest levels in EBV-transformed lymphocytes and testis (https://www.gtexportal.org).	*MMS22L* might an oncogene involved in lung and esophageal carcinogenesis[137] and it is part of a 15-gene expression signature associated with the development of bone metastases in breast cancer[138].	Bipolar disorder[139, 140], Intelligence[83], Cognitive function[141], Educational attainment [50, 67, 142, 143]
6	*POU3F2*[*]	rs2388334 (98591622)	MTAG Edu: $3.3 \cdot 10^{-12}$	*POU3F2* encodes POU domain, class 3, transcription factor 2 (alternatively Brn-2, Oct-7 and OTF-7). POU3F is a member of the POU-III class of neural octamer-binding transcription factors[144]. In mouse, *POU3F2* is essential for the development of the PVN and SON neuronal lineages in the hypothalamus[145]. *POU3F2* and *POU3F3* are co-expressed in the developing neocortex where they redundantly regulate cortical neuron migration and layer production[146, 147]. *POU3F2* is a downstream target of the SIM1-ARNT2 complex in the leptin-melanocortin-SIM1 pathway playing an important role in regulating expression of oxytocin in the hypothalamus[148].	*POU3F2* seems to be exclusively expressed in brain and tibial nerve with lowest levels in cerebellum (https://www.gtexportal.org). *POU3F2* is further plentifully expressed during all stages of neurogenesis and in distinct neural subsets in the adult central nervous system (although at lower levels), including the PVN and SON of the hypothalamus[149].	Small deletions including *POU3F2* are causing susceptibility to obesity, variable developmental delay with intellectual disability and autism[148, 150]. Heterozygous *POU3F2* knockout mice show deficits in adult social behavior and increased repetitive behavior in the marble burying test combined with embryonic ventricular zone and cortical plate expansion[151]. Deregulation of a β-catenin/*POU3F2*/Tbr2 transcriptional cascade may be responsible for embryonic expansion of basal neural progenitor cells and adult social and repetitive behavioral abnormalities[151]. Homopolymeric amino acid repeat-deleted POU3F2 mice show impairments in maternal behavior and pup recognition, cognitive deficits and impaired adult hippocampal neurogenesis[152, 153]. Besides, *POU3F2* is involved in melanocytic growth, tumorgenesis and metastatic growth after dissemination of melanoma, [154] and references herein.	Bipolar disorder[139, 140], Intelligence[83], Cognitive function[141], Educational attainment [50, 67, 142, 143]

continues on the next page...

Supplementary Table 4 — continued from the previous page

Chr	Gene	Index SNP (BP)	Analysis P-value	Function	Tissue specificity	Disease	Previous GWS hits in locus[†]
7	*KMT2E (MLL5)*	rs111931861 (104744219)	Comb: $3.5 \cdot 10^{-8}$	*KMT2E* (alternatively *MLL5*) encodes Histone-lysine N-methyltransferase 2E. KMT2E was initially categorized into the KMT2 (MLL) family, however phylogenetic analysis has shown that *KMT2E* is distinct from the MLL1-4, SETD1A, and SETD1B group of proteins and forms a family together with another mammalian protein, the SET containing-domain 5 (SETD5)[155, 156]. The molecular function of *KMT2E* is uncertain since it has been suggested that *KMT2E* unlike other KMT2 (MLL) proteins lack intrinsic methyltransferase activity[155]. Several lines of evidence however support that recognition of the histone H3K4me3 mark by the *KMT2E* PHD finger can facilitate the recruitment of *KMT2E* to active transcription chromatin regions[157, 158]. *KMT2E* play important roles in controlling cell cycle progression, maintaining genomic stability, as well as regulating hematopoiesis and spermatogenesis (for review see[159]).	*KMT2E* is expressed in various tissues with highest levels in cerebellum and low levels in other brain regions (https://www.gtexportal.org).	*KMT2E* has been suggested as an ASD risk gene[160]. Evidence include identification of two different *KMT2E de novo* frameshift variants in two unrelated ASD cases[161, 162] and identification of a maternally inherited frameshift variant in a Chinese ASD case[160].	Schizophrenia[8, 82], Meta-analysis of autism spectrum disorder and schizophrenia[24]**
7	*SRPK2*	rs111931861 (104744219)	Comb: $3.5 \cdot 10^{-8}$	*SRPK2* encodes the SRSF protein kinase 2 which is a cell cycle-regulated kinase that phosphorylates serine residues in the serine/arginine domain of various mRNA splicing factors and mediates pre-mRNA splicing[163, 164]. *SRPK2* also phosphorylates tau, suppresses tau-dependent microtubule polymerization, and inhibits axonal elongation in neurons[165]. Interaction of Akt-phosphorylated *SRPK2* with 14-3-3 mediates cell cycle and cell death in neurons[166]. Depletion of SRPK2 in dentate gyrus inhibits tau phosphorylation in the APP/PS1 mouse and alleviates impaired cognitive behaviors[165].	*SRPK2* is mainly expressed in brain but also at high levels in testis (https://www.gtexportal.org)	Activity of *SRPK2* is elevated in pathological structures of human Alzheimer's disease brain[165].	
8	*C8orf74*	rs10099100 (10576775)	ASD: $1.1 \cdot 10^{-8}$ Comb: $9.6 \cdot 10^{-9}$ MTAG Edu: $1.6 \cdot 10^{-8}$	*C8orf74* encodes a protein C8orf74 that is not yet characterized. C8orf74 has experimentally been shown to interact with histone-lysine-N methyltransferases SUV39H1 and H2, protein arginine N-methyltransferase 6 (ANM6) and Lysine-specific histone demethylase 1A (KDM1A) (IntAct database).	*C8orf74* is abundantly expressed in testis and is furthermore detected in pineal gland tissue (https://www.gtexportal.org).		Schizophrenia[82], Extraversion[167], Neuroticism[62, 167]

continues on the next page...

Supplementary Table 4 — continued from the previous page

Chr	Gene	Index SNP (BP)	Analysis P-value	Function	Tissue specificity	Disease	Previous GWS hits in locus[†]
8	*SOX7*	rs10099100 (10576775)	ASD: $1.1 \cdot 10^{-8}$ Comb: $9.6 \cdot 10^{-9}$ MTAG Edu: $1.6 \cdot 10^{-8}$	*SOX7* encodes Transcription factor SOX-7. *SOX7* is both a potent activator[168], and repressor[168] and it functions in several early developmental signaling pathways, including VEGF/Flk1 signaling, Wnt signaling, and Notch pathway[169]. *SOX7* is implicated in embryonic stem cell differentiation[170, 171] and in the regulation of embryonic development[172] and vascular development in particular[169]. *SOX7* acts as a tumor suppressor through the Wnt/β-catenin signaling pathway[173].	*SOX7* mRNA is detected during embryonic development in many tissues, most abundantly in brain, heart, lung, kidney, prostate, colon and spleen[168, 169]. In adults, *Sox7* is expressed in various tissues with highest levels in vagina and ectocervix but low levels in brain tissues (https://www.gtexportal.org).		Schizophrenia[82], Extraversion[167], Neuroticism[62, 167]
8	*PINX1*	rs10099100 (10576775)	ASD: $1.1 \cdot 10^{-8}$ Comb: $9.6 \cdot 10^{-9}$ MTAG Edu: $1.6 \cdot 10^{-8}$	*PINX1* encodes PIN2/TERF1-interacting telomerase inhibitor 1, a microtubule-binding protein essential for faithful chromosome segregation[174, 175]. *PINX1* interact with telomere repeat binding factor 1 (TRF1) and telomerase[176] and can potently inhibit telomerase activation and telomeres elongation in cancer cells[177, 178]. *PINX1* is further implicated in regulating chromosome stability[179]. *PINX1* overexpression significantly suppresses the growth of hepatocellular carcinoma cells, whereas *PINX1* inhibition potently enhances cell growth[180]. Depletion of *PINX1* also increases tumorigenicity in nude mice[181]. *PINX1* might be a putative tumor suppressor[182].	*PINX1* is ubiquitously expressed including in the brain, where *PINX1* mRNA is more abundant in cerebellar tissue than in other brain regions (https://www.gtexportal.org).	Rare variants in the *PINX1* gene have been identified in individuals with ASD[183].	Schizophrenia[82], Extraversion[167], Neuroticism[62, 167]
8	*MROH5*[*]	rs11787216 (142615222)	MTAG Edu: $2.0 \cdot 10^{-9}$	*MROH5* encodes Maestro heat-like repeat family member 5. *MROH5* interactions with the *GPSM3* G-protein-signaling modulator 3 and the *CHCHD2* transcription factor have been demonstrated experimentally (IntAct database). Otherwise, *MROH5* is largely uncharacterized.	*MROH5* seems to be exclusively expressed in testis (https://www.gtexportal.org).		Educational attainment[50]

continues on the next page...

Supplementary Table 4 — continued from the previous page

Chr	Gene	Index SNP (BP)	Analysis P-value	Function	Tissue specificity	Disease	Previous GWS hits in locus[†]
14	*MARK3*	rs10149470 (104017953)	MTAG MD: $8.5 \cdot 10^{-9}$	*MARK3* (also known as *CTAK1* or *EMK2*) encodes MAP/microtubule affinity-regulating kinase 3. *MARK3* belongs to family of four highly conserved kinases, *MARK1-4*. *MARK*s are evolutionarily conserved and required for polarity in various species including mammals (references within[184]). *MARK*s have numerous different upstream regulators (e.g. Pim-1, LKB1, and CaMKI) as well as downstream substrates (e.g. Pkp2, Cdc25C, Class II HDAC, Dlg/PSD-95, and MAP2/4/TAU)[184] illuminating an extreme multifunctionality. Specifically, *MARK3* negatively regulates the Hippo signaling pathway (controlling organ size in animals) and antagonizes the phosphorylation of LATS1[185]. *MARK3* has also been been implicated in hippocampal function[186] and CagA (Helicobacter pylori)-associated epithelial cell polarity disruption[187].	*MARK3* transcripts are ubiquitously expressed with highest levels in cerebellum (https://www.gtexportal.org).	*MARK3* (together with *SPTBN1*) has been associated with bone mineral density[188, 189]. Loss of MARK3 in mice leads to a hypermetabolic state with reduced body weight, decreased adiposity, resistance to hepatic steatosis, and hypofertility[184]. MARK1 has been associated with autism, overexpression in prefrontal cortex in post-mortem brains from patients, and accelerated evolution in the human lineage. Modulation of *MARK1* expression seems to modify both dendrite length and the velocity of mitochondrial transport along microtubules in primary cultures of mouse cortical neurons[190].	Schizophrenia[8, 82], Meta-analysis of autism spectrum disorder and schizophrenia[24]**
14	*CKB*	rs10149470 (104017953)	MTAG MD: $8.5 \cdot 10^{-9}$	*CKB* encodes Creatine kinase B-type (also known as brain creatinine kinase, B-CK). *CKB* is one of two cytosolic creatinine kinase isoforms that control energy demand through phosphocreatine consumption for local ATP production at subcellular sites of high energy demand[191, 192]. *CKB* plays a crucial role in brain energy homeostasis and in GABA neurons by activating *KCC2*[193].	*CKB* is highly expressed in brain, colon, esophagus, prostate and stomach (https://www.gtexportal.org).	ASD is part of the clinical symptoms seen in creatine deficiency syndrome (CDS) along with intellectual disability, speech and language delay, and epilepsy[194]. Serum CKB has been found to be elevated in ASD and to be associated with disease severity[195]. CKB has been found to be decreased in the brains of patients with Alzheimer disease, Huntington disease, and Pick disease[196] and references herein. Mutant huntingtin (mHTT) seems to act directly on the *CKB* promoter to repress its activity and overexpression of *CKB* has been shown to rescue the ATP depletion, aggregate formation, impaired proteasome activity, and shortened neurites induced by mHTT[196]. *CKB* has also been implicated with schizophrenia by proteomics[197] and proteomics-based reverse genetics[198]. Upstream regions of the *CKB* gene has been found to be differential methylated in fibroblasts from a discordant monozygotic twin pair with Rett syndrome[199].	Schizophrenia[8, 82], Meta-analysis of autism spectrum disorder and schizophrenia[24]**
14	*TRMT61A*	rs10149470 (104017953)	MTAG MD: $8.5 \cdot 10^{-9}$	*TRMT61A* encodes tRNA (adenine(58)-N(1))-methyltransferase catalytic subunit *TRMT61A*. tRNA (adenine-N1-)-methyltransferase catalyzes the formation of N1-methyladenine at position 58 (m1A58) in initiator methionyl-tRNA[200].	*TRMT61A* is ubiquitously expressed (https://www.gtexportal.org).		Schizophrenia[8, 82], Meta-analysis of autism spectrum disorder and schizophrenia[24]**

continues on the next page...

Supplementary Table 4 — continued from the previous page

Chr	Gene	Index SNP (BP)	Analysis P-value	Function	Tissue specificity	Disease	Previous GWS hits in locus[†]
14	*BAG5*	rs10149470 (104017953)	MTAG MD: $8.5 \cdot 10^{-9}$	*BAG5* encodes BAG family molecular chaperone regulator 5 (also known as Bcl-2-associated athanogene 5). *BAG5* is special to the BAG family of proteins since it consists entirely of five Bag domains[201]. Bag domains mediates direct interaction with the ATPase domain of Hsp70/Hsc70 molecular chaperones and *BAG5* function thereby as a nucleotide exchange factor to enhance Hsp70-mediated protein refolding[202].	*BAG5* is ubiquitously expressed with highest levels in testis (https://www.gtexportal.org). *BAG5* expression has been shown to increase during endoplamic reticulum (ER) stress in cardiomyocytes and this apparently modulates Hsps70 protein stability and reduces ER stress[203].	*BAG5* seems to be involved in neuroprotection in Parkinsons disease[204–207], Alzheimers disease[208], and spinocerebellar ataxia type-3 (SCA3)[209].	Schizophrenia[8, 82], Meta-analysis of autism spectrum disorder and schizophrenia[24]**
14	*APOPT1*	rs10149470 (104017953)	MTAG MD: $8.5 \cdot 10^{-9}$	*APOPT1* (previously *C14ORF153*) encodes Apoptogenic protein 1, mitochondrial. Mitochondrial localization of *APOPT1* has been experimentally validated[210].	*APOPT1* is ubiquitously expressed with highest levels in skeletal muscle and testis (https://www.gtexportal.org).	Mutations in *APOPT1* are causing cavitating leukoencephalopathy with Cytochrome c oxidase deficiency[210]. Alternative splicing of *APOPT1* has been suggested as the underlying mechanism of the association signal of the locus containing *APOPT1* in schizophrenia[211].	Schizophrenia[8, 82], Meta-analysis of autism spectrum disorder and schizophrenia[24]**
14	*KLC1*	rs10149470 (104017953)	MTAG MD: $8.5 \cdot 10^{-9}$	*KLC1* encodes Kinesin light chain 1. Kinesin is a microtubule-associated force-producing protein involved in organelle transport. *KCL1* may play a role in coupling of cargo to the Kinesin heavy chain or in modulation of its ATPase activity[212, 213]. Fast anterograde axonal transport of APP is mediated by direct binding between APP and *KLC1*[214].	*KLC1* is highly expressed in many tissues with very high levels in brain (https://www.gtexportal.org).	*KLC1* has been suggested to be involved in Alzheimers disease[215], age-related macular degeneration[216], and cortical cataracts[217].	Schizophrenia[8, 82], Meta-analysis of autism spectrum disorder and schizophrenia[24]**
14	*XRCC3*	rs10149470 (104017953)	MTAG MD: $8.5 \cdot 10^{-9}$	*XRCC3* encodes DNA repair protein *XRCC3*. *XRCC3* is part of the RAD51-related protein family[218] and forms the CX3 complex with one of them, RAD51C[219]. *XRCC3* is involved in homologous recombination repair of DNA double-strand breaks[220] and plays an important role in maintaining chromosome stability and DNA damage repair[221].	*XRCC3* is expressed in many tissues with highest levels in spleen and low levels in all brain parts except cerebellum (https://www.gtexportal.org).	*XRCC3* SNPs have been suggested as a modifier of various different cancers e.g. bladder, breast, non-melanoma skin, and colorectal cancers, [222] and references herein.	Schizophrenia[8, 82], Meta-analysis of autism spectrum disorder and schizophrenia[24]**
20	*MACROD2*	rs71190156 (14760747)	ASD $2.8 \cdot 10^{-8}$ Comb $3.0 \cdot 10^{-8}$ MTAG Edu ·10	*MACROD2* (also known as *C20orf133*) encodes O-acetyl-ADP-ribose deacetylase MACROD2, an enzyme in the nucleus, that binds to mono-ADP-ribosylated (MARylated) proteins and functions as an eraser of mono-ADP-ribosylation[223]. Intracellular MARylated histones and GSK3β are substrates of macroD2, and the removal of MAR from GSK3β is responsible for reactivating of its kinase activity [223].	*MACROD2* is expressed in EPV-transformed lymphocytes, lung and multiple regions of the brain. Low or no expression across most other tissue (https://www.gtexportal.org).	A heterozygous *de novo* 250-kb deletion in the *MACROD2*, initially identified in a patient with Kabuki syndrome (a congenital mental retardation syndrome)[224], was later found not to be the cause of the syndrome[225].	Autism spectrum disorder[20]

continues on the next page...

Supplementary Table 4 — continued from the previous page

Chr	Gene	Index SNP (BP)	Analysis P-value	Function	Tissue specificity	Disease	Previous GWS hits in locus[†]
20	*XRN2*	rs910805 (21248116)	ASD $2.0 \cdot 10^{-9}$ MTAG SCZ $1.5 \cdot 10^{-10}$ MTAG Edu $1.3 \cdot 10^{-8}$	*XRN2* encodes the 5'-3' exoribonuclease 2 promoting transcription termination at the 3' ends of genes[226]. In differentiated rat neurons, *XRN2* is involved in cleavage of miRNA precursors, suggesting that the gene is involved in a novel mechanism for control of miRNA expression[227].	*XRN2* is transcribed uniformly across most tissues, with lowest levels in all brain regions except cerebellum where levels are substantially higher (https://www.gtexportal.org).		
20	*KIZ*	rs910805 (21248116)	ASD $2.0 \cdot 10^{-9}$ MTAG SCZ $1.5 \cdot 10^{-10}$ MTAG Edu $1.3 \cdot 10^{-8}$	*KIZ* encodes centrosomal protein Kizuna. The gene is also known as *C20orf19* or PLK1S1. Protects mature centrosomes from collapse during spindle formation[228]. KIZ-depleted cells has been shown to grow more slowly, have nuclear abnormalities, and undergoing cell cycle arrest[228].	*KIZ* is expressed across a wide range of tissues including the brain, highest in cerebellum and cerebellar hemisphere (https://www.gtexportal.org).		
20	*NKX2-4*	rs910805 (21248116)	ASD $2.0 \cdot 10^{-9}$ MTAG SCZ $1.5 \cdot 10^{-10}$ MTAG Edu $1.3 \cdot 10^{-8}$	*NKX2-4* encodes Homeobox protein Nkx-2.4. *NKX2-4* belong to the large family of homeobox-containing transcription factors, distinguished by a 60-amino acid evolutionarily conserved DNA-binding homeodomain. Morpholino knockdown of the zebrafish orthologs of *NKX2-1* and *NKX2-4* (Nkx2.4a and Nkx2.4b) revealed a contribution of these transcription factors to neural patterning and neuronal differentiation in zebrafish brain the development of the hypothalamus, preoptic region, and pallidum [229].	*NKX2-4* is exclusively expressed in hypothalamus, pituitary and testis (https://www.gtexportal.org).	Given the expression pattern and the effects of *NKX2-4* knockdown in zebrafish, *NKX2-4* might be important in hypothalamus-pituitary function and eventually oxytocin production. Of special note, deletions affecting 20p11-20p12 have been described in patients with panhypopituarism[230] and hypopituitarism has been associated with lower saliva oxytocin concentrations and reduced empathic ability[231].	
20	*NKX2-2*	rs910805 (21248116)	ASD $2.0 \cdot 10^{-9}$ MTAG SCZ $1.5 \cdot 10^{-10}$ MTAG Edu $1.3 \cdot 10^{-8}$	*NKX2-2* encodes Homeobox protein Nkx-2.2. This homeo domain transcription factor has an essential role in interpreting the Sonic hedgehog signals and selecting neuronal identity[232] The gene is part of the networks controlling the development of midbrain dopaminergic neurons in the mouse brain[233].	*NKX2-2* transcripts are found in different regions of the brain and pituitary (https://www.gtexportal.org).		

3.2.2 Genetic correlation with other phenotypes

Supplementary Table 5: The complete output from LD Hub (except for 'Years of schooling (proxy cognitive performance)' and 'Years of schooling 2013' and 5 other removed out of redundancy and ASD and PGC cross-disorder due to sample overlap) with a few extra phenotypes added that had not yet been included in LD Hub. Altogether there are 234 phenotypes. The colums are trait, PMID of the publication, Category as defined by LD Hub, Ethnicity, SNP correlation, r_G, standard error of r_G, z-score of r_G, p-value for r_G, SNP heritability on the observed scale, h^2_G obs, and its standard error, h^2_G Int is the intercept of h^2_G obs, and it comes with its own standard error, and finally GCOV Int is the cross-trait LD Score regression intercept with standard error. The colour of the estimate of genetic correlation, r_G, signifies whether the correlation is positive, blue, or negative, red, and p-values (estimated from z-test) that are significant after Bonferroni correction on the number of tests are painted red. The PMID is hyperlinked to the particular pubmed page. For tables conserning genetic overlap between subtypes of ASD, see section 3.3.
* Values from in-house analyses of new summary statistics not yet included in LD Hub. The major depression is the latest PGC MD scan (excluding the iPSYCH samples.
** Values from in-house LD score pipeline as the values from LD Hub are invalid due to erroneous summary stat files at LD Hub.

Trait	PMID	Category	Ethnicity	r_G	se	Z	P	h^2_G obs (se)	h^2_G Int (se)	GCOV Int (se)
Fathers age at death	27015805	aging	European	0.138	0.090	1.540	$1.24 \cdot 10^{-1}$	0.041 (0.007)	1.017 (0.008)	-0.004 (0.007)
Mothers age at death	27015805	aging	European	0.095	0.085	1.123	$2.62 \cdot 10^{-1}$	0.041 (0.007)	1.004 (0.008)	-0.011 (0.006)
Parents age at death	27015805	aging	European	−0.023	0.100	−0.235	$8.14 \cdot 10^{-1}$	0.031 (0.007)	1.013 (0.008)	0.000 (0.007)
Birth weight	27680694	anthropometric	European	−0.008	0.045	−0.183	$8.55 \cdot 10^{-1}$	0.100 (0.007)	1.047 (0.012)	0.008 (0.006)
Body fat	26833246	anthropometric	Mixed	0.027	0.060	0.445	$6.56 \cdot 10^{-1}$	0.111 (0.009)	0.898 (0.008)	0.001 (0.006)
Body mass index	20935630	anthropometric	European	0.078	0.043	1.817	$6.93 \cdot 10^{-2}$	0.192 (0.010)	1.006 (0.013)	0.001 (0.007)
Child birth length	25281659	anthropometric	European	0.136	0.089	1.533	$1.25 \cdot 10^{-1}$	0.161 (0.025)	0.995 (0.009)	-0.015 (0.008)
Child birth weight	23202124	anthropometric	European	0.059	0.080	0.733	$4.64 \cdot 10^{-1}$	0.108 (0.020)	1.006 (0.007)	-0.008 (0.005)
Childhood obesity	22484627	anthropometric	European	0.057	0.061	0.934	$3.50 \cdot 10^{-1}$	0.439 (0.047)	0.920 (0.009)	-0.004 (0.006)
Diff in height btwn adoles and adulth; age 14	23449627	anthropometric	European	−0.143	0.105	−1.361	$1.74 \cdot 10^{-1}$	0.448 (0.117)	0.981 (0.008)	-0.000 (0.006)
Diff in height btwn childh and adulth; age 8	23449627	anthropometric	European	−0.027	0.095	−0.290	$7.72 \cdot 10^{-1}$	0.330 (0.060)	0.973 (0.010)	-0.000 (0.007)
Extreme bmi	23563607	anthropometric	European	0.071	0.060	1.193	$2.33 \cdot 10^{-1}$	0.687 (0.059)	1.031 (0.013)	0.004 (0.009)
Extreme height	23563607	anthropometric	European	0.017	0.046	0.365	$7.15 \cdot 10^{-1}$	1.266 (0.119)	1.024 (0.023)	0.004 (0.009)
Extreme waist-to-hip ratio	23563607	anthropometric	European	0.179	0.083	2.158	$3.10 \cdot 10^{-2}$	0.361 (0.066)	0.978 (0.009)	-0.018 (0.008)
Height2010	20881960	anthropometric	European	0.036	0.034	1.067	$2.86 \cdot 10^{-1}$	0.283 (0.018)	1.022 (0.022)	-0.010 (0.008)
Height; Females at age 10 and males at age 12	23449627	anthropometric	European	0.066	0.074	0.883	$3.77 \cdot 10^{-1}$	0.416 (0.051)	0.957 (0.010)	0.000 (0.007)
Hip circumference	25673412	anthropometric	European	0.091	0.041	2.236	$2.54 \cdot 10^{-2}$	0.130 (0.006)	0.852 (0.010)	0.002 (0.006)
Infant head circumference	22504419	anthropometric	European	0.086	0.091	0.936	$3.50 \cdot 10^{-1}$	0.216 (0.048)	0.994 (0.008)	-0.013 (0.006)
Obesity class 1	23563607	anthropometric	European	0.092	0.046	2.012	$4.42 \cdot 10^{-2}$	0.216 (0.012)	1.018 (0.013)	0.004 (0.008)
Obesity class 2	23563607	anthropometric	European	0.092	0.055	1.695	$9.01 \cdot 10^{-2}$	0.181 (0.014)	1.006 (0.011)	0.006 (0.008)
Obesity class 3	23563607	anthropometric	European	0.127	0.063	2.027	$4.27 \cdot 10^{-2}$	0.119 (0.015)	0.982 (0.011)	0.003 (0.007)
Overweight	23563607	anthropometric	European	0.084	0.049	1.720	$8.55 \cdot 10^{-2}$	0.110 (0.007)	1.022 (0.011)	-0.004 (0.007)
Sitting height ratio	25865494	anthropometric	European	0.088	0.078	1.130	$2.59 \cdot 10^{-1}$	0.220 (0.029)	0.982 (0.009)	-0.010 (0.007)
Waist circumference	25673412	anthropometric	European	0.078	0.040	1.963	$4.97 \cdot 10^{-2}$	0.123 (0.005)	0.839 (0.009)	0.001 (0.006)

Continues on the next page

Supplementary Table 5 – continued from previous page

Trait	PMID	Category	Ethnicity	r_G	se	Z	P	h^2_G obs (se)	h^2_G Int (se)	GCOV Int (se)
Waist-to-hip ratio	25673412	anthropometric	European	0.068	0.041	1.659	$9.71 \cdot 10^{-2}$	0.115 (0.008)	0.915 (0.012)	-0.006 (0.007)
Asthma	17611496	autoimmune	European	0.054	0.093	0.573	$5.67 \cdot 10^{-1}$	0.125 (0.030)	1.007 (0.010)	0.004 (0.007)
Celiac disease	20190752	autoimmune	European	0.062	0.087	0.715	$4.75 \cdot 10^{-1}$	0.249 (0.051)	1.085 (0.012)	0.007 (0.008)
Crohns disease	26192919	autoimmune	European	−0.027	0.056	−0.491	$6.24 \cdot 10^{-1}$	0.484 (0.064)	1.029 (0.015)	0.001 (0.007)
Eczema	26482879	autoimmune	Mixed	−0.131	0.098	−1.333	$1.82 \cdot 10^{-1}$	0.065 (0.016)	1.026 (0.009)	0.023 (0.006)
Inflammatory Bowel Disease (Euro)	26192919	autoimmune	European	−0.029	0.053	−0.550	$5.82 \cdot 10^{-1}$	0.316 (0.037)	1.064 (0.015)	0.003 (0.007)
Multiple sclerosis	21833088	autoimmune	European	−0.030	0.156	−0.191	$8.49 \cdot 10^{-1}$	0.049 (0.029)	1.064 (0.011)	-0.004 (0.008)
Primary biliary cirrhosis	26394269	autoimmune	European	−0.100	0.074	−1.350	$1.77 \cdot 10^{-1}$	0.386 (0.068)	1.002 (0.011)	0.013 (0.007)
Rheumatoid Arthritis	24390342	autoimmune	European	−0.134	0.056	−2.382	$1.72 \cdot 10^{-2}$	0.153 (0.034)	1.033 (0.026)	0.010 (0.006)
Systemic lupus erythematosus	26502338	autoimmune	European	−0.168	0.094	−1.781	$7.49 \cdot 10^{-2}$	0.378 (0.075)	1.110 (0.013)	0.011 (0.009)
Ulcerative colitis	26192919	autoimmune	European	−0.010	0.065	−0.160	$8.73 \cdot 10^{-1}$	0.238 (0.033)	1.058 (0.013)	0.005 (0.006)
Femoral neck bone mineral density	22504420	bone	Mixed	0.016	0.047	0.328	$7.43 \cdot 10^{-1}$	0.300 (0.028)	0.983 (0.012)	0.001 (0.006)
Femoral Neck bone mineral density	26367794	bone	Mixed	−0.044	0.059	−0.747	$4.55 \cdot 10^{-1}$	0.124 (0.015)	0.978 (0.009)	0.004 (0.006)
Forearm Bone mineral density	26367794	bone	Mixed	0.060	0.147	0.405	$6.86 \cdot 10^{-1}$	0.072 (0.046)	1.016 (0.008)	-0.004 (0.006)
Lumbar spine bone mineral density	22504420	bone	Mixed	0.057	0.055	1.040	$2.98 \cdot 10^{-1}$	0.262 (0.026)	1.018 (0.011)	-0.005 (0.006)
Lumbar Spine bone mineral density	26367794	bone	Mixed	−0.016	0.063	−0.258	$7.96 \cdot 10^{-1}$	0.124 (0.018)	0.983 (0.010)	0.004 (0.006)
ICV**	25607358	brainvolume	European	0.137	0.095	1.450	$1.47 \cdot 10^{-1}$	0.175 (0.048)	1.018 (0.008)	-0.004 (0.005)
Mean Accumbens	25607358	brainvolume	European	−0.081	0.145	−0.557	$5.77 \cdot 10^{-1}$	0.096 (0.037)	0.977 (0.007)	0.000 (0.006)
Mean Caudate	25607358	brainvolume	European	−0.044	0.072	−0.612	$5.40 \cdot 10^{-1}$	0.251 (0.040)	0.967 (0.008)	0.006 (0.006)
Mean Hippocampus	25607358	brainvolume	European	−0.046	0.117	−0.389	$6.97 \cdot 10^{-1}$	0.133 (0.044)	0.990 (0.009)	-0.000 (0.007)
Mean Pallidum	25607358	brainvolume	European	−0.065	0.098	−0.665	$5.06 \cdot 10^{-1}$	0.165 (0.047)	0.978 (0.009)	-0.002 (0.006)
Mean Putamen**	25607358	brainvolume	European	0.004	0.081	0.053	$9.58 \cdot 10^{-1}$	0.303 (0.052)	1.000 (0.009)	0.001 (0.006)
Mean Thalamus	25607358	brainvolume	European	0.024	0.128	0.186	$8.53 \cdot 10^{-1}$	0.128 (0.039)	0.983 (0.008)	-0.008 (0.006)
Lung adenocarcinoma	27488534	cancer	European	−0.006	0.113	−0.049	$9.61 \cdot 10^{-1}$	0.031 (0.013)	1.019 (0.008)	-0.011 (0.005)
Lung cancer	27488534	cancer	European	−0.089	0.079	−1.120	$2.63 \cdot 10^{-1}$	0.315 (0.072)	1.015 (0.009)	-0.004 (0.006)
Lung cancer (all)	24880342	cancer	European	−0.061	0.088	−0.692	$4.89 \cdot 10^{-1}$	0.126 (0.033)	1.009 (0.009)	-0.004 (0.006)
Lung cancer (squamous cell)	24880342	cancer	European	0.129	0.145	0.888	$3.75 \cdot 10^{-1}$	0.036 (0.020)	1.016 (0.007)	-0.005 (0.006)
Squamous cell lung cancer	27488534	cancer	European	0.087	0.125	0.698	$4.85 \cdot 10^{-1}$	0.031 (0.012)	1.019 (0.008)	-0.004 (0.006)
Adiponectin	22479202	cardiometabolic	Mixed	−0.125	0.079	−1.575	$1.15 \cdot 10^{-1}$	0.122 (0.027)	1.020 (0.013)	0.006 (0.007)
Coronary artery disease	26343387	cardiometabolic	Mixed	−0.050	0.041	−1.215	$2.25 \cdot 10^{-1}$	0.077 (0.006)	1.052 (0.013)	0.001 (0.006)
IQ*	28530673	cognition	European	0.199	0.048	4.122	$3.76 \cdot 10^{-5}$	0.201 (0.011)	1.007 (0.010)	0.004 (0.007)
Memory*	27046643	cognition	European	−0.021	0.066	−0.316	$7.52 \cdot 10^{-1}$	0.044 (0.006)	0.997 (0.009)	0.004 (0.006)
Reaction time*	27046643	cognition	European	−0.028	0.060	−0.469	$6.39 \cdot 10^{-1}$	0.072 (0.006)	1.014 (0.009)	-0.005 (0.006)
Verbal-Numerical reasoning*	27046643	cognition	European	0.200	0.061	3.261	$1.10 \cdot 10^{-3}$	0.217 (0.020)	1.012 (0.009)	-0.002 (0.007)
Childhood IQ	23358156	education	European	0.234	0.073	3.223	$1.30 \cdot 10^{-3}$	0.274 (0.046)	1.002 (0.011)	-0.005 (0.006)
College*	27046643	education	European	0.274	0.041	6.649	$2.94 \cdot 10^{-11}$	0.155 (0.009)	1.033 (0.011)	-0.009 (0.007)
College completion	23722424	education	European	0.167	0.055	3.032	$2.40 \cdot 10^{-3}$	0.080 (0.006)	1.020 (0.010)	0.003 (0.007)
Educational Attainment	27225129	education	European	0.199	0.033	5.958	$2.56 \cdot 10^{-9}$	0.124 (0.004)	0.942 (0.013)	-0.001 (0.008)

Continues on the next page

Supplementary Table 5 – continued from previous page

Trait	PMID	Category	Ethnicity	r_G	se	Z	P	h^2_G obs (se)	h^2_G Int (se)	GCOV Int (se)
Income*	27818178	education	SES	−0.034	0.059	−0.570	$5.69 \cdot 10^{-1}$	0.062 (0.006)	1.025 (0.009)	-0.007 (0.006)
2hr glucose adjusted for BMI	20081857	glycemic	European	0.016	0.111	0.143	$8.87 \cdot 10^{-1}$	0.101 (0.036)	0.993 (0.008)	-0.005 (0.006)
Fasting glucose main effect	22581228	glycemic	European	−0.023	0.063	−0.372	$7.10 \cdot 10^{-1}$	0.097 (0.021)	1.001 (0.013)	-0.001 (0.006)
Fasting insulin main effect	22581228	glycemic	European	0.017	0.072	0.241	$8.10 \cdot 10^{-1}$	0.075 (0.011)	1.009 (0.009)	-0.002 (0.006)
Fasting proinsulin	20081858	glycemic	European	−0.052	0.087	−0.598	$5.50 \cdot 10^{-1}$	0.222 (0.099)	0.973 (0.012)	0.002 (0.006)
HbA1C	20858683	glycemic	European	0.020	0.091	0.225	$8.22 \cdot 10^{-1}$	0.059 (0.013)	1.006 (0.009)	-0.008 (0.007)
HOMA-B	20081858	glycemic	European	0.027	0.108	0.250	$8.03 \cdot 10^{-1}$	0.080 (0.015)	0.996 (0.008)	0.000 (0.007)
HOMA-IR	20081858	glycemic	European	0.029	0.107	0.271	$7.87 \cdot 10^{-1}$	0.070 (0.014)	1.002 (0.007)	-0.002 (0.007)
Type 2 Diabetes	22885922	glycemic	European	0.008	0.070	0.111	$9.11 \cdot 10^{-1}$	0.087 (0.010)	1.010 (0.009)	0.005 (0.007)
Heart rate	23583979	haemotological	Mixed	−0.057	0.055	−1.037	$3.00 \cdot 10^{-1}$	0.085 (0.009)	1.011 (0.010)	0.004 (0.006)
Mean platelet volume	22139419	haemotological	European	−0.072	0.071	−1.006	$3.14 \cdot 10^{-1}$	0.321 (0.054)	0.980 (0.012)	0.002 (0.007)
Platelet count	22139419	haemotological	European	−0.027	0.058	−0.463	$6.43 \cdot 10^{-1}$	0.114 (0.012)	0.994 (0.011)	-0.001 (0.006)
LeptinadjBMI	26833098	hormone	European	−0.010	0.084	−0.121	$9.04 \cdot 10^{-1}$	0.096 (0.019)	1.003 (0.009)	0.000 (0.006)
LeptinnotadjBMI	26833098	hormone	European	0.070	0.082	0.849	$3.96 \cdot 10^{-1}$	0.103 (0.016)	0.992 (0.008)	-0.002 (0.006)
Chronic Kidney Disease	26831199	kidney	Mixed	−0.050	0.106	−0.476	$6.34 \cdot 10^{-1}$	0.020 (0.006)	1.013 (0.011)	0.020 (0.007)
Serum creatinine	26831199	kidney	Mixed	−0.035	0.052	−0.665	$5.06 \cdot 10^{-1}$	0.107 (0.011)	0.975 (0.018)	-0.000 (0.008)
Serum creatinine (non-diab)	26831199	kidney	Mixed	−0.056	0.051	−1.094	$2.74 \cdot 10^{-1}$	0.115 (0.013)	0.977 (0.017)	-0.000 (0.007)
Serum cystatin c	26831199	kidney	Mixed	−0.030	0.058	−0.509	$6.11 \cdot 10^{-1}$	0.178 (0.074)	0.955 (0.018)	0.003 (0.006)
Urinary alb-to-cret ratio	26631737	kidney	European	−0.037	0.091	−0.402	$6.87 \cdot 10^{-1}$	0.045 (0.009)	0.998 (0.008)	0.003 (0.006)
Urinary alb-to-cret ratio (non-diab)	26631737	kidney	European	−0.131	0.096	−1.364	$1.73 \cdot 10^{-1}$	0.050 (0.011)	0.999 (0.008)	0.010 (0.007)
HDL cholest	20686565	lipids	European	−0.019	0.050	−0.377	$7.06 \cdot 10^{-1}$	0.117 (0.029)	1.080 (0.065)	-0.002 (0.006)
LDL cholest	20686565	lipids	European	−0.005	0.054	−0.082	$9.35 \cdot 10^{-1}$	0.091 (0.035)	1.078 (0.065)	-0.004 (0.006)
Tot Cholesterol	20686565	lipids	European	0.014	0.047	0.303	$7.62 \cdot 10^{-1}$	0.123 (0.029)	1.044 (0.048)	-0.004 (0.006)
Trigly	20686565	lipids	European	0.090	0.054	1.659	$9.72 \cdot 10^{-2}$	0.167 (0.032)	0.972 (0.022)	-0.005 (0.008)
Forced expiratory volume in 1 second (FEV1)	21946350	lungfunction	European	0.202	0.080	2.516	$1.19 \cdot 10^{-2}$	0.171 (0.023)	0.882 (0.013)	0.000 (0.010)
Forced expiratory volume in 1 second (FEV1)	26635082	lungfunction	European	0.010	0.066	0.147	$8.83 \cdot 10^{-1}$	0.144 (0.018)	0.989 (0.009)	-0.004 (0.006)
Forced expiratory volume in 1 second (FEV1)	28166213	lungfunction	European	0.086	0.054	1.599	$1.10 \cdot 10^{-1}$	0.269 (0.018)	0.967 (0.009)	-0.016 (0.008)
Forced expiratory volume in 1 second (FEV1)/Forced Vital capacity(FVC)	21946350	lungfunction	European	−0.037	0.060	−0.615	$5.39 \cdot 10^{-1}$	0.125 (0.015)	0.927 (0.009)	0.007 (0.006)
Forced expiratory volume in 1 second (FEV1)/Forced Vital capacity(FVC)	26635082	lungfunction	European	−0.005	0.082	−0.059	$9.53 \cdot 10^{-1}$	0.116 (0.017)	0.980 (0.008)	-0.003 (0.006)
Forced expiratory volume in 1 second (FEV1)/Forced Vital capacity(FVC)	28166213	lungfunction	European	0.079	0.060	1.330	$1.83 \cdot 10^{-1}$	0.254 (0.022)	0.979 (0.011)	-0.013 (0.007)
Forced Vital capacity(FVC)	26635082	lungfunction	European	0.021	0.066	0.313	$7.54 \cdot 10^{-1}$	0.149 (0.016)	0.984 (0.008)	-0.004 (0.006)
Forced Vital capacity(FVC)	28166213	lungfunction	European	0.078	0.050	1.548	$1.22 \cdot 10^{-1}$	0.269 (0.017)	0.968 (0.010)	-0.015 (0.007)
18:2 linoleic acid (LA)	27005778	metabolites	European	0.085	0.117	0.728	$4.67 \cdot 10^{-1}$	0.113 (0.055)	1.008 (0.012)	-0.005 (0.006)
22:6 docosahexaenoic acid	27005778	metabolites	European	−0.050	0.095	−0.533	$5.94 \cdot 10^{-1}$	0.123 (0.039)	0.998 (0.009)	0.002 (0.006)
Acetate	27005778	metabolites	European	0.383	0.147	2.610	$9.00 \cdot 10^{-3}$	0.047 (0.019)	1.007 (0.007)	-0.012 (0.006)
Acetoacetate	27005778	metabolites	European	0.145	0.115	1.266	$2.06 \cdot 10^{-1}$	0.085 (0.030)	0.975 (0.009)	-0.005 (0.006)
Alanine	27005778	metabolites	European	−0.008	0.085	−0.089	$9.29 \cdot 10^{-1}$	0.094 (0.030)	1.007 (0.009)	0.001 (0.006)
Albumin	27005778	metabolites	European	−0.031	0.140	−0.225	$8.22 \cdot 10^{-1}$	0.061 (0.027)	0.990 (0.008)	-0.001 (0.006)

Continues on the next page

Supplementary Table 5 – continued from previous page

Trait	PMID	Category	Ethnicity	r_G	se	Z	P	h^2_G obs (se)	h^2_G Int (se)	GCOV Int (se)
Apolipoprotein A-I	27005778	metabolites	European	−0.035	0.111	−0.320	$7.49 \cdot 10^{-1}$	0.091 (0.035)	0.999 (0.015)	-0.001 (0.006)
Apolipoprotein B	27005778	metabolites	European	0.077	0.115	0.673	$5.01 \cdot 10^{-1}$	0.079 (0.049)	1.010 (0.021)	-0.007 (0.006)
Av no of dbl bonds in a fatty acid chain	27005778	metabolites	European	0.135	0.085	1.593	$1.11 \cdot 10^{-1}$	0.173 (0.052)	1.002 (0.010)	-0.011 (0.006)
Av no of meth grps per a dbl bond	27005778	metabolites	European	−0.081	0.080	−1.023	$3.06 \cdot 10^{-1}$	0.213 (0.073)	0.993 (0.011)	0.009 (0.006)
Cholesterol esters in large HDL	27005778	metabolites	European	−0.118	0.103	−1.140	$2.54 \cdot 10^{-1}$	0.103 (0.037)	1.010 (0.019)	0.006 (0.006)
Cholesterol esters in large LDL	27005778	metabolites	European	0.054	0.138	0.390	$6.96 \cdot 10^{-1}$	0.062 (0.068)	1.018 (0.031)	-0.008 (0.006)
Cholesterol esters in large VLDL	27005778	metabolites	European	0.061	0.084	0.731	$4.65 \cdot 10^{-1}$	0.166 (0.037)	0.978 (0.009)	0.003 (0.006)
Cholesterol esters in medium HDL	27005778	metabolites	European	−0.195	0.136	−1.432	$1.52 \cdot 10^{-1}$	0.051 (0.033)	1.003 (0.011)	0.002 (0.006)
Cholesterol esters in medium LDL	27005778	metabolites	European	0.081	0.129	0.622	$5.34 \cdot 10^{-1}$	0.069 (0.065)	1.015 (0.029)	-0.009 (0.006)
Cholesterol esters in medium VLDL	27005778	metabolites	European	0.105	0.083	1.271	$2.04 \cdot 10^{-1}$	0.144 (0.040)	0.989 (0.010)	-0.005 (0.006)
Citrate	27005778	metabolites	European	0.072	0.113	0.641	$5.22 \cdot 10^{-1}$	0.068 (0.022)	1.013 (0.008)	-0.013 (0.006)
Conc of chylom and lrgst VLDL prt	27005778	metabolites	European	−0.143	0.103	−1.381	$1.67 \cdot 10^{-1}$	0.121 (0.029)	0.987 (0.008)	0.006 (0.006)
Conc of IDL prt	27005778	metabolites	European	0.001	0.135	0.009	$9.93 \cdot 10^{-1}$	0.059 (0.054)	1.025 (0.025)	-0.006 (0.006)
Conc of large HDL prt	27005778	metabolites	European	−0.144	0.101	−1.430	$1.53 \cdot 10^{-1}$	0.109 (0.037)	1.010 (0.020)	0.006 (0.006)
Conc of large LDL prt	27005778	metabolites	European	0.032	0.135	0.235	$8.14 \cdot 10^{-1}$	0.061 (0.066)	1.022 (0.030)	-0.007 (0.006)
Conc of large VLDL prt	27005778	metabolites	European	0.093	0.086	1.091	$2.75 \cdot 10^{-1}$	0.137 (0.037)	0.972 (0.009)	-0.000 (0.006)
Conc of medium HDL prt	27005778	metabolites	European	−0.182	0.115	−1.585	$1.13 \cdot 10^{-1}$	0.067 (0.031)	0.995 (0.009)	0.002 (0.006)
Conc of medium LDL prt	27005778	metabolites	European	0.069	0.125	0.548	$5.84 \cdot 10^{-1}$	0.070 (0.063)	1.016 (0.028)	-0.009 (0.006)
Conc of medium VLDL prt	27005778	metabolites	European	0.084	0.087	0.960	$3.37 \cdot 10^{-1}$	0.144 (0.038)	0.984 (0.010)	0.001 (0.006)
Conc of small LDL prt	27005778	metabolites	European	0.067	0.105	0.640	$5.22 \cdot 10^{-1}$	0.094 (0.053)	1.007 (0.022)	-0.008 (0.006)
Conc of small VLDL prt	27005778	metabolites	European	0.116	0.080	1.446	$1.48 \cdot 10^{-1}$	0.151 (0.039)	0.990 (0.010)	-0.005 (0.006)
Conc of very large HDL prt	27005778	metabolites	European	−0.156	0.148	−1.057	$2.91 \cdot 10^{-1}$	0.049 (0.033)	1.009 (0.019)	0.008 (0.006)
Conc of very large VLDL prt	27005778	metabolites	European	0.044	0.104	0.420	$6.74 \cdot 10^{-1}$	0.135 (0.033)	0.980 (0.009)	-0.001 (0.006)
Conc of very small VLDL prt	27005778	metabolites	European	0.039	0.094	0.412	$6.80 \cdot 10^{-1}$	0.104 (0.041)	1.010 (0.016)	-0.005 (0.006)
Creatinine	27005778	metabolites	European	0.164	0.089	1.843	$6.54 \cdot 10^{-2}$	0.112 (0.028)	1.013 (0.009)	-0.011 (0.006)
Desc of av fatty acid chain length;	27005778	metabolites	European	0.024	0.101	0.235	$8.15 \cdot 10^{-1}$	0.120 (0.039)	0.977 (0.009)	-0.000 (0.006)
Free cholest	27005778	metabolites	European	−0.061	0.159	−0.387	$6.99 \cdot 10^{-1}$	0.071 (0.049)	1.022 (0.013)	-0.006 (0.006)
Free cholest in IDL	27005778	metabolites	European	0.016	0.137	0.119	$9.06 \cdot 10^{-1}$	0.053 (0.054)	1.029 (0.028)	-0.006 (0.006)
Free cholest in large HDL	27005778	metabolites	European	−0.125	0.104	−1.211	$2.26 \cdot 10^{-1}$	0.088 (0.033)	1.017 (0.019)	0.005 (0.006)
Free cholest in large LDL	27005778	metabolites	European	−0.010	0.143	−0.070	$9.44 \cdot 10^{-1}$	0.049 (0.065)	1.024 (0.034)	-0.006 (0.006)
Free cholest in large VLDL	27005778	metabolites	European	0.077	0.085	0.900	$3.68 \cdot 10^{-1}$	0.129 (0.032)	0.987 (0.009)	0.000 (0.006)
Free cholest in medium HDL	27005778	metabolites	European	−0.208	0.109	−1.916	$5.54 \cdot 10^{-2}$	0.067 (0.027)	0.999 (0.011)	0.002 (0.006)
Free cholest in medium VLDL	27005778	metabolites	European	0.089	0.092	0.971	$3.32 \cdot 10^{-1}$	0.108 (0.035)	0.998 (0.009)	-0.001 (0.006)
Free cholest in small VLDL	27005778	metabolites	European	0.165	0.097	1.709	$8.75 \cdot 10^{-2}$	0.102 (0.036)	1.004 (0.011)	-0.008 (0.006)
Free cholest in very large HDL	27005778	metabolites	European	−0.162	0.166	−0.974	$3.30 \cdot 10^{-1}$	0.035 (0.029)	1.022 (0.019)	0.007 (0.006)
Free cholest to esterified cholest ratio	27005778	metabolites	European	0.004	0.185	0.024	$9.81 \cdot 10^{-1}$	0.051 (0.060)	1.016 (0.016)	-0.007 (0.006)
Glucose	27005778	metabolites	European	0.043	0.100	0.432	$6.66 \cdot 10^{-1}$	0.086 (0.024)	0.995 (0.008)	-0.008 (0.006)
Glutamine	27005778	metabolites	European	0.108	0.124	0.870	$3.84 \cdot 10^{-1}$	0.057 (0.023)	1.020 (0.010)	-0.009 (0.006)

Continues on the next page

Supplementary Table 5 – continued from previous page

Trait	PMID	Category	Ethnicity	r_G	se	Z	P	h^2_G obs (se)	h^2_G Int (se)	GCOV Int (se)
Glycop acetyls; mainly a1-acid glycop	27005778	metabolites	European	0.029	0.099	0.296	$7.67 \cdot 10^{-1}$	0.107 (0.030)	0.983 (0.008)	-0.001 (0.006)
Isoleucine	27005778	metabolites	European	0.089	0.108	0.822	$4.11 \cdot 10^{-1}$	0.065 (0.025)	0.998 (0.008)	-0.003 (0.006)
Leucine	27005778	metabolites	European	0.127	0.133	0.959	$3.38 \cdot 10^{-1}$	0.047 (0.023)	1.008 (0.008)	-0.003 (0.006)
Mean diameter for HDL prt	27005778	metabolites	European	−0.116	0.117	−0.994	$3.20 \cdot 10^{-1}$	0.088 (0.041)	1.022 (0.026)	0.007 (0.006)
Mean diameter for LDL prt	27005778	metabolites	European	−0.020	0.132	−0.154	$8.78 \cdot 10^{-1}$	0.048 (0.031)	1.001 (0.015)	-0.001 (0.005)
Mean diameter for VLDL prt	27005778	metabolites	European	0.119	0.092	1.286	$1.99 \cdot 10^{-1}$	0.121 (0.039)	0.997 (0.011)	0.002 (0.006)
Mono-unsaturated fatty acids	27005778	metabolites	European	−0.116	0.111	−1.044	$2.97 \cdot 10^{-1}$	0.105 (0.045)	0.988 (0.008)	0.003 (0.006)
Omega-3 fatty acids	27005778	metabolites	European	−0.037	0.094	−0.390	$6.97 \cdot 10^{-1}$	0.136 (0.043)	0.996 (0.009)	0.003 (0.006)
Omega-9 and saturated fatty acids	27005778	metabolites	European	−0.130	0.131	−0.997	$3.19 \cdot 10^{-1}$	0.082 (0.045)	0.998 (0.009)	0.003 (0.006)
Phenylalanine	27005778	metabolites	European	0.007	0.119	0.063	$9.50 \cdot 10^{-1}$	0.057 (0.024)	1.004 (0.008)	-0.002 (0.006)
PhosLip in chylom and lrgst VLDL prt	27005778	metabolites	European	−0.024	0.094	−0.256	$7.98 \cdot 10^{-1}$	0.119 (0.028)	0.975 (0.008)	0.003 (0.006)
PhosLip in IDL	27005778	metabolites	European	0.021	0.149	0.140	$8.88 \cdot 10^{-1}$	0.043 (0.052)	1.029 (0.027)	-0.006 (0.006)
PhosLip in large HDL	27005778	metabolites	European	−0.151	0.102	−1.490	$1.36 \cdot 10^{-1}$	0.106 (0.036)	1.008 (0.019)	0.005 (0.006)
PhosLip in large LDL	27005778	metabolites	European	−0.006	0.141	−0.039	$9.69 \cdot 10^{-1}$	0.048 (0.059)	1.024 (0.030)	-0.007 (0.006)
PhosLip in large VLDL	27005778	metabolites	European	0.024	0.094	0.258	$7.96 \cdot 10^{-1}$	0.116 (0.033)	0.990 (0.009)	0.004 (0.006)
PhosLip in medium HDL	27005778	metabolites	European	−0.202	0.109	−1.851	$6.42 \cdot 10^{-2}$	0.067 (0.028)	0.996 (0.010)	0.002 (0.006)
PhosLip in medium LDL	27005778	metabolites	European	0.079	0.120	0.662	$5.08 \cdot 10^{-1}$	0.067 (0.055)	1.012 (0.027)	-0.010 (0.006)
PhosLip in medium VLDL	27005778	metabolites	European	0.079	0.092	0.862	$3.89 \cdot 10^{-1}$	0.106 (0.035)	0.999 (0.009)	-0.001 (0.006)
PhosLip in small VLDL	27005778	metabolites	European	0.126	0.092	1.377	$1.69 \cdot 10^{-1}$	0.106 (0.037)	1.003 (0.011)	-0.006 (0.006)
PhosLip in very large HDL	27005778	metabolites	European	−0.045	0.121	−0.370	$7.12 \cdot 10^{-1}$	0.068 (0.038)	1.018 (0.023)	0.004 (0.006)
PhosLip in very large VLDL	27005778	metabolites	European	0.018	0.094	0.197	$8.44 \cdot 10^{-1}$	0.117 (0.030)	0.982 (0.008)	0.003 (0.006)
PhosLip in very small VLDL	27005778	metabolites	European	0.017	0.119	0.143	$8.86 \cdot 10^{-1}$	0.067 (0.044)	1.022 (0.020)	-0.006 (0.006)
Ratio of bisal grps to dbl bonds	27005778	metabolites	European	−0.013	0.064	−0.211	$8.33 \cdot 10^{-1}$	0.306 (0.102)	0.975 (0.012)	0.000 (0.006)
Ratio of bisal grps to tot fatty acids	27005778	metabolites	European	0.039	0.070	0.560	$5.75 \cdot 10^{-1}$	0.287 (0.091)	0.983 (0.011)	-0.006 (0.006)
Serum tot cholest	27005778	metabolites	European	0.065	0.131	0.497	$6.19 \cdot 10^{-1}$	0.059 (0.047)	1.024 (0.021)	-0.008 (0.006)
Serum tot triglycerides	27005778	metabolites	European	0.063	0.079	0.798	$4.25 \cdot 10^{-1}$	0.133 (0.037)	0.989 (0.010)	-0.001 (0.006)
Tot cholest in HDL	27005778	metabolites	European	−0.158	0.105	−1.507	$1.32 \cdot 10^{-1}$	0.085 (0.033)	1.012 (0.017)	0.004 (0.006)
Tot cholest in IDL	27005778	metabolites	European	0.003	0.148	0.017	$9.87 \cdot 10^{-1}$	0.052 (0.060)	1.027 (0.028)	-0.006 (0.006)
Tot cholest in large HDL	27005778	metabolites	European	−0.158	0.106	−1.488	$1.37 \cdot 10^{-1}$	0.085 (0.034)	1.016 (0.020)	0.007 (0.006)
Tot cholest in large LDL	27005778	metabolites	European	0.025	0.139	0.178	$8.59 \cdot 10^{-1}$	0.051 (0.063)	1.022 (0.032)	-0.007 (0.006)
Tot cholest in large VLDL	27005778	metabolites	European	0.073	0.086	0.846	$3.98 \cdot 10^{-1}$	0.121 (0.032)	0.990 (0.008)	0.001 (0.006)
Tot cholest in LDL	27005778	metabolites	European	0.085	0.133	0.640	$5.22 \cdot 10^{-1}$	0.059 (0.068)	1.019 (0.034)	-0.009 (0.006)
Tot cholest in medium HDL	27005778	metabolites	European	−0.222	0.125	−1.785	$7.42 \cdot 10^{-2}$	0.051 (0.029)	1.001 (0.011)	0.003 (0.006)
Tot cholest in medium LDL	27005778	metabolites	European	0.084	0.131	0.638	$5.23 \cdot 10^{-1}$	0.059 (0.063)	1.018 (0.032)	-0.010 (0.006)
Tot cholest in medium VLDL	27005778	metabolites	European	0.103	0.088	1.178	$2.39 \cdot 10^{-1}$	0.117 (0.037)	0.996 (0.010)	-0.004 (0.006)
Tot cholest in small LDL	27005778	metabolites	European	0.135	0.136	0.990	$3.22 \cdot 10^{-1}$	0.066 (0.056)	1.018 (0.027)	-0.009 (0.006)
Tot cholest in small VLDL	27005778	metabolites	European	0.186	0.118	1.584	$1.13 \cdot 10^{-1}$	0.072 (0.036)	1.014 (0.013)	-0.010 (0.006)
Tot cholest in very large HDL	27005778	metabolites	European	−0.195	0.200	−0.977	$3.29 \cdot 10^{-1}$	0.028 (0.028)	1.017 (0.016)	0.007 (0.006)

Continues on the next page

Supplementary Table 5 – continued from previous page

Trait	PMID	Category	Ethnicity	r_G	se	Z	P	h^2_G obs (se)	h^2_G Int (se)	GCOV Int (se)
Tot lipids in chylom and lrgst VLDL prt	27005778	metabolites	European	−0.027	0.093	−0.292	$7.71 \cdot 10^{-1}$	0.141 (0.029)	0.982 (0.008)	0.003 (0.006)
Tot lipids in IDL	27005778	metabolites	European	0.002	0.140	0.014	$9.89 \cdot 10^{-1}$	0.056 (0.057)	1.027 (0.026)	-0.006 (0.006)
Tot lipids in large HDL	27005778	metabolites	European	−0.137	0.101	−1.353	$1.76 \cdot 10^{-1}$	0.108 (0.037)	1.011 (0.020)	0.006 (0.006)
Tot lipids in large LDL	27005778	metabolites	European	0.038	0.138	0.279	$7.81 \cdot 10^{-1}$	0.061 (0.068)	1.021 (0.031)	-0.008 (0.006)
Tot lipids in large VLDL	27005778	metabolites	European	0.042	0.094	0.449	$6.54 \cdot 10^{-1}$	0.141 (0.033)	0.985 (0.009)	0.003 (0.007)
Tot lipids in medium HDL	27005778	metabolites	European	−0.197	0.121	−1.633	$1.03 \cdot 10^{-1}$	0.062 (0.031)	0.997 (0.010)	0.002 (0.006)
Tot lipids in medium LDL	27005778	metabolites	European	0.066	0.126	0.520	$6.03 \cdot 10^{-1}$	0.071 (0.065)	1.014 (0.029)	-0.008 (0.006)
Tot lipids in medium VLDL	27005778	metabolites	European	0.083	0.086	0.973	$3.30 \cdot 10^{-1}$	0.141 (0.037)	0.986 (0.009)	-0.001 (0.006)
Tot lipids in small HDL	27005778	metabolites	European	−0.020	0.133	−0.149	$8.82 \cdot 10^{-1}$	0.051 (0.030)	1.004 (0.009)	-0.006 (0.006)
Tot lipids in small LDL	27005778	metabolites	European	0.078	0.116	0.671	$5.02 \cdot 10^{-1}$	0.081 (0.057)	1.010 (0.025)	-0.008 (0.006)
Tot lipids in small VLDL	27005778	metabolites	European	0.121	0.084	1.441	$1.50 \cdot 10^{-1}$	0.142 (0.039)	0.993 (0.010)	-0.006 (0.006)
Tot lipids in very large HDL	27005778	metabolites	European	−0.066	0.149	−0.443	$6.58 \cdot 10^{-1}$	0.044 (0.035)	1.024 (0.021)	0.004 (0.006)
Tot lipids in very large VLDL	27005778	metabolites	European	0.037	0.090	0.408	$6.83 \cdot 10^{-1}$	0.152 (0.032)	0.973 (0.008)	0.000 (0.006)
Tot lipids in very small VLDL	27005778	metabolites	European	0.031	0.101	0.309	$7.57 \cdot 10^{-1}$	0.092 (0.041)	1.016 (0.016)	-0.005 (0.006)
Trigly in chylom and lrgst VLDL prt	27005778	metabolites	European	−0.039	0.091	−0.425	$6.71 \cdot 10^{-1}$	0.107 (0.029)	0.984 (0.009)	0.006 (0.006)
Trigly in IDL	27005778	metabolites	European	0.027	0.096	0.280	$7.80 \cdot 10^{-1}$	0.098 (0.041)	1.013 (0.019)	-0.005 (0.006)
Trigly in large VLDL	27005778	metabolites	European	0.044	0.093	0.476	$6.34 \cdot 10^{-1}$	0.116 (0.031)	0.987 (0.009)	0.004 (0.006)
Trigly in medium VLDL	27005778	metabolites	European	0.079	0.100	0.789	$4.30 \cdot 10^{-1}$	0.094 (0.032)	1.000 (0.009)	0.002 (0.006)
Trigly in small HDL	27005778	metabolites	European	0.157	0.114	1.372	$1.70 \cdot 10^{-1}$	0.059 (0.029)	1.002 (0.010)	-0.007 (0.005)
Trigly in small VLDL	27005778	metabolites	European	0.125	0.086	1.458	$1.45 \cdot 10^{-1}$	0.124 (0.037)	0.993 (0.010)	-0.004 (0.006)
Trigly in very large HDL	27005778	metabolites	European	−0.003	0.113	−0.027	$9.78 \cdot 10^{-1}$	0.066 (0.040)	1.023 (0.037)	0.001 (0.006)
Trigly in very large VLDL	27005778	metabolites	European	0.040	0.085	0.472	$6.37 \cdot 10^{-1}$	0.136 (0.030)	0.974 (0.008)	0.001 (0.006)
Trigly in very small VLDL	27005778	metabolites	European	0.085	0.079	1.069	$2.85 \cdot 10^{-1}$	0.143 (0.039)	0.996 (0.012)	-0.005 (0.006)
Tyrosine	27005778	metabolites	European	−0.072	0.107	−0.678	$4.98 \cdot 10^{-1}$	0.067 (0.029)	1.004 (0.008)	0.004 (0.006)
Valine	27005778	metabolites	European	0.081	0.116	0.699	$4.84 \cdot 10^{-1}$	0.062 (0.022)	1.014 (0.008)	-0.001 (0.006)
Ferritin	25352340	metal	European	0.008	0.101	0.074	$9.41 \cdot 10^{-1}$	0.086 (0.030)	1.030 (0.011)	-0.003 (0.007)
Transferrin	25352340	metal	European	0.039	0.085	0.451	$6.52 \cdot 10^{-1}$	0.162 (0.079)	1.062 (0.027)	-0.001 (0.007)
Alzheimers disease	24162737	neurological	European	0.055	0.104	0.525	$6.00 \cdot 10^{-1}$	0.039 (0.029)	1.074 (0.042)	-0.002 (0.006)
Amyotrophic lateral sclerosis	27455348	neurological	European	−0.005	0.125	−0.041	$9.67 \cdot 10^{-1}$	0.051 (0.014)	0.993 (0.008)	-0.003 (0.006)
Parkinsons disease	19915575	neurological	European	0.103	0.071	1.463	$1.44 \cdot 10^{-1}$	0.341 (0.127)	1.130 (0.011)	-0.008 (0.005)
Male pat baldness*	28196072	other	European	−0.133	0.043	−3.106	$1.90 \cdot 10^{-3}$	0.298 (0.049)	1.038 (0.028)	0.017 (0.007)
SCDC*	28044064	other	European	0.375	0.126	2.986	$2.80 \cdot 10^{-3}$	0.304 (0.096)	0.986 (0.008)	-0.010 (0.006)
Self-rated health*	27864402	other	European	0.081	0.059	1.386	$1.66 \cdot 10^{-1}$	0.095 (0.006)	1.018 (0.009)	0.010 (0.007)
Self-reported tiredness*	28194004	other	European	0.331	0.055	5.992	$2.07 \cdot 10^{-9}$	0.068 (0.006)	0.994 (0.008)	-0.007 (0.006)
Urate	23263486	other	European	0.012	0.042	0.284	$7.77 \cdot 10^{-1}$	0.186 (0.068)	0.934 (0.070)	0.002 (0.007)
Neo-conscientiousness	21173776	personality	European	−0.173	0.152	−1.142	$2.54 \cdot 10^{-1}$	0.072 (0.032)	1.002 (0.009)	-0.009 (0.007)
Neo-openness to experience	21173776	personality	European	0.339	0.105	3.246	$1.20 \cdot 10^{-3}$	0.123 (0.029)	0.985 (0.008)	0.002 (0.006)
Neuroticism	24828478	personality	European	0.217	0.116	1.879	$6.03 \cdot 10^{-2}$	0.012 (0.004)	1.018 (0.008)	-0.006 (0.007)

Continues on the next page

Supplementary Table 5 – continued from previous page

Trait	PMID	Category	Ethnicity	r_G	se	Z	P	h^2_G obs (se)	h^2_G Int (se)	GCOV Int (se)
Neuroticism	27089181	personality	European	0.270	0.067	4.065	$4.81 \cdot 10^{-5}$	0.090 (0.009)	0.987 (0.017)	-0.012 (0.011)
ADHD*	30478444	psychiatric	Mixed	0.360	0.051	7.101	$1.24 \cdot 10^{-12}$	0.229 (0.015)	1.034 (0.010)	0.351 (0.008)
Anorexia Nervosa	24514567	psychiatric	European	0.059	0.064	0.923	$3.56 \cdot 10^{-1}$	0.388 (0.033)	0.960 (0.009)	0.008 (0.006)
Bipolar disorder	21926972	psychiatric	European	0.110	0.066	1.677	$9.36 \cdot 10^{-2}$	0.396 (0.041)	1.038 (0.009)	0.004 (0.007)
Depressive symptoms	27089181	psychiatric	European	0.320	0.063	5.106	$3.28 \cdot 10^{-7}$	0.046 (0.004)	1.007 (0.009)	-0.001 (0.007)
Major depression*	29700475	psychiatric	European	0.412	0.039	10.454	$1.40 \cdot 10^{-25}$	0.056 (0.003)	1.006 (0.012)	-0.000 (0.007)
Schizophrenia	25056061	psychiatric	Mixed	0.211	0.048	4.410	$1.03 \cdot 10^{-5}$	0.424 (0.020)	1.110 (0.016)	0.018 (0.009)
Subjective well being	27089181	psychiatric	European	−0.491	0.055	−8.876	$6.93 \cdot 10^{-19}$	0.025 (0.002)	1.002 (0.009)	0.009 (0.007)
Age at Menarche	25231870	reproductive	European	−0.108	0.036	−3.029	$2.50 \cdot 10^{-3}$	0.211 (0.011)	0.931 (0.015)	-0.002 (0.007)
Age at Menopause	26414677	reproductive	European	−0.014	0.054	−0.263	$7.93 \cdot 10^{-1}$	0.135 (0.017)	0.992 (0.017)	0.005 (0.007)
Age of first birth	27798627	reproductive	European	0.005	0.051	0.104	$9.17 \cdot 10^{-1}$	0.062 (0.004)	0.957 (0.011)	-0.003 (0.007)
Number of children ever born	27798627	reproductive	European	−0.024	0.051	−0.464	$6.42 \cdot 10^{-1}$	0.026 (0.002)	0.968 (0.008)	-0.009 (0.006)
Social deprivation*	27864402	SES	European	0.224	0.075	2.985	$2.80 \cdot 10^{-3}$	0.038 (0.005)	1.012 (0.009)	0.004 (0.006)
Chronotype	27494321	sleeping	European	−0.209	0.047	−4.420	$9.88 \cdot 10^{-6}$	0.103 (0.006)	1.011 (0.010)	0.009 (0.006)
Sleep duration	27494321	sleeping	European	−0.080	0.077	−1.043	$2.97 \cdot 10^{-1}$	0.053 (0.006)	1.027 (0.010)	0.006 (0.007)
Age of smoking initiation	20418890	smokingbehaviour	European	−0.127	0.135	−0.943	$3.46 \cdot 10^{-1}$	0.060 (0.020)	1.000 (0.008)	0.007 (0.007)
Cigarettes smoked per day	20418890	smokingbehaviour	European	0.080	0.104	0.762	$4.46 \cdot 10^{-1}$	0.055 (0.017)	1.009 (0.008)	-0.003 (0.006)
Ever vs never smoked	20418890	smokingbehaviour	European	0.063	0.062	1.012	$3.12 \cdot 10^{-1}$	0.068 (0.007)	1.008 (0.007)	-0.009 (0.005)
Former vs Current smoker	20418890	smokingbehaviour	European	0.046	0.112	0.409	$6.83 \cdot 10^{-1}$	0.054 (0.012)	1.009 (0.008)	0.006 (0.006)
Serumurate overweight	25811787	uricacid	European	−0.082	0.068	−1.194	$2.33 \cdot 10^{-1}$	0.535 (0.348)	0.969 (0.037)	0.005 (0.006)

3.2.3 MTAG analysis and tophits in related phenotypes

Supplementary Table 6: Top hits of MTAG analyses: An extended version of Table 1b of the main manuscript including also the effect size and p-value for the contributing secondary phenotypes as well as the original GWAS signal: Loci from the three MTAG analyses with schizophrenia (SCZ)[8], educational attainment (Edu)[50] and major depression (MD)[48] — loci not already represented in the ASD scan. Independent loci ($r^2 < 0.1$, distance > 400kb) with index variant (Index var), chromosome (CHR), chromosomal position (BP), MTAG estimate of effect (β) with respect to A1, standard error of β (SE), the association p-value of the index variant (P), and max FDR (mFDR), alleles (A1/A2), allele frequency of A1 (FRQ). The "Analysis" column shows the analysis that generated the particular MTAG result. The corresponding P-value (P) and effect size (β) from the ASD scan (logistic regression and inverse variance weighted meta-analysis) and the secondary phenotype (logistic regression and inverse variance weighted meta-analysis except for educational attainment which linear regression) is provided together with the weight assigned to the secondary phenotype by MTAG (Weight). All p-values are derived from z-scores. The column "Nearest genes" lists nearest genes from within 50kb of the $r^2 \geq 0.6$ LD friends of the index variant. The loci also found in the 88-loci follow-up sample (Table 3) are marked with *. They all show same direction of effect. Figures 49–55 show regional plot for the 7 loci.

			MTAG							ASD scan		Secundary phenotype			
Index var	CHR	BP	P	β	SE	mFDR	A1/A2	FRQ	Analysis	P	β	P	β	Weight	Nearest genes
rs2388334*	6	98,591,622	$3.34 \cdot 10^{-12}$	−0.065	0.009	0.021	A/G	0.517	ASD-Edu	$1.00 \cdot 10^{-6}$	−0.068	$6.56 \cdot 10^{-21}$	−0.023	0.108	MMS22L, POU3F2
rs325506*	5	104,012,303	$3.26 \cdot 10^{-11}$	0.057	0.009	0.012	C/G	0.423	ASD-MD	$3.50 \cdot 10^{-7}$	0.071	$2.17 \cdot 10^{-7}$	0.026	0.244	NUD12
rs11787216*	8	142,615,222	$2.00 \cdot 10^{-9}$	−0.058	0.010	0.021	T/C	0.364	ASD-Edu	$2.59 \cdot 10^{-6}$	−0.030	$6.12 \cdot 10^{-10}$	−0.016	0.108	MROH5
rs1452075*	3	62,481,063	$3.17 \cdot 10^{-9}$	0.061	0.010	0.021	T/C	0.721	ASD-Edu	$2.07 \cdot 10^{-7}$	0.035	$7.44 \cdot 10^{-5}$	0.011	0.108	CADPS
rs1620977	1	72,729,142	$6.66 \cdot 10^{-9}$	0.056	0.010	0.012	A/G	0.260	ASD-MD	$1.19 \cdot 10^{-4}$	0.062	$7.64 \cdot 10^{-9}$	0.032	0.244	NEGR1
rs10149470	14	104,017,953	$8.52 \cdot 10^{-9}$	−0.049	0.008	0.012	A/G	0.487	ASD-MD	$8.49 \cdot 10^{-5}$	−0.056	$3.57 \cdot 10^{-8}$	−0.028	0.244	MARK3, CKB, TRMT61A, BAG5, APOPT1, KLC1, XRCC3
rs16854048	4	42,123,728	$1.29 \cdot 10^{-8}$	0.069	0.012	0.012	A/C	0.858	ASD-MD	$5.87 \cdot 10^{-5}$	0.082	$2.44 \cdot 10^{-7}$	0.038	0.244	SLC30A9, BEND4, TMEM33, DCAF4L1

Supplementary Table 7: Look-up in the ASD scan of the top major depression loci[48] shown together with the results from the corresponding MTAG analysis. The 40 loci represented in the ASD summary statistics are shown. The columns are chromosome (CHR), marker name in the major depression scan (SNP), chromosomal position (BP), logistic regression effect size (β), standard error of effect (SE), p-value (P) in major depression, ASD and the ASD-major-depression MTAG analysis, allele names (A1A2), minor allele frequency in ASD cases (FRQ A) and controls (FRQ U). The results are presented in order of the p-values in the major depression scan, and statistically significant MTAG results ($P < 1.667 \cdot 10^{-8}$) are presented in red. The effect measures of ASD and major depression were estimated using logistic regression and inverse variance weighted meta-analysis, and all p-values were estimated from the z-scores.

			Major Depression			ASD			ASD-MD MTAG					
CHR	SNP	BP	β	SE	P	β	SE	P	β	SE	P	A1/A2	FRQ A	FRQ U
13	rs12552	53,625,781	0.039	0.005	$6.10 \cdot 10^{-19}$	0.032	0.014	$2.18 \cdot 10^{-2}$	0.047	0.009	$3.72 \cdot 10^{-8}$	A/G	0.434	0.424
1	rs1432639	72,813,218	0.039	0.005	$4.60 \cdot 10^{-15}$	0.036	0.014	$1.04 \cdot 10^{-2}$	0.045	0.009	$1.32 \cdot 10^{-7}$	A/C	0.611	0.598
15	rs8025231	37,648,402	−0.030	0.005	$2.40 \cdot 10^{-12}$	0.014	0.014	$3.15 \cdot 10^{-1}$	−0.017	0.009	$4.78 \cdot 10^{-2}$	A/C	0.560	0.556
1	rs12129573	73,768,366	0.039	0.005	$4.00 \cdot 10^{-12}$	0.026	0.014	$7.23 \cdot 10^{-2}$	0.037	0.009	$2.41 \cdot 10^{-5}$	A/C	0.371	0.364
18	rs12958048	53,101,598	0.030	0.005	$3.60 \cdot 10^{-11}$	−0.004	0.015	$7.78 \cdot 10^{-1}$	0.021	0.009	$1.82 \cdot 10^{-2}$	A/G	0.327	0.328
5	chr5:87992715:I	87,992,715	−0.030	0.005	$7.90 \cdot 10^{-11}$	−0.003	0.014	$8.31 \cdot 10^{-1}$				T/TA	0.407	0.405
10	rs61867293	106,563,924	−0.041	0.006	$7.00 \cdot 10^{-10}$	−0.051	0.017	$2.86 \cdot 10^{-3}$	−0.050	0.010	$1.24 \cdot 10^{-6}$	T/C	0.207	0.216
14	rs915057	64,686,207	−0.030	0.005	$7.60 \cdot 10^{-10}$	−0.026	0.014	$6.74 \cdot 10^{-2}$	−0.033	0.009	$9.39 \cdot 10^{-5}$	A/G	0.430	0.439
5	rs11135349	164,523,472	−0.030	0.005	$1.10 \cdot 10^{-9}$	0.013	0.014	$3.69 \cdot 10^{-1}$	−0.014	0.009	$9.49 \cdot 10^{-2}$	A/C	0.441	0.432
11	rs1806153	31,850,105	0.039	0.006	$1.20 \cdot 10^{-9}$	0.058	0.017	$6.59 \cdot 10^{-4}$	0.057	0.010	$4.14 \cdot 10^{-8}$	T/G	0.222	0.213
14	rs4904738	42,179,732	−0.030	0.005	$2.60 \cdot 10^{-9}$	−0.013	0.014	$3.46 \cdot 10^{-1}$	−0.026	0.009	$2.13 \cdot 10^{-3}$	T/C	0.561	0.566
3	rs7430565	158,107,180	−0.030	0.005	$2.90 \cdot 10^{-9}$	−0.025	0.014	$7.67 \cdot 10^{-2}$	−0.034	0.009	$7.51 \cdot 10^{-5}$	A/G	0.566	0.570
14	rs10149470	104,017,953	−0.030	0.005	$3.10 \cdot 10^{-9}$	−0.056	0.014	$8.49 \cdot 10^{-5}$	−0.049	0.008	$8.52 \cdot 10^{-9}$	A/G	0.476	0.487
4	rs34215985	42,047,778	−0.041	0.006	$3.10 \cdot 10^{-9}$	−0.057	0.017	$9.48 \cdot 10^{-4}$	−0.055	0.010	$1.59 \cdot 10^{-7}$	C/G	0.202	0.211
2	rs11682175	57,987,593	−0.030	0.005	$4.70 \cdot 10^{-9}$	−0.024	0.014	$8.48 \cdot 10^{-2}$	−0.033	0.008	$1.01 \cdot 10^{-4}$	T/C	0.529	0.536
9	rs10959913	11,544,964	0.030	0.006	$5.10 \cdot 10^{-9}$	−0.031	0.016	$5.80 \cdot 10^{-2}$	0.007	0.010	$4.69 \cdot 10^{-1}$	T/G	0.746	0.751
5	rs4869056	166,992,078	−0.030	0.005	$6.80 \cdot 10^{-9}$	−0.025	0.014	$7.84 \cdot 10^{-2}$	−0.032	0.009	$2.51 \cdot 10^{-4}$	A/G	0.629	0.635
16	rs8063603	6,310,645	−0.030	0.005	$6.90 \cdot 10^{-9}$	−0.042	0.015	$5.62 \cdot 10^{-3}$	−0.041	0.009	$6.97 \cdot 10^{-6}$	A/G	0.662	0.673
5	rs116755193	124,251,883	−0.030	0.005	$7.00 \cdot 10^{-9}$	−0.009	0.015	$5.37 \cdot 10^{-1}$	−0.025	0.009	$3.64 \cdot 10^{-3}$	T/C	0.386	0.391
22	rs5758265	41,617,897	0.030	0.005	$7.60 \cdot 10^{-9}$	0.024	0.016	$1.20 \cdot 10^{-1}$	0.036	0.010	$1.70 \cdot 10^{-4}$	A/G	0.278	0.271
17	rs17727765	27,576,962	−0.051	0.009	$8.50 \cdot 10^{-9}$	0.014	0.027	$5.92 \cdot 10^{-1}$	−0.029	0.016	$7.11 \cdot 10^{-2}$	T/C	0.923	0.923
9	rs7856424	119,733,595	−0.030	0.005	$8.50 \cdot 10^{-9}$	0.000	0.015	$9.94 \cdot 10^{-1}$	−0.021	0.009	$2.80 \cdot 10^{-2}$	T/C	0.287	0.286
16	rs7198928	7,666,402	0.030	0.005	$1.00 \cdot 10^{-8}$	−0.005	0.014	$7.22 \cdot 10^{-1}$	0.019	0.009	$2.54 \cdot 10^{-2}$	T/C	0.610	0.610
1	rs2389016	80,799,329	0.030	0.005	$1.00 \cdot 10^{-8}$	0.011	0.015	$4.86 \cdot 10^{-1}$	0.029	0.009	$2.35 \cdot 10^{-3}$	T/C	0.284	0.283
1	rs4261101	90,796,053	−0.030	0.005	$1.00 \cdot 10^{-8}$	−0.011	0.014	$4.67 \cdot 10^{-1}$	−0.026	0.009	$2.74 \cdot 10^{-3}$	A/G	0.357	0.357
18	rs62099069	36,883,737	−0.030	0.005	$1.30 \cdot 10^{-8}$	−0.008	0.014	$5.53 \cdot 10^{-1}$	−0.024	0.009	$5.74 \cdot 10^{-3}$	A/T	0.414	0.417
7	rs12666117	109,105,611	0.030	0.005	$1.40 \cdot 10^{-8}$	0.007	0.014	$6.22 \cdot 10^{-1}$	0.024	0.008	$3.86 \cdot 10^{-3}$	A/G	0.474	0.474
18	rs11663393	50,614,732	0.030	0.005	$1.60 \cdot 10^{-8}$	0.005	0.014	$7.09 \cdot 10^{-1}$	0.022	0.008	$9.85 \cdot 10^{-3}$	A/G	0.490	0.493
16	rs7200826	13,066,833	0.030	0.006	$2.40 \cdot 10^{-8}$	0.003	0.016	$8.61 \cdot 10^{-1}$	0.022	0.010	$2.40 \cdot 10^{-2}$	T/C	0.257	0.258
2	rs1226412	157,111,313	0.030	0.006	$2.40 \cdot 10^{-8}$	0.012	0.017	$4.84 \cdot 10^{-1}$	0.032	0.011	$2.60 \cdot 10^{-3}$	T/C	0.802	0.801
9	rs1354115	2,983,774	0.030	0.005	$2.40 \cdot 10^{-8}$	−0.009	0.014	$5.22 \cdot 10^{-1}$	0.015	0.009	$9.35 \cdot 10^{-2}$	A/C	0.626	0.631
13	rs4143229	44,327,799	−0.051	0.009	$2.50 \cdot 10^{-8}$	−0.002	0.027	$9.35 \cdot 10^{-1}$	−0.037	0.017	$2.57 \cdot 10^{-2}$	A/C	0.929	0.930
7	rs10950398	12,264,871	0.030	0.005	$2.60 \cdot 10^{-8}$	−0.017	0.014	$2.16 \cdot 10^{-1}$	0.010	0.009	$2.34 \cdot 10^{-1}$	A/G	0.418	0.424
9	rs7029033	126,682,068	0.049	0.009	$2.70 \cdot 10^{-8}$	−0.014	0.025	$5.87 \cdot 10^{-1}$	0.027	0.015	$7.65 \cdot 10^{-2}$	T/C	0.080	0.083
6	rs9402472	99,566,521	0.030	0.006	$2.80 \cdot 10^{-8}$	0.004	0.016	$8.31 \cdot 10^{-1}$	0.023	0.010	$2.14 \cdot 10^{-2}$	A/G	0.235	0.234
12	rs4074723	23,947,737	−0.030	0.005	$3.10 \cdot 10^{-8}$	−0.010	0.014	$4.78 \cdot 10^{-1}$	−0.023	0.009	$7.03 \cdot 10^{-3}$	A/C	0.403	0.404
1	rs9427672	197,754,741	−0.030	0.006	$3.10 \cdot 10^{-8}$	0.041	0.017	$1.49 \cdot 10^{-2}$	−0.005	0.010	$6.26 \cdot 10^{-1}$	A/G	0.227	0.218
1	rs159963	8,504,421	−0.030	0.005	$3.20 \cdot 10^{-8}$	−0.021	0.014	$1.36 \cdot 10^{-1}$	−0.031	0.009	$3.32 \cdot 10^{-4}$	A/C	0.569	0.577
16	rs11643192	72,214,276	0.030	0.005	$3.40 \cdot 10^{-8}$	0.035	0.014	$1.31 \cdot 10^{-2}$	0.038	0.009	$1.14 \cdot 10^{-5}$	A/C	0.388	0.375
3	chr3:44287760:I	44,287,760	0.030	0.005	$4.60 \cdot 10^{-8}$	0.010	0.015	$4.99 \cdot 10^{-1}$				A/AT	0.670	0.670

Supplementary Table 8: Look-up in the ASD scan of the top educational attainment loci[50] shown together with the results from the corresponding MTAG analysis. The 73 loci represented in the ASD summary statistics are shown. The columns are chromosome (CHR), marker name in educational attainment scan (SNP), chromosomal position (BP), linear regression effect size (β), standard error of effect (SE), p-value (P) in educational attainment, ASD and the ASD-educational-attainment MTAG analysis, allele names (A1A2), minor allele frequency in ASD cases (FRQ A) and controls (FRQ U). The results are presented in order of the p-values in the major depression scan, and statistically significant MTAG results ($P < 1.667 \cdot 10^{-8}$) are presented in red. The effect measures of ASD were estimated using logistic regression and inverse variance weighted meta-analysis and those fore educational attainment by linear regression. P-values were estimated from the z-scores.

			Educational Attainment			ASD			ASD-Edu MTAG					
CHR	SNP	BP	β	SE	P	β	SE	P	β	SE	P	A1/A2	FRQ A	FRQ U
3	rs11712056	49,914,397	0.025	0.002	$7.53 \cdot 10^{-24}$	0.026	0.014	$6.01 \cdot 10^{-2}$	0.040	0.009	$2.04 \cdot 10^{-5}$	T/C	0.563	0.558
3	rs148734725	49,406,708	0.027	0.003	$1.25 \cdot 10^{-23}$	0.028	0.015	$6.21 \cdot 10^{-2}$	0.043	0.010	$2.29 \cdot 10^{-5}$	A/G	0.304	0.298
9	rs13294439	23,358,875	−0.025	0.003	$6.63 \cdot 10^{-23}$	−0.040	0.014	$4.71 \cdot 10^{-3}$	−0.048	0.009	$3.22 \cdot 10^{-7}$	A/C	0.589	0.596
6	rs9320913	98,584,733	0.024	0.002	$2.05 \cdot 10^{-21}$	0.067	0.014	$1.51 \cdot 10^{-6}$	0.064	0.009	$4.66 \cdot 10^{-12}$	A/C	0.498	0.483

Continues on the next page

Supplementary Table 8 – continued from previous page

			Educational Attainment			ASD			ASD-Edu MTAG					
CHR	SNP	BP	β	SE	P	β	SE	P	β	SE	P	A1/A2	FRQ A	FRQ U
2	rs12987662	100,821,548	0.022	0.003	$3.25 \cdot 10^{-18}$	0.005	0.014	$7.14 \cdot 10^{-1}$	0.023	0.009	$1.31 \cdot 10^{-2}$	A/C	0.399	0.399
13	rs9537821	58,402,771	0.023	0.003	$8.61 \cdot 10^{-17}$	−0.023	0.015	$1.26 \cdot 10^{-1}$	0.006	0.010	$5.63 \cdot 10^{-1}$	A/G	0.708	0.709
1	rs34305371	72,733,610	0.036	0.004	$2.34 \cdot 10^{-16}$	0.024	0.025	$3.35 \cdot 10^{-1}$	0.047	0.016	$3.40 \cdot 10^{-3}$	A/G	0.095	0.092
12	rs7306755	123,767,929	0.025	0.003	$4.23 \cdot 10^{-16}$	0.002	0.017	$9.03 \cdot 10^{-1}$	0.024	0.012	$3.50 \cdot 10^{-2}$	A/G	0.202	0.202
2	rs17824247	144,152,539	−0.018	0.003	$5.29 \cdot 10^{-13}$	−0.026	0.014	$6.79 \cdot 10^{-2}$	−0.033	0.009	$4.48 \cdot 10^{-4}$	T/C	0.574	0.578
5	rs61160187	60,111,579	−0.018	0.003	$5.93 \cdot 10^{-13}$	−0.026	0.014	$7.07 \cdot 10^{-2}$	−0.033	0.009	$4.86 \cdot 10^{-4}$	A/G	0.593	0.598
10	rs11191193	103,802,408	0.019	0.003	$6.97 \cdot 10^{-13}$	−0.005	0.014	$7.35 \cdot 10^{-1}$	0.014	0.010	$1.51 \cdot 10^{-1}$	A/G	0.634	0.630
1	rs11588857	204,587,047	0.022	0.003	$1.31 \cdot 10^{-12}$	0.001	0.017	$9.35 \cdot 10^{-1}$	0.021	0.011	$6.94 \cdot 10^{-2}$	A/G	0.213	0.214
12	rs2456973	56,416,928	−0.018	0.003	$1.58 \cdot 10^{-12}$	−0.015	0.015	$2.95 \cdot 10^{-1}$	−0.027	0.010	$6.33 \cdot 10^{-3}$	A/C	0.673	0.676
4	rs4863692	140,764,124	0.018	0.003	$3.80 \cdot 10^{-12}$	0.001	0.015	$9.67 \cdot 10^{-1}$	0.017	0.010	$8.16 \cdot 10^{-2}$	T/G	0.312	0.312
18	rs12969294	35,186,122	−0.018	0.003	$1.11 \cdot 10^{-11}$	−0.001	0.015	$9.22 \cdot 10^{-1}$	−0.017	0.010	$7.87 \cdot 10^{-2}$	A/G	0.336	0.336
3	rs112634398	50,075,494	0.041	0.006	$2.45 \cdot 10^{-11}$	−0.002	0.035	$9.62 \cdot 10^{-1}$	0.034	0.021	$1.12 \cdot 10^{-1}$	A/G	0.952	0.951
1	rs1008078	91,189,731	−0.016	0.003	$7.88 \cdot 10^{-11}$	−0.034	0.014	$1.70 \cdot 10^{-2}$	−0.036	0.009	$1.09 \cdot 10^{-4}$	T/C	0.399	0.409
14	rs17119973	84,913,111	−0.018	0.003	$8.39 \cdot 10^{-11}$	−0.021	0.016	$1.77 \cdot 10^{-1}$	−0.030	0.010	$3.99 \cdot 10^{-3}$	A/G	0.260	0.266
1	rs11210860	43,982,527	0.016	0.003	$9.73 \cdot 10^{-11}$	0.016	0.014	$2.54 \cdot 10^{-1}$	0.025	0.010	$7.50 \cdot 10^{-3}$	A/G	0.385	0.384
10	rs12772375	104,082,688	−0.016	0.003	$1.36 \cdot 10^{-10}$	−0.020	0.014	$1.61 \cdot 10^{-1}$	−0.027	0.009	$3.63 \cdot 10^{-3}$	T/G	0.424	0.429
14	rs1043209	23,373,986	0.016	0.003	$1.37 \cdot 10^{-10}$	−0.005	0.014	$7.01 \cdot 10^{-1}$	0.011	0.009	$2.27 \cdot 10^{-1}$	A/G	0.607	0.609
2	rs16845580	161,920,884	0.016	0.003	$2.07 \cdot 10^{-10}$	0.011	0.014	$4.52 \cdot 10^{-1}$	0.022	0.010	$2.29 \cdot 10^{-2}$	T/C	0.626	0.625
12	rs7955289	14,653,667	0.016	0.003	$3.49 \cdot 10^{-10}$	−0.004	0.014	$8.00 \cdot 10^{-1}$	0.012	0.010	$1.95 \cdot 10^{-1}$	A/T	0.618	0.618
5	rs10061788	87,934,707	0.021	0.003	$5.92 \cdot 10^{-10}$	−0.025	0.019	$1.88 \cdot 10^{-1}$	0.003	0.012	$7.93 \cdot 10^{-1}$	A/G	0.172	0.171
2	rs2457660	60,757,419	−0.016	0.003	$7.33 \cdot 10^{-10}$	−0.008	0.015	$5.82 \cdot 10^{-1}$	−0.019	0.010	$4.19 \cdot 10^{-2}$	T/C	0.623	0.626
1	rs2992632	243,503,764	0.017	0.003	$7.64 \cdot 10^{-10}$	−0.008	0.015	$5.85 \cdot 10^{-1}$	0.010	0.010	$3.24 \cdot 10^{-1}$	A/T	0.708	0.710
9	rs1871109	1,746,016	−0.015	0.002	$1.18 \cdot 10^{-9}$	−0.008	0.014	$5.86 \cdot 10^{-1}$				T/G	0.555	0.559
5	rs1402025	113,987,898	0.018	0.003	$1.51 \cdot 10^{-9}$	0.062	0.017	$1.57 \cdot 10^{-4}$	0.055	0.011	$3.67 \cdot 10^{-7}$	T/C	0.774	0.763
6	rs56231335	98,187,291	−0.016	0.003	$1.62 \cdot 10^{-9}$	−0.002	0.016	$9.17 \cdot 10^{-1}$	−0.016	0.010	$1.15 \cdot 10^{-1}$	T/C	0.692	0.694
3	rs62263923	85,674,790	−0.016	0.003	$1.63 \cdot 10^{-9}$	0.001	0.015	$9.53 \cdot 10^{-1}$	−0.014	0.010	$1.55 \cdot 10^{-1}$	A/G	0.645	0.646
3	rs35761247	48,623,124	0.034	0.006	$2.59 \cdot 10^{-9}$	−0.004	0.033	$9.11 \cdot 10^{-1}$	0.029	0.021	$1.76 \cdot 10^{-1}$	A/G	0.049	0.049
2	rs13402908	100,333,377	−0.015	0.002	$2.91 \cdot 10^{-9}$	0.012	0.014	$4.02 \cdot 10^{-1}$	−0.006	0.009	$5.12 \cdot 10^{-1}$	T/C	0.461	0.454
2	rs4500960	162,818,621	−0.014	0.002	$6.55 \cdot 10^{-9}$	−0.025	0.014	$7.43 \cdot 10^{-2}$	−0.029	0.009	$1.78 \cdot 10^{-3}$	T/C	0.459	0.464
17	rs192818565	43,991,515	0.019	0.003	$7.69 \cdot 10^{-9}$	−0.077	0.017	$9.01 \cdot 10^{-6}$				T/G	0.795	0.810
7	rs12671937	92,654,365	0.014	0.003	$1.02 \cdot 10^{-8}$	−0.041	0.014	$4.22 \cdot 10^{-3}$	−0.012	0.009	$1.85 \cdot 10^{-1}$	A/G	0.525	0.534
7	rs17167170	133,302,345	0.017	0.003	$1.62 \cdot 10^{-8}$	0.041	0.017	$1.72 \cdot 10^{-2}$	0.042	0.012	$2.55 \cdot 10^{-4}$	A/G	0.805	0.800
5	rs2964197	57,535,206	0.014	0.002	$2.01 \cdot 10^{-8}$	0.022	0.014	$1.17 \cdot 10^{-1}$	0.027	0.009	$4.12 \cdot 10^{-3}$	T/C	0.485	0.475
5	rs4493682	45,188,024	0.019	0.003	$2.27 \cdot 10^{-8}$	−0.005	0.019	$7.85 \cdot 10^{-1}$	0.014	0.012	$2.67 \cdot 10^{-1}$	C/G	0.168	0.165
8	rs12682297	145,712,860	−0.014	0.002	$2.29 \cdot 10^{-8}$	0.036	0.015	$1.34 \cdot 10^{-2}$	0.009	0.009	$3.23 \cdot 10^{-1}$	A/T	0.483	0.474
2	rs4851251	100,753,490	−0.015	0.003	$2.83 \cdot 10^{-8}$	0.001	0.015	$9.51 \cdot 10^{-1}$	−0.013	0.010	$1.93 \cdot 10^{-1}$	T/C	0.280	0.280
11	rs7945718	12,748,819	0.014	0.003	$2.85 \cdot 10^{-8}$	0.005	0.014	$7.27 \cdot 10^{-1}$	0.016	0.009	$9.03 \cdot 10^{-2}$	A/G	0.608	0.605
2	rs55830725	237,056,854	−0.018	0.003	$3.05 \cdot 10^{-8}$	0.008	0.019	$6.85 \cdot 10^{-1}$	−0.012	0.012	$3.32 \cdot 10^{-1}$	A/T	0.168	0.166
2	rs1606974	51,873,599	0.021	0.004	$4.03 \cdot 10^{-8}$	−0.012	0.021	$5.44 \cdot 10^{-1}$				A/G	0.132	0.135
1	rs1777827	211,613,114	0.014	0.003	$4.19 \cdot 10^{-8}$	0.008	0.014	$5.76 \cdot 10^{-1}$	0.018	0.010	$6.04 \cdot 10^{-2}$	A/G	0.618	0.619
9	rs895606	88,003,668	0.013	0.002	$6.90 \cdot 10^{-8}$	−0.006	0.014	$6.65 \cdot 10^{-1}$	0.008	0.009	$3.63 \cdot 10^{-1}$	A/G	0.436	0.434
12	rs7131944	92,159,557	0.013	0.003	$1.74 \cdot 10^{-7}$	0.005	0.014	$7.08 \cdot 10^{-1}$	0.016	0.009	$1.01 \cdot 10^{-1}$	A/T	0.613	0.607
1	rs2568955	72,762,169	−0.015	0.003	$1.82 \cdot 10^{-7}$	−0.036	0.016	$2.54 \cdot 10^{-2}$	−0.035	0.010	$6.49 \cdot 10^{-4}$	T/C	0.281	0.293
7	rs11768238	135,227,513	−0.014	0.003	$2.12 \cdot 10^{-7}$	−0.004	0.015	$7.87 \cdot 10^{-1}$	−0.015	0.010	$1.26 \cdot 10^{-1}$	A/G	0.328	0.327
1	rs301800	8,490,603	0.017	0.003	$2.43 \cdot 10^{-7}$	0.016	0.018	$3.74 \cdot 10^{-1}$	0.026	0.012	$3.46 \cdot 10^{-2}$	T/C	0.175	0.169
21	rs2837992	42,620,520	0.013	0.003	$3.08 \cdot 10^{-7}$	0.004	0.015	$7.94 \cdot 10^{-1}$	0.014	0.010	$1.33 \cdot 10^{-1}$	T/C	0.375	0.373
2	rs76076331	10,977,585	0.018	0.004	$3.72 \cdot 10^{-7}$	−0.065	0.020	$1.30 \cdot 10^{-3}$	−0.024	0.013	$6.87 \cdot 10^{-2}$	T/C	0.136	0.146
9	rs7854982	124,644,562	−0.013	0.002	$4.05 \cdot 10^{-7}$	0.030	0.014	$3.12 \cdot 10^{-2}$	0.008	0.009	$4.16 \cdot 10^{-1}$	T/C	0.469	0.461
4	rs12646808	3,249,828	0.013	0.003	$4.40 \cdot 10^{-7}$	−0.007	0.015	$6.29 \cdot 10^{-1}$	0.008	0.010	$4.37 \cdot 10^{-1}$	T/C	0.654	0.654
2	rs6739979	193,731,929	−0.013	0.003	$6.53 \cdot 10^{-7}$	0.015	0.014	$2.99 \cdot 10^{-1}$	−0.002	0.010	$8.19 \cdot 10^{-1}$	T/C	0.628	0.627
5	rs324886	87,896,602	−0.012	0.003	$9.67 \cdot 10^{-7}$	0.056	0.014	$7.94 \cdot 10^{-5}$	0.024	0.009	$1.04 \cdot 10^{-2}$	T/C	0.403	0.395
2	rs11690172	57,387,094	0.012	0.003	$1.44 \cdot 10^{-6}$	−0.005	0.014	$7.47 \cdot 10^{-1}$	0.008	0.009	$3.82 \cdot 10^{-1}$	A/G	0.586	0.584
7	rs12531458	39,090,698	0.011	0.002	$3.47 \cdot 10^{-6}$	0.015	0.014	$2.90 \cdot 10^{-1}$	0.020	0.009	$3.18 \cdot 10^{-2}$	A/C	0.524	0.520
5	rs62379838	120,102,028	0.012	0.003	$4.00 \cdot 10^{-6}$	−0.010	0.015	$5.09 \cdot 10^{-1}$	0.005	0.010	$6.17 \cdot 10^{-1}$	T/C	0.696	0.696
5	rs2431108	103,947,968	0.012	0.003	$4.56 \cdot 10^{-6}$	−0.048	0.015	$1.08 \cdot 10^{-3}$	−0.020	0.010	$4.63 \cdot 10^{-2}$	T/C	0.666	0.677
2	rs10496091	61,482,261	−0.012	0.003	$5.61 \cdot 10^{-6}$	0.026	0.015	$9.64 \cdot 10^{-2}$	0.005	0.010	$6.36 \cdot 10^{-1}$	A/G	0.278	0.272
6	rs7767938	153,367,613	0.013	0.003	$5.75 \cdot 10^{-6}$	−0.016	0.016	$3.14 \cdot 10^{-1}$	0.002	0.011	$8.79 \cdot 10^{-1}$	T/C	0.746	0.750
2	rs2245901	194,296,294	−0.011	0.003	$5.98 \cdot 10^{-6}$	0.010	0.014	$4.98 \cdot 10^{-1}$	−0.004	0.009	$6.44 \cdot 10^{-1}$	A/G	0.408	0.407
7	rs113520408	128,402,782	0.013	0.003	$6.59 \cdot 10^{-6}$	−0.010	0.016	$5.27 \cdot 10^{-1}$	0.005	0.010	$6.17 \cdot 10^{-1}$	A/G	0.265	0.266
3	rs6799130	160,847,801	−0.011	0.002	$8.01 \cdot 10^{-6}$	−0.005	0.014	$7.04 \cdot 10^{-1}$	−0.014	0.009	$1.45 \cdot 10^{-1}$	C/G	0.536	0.540
2	rs11689269	15,621,917	0.012	0.003	$8.35 \cdot 10^{-6}$	−0.029	0.015	$4.68 \cdot 10^{-2}$	−0.008	0.010	$4.21 \cdot 10^{-1}$	C/G	0.326	0.334
12	rs572016	121,279,083	0.011	0.002	$1.08 \cdot 10^{-5}$	0.009	0.014	$5.40 \cdot 10^{-1}$	0.015	0.009	$9.64 \cdot 10^{-2}$	A/G	0.509	0.510
22	rs165633	29,880,773	−0.012	0.003	$1.47 \cdot 10^{-5}$	−0.018	0.017	$2.72 \cdot 10^{-1}$	−0.023	0.011	$3.49 \cdot 10^{-2}$	A/G	0.761	0.764
3	rs62259535	48,939,052	0.032	0.008	$2.35 \cdot 10^{-5}$	0.065	0.037	$7.62 \cdot 10^{-2}$	0.064	0.023	$6.39 \cdot 10^{-3}$	A/G	0.963	0.959
2	rs114598875	60,976,384	−0.014	0.003	$2.71 \cdot 10^{-5}$	−0.006	0.017	$7.05 \cdot 10^{-1}$	−0.016	0.011	$1.65 \cdot 10^{-1}$	A/G	0.793	0.795
4	rs34072092	28,801,221	0.016	0.004	$1.06 \cdot 10^{-4}$	0.018	0.023	$4.42 \cdot 10^{-1}$	0.026	0.016	$9.22 \cdot 10^{-2}$	T/C	0.903	0.902
7	rs2615691	23,402,104	−0.023	0.007	$3.42 \cdot 10^{-4}$	−0.056	0.037	$1.33 \cdot 10^{-1}$	−0.055	0.024	$2.09 \cdot 10^{-2}$	A/G	0.037	0.040
4	rs2610986	18,037,231	−0.010	0.003	$3.63 \cdot 10^{-4}$	−0.014	0.016	$3.78 \cdot 10^{-1}$	−0.017	0.010	$8.64 \cdot 10^{-2}$	T/C	0.665	0.667
4	rs3101246	42,649,935	−0.008	0.003	$8.88 \cdot 10^{-4}$	−0.015	0.014	$3.04 \cdot 10^{-1}$	−0.017	0.009	$7.28 \cdot 10^{-2}$	T/G	0.597	0.602

Supplementary Table 9: Look-up in the ASD scan of the top schizophrenia loci[8] shown together with the results from the corresponding MTAG analysis. The 119 loci represented in the ASD summary statistics directly or by proxy are shown. The columns are chromosome (CHR), marker name in schizophrenia scan (SNP), chromosomal position (BP), logistic regression effect size (β), standard error of effect (SE), p-value (P) in schizophrenia, ASD and the ASD-schizophrenia MTAG analysis, minor allele names (A1A2), minor allele frequency in ASD cases (FRQ A) and controls (FRQ U), and proxies where appropriate, - elsewhere (Proxy). The results are presented in order of the p-values in the major depression scan. There were no statistically significant MTAG results ($P < 1.667 \cdot 10^{-8}$) in this range of loci. . The effect measures of ASD and schizophrenia were estimated using logistic regression and inverse variance weighted meta-analysis, and all p-values were estimated from the z-scores.

			Schizophrenia			ASD			ASD-SCZ MTAG						
CHR	SNP	BP	β	SE	P	β	SE	P	β	SE	P	A1/A2	FRQ A	FRQ U	Proxy
6	rs115329265	28,712,247	0.186	0.016	$3.48 \cdot 10^{-31}$	0.029	0.020	$1.49 \cdot 10^{-1}$				A/G	0.863	0.860	-
1	rs1702294	98,501,984	−0.119	0.013	$3.36 \cdot 10^{-19}$	−0.037	0.018	$3.65 \cdot 10^{-2}$	−0.046	0.012	$6.01 \cdot 10^{-5}$	T/C	0.190	0.199	-
10	rs11191419	104,612,335	−0.099	0.011	$6.20 \cdot 10^{-19}$	−0.008	0.015	$5.71 \cdot 10^{-1}$	−0.025	0.010	$8.15 \cdot 10^{-3}$	A/T	0.350	0.351	-
12	rs2007044	2,344,960	−0.092	0.011	$3.22 \cdot 10^{-18}$	0.030	0.014	$3.59 \cdot 10^{-2}$	−0.002	0.009	$8.48 \cdot 10^{-1}$	A/G	0.606	0.596	-
8	rs4129585	143,312,933	0.083	0.010	$1.74 \cdot 10^{-15}$	0.008	0.014	$5.90 \cdot 10^{-1}$	0.021	0.009	$2.15 \cdot 10^{-2}$	A/C	0.440	0.438	-
4	rs35518360	103,146,890	−0.155	0.020	$7.98 \cdot 10^{-15}$	−0.047	0.029	$1.05 \cdot 10^{-1}$	−0.063	0.019	$1.16 \cdot 10^{-3}$	A/T	0.933	0.940	-
7	chr7:2025096:I	2,025,096	−0.081	0.011	$8.20 \cdot 10^{-15}$	−0.003	0.014	$8.61 \cdot 10^{-1}$				A/ACT	0.416	0.417	-
5	rs4391122	60,598,543	−0.081	0.010	$1.10 \cdot 10^{-14}$	0.030	0.014	$3.03 \cdot 10^{-2}$	0.002	0.009	$8.39 \cdot 10^{-1}$	A/G	0.514	0.506	-
12	rs2851447	123,665,113	−0.089	0.012	$1.86 \cdot 10^{-14}$	0.010	0.016	$5.58 \cdot 10^{-1}$	−0.015	0.011	$1.64 \cdot 10^{-1}$	C/G	0.762	0.762	-
15	rs4702	91,426,560	−0.081	0.011	$8.30 \cdot 10^{-14}$	−0.023	0.014	$1.05 \cdot 10^{-1}$	−0.031	0.009	$9.12 \cdot 10^{-4}$	A/G	0.560	0.567	-
3	rs75968099	36,858,583	0.082	0.011	$1.05 \cdot 10^{-13}$	−0.007	0.014	$6.13 \cdot 10^{-1}$	0.012	0.010	$2.09 \cdot 10^{-1}$	T/C	0.362	0.365	-
14	rs12887734	104,046,834	0.084	0.011	$1.36 \cdot 10^{-13}$	0.033	0.015	$2.78 \cdot 10^{-2}$	0.039	0.010	$1.04 \cdot 10^{-4}$	T/G	0.301	0.296	-
15	rs8042374	78,908,032	0.089	0.012	$2.44 \cdot 10^{-13}$	0.016	0.016	$3.17 \cdot 10^{-1}$	0.028	0.011	$9.32 \cdot 10^{-3}$	A/G	0.772	0.770	-
7	rs13240464	110,898,915	0.080	0.011	$3.03 \cdot 10^{-13}$	0.004	0.015	$7.69 \cdot 10^{-1}$	0.021	0.010	$3.69 \cdot 10^{-2}$	T/C	0.674	0.679	-
11	rs10791097	130,718,630	0.074	0.010	$1.09 \cdot 10^{-12}$	0.000	0.014	$9.76 \cdot 10^{-1}$	0.017	0.009	$7.43 \cdot 10^{-2}$	T/G	0.452	0.449	-
2	rs11693094	185,601,420	−0.074	0.010	$1.53 \cdot 10^{-12}$	0.029	0.014	$3.52 \cdot 10^{-2}$	0.003	0.009	$7.14 \cdot 10^{-1}$	T/C	0.477	0.475	-
10	rs7893279	18,745,105	0.117	0.017	$1.97 \cdot 10^{-12}$	0.051	0.022	$2.17 \cdot 10^{-2}$	0.054	0.014	$1.99 \cdot 10^{-4}$	T/G	0.891	0.885	-
12	rs12826178	57,622,371	−0.167	0.024	$2.02 \cdot 10^{-12}$	−0.045	0.028	$1.04 \cdot 10^{-1}$	−0.056	0.018	$1.69 \cdot 10^{-3}$	T/G	0.069	0.072	-
1	rs12129573	73,768,366	0.075	0.011	$2.03 \cdot 10^{-12}$	0.026	0.014	$7.23 \cdot 10^{-2}$	0.031	0.010	$1.27 \cdot 10^{-3}$	A/C	0.371	0.364	-
2	rs6704768	233,592,501	−0.073	0.010	$2.32 \cdot 10^{-12}$	0.030	0.014	$3.28 \cdot 10^{-2}$	0.003	0.009	$7.57 \cdot 10^{-1}$	A/G	0.564	0.557	-
11	rs55661361	124,613,957	−0.077	0.011	$2.80 \cdot 10^{-12}$	−0.048	0.015	$1.19 \cdot 10^{-3}$	−0.047	0.010	$9.97 \cdot 10^{-7}$	A/G	0.336	0.348	-
18	rs9636107	53,200,117	−0.073	0.010	$3.34 \cdot 10^{-12}$	−0.019	0.014	$1.74 \cdot 10^{-1}$	−0.028	0.009	$2.86 \cdot 10^{-3}$	A/G	0.541	0.549	-
11	chr11:46350213:D	46,350,213	−0.098	0.015	$1.26 \cdot 10^{-11}$	0.038	0.020	$5.48 \cdot 10^{-2}$				A/AG	0.157	0.152	rs61126341:1
3	chr3:180594593:I	180,594,593	−0.090	0.013	$1.30 \cdot 10^{-11}$	−0.009	0.017	$5.88 \cdot 10^{-1}$				T/TA	0.783	0.788	-
20	rs6065094	37,453,194	−0.074	0.011	$1.46 \cdot 10^{-11}$	−0.001	0.015	$9.31 \cdot 10^{-1}$	−0.017	0.010	$9.35 \cdot 10^{-2}$	A/G	0.306	0.305	-
2	rs11682175	57,987,593	−0.070	0.010	$1.47 \cdot 10^{-11}$	−0.024	0.014	$8.48 \cdot 10^{-2}$	−0.031	0.009	$7.62 \cdot 10^{-4}$	T/C	0.529	0.536	-
15	rs950169	84,706,461	−0.080	0.012	$1.62 \cdot 10^{-11}$	−0.036	0.016	$1.81 \cdot 10^{-2}$	−0.040	0.010	$8.67 \cdot 10^{-5}$	T/C	0.269	0.277	-
18	rs72934570	53,533,189	−0.135	0.020	$1.97 \cdot 10^{-11}$	−0.038	0.025	$1.22 \cdot 10^{-1}$	−0.050	0.016	$2.05 \cdot 10^{-3}$	T/C	0.085	0.089	-
2	rs6434928	198,304,577	−0.074	0.011	$2.06 \cdot 10^{-11}$	−0.021	0.015	$1.48 \cdot 10^{-1}$	−0.029	0.010	$3.13 \cdot 10^{-3}$	A/G	0.678	0.681	-
22	rs9607782	41,587,556	0.083	0.012	$2.07 \cdot 10^{-11}$	0.025	0.016	$1.16 \cdot 10^{-1}$	0.034	0.011	$1.64 \cdot 10^{-3}$	A/T	0.248	0.243	-
8	rs36068923	111,485,761	−0.085	0.013	$2.61 \cdot 10^{-11}$	−0.038	0.017	$2.60 \cdot 10^{-2}$	−0.042	0.011	$1.85 \cdot 10^{-4}$	A/G	0.787	0.791	-
3	rs17194490	2,547,786	0.096	0.014	$2.69 \cdot 10^{-11}$	0.031	0.019	$1.05 \cdot 10^{-1}$	0.041	0.013	$1.11 \cdot 10^{-3}$	T/G	0.165	0.160	-
11	rs2514218	113,392,994	−0.075	0.011	$2.75 \cdot 10^{-11}$	0.006	0.015	$6.54 \cdot 10^{-1}$	−0.012	0.010	$2.06 \cdot 10^{-1}$	T/C	0.347	0.343	-
11	rs75059851	133,822,569	0.087	0.013	$3.87 \cdot 10^{-11}$	0.004	0.017	$7.90 \cdot 10^{-1}$	0.021	0.011	$5.19 \cdot 10^{-2}$	A/G	0.776	0.771	-
3	rs2535627	52,845,105	0.068	0.010	$4.26 \cdot 10^{-11}$	0.052	0.014	$1.91 \cdot 10^{-4}$	0.047	0.009	$2.51 \cdot 10^{-7}$	T/C	0.530	0.516	-
16	rs12691307	29,939,877	0.071	0.011	$4.55 \cdot 10^{-11}$	0.023	0.014	$1.05 \cdot 10^{-1}$	0.029	0.009	$1.55 \cdot 10^{-3}$	A/G	0.456	0.449	-
3	rs7432375	136,288,405	−0.069	0.011	$7.26 \cdot 10^{-11}$	0.017	0.014	$2.20 \cdot 10^{-1}$	−0.004	0.009	$6.32 \cdot 10^{-1}$	A/G	0.414	0.412	-
18	chr18:52749216:D	52,749,216	0.069	0.011	$8.03 \cdot 10^{-11}$	0.005	0.014	$7.12 \cdot 10^{-1}$				GA/G	0.588	0.585	-
5	rs111294930	152,177,121	0.090	0.014	$1.06 \cdot 10^{-10}$	−0.004	0.015	$7.83 \cdot 10^{-1}$	0.012	0.010	$2.17 \cdot 10^{-1}$	A/G	0.693	0.691	-
5	rs2973155	152,608,619	−0.069	0.011	$1.11 \cdot 10^{-10}$	−0.015	0.014	$3.03 \cdot 10^{-1}$	−0.023	0.010	$1.50 \cdot 10^{-2}$	T/C	0.354	0.358	-
17	rs4523957	2,208,899	0.069	0.011	$2.86 \cdot 10^{-10}$	0.011	0.014	$4.60 \cdot 10^{-1}$	0.021	0.009	$2.51 \cdot 10^{-2}$	T/G	0.624	0.619	-
7	rs12704290	86,427,626	−0.101	0.016	$3.33 \cdot 10^{-10}$	−0.030	0.021	$1.57 \cdot 10^{-1}$	−0.042	0.014	$3.11 \cdot 10^{-3}$	A/G	0.120	0.122	-
15	rs12903146	61,854,663	0.065	0.010	$3.38 \cdot 10^{-10}$	−0.011	0.014	$4.11 \cdot 10^{-1}$	0.007	0.009	$4.44 \cdot 10^{-1}$	A/G	0.541	0.543	-
1	rs11210892	44,100,084	−0.069	0.011	$3.39 \cdot 10^{-10}$	−0.011	0.015	$4.60 \cdot 10^{-1}$	−0.022	0.010	$2.60 \cdot 10^{-2}$	A/G	0.672	0.675	-
19	rs2905426	19,478,022	−0.069	0.011	$3.63 \cdot 10^{-10}$	−0.025	0.014	$7.88 \cdot 10^{-2}$	−0.029	0.010	$1.99 \cdot 10^{-3}$	T/G	0.621	0.626	-
1	rs140505938	150,031,490	−0.090	0.014	$4.49 \cdot 10^{-10}$	0.028	0.018	$1.24 \cdot 10^{-1}$	−0.001	0.012	$9.33 \cdot 10^{-1}$	T/C	0.170	0.167	-
1	rs4648845	2,387,101	0.070	0.011	$8.70 \cdot 10^{-10}$	−0.025	0.016	$1.18 \cdot 10^{-1}$	0.001	0.009	$9.43 \cdot 10^{-1}$	T/C	0.505	0.513	-
16	rs7405404	13,749,859	0.075	0.012	$1.00 \cdot 10^{-9}$	0.057	0.017	$5.67 \cdot 10^{-4}$	0.054	0.011	$1.47 \cdot 10^{-6}$	T/C	0.226	0.215	-
7	rs6466055	104,929,064	0.066	0.011	$1.13 \cdot 10^{-9}$	0.050	0.015	$5.75 \cdot 10^{-4}$	0.046	0.010	$1.82 \cdot 10^{-6}$	A/C	0.357	0.345	-
1	chr1:8424984:D	8,424,984	0.068	0.011	$1.17 \cdot 10^{-9}$	0.004	0.015	$7.76 \cdot 10^{-1}$				GA/G	0.342	0.343	-
12	rs4766428	110,723,245	0.065	0.011	$1.40 \cdot 10^{-9}$	0.002	0.014	$8.59 \cdot 10^{-1}$	0.016	0.009	$8.39 \cdot 10^{-2}$	T/C	0.445	0.442	-
4	rs10520163	170,626,552	0.063	0.010	$1.47 \cdot 10^{-9}$	0.030	0.014	$2.90 \cdot 10^{-2}$	0.032	0.009	$4.54 \cdot 10^{-4}$	T/C	0.502	0.497	-
6	rs117074560	96,459,651	−0.163	0.027	$1.64 \cdot 10^{-9}$	−0.029	0.033	$3.81 \cdot 10^{-1}$	−0.051	0.022	$2.06 \cdot 10^{-2}$	T/C	0.046	0.047	-
22	rs6002655	42,603,814	0.064	0.011	$1.71 \cdot 10^{-9}$	0.031	0.014	$3.05 \cdot 10^{-2}$	0.033	0.009	$4.15 \cdot 10^{-4}$	T/C	0.431	0.424	-
2	chr2:146436222:I	146,436,222	0.083	0.014	$1.81 \cdot 10^{-9}$	−0.016	0.018	$3.83 \cdot 10^{-1}$				TC/T	0.172	0.175	rs56807175:1
11	rs9420	57,510,294	0.066	0.011	$2.24 \cdot 10^{-9}$	0.032	0.015	$2.74 \cdot 10^{-2}$	0.033	0.010	$7.00 \cdot 10^{-4}$	A/G	0.331	0.324	-
11	rs11027857	24,403,620	0.062	0.010	$2.55 \cdot 10^{-9}$	0.002	0.014	$8.77 \cdot 10^{-1}$	0.015	0.009	$9.56 \cdot 10^{-2}$	A/G	0.511	0.509	-
1	rs1498232	30,433,951	0.067	0.011	$2.86 \cdot 10^{-9}$	0.019	0.015	$1.91 \cdot 10^{-1}$	0.027	0.010	$6.59 \cdot 10^{-3}$	T/C	0.321	0.319	-
7	rs3735025	137,074,844	0.064	0.011	$3.28 \cdot 10^{-9}$	0.030	0.015	$4.19 \cdot 10^{-2}$	0.033	0.010	$7.12 \cdot 10^{-4}$	T/C	0.654	0.648	-
9	rs11139497	84,739,941	0.066	0.011	$3.61 \cdot 10^{-9}$	0.018	0.015	$2.26 \cdot 10^{-1}$	0.026	0.010	$9.44 \cdot 10^{-3}$	A/T	0.319	0.314	-

Continues on the next page

Supplementary Table 9 – continued from previous page

			Schizophrenia			ASD			ASD-SCZ MTAG						
CHR	SNP	BP	β	SE	P	β	SE	P	β	SE	P	A1/A2	FRQ A	FRQ U	Proxy
1	rs77149735	243,555,105	0.276	0.047	$3.73 \cdot 10^{-9}$	0.107	0.041	$8.11 \cdot 10^{-3}$				A/G	0.032	0.030	-
15	rs56205728	40,567,237	0.071	0.012	$4.18 \cdot 10^{-9}$	0.006	0.016	$7.09 \cdot 10^{-1}$	0.017	0.010	$9.38 \cdot 10^{-2}$	A/G	0.281	0.278	-
19	rs2053079	30,987,423	−0.071	0.012	$4.49 \cdot 10^{-9}$	0.023	0.016	$1.59 \cdot 10^{-1}$	−0.001	0.011	$9.18 \cdot 10^{-1}$	A/G	0.761	0.755	-
5	rs16867576	88,746,331	0.097	0.017	$4.61 \cdot 10^{-9}$	0.033	0.020	$9.65 \cdot 10^{-2}$	0.039	0.013	$2.93 \cdot 10^{-3}$	A/G	0.860	0.854	-
3	rs4330281	17,859,366	−0.062	0.011	$4.64 \cdot 10^{-9}$	0.014	0.014	$3.05 \cdot 10^{-1}$	−0.003	0.009	$7.24 \cdot 10^{-1}$	T/C	0.512	0.506	-
5	rs3849046	137,851,192	0.061	0.010	$4.67 \cdot 10^{-9}$	0.018	0.014	$1.94 \cdot 10^{-1}$	0.024	0.009	$8.27 \cdot 10^{-3}$	T/C	0.555	0.553	-
14	rs2693698	99,719,219	−0.063	0.011	$4.80 \cdot 10^{-9}$	−0.018	0.014	$2.09 \cdot 10^{-1}$	−0.024	0.009	$1.05 \cdot 10^{-2}$	A/G	0.463	0.469	-
14	rs2332700	72,417,326	0.070	0.012	$4.86 \cdot 10^{-9}$	0.034	0.016	$3.37 \cdot 10^{-2}$	0.037	0.011	$4.84 \cdot 10^{-4}$	C/G	0.260	0.255	-
5	rs1501357	45,364,875	−0.077	0.013	$5.00 \cdot 10^{-9}$	0.000	0.018	$9.76 \cdot 10^{-1}$	−0.017	0.012	$1.71 \cdot 10^{-1}$	T/C	0.822	0.823	-
8	rs6984242	60,700,469	−0.061	0.011	$6.00 \cdot 10^{-9}$	−0.004	0.014	$7.74 \cdot 10^{-1}$	−0.016	0.009	$9.08 \cdot 10^{-2}$	A/G	0.608	0.612	-
1	chr1:243881945:I	243,881,945	0.066	0.011	$6.53 \cdot 10^{-9}$	−0.008	0.015	$5.90 \cdot 10^{-1}$				A/AT	0.317	0.317	-
5	rs79212538	151,993,104	0.144	0.025	$7.00 \cdot 10^{-9}$	0.039	0.033	$2.37 \cdot 10^{-1}$	0.055	0.022	$1.28 \cdot 10^{-2}$	T/G	0.047	0.046	-
2	rs3768644	72,361,505	−0.101	0.017	$7.39 \cdot 10^{-9}$	−0.012	0.023	$6.09 \cdot 10^{-1}$	−0.026	0.015	$7.96 \cdot 10^{-2}$	A/G	0.106	0.107	-
11	rs77502336	123,394,636	0.064	0.011	$7.54 \cdot 10^{-9}$	0.016	0.015	$3.04 \cdot 10^{-1}$	0.025	0.010	$1.27 \cdot 10^{-2}$	C/G	0.309	0.303	-
2	rs6704641	200,164,252	0.078	0.014	$8.33 \cdot 10^{-9}$	−0.016	0.018	$3.83 \cdot 10^{-1}$	0.007	0.012	$5.77 \cdot 10^{-1}$	A/G	0.817	0.818	-
2	rs59979824	193,848,340	−0.065	0.011	$8.41 \cdot 10^{-9}$	−0.021	0.015	$1.48 \cdot 10^{-1}$	−0.027	0.010	$4.63 \cdot 10^{-3}$	A/C	0.344	0.351	-
4	rs1106568	176,861,301	−0.068	0.012	$9.47 \cdot 10^{-9}$	−0.024	0.016	$1.23 \cdot 10^{-1}$	−0.030	0.011	$4.89 \cdot 10^{-3}$	A/G	0.742	0.744	-
8	rs10503253	4,180,844	0.071	0.012	$1.06 \cdot 10^{-8}$	−0.001	0.017	$9.43 \cdot 10^{-1}$	0.015	0.011	$1.87 \cdot 10^{-1}$	A/C	0.207	0.208	-
5	rs10043984	137,712,121	0.067	0.012	$1.09 \cdot 10^{-8}$	0.033	0.016	$4.21 \cdot 10^{-2}$	0.035	0.011	$1.05 \cdot 10^{-3}$	T/C	0.249	0.239	-
2	rs11685299	225,391,296	−0.063	0.011	$1.12 \cdot 10^{-8}$	0.037	0.015	$1.22 \cdot 10^{-2}$	0.009	0.010	$3.79 \cdot 10^{-1}$	A/C	0.333	0.322	-
8	rs7819570	89,588,626	0.076	0.013	$1.22 \cdot 10^{-8}$	0.006	0.018	$7.34 \cdot 10^{-1}$	0.021	0.012	$7.97 \cdot 10^{-2}$	T/G	0.179	0.178	-
18	rs715170	53,795,514	−0.067	0.012	$1.27 \cdot 10^{-8}$	0.048	0.016	$2.05 \cdot 10^{-3}$	0.016	0.010	$1.14 \cdot 10^{-1}$	T/C	0.275	0.265	-
16	rs9922678	9,946,319	0.065	0.011	$1.28 \cdot 10^{-8}$	0.026	0.015	$8.46 \cdot 10^{-2}$	0.031	0.010	$2.90 \cdot 10^{-3}$	A/G	0.284	0.276	-
18	rs78322266	53,063,676	0.173	0.030	$1.32 \cdot 10^{-8}$	0.060	0.042	$1.55 \cdot 10^{-1}$	0.081	0.029	$5.13 \cdot 10^{-3}$	T/G	0.029	0.026	-
14	rs2068012	30,190,316	−0.070	0.012	$1.41 \cdot 10^{-8}$	−0.010	0.016	$5.46 \cdot 10^{-1}$	−0.020	0.011	$6.11 \cdot 10^{-2}$	T/C	0.759	0.759	-
3	rs832187	63,833,050	−0.060	0.011	$1.43 \cdot 10^{-8}$	−0.025	0.015	$8.42 \cdot 10^{-2}$	−0.029	0.010	$2.48 \cdot 10^{-3}$	T/C	0.637	0.644	-
16	rs8044995	68,189,340	0.078	0.014	$1.51 \cdot 10^{-8}$	−0.017	0.019	$3.52 \cdot 10^{-1}$	0.007	0.012	$5.68 \cdot 10^{-1}$	A/G	0.167	0.170	-
2	chr2:149429178:D	149,429,178	−0.154	0.027	$1.59 \cdot 10^{-8}$	0.055	0.030	$6.71 \cdot 10^{-2}$				A/AT	0.059	0.057	rs200327371:1
17	rs8082590	17,958,402	−0.063	0.011	$1.77 \cdot 10^{-8}$	0.037	0.015	$1.51 \cdot 10^{-2}$	0.008	0.010	$4.44 \cdot 10^{-1}$	A/G	0.698	0.694	-
15	rs12148337	70,589,272	0.058	0.010	$1.79 \cdot 10^{-8}$	0.006	0.014	$6.67 \cdot 10^{-1}$	0.016	0.009	$7.73 \cdot 10^{-2}$	T/C	0.456	0.453	-
16	rs12325245	58,681,393	−0.084	0.015	$1.87 \cdot 10^{-8}$	−0.013	0.020	$5.34 \cdot 10^{-1}$	−0.028	0.014	$3.99 \cdot 10^{-2}$	A/T	0.863	0.867	-
12	rs2239063	2,511,831	0.065	0.012	$1.93 \cdot 10^{-8}$	−0.004	0.016	$8.00 \cdot 10^{-1}$	0.013	0.010	$2.05 \cdot 10^{-1}$	A/C	0.725	0.727	-
5	rs12522290	152,797,656	0.081	0.014	$1.99 \cdot 10^{-8}$	0.012	0.018	$5.08 \cdot 10^{-1}$	0.024	0.012	$4.97 \cdot 10^{-2}$	C/G	0.826	0.823	-
1	rs10803138	243,555,219	−0.069	0.012	$2.03 \cdot 10^{-8}$	0.010	0.016	$5.28 \cdot 10^{-1}$	−0.008	0.011	$4.33 \cdot 10^{-1}$	A/G	0.259	0.258	-
8	rs73229090	27,442,127	−0.097	0.017	$2.10 \cdot 10^{-8}$	−0.030	0.022	$1.81 \cdot 10^{-1}$	−0.039	0.015	$7.31 \cdot 10^{-3}$	A/C	0.110	0.113	-
12	rs324017	57,487,814	−0.064	0.011	$2.13 \cdot 10^{-8}$	0.002	0.015	$8.94 \cdot 10^{-1}$	−0.012	0.010	$2.40 \cdot 10^{-1}$	A/C	0.292	0.294	-
10	rs55833108	104,741,583	0.073	0.013	$2.23 \cdot 10^{-8}$	0.007	0.017	$6.96 \cdot 10^{-1}$	0.021	0.011	$6.23 \cdot 10^{-2}$	T/G	0.208	0.209	-
3	rs9841616	181,167,585	−0.078	0.014	$2.35 \cdot 10^{-8}$	−0.020	0.019	$2.86 \cdot 10^{-1}$	−0.031	0.013	$1.49 \cdot 10^{-2}$	A/T	0.158	0.157	-
1	rs76869799	97,834,525	−0.167	0.030	$2.64 \cdot 10^{-8}$	0.048	0.042	$2.49 \cdot 10^{-1}$	−0.004	0.026	$8.65 \cdot 10^{-1}$	C/G	0.968	0.967	-
6	rs1339227	73,155,701	−0.060	0.011	$2.69 \cdot 10^{-8}$	−0.026	0.015	$7.58 \cdot 10^{-2}$	−0.028	0.010	$2.81 \cdot 10^{-3}$	T/C	0.358	0.369	-
7	chr7:24747494:D	24,747,494	0.096	0.017	$2.85 \cdot 10^{-8}$	−0.065	0.023	$5.06 \cdot 10^{-3}$				CTA/C	0.896	0.901	-
5	rs4388249	109,036,066	0.073	0.013	$3.05 \cdot 10^{-8}$	0.012	0.019	$5.20 \cdot 10^{-1}$	0.023	0.012	$6.00 \cdot 10^{-2}$	T/C	0.174	0.172	-
4	rs215411	23,423,603	0.062	0.011	$3.06 \cdot 10^{-8}$	0.026	0.015	$6.98 \cdot 10^{-2}$	0.029	0.010	$2.28 \cdot 10^{-3}$	A/T	0.348	0.346	-
5	rs11740474	153,680,747	−0.060	0.011	$3.15 \cdot 10^{-8}$	−0.020	0.014	$1.57 \cdot 10^{-1}$	−0.025	0.009	$6.17 \cdot 10^{-3}$	A/T	0.572	0.575	-
22	rs1023500	42,340,844	0.073	0.013	$3.43 \cdot 10^{-8}$	0.023	0.018	$2.14 \cdot 10^{-1}$	0.031	0.012	$9.73 \cdot 10^{-3}$	T/C	0.821	0.821	-
11	rs12421382	109,378,071	−0.061	0.011	$3.70 \cdot 10^{-8}$	−0.020	0.015	$1.76 \cdot 10^{-1}$	−0.026	0.010	$7.52 \cdot 10^{-3}$	T/C	0.333	0.341	-
7	rs211829	110,048,893	0.059	0.011	$3.71 \cdot 10^{-8}$	0.045	0.014	$1.60 \cdot 10^{-3}$	0.039	0.009	$3.77 \cdot 10^{-5}$	T/C	0.631	0.619	-
12	rs679087	29,917,265	−0.061	0.011	$3.91 \cdot 10^{-8}$	0.001	0.014	$9.38 \cdot 10^{-1}$	−0.012	0.010	$2.23 \cdot 10^{-1}$	A/C	0.361	0.363	-
2	rs75575209	58,138,192	−0.103	0.019	$3.95 \cdot 10^{-8}$	−0.016	0.025	$5.20 \cdot 10^{-1}$	−0.033	0.017	$4.94 \cdot 10^{-2}$	A/T	0.914	0.917	-
7	rs7801375	131,567,263	−0.079	0.014	$4.42 \cdot 10^{-8}$	−0.026	0.019	$1.60 \cdot 10^{-1}$	−0.034	0.012	$6.59 \cdot 10^{-3}$	A/G	0.158	0.162	-
1	rs14403	243,663,893	−0.068	0.013	$4.42 \cdot 10^{-8}$	0.000	0.017	$9.88 \cdot 10^{-1}$	−0.015	0.011	$1.63 \cdot 10^{-1}$	T/C	0.221	0.223	-
1	rs6670165	177,280,121	0.072	0.013	$4.45 \cdot 10^{-8}$	0.033	0.017	$5.74 \cdot 10^{-2}$	0.037	0.012	$1.50 \cdot 10^{-3}$	T/C	0.202	0.198	-
1	rs7523273	207,977,083	0.061	0.011	$4.47 \cdot 10^{-8}$	−0.010	0.015	$5.00 \cdot 10^{-1}$	0.006	0.010	$5.36 \cdot 10^{-1}$	A/G	0.645	0.642	-
20	rs7267348	48,131,036	−0.065	0.012	$4.56 \cdot 10^{-8}$	−0.027	0.016	$8.79 \cdot 10^{-2}$	−0.032	0.011	$3.14 \cdot 10^{-3}$	T/C	0.754	0.761	-
12	rs4240748	92,246,786	−0.059	0.011	$4.59 \cdot 10^{-8}$	0.006	0.014	$6.66 \cdot 10^{-1}$	−0.009	0.010	$3.64 \cdot 10^{-1}$	C/G	0.376	0.375	-
2	rs2909457	162,845,855	−0.058	0.011	$4.62 \cdot 10^{-8}$	0.020	0.014	$1.46 \cdot 10^{-1}$	0.000	0.009	$9.99 \cdot 10^{-1}$	A/G	0.558	0.553	-
19	rs56873913	50,091,199	0.069	0.013	$4.69 \cdot 10^{-8}$	0.004	0.016	$8.06 \cdot 10^{-1}$	0.017	0.011	$1.13 \cdot 10^{-1}$	T/G	0.753	0.750	-
12	rs10860964	103,596,455	0.059	0.011	$4.84 \cdot 10^{-8}$	0.010	0.014	$4.79 \cdot 10^{-1}$	0.018	0.009	$6.07 \cdot 10^{-2}$	T/C	0.622	0.620	-
5	chr5:140143664:I	140,143,664	0.056	0.010	$4.85 \cdot 10^{-8}$	0.015	0.014	$2.79 \cdot 10^{-1}$				CATTGAAAGAAA/C	0.474	0.470	rs111896713:1

3.2.4 Gene-based association and gene-set enrichment

Supplementary Table 10: Top 25 results from Magma gene-based association from the iPSYCH-PGC meta analysis of ASD. Red means the gene is significant after Bonferroni correction, *slanted* gene name that no single SNP in the gene was genome wide significant, ***bold face*** gene name that no single SNP in the gene was significant at the Bonferroni level (significance from z-scores).

Gene	Chr	BP start	BP stop	N SNPs	N param	N	Z-stat	P	Bonf P
XRN2	20	21,283,942	21,370,463	174	17	21,104	6.003	$9.69 \cdot 10^{-10}$	$1.73 \cdot 10^{-5}$
KCNN2	5	113,698,016	113,832,197	306	39	21,009	5.995	$1.02 \cdot 10^{-9}$	$1.82 \cdot 10^{-5}$
KIZ	20	21,106,624	21,227,260	200	12	21,080	5.725	$5.17 \cdot 10^{-9}$	$9.23 \cdot 10^{-5}$
KANSL1	17	44,107,282	44,302,740	89	14	21,038	5.169	$1.18 \cdot 10^{-7}$	$2.10 \cdot 10^{-3}$
MACROD2	20	13,976,146	16,033,842	6,037	256	21,104	5.137	$1.40 \cdot 10^{-7}$	$2.49 \cdot 10^{-3}$
WNT3	17	44,841,686	44,896,082	74	11	20,952	4.934	$4.03 \cdot 10^{-7}$	$7.19 \cdot 10^{-3}$
MAPT	17	43,971,748	44,105,700	72	8	21,020	4.891	$5.01 \cdot 10^{-7}$	$8.94 \cdot 10^{-3}$
MFHAS1	8	8,641,999	8,751,131	497	28	21,081	4.870	$5.58 \cdot 10^{-7}$	$9.96 \cdot 10^{-3}$
XKR6	8	10,753,654	11,058,875	1,013	28	21,102	4.798	$8.01 \cdot 10^{-7}$	$1.43 \cdot 10^{-2}$
MSRA	8	9,911,830	10,286,401	1,547	62	21,112	4.771	$9.15 \cdot 10^{-7}$	$1.63 \cdot 10^{-2}$
CRHR1	17	43,697,710	43,913,194	276	21	21,133	4.740	$1.07 \cdot 10^{-6}$	$1.91 \cdot 10^{-2}$
SOX7	8	10,581,278	10,588,022	24	5	21,199	4.709	$1.24 \cdot 10^{-6}$	$2.22 \cdot 10^{-2}$
NTM	11	131,240,371	132,206,716	2,938	213	21,113	4.698	$1.32 \cdot 10^{-6}$	$2.35 \cdot 10^{-2}$
MMP12	11	102,733,464	102,745,764	22	8	21,104	4.584	$2.28 \cdot 10^{-6}$	$4.07 \cdot 10^{-2}$
BLK	8	11,351,521	11,422,108	269	21	21,161	4.569	$2.45 \cdot 10^{-6}$	$4.37 \cdot 10^{-2}$
MANBA	4	103,552,643	103,682,151	210	13	21,114	4.468	$3.96 \cdot 10^{-6}$	$7.06 \cdot 10^{-2}$
ADTRP	6	11,713,888	11,779,280	247	25	21,083	4.463	$4.04 \cdot 10^{-6}$	$7.21 \cdot 10^{-2}$
WDPCP	2	63,348,518	63,815,867	955	25	21,121	4.413	$5.11 \cdot 10^{-6}$	$9.11 \cdot 10^{-2}$
PINX1	8	10,622,884	10,697,299	416	17	21,155	4.326	$7.60 \cdot 10^{-6}$	$1.36 \cdot 10^{-1}$
PKP4	2	159,313,476	159,537,941	605	19	21,070	4.312	$8.11 \cdot 10^{-6}$	$1.45 \cdot 10^{-1}$
PLEKHM1	17	43,513,266	43,568,146	64	9	20,916	4.289	$8.99 \cdot 10^{-6}$	$1.60 \cdot 10^{-1}$
C8orf74	8	10,530,147	10,558,103	31	9	21,199	4.225	$1.20 \cdot 10^{-5}$	$2.14 \cdot 10^{-1}$
MDH1	2	63,815,743	63,834,331	38	6	21,008	4.203	$1.32 \cdot 10^{-5}$	$2.35 \cdot 10^{-1}$
HDAC4	2	239,969,864	240,322,643	1,109	80	21,125	4.165	$1.56 \cdot 10^{-5}$	$2.77 \cdot 10^{-1}$
WNT5B	12	1,726,222	1,756,378	115	29	21,191	4.054	$2.52 \cdot 10^{-5}$	$4.50 \cdot 10^{-1}$

Supplementary Table 11: Gene set analysis of candidate gene sets, M13, M16 and M17 from [41], constrained genes of [42, 43] with a high probability of being loss-of-function intolerant (pLI > 0.9), the 65 genes at FDR< 0.1 in [234], and the highly curated list of ASD genes (`https://spark-sf.s3.amazonaws.com/SPARK_gene_list.pdf`) from SPARK[235]. The effect sizes estimated by MAGMA indicate the extent to which the z-scores for the genes in the set are higher than those in the complement, adjusted among other features the gene length (see section 2.1.2 for details). The β_{std} are semi-standardized regression coefficients, and the p-values are from a z-test.

Gene set	N Genes	β	β_{std}	SD(β)	P
M13	603	−0.015	−0.003	0.035	0.662
M16	401	0.069	0.010	0.042	0.050
M17	694	−0.022	−0.004	0.033	0.749
Constrained	2,939	0.038	0.014	0.017	0.014
Sanders	65	0.164	0.010	0.107	0.063
SPARK	77	0.272	0.017	0.100	0.003

Supplementary Table 12: Top 25 genesets from gene set analysis of 863 gene sets from the Gene Oncology[44, 45] 'molecular functions' of MsigDB[46] including 'BioCarta'. MAGMA estimates the effect sizes in a regression adjusted among other features the gene length (see section 2.1.2 for details). The βs indicate the extent to which the z-scores for the genes in the set are higher than those in the complement, the β_{std} are semi-standardized regression coefficients, and p-values are from a z-test.

Gene set	N Genes	β	β_{std}	SD(β)	P
GO ION GATED CHANNEL ACTIVITY	41	0.435	0.021	0.144	0.001
GO PHOSPHATIDYLINOSITOL MONOPHOSPHATE PHOSPHATASE ACTIVITY	11	0.724	0.018	0.244	0.002
GO CALCIUM ACTIVATED POTASSIUM CHANNEL ACTIVITY	17	0.686	0.021	0.234	0.002
GO UBIQUITIN LIKE PROTEIN SPECIFIC PROTEASE ACTIVITY	85	0.236	0.016	0.082	0.002
GO PHOSPHATIDYLINOSITOL PHOSPHATE BINDING	106	0.241	0.019	0.085	0.002
GO PHOSPHATIDYLINOSITOL BINDING	184	0.174	0.018	0.062	0.003
GO CALCIUM ACTIVATED CATION CHANNEL ACTIVITY	28	0.475	0.019	0.170	0.003
GO RNA POLYMERASE II TRANSCRIPTION COREPRESSOR ACTIVITY	22	0.475	0.017	0.172	0.003
GO HISTONE DEMETHYLASE ACTIVITY	19	0.523	0.017	0.192	0.003
GO PROTEOGLYCAN BINDING	26	0.450	0.017	0.173	0.005
GO CYSTEINE TYPE PEPTIDASE ACTIVITY	144	0.170	0.015	0.066	0.005
GO OXIDOREDUCTASE ACTIVITY OXIDIZING METAL IONS	16	0.550	0.017	0.216	0.005
GO PROTEIN SERINE THREONINE PHOSPHATASE ACTIVITY	61	0.263	0.015	0.104	0.006
GO PHOSPHATIDYLINOSITOL 3 4 5 TRISPHOSPHATE BINDING	30	0.405	0.017	0.160	0.006
GO PHOSPHOLIPID BINDING	326	0.117	0.016	0.048	0.007
GO INSULIN LIKE GROWTH FACTOR BINDING	25	0.434	0.016	0.181	0.008
GO OXIDOREDUCTASE ACTIVITY ACTING ON PEROXIDE AS ACCEPTOR	35	0.343	0.015	0.143	0.008
GO KINASE BINDING	577	0.083	0.015	0.035	0.008
GO PHOSPHORIC ESTER HYDROLASE ACTIVITY	339	0.106	0.015	0.045	0.009
GO MHC PROTEIN BINDING	22	0.400	0.014	0.172	0.010
GO DIPEPTIDASE ACTIVITY	14	0.456	0.013	0.204	0.013
GO COA HYDROLASE ACTIVITY	19	0.445	0.015	0.201	0.013
GO NOTCH BINDING	18	0.469	0.015	0.211	0.013
GO PROTEIN TYROSINE PHOSPHATASE ACTIVITY	92	0.196	0.014	0.089	0.014
GO DIPEPTIDYL PEPTIDASE ACTIVITY	11	0.489	0.012	0.225	0.015

3.3 Polygenic qualities of subtypes

This section presents results on heritability of and genetic overlap between subtypes of ASD. For results on genetic correlation with other phenotypes, see Table 5.

3.3.1 Heritability and genetic correlation across subtypes

Supplementary Table 13: Definition of the hierarchical ASD subtypes from the ICD10 diagnosis categories. See Table 1 for counts.

Name	Diagnosis
(h)CHA	Childhood autism (ICD10 F84.0)
hATA	those with ATA and no CHA (ICD10 F84.1)
hAsp	Asperger's syndrome and no CHA and no ATA (ICD10 F84.5)
hPDM	those with PDM (pervasive disorders, unspecified and other, ICD10 F84.8+9) and none of the above.

Supplementary Table 14: Heritability estimates from GCTA for subtypes and substrata on the observed as well as the liability scale. The number of samples are: ASD 13 076, ASD wID 1 873, ASD woID 11 203, CHA and hCHA 3 310, ATA 1 607, Asp 4 622, OPDD 2 042, PDDU 3 753, PDM 5 460, hATA 1 494, hAsp 4 417, hPDM 3 855. For a graphical representation, see Figure 82.

Summary Stats	Pop Prev	h^2_G Obs	SE(h^2_G Obs)	h^2_G Liab	SE(h^2_G Liab)
ASD	0.012	0.129	0.008	0.080	0.005
ASD wID	0.002	0.020	0.009	0.029	0.013
ASD woID	0.010	0.137	0.008	0.086	0.005
CHA	0.003	0.049	0.009	0.048	0.009
ATA	0.002	0.008	0.009	0.012	0.013
Asp	0.004	0.120	0.010	0.097	0.008
OPDD	0.002	0.024	0.009	0.031	0.012
PDDU	0.004	0.047	0.009	0.042	0.008
PDM	0.005	0.062	0.009	0.047	0.007
hCHA	0.003	0.049	0.009	0.048	0.009
hATA	0.001	0.010	0.009	0.016	0.014
hAsp	0.004	0.116	0.010	0.096	0.008
hPDM	0.004	0.050	0.009	0.045	0.008

Supplementary Table 15: GCTA based genetic correlation, r_G, between ASD subtypes. The number of samples are: ASD 13 076, ASD wID 1 873, ASD woID 11 203, CHA and hCHA 3 310, ATA 1 607, Asp 4 622, OPDD 2 042, PDDU 3 753, PDM 5 460, hATA 1 494, hAsp 4 417, hPDM 3 855. For a graphical presentation, see Figure 83.

Trait 1	Trait 2	$h^2_{G,1}$	se($h^2_{G,1}$)	$h^2_{G,2}$	se($h^2_{G,2}$)	r_G	se(r_G)
ASD woID	ASD wID	0.140	0.009	0.065	0.040	1.000	0.312
CHA	hATA	0.060	0.012	0.070	0.026	0.891	0.250
CHA	hAsp	0.083	0.018	0.136	0.015	1.000	0.141
CHA	hPDM	0.093	0.017	0.083	0.015	0.965	0.151
hATA	hPDM	0.038	0.028	0.056	0.012	1.000	0.459
hATA	hAsp	0.065	0.030	0.141	0.012	0.718	0.206
hAsp	hPDM	0.170	0.016	0.077	0.016	0.955	0.121
CHA woID	hPDM woID	0.070	0.020	0.066	0.014	1.000	0.229
hATA woID	hAsp woID	0.080	0.037	0.131	0.012	0.908	0.241
CHA woID	hATA woID	0.062	0.013	0.034	0.025	1.000	0.424
hATA woID	hPDM woID	0.038	0.032	0.048	0.011	1.000	0.522
hAsp woID	hPDM woID	0.160	0.015	0.066	0.017	1.000	0.156
CHA woID	hAsp woID	0.093	0.022	0.159	0.014	0.893	0.132

3.4 Hi-C analysis

Supplementary Table 16: Altogether 380 credible SNPs were identified from 28 loci that could be assigned to 95 genes (of which 40 are protein-coding genes), including 39 promoter SNPs assigned to 9 genes, and 16 functional SNPs within 8 genes. Hi-C identified 86 genes interacting with credible SNPs in either GZ or CP. Among these genes, 34 genes are interacting with credible SNPs in both CP and GZ, which represent a high-confidence gene list (these are coloured blue)..

CHR	BP	CredSNP	IndexSNP	Index P	ENSGID_CP	ENSGID_GZ	ENSGID Promoter	ENSGID functional	Chrom HMM	Histone	HGNC_CP	HGNC_GZ	HGNC Promoter	HGNC functional
chr10	72,748,374	chr10:72748374	rs78827416	9.0e-07	NA	NA	NA	NA	15_Quies		NA	NA	NA	NA
chr17	44,104,576	chr17:44104576	rs142920272, rs147317628	2.9e-07, 1.1e-06	ENSG00000131484(3.118e-13), ENSG00000176681(5.735e-113), ENSG00000214425(3.118e-13), ENSG00000228696(5.735e-113), ENSG00000260075(2.751e-15), ENSG00000266918(3.118e-13)	ENSG00000073969(1.064e-07), ENSG00000120071(2.801e-05), ENSG00000136448(5.713e-08), ENSG00000172992(5.713e-08), ENSG00000228696(6.468e-09), ENSG00000238723(2.941e-05), ENSG00000262500(5.235e-05)	NA	NA	5_TxWk		LRRC37A, LRRC37A4P, ARL17B, NSFP1	NSF, KANSL1, NMT1, DCAKD, ARL17B	NA	NA
chr17	44,122,345	chr17:44122345	rs142920272, rs147317628	2.9e-07, 1.1e-06	ENSG00000108433(7.417e-05), ENSG00000120071(2.093e-15), ENSG00000176681(4.187e-13), ENSG00000214401(7.753e-08), ENSG00000228696(4.187e-13), ENSG00000238723(2.093e-15), ENSG00000262500(1.238e-14), ENSG00000262633(7.417e-05), ENSG00000262879(7.417e-05), ENSG00000263142(7.417e-05)	ENSG00000108433(4.841e-06), ENSG00000120071(1.708e-15), ENSG00000176681(1.036e-29), ENSG00000214401(8.406e-08), ENSG00000228696(1.036e-29), ENSG00000238723(1.708e-15), ENSG00000262500(5.602e-15), ENSG00000262633(4.841e-06), ENSG00000262879(4.841e-06), ENSG00000263142(4.841e-06), ENSG00000266497(2.301e-06)	NA	NA	5_TxWk		GOSR2, KANSL1, LRRC37A, KANSL1-AS1, ARL17B, LRRC37A17P	GOSR2, KANSL1, LRRC37A, KANSL1-AS1, ARL17B, LRRC37A17P	NA	NA
chr17	44,122,348	chr17:44122348	rs142920272, rs147317628	2.9e-07, 1.1e-06	ENSG00000108433(7.417e-05), ENSG00000120071(2.093e-15), ENSG00000176681(4.187e-13), ENSG00000214401(7.753e-08), ENSG00000228696(4.187e-13), ENSG00000238723(2.093e-15), ENSG00000262500(1.238e-14), ENSG00000262633(7.417e-05), ENSG00000262879(7.417e-05), ENSG00000263142(7.417e-05)	ENSG00000108433(4.841e-06), ENSG00000120071(1.708e-15), ENSG00000176681(1.036e-29), ENSG00000214401(8.406e-08), ENSG00000228696(1.036e-29), ENSG00000238723(1.708e-15), ENSG00000262500(5.602e-15), ENSG00000262633(4.841e-06), ENSG00000262879(4.841e-06), ENSG00000263142(4.841e-06), ENSG00000266497(2.301e-06)	NA	NA	5_TxWk		GOSR2, KANSL1, LRRC37A, KANSL1-AS1, ARL17B, LRRC37A17P	GOSR2, KANSL1, LRRC37A, KANSL1-AS1, ARL17B, LRRC37A17P	NA	NA
chr17	44,122,354	chr17:44122354	rs147317628	1.1e-06	ENSG00000108433(7.417e-05), ENSG00000120071(2.093e-15), ENSG00000176681(4.187e-13), ENSG00000214401(7.753e-08), ENSG00000228696(4.187e-13), ENSG00000238723(2.093e-15), ENSG00000262500(1.238e-14), ENSG00000262633(7.417e-05), ENSG00000262879(7.417e-05), ENSG00000263142(7.417e-05)	ENSG00000108433(4.841e-06), ENSG00000120071(1.708e-15), ENSG00000176681(1.036e-29), ENSG00000214401(8.406e-08), ENSG00000228696(1.036e-29), ENSG00000238723(1.708e-15), ENSG00000262500(5.602e-15), ENSG00000262633(4.841e-06), ENSG00000262879(4.841e-06), ENSG00000263142(4.841e-06), ENSG00000266497(2.301e-06)	NA	NA	5_TxWk		GOSR2, KANSL1, LRRC37A, KANSL1-AS1, ARL17B, LRRC37A17P	GOSR2, KANSL1, LRRC37A, KANSL1-AS1, ARL17B, LRRC37A17P	NA	NA
chr17	44,125,277	chr17:44125277	rs142920272, rs147317628	2.9e-07, 1.1e-06			ENSG00000120071		5_TxWk				KANSL1	
chr17	44,126,473	chr17:44126473	rs142920272, rs147317628	2.9e-07, 1.1e-06	ENSG00000108433(7.417e-05), ENSG00000120071(2.093e-15), ENSG00000176681(4.187e-13), ENSG00000214401(7.753e-08), ENSG00000228696(4.187e-13), ENSG00000238723(2.093e-15), ENSG00000262500(1.238e-14), ENSG00000262633(7.417e-05), ENSG00000262879(7.417e-05), ENSG00000263142(7.417e-05)	ENSG00000108433(4.841e-06), ENSG00000120071(1.708e-15), ENSG00000176681(1.036e-29), ENSG00000214401(8.406e-08), ENSG00000228696(1.036e-29), ENSG00000238723(1.708e-15), ENSG00000262500(5.602e-15), ENSG00000262633(4.841e-06), ENSG00000262879(4.841e-06), ENSG00000263142(4.841e-06), ENSG00000266497(2.301e-06)	NA	NA	5_TxWk		GOSR2, KANSL1, LRRC37A, KANSL1-AS1, ARL17B, LRRC37A17P	GOSR2, KANSL1, LRRC37A, KANSL1-AS1, ARL17B, LRRC37A17P	NA	NA

Continues on the next page

Supplementary Table 16 – continued from previous page

CHR	BP	CredSNP	IndexSNP	Index P	ENSGID_CP	ENSGID_GZ	ENSGID Promoter	ENSGID functional	Chrom HMM	Histone	HGNC_CP	HGNC_GZ	HGNC Promoter	HGNC functional
chr17	44,126,477	chr17:44126477	rs142920272	2.9e-07	ENSG00000108433(7.417e-05), ENSG00000120071(2.093e-15), ENSG00000176681(4.187e-13), ENSG00000214401(7.753e-08), ENSG00000228696(4.187e-13), ENSG00000238723(2.093e-15), ENSG00000262500(1.238e-14), ENSG00000262633(7.417e-05), ENSG00000262879(7.417e-05), ENSG00000263142(7.417e-05)	ENSG00000108433(4.841e-06), ENSG00000120071(1.708e-15), ENSG00000176681(1.036e-29), ENSG00000214401(8.406e-08), ENSG00000228696(1.036e-29), ENSG00000238723(1.708e-15), ENSG00000262500(5.602e-15), ENSG00000262633(4.841e-06), ENSG00000262879(4.841e-06), ENSG00000263142(4.841e-06), ENSG00000266497(2.301e-06)	NA	NA	5_TxWk		GOSR2, KANSL1, LRRC37A, KANSL1-AS1, ARL17B, LRRC37A17P	GOSR2, KANSL1, LRRC37A, KANSL1-AS1, ARL17B, LRRC37A17P	NA	NA
chr17	44,126,478	chr17:44126478	rs142920272, rs147317628	2.9e-07, 1.1e-06	ENSG00000108433(7.417e-05), ENSG00000120071(2.093e-15), ENSG00000176681(4.187e-13), ENSG00000214401(7.753e-08), ENSG00000228696(4.187e-13), ENSG00000238723(2.093e-15), ENSG00000262500(1.238e-14), ENSG00000262633(7.417e-05), ENSG00000262879(7.417e-05), ENSG00000263142(7.417e-05)	ENSG00000108433(4.841e-06), ENSG00000120071(1.708e-15), ENSG00000176681(1.036e-29), ENSG00000214401(8.406e-08), ENSG00000228696(1.036e-29), ENSG00000238723(1.708e-15), ENSG00000262500(5.602e-15), ENSG00000262633(4.841e-06), ENSG00000262879(4.841e-06), ENSG00000263142(4.841e-06), ENSG00000266497(2.301e-06)	NA	NA	5_TxWk		GOSR2, KANSL1, LRRC37A, KANSL1-AS1, ARL17B, LRRC37A17P	GOSR2, KANSL1, LRRC37A, KANSL1-AS1, ARL17B, LRRC37A17P	NA	NA
chr17	44,227,623	chr17:44227623	rs142920272, rs147317628	2.9e-07, 1.1e-06	ENSG00000267198(1.976e-05)	ENSG00000131484(1.08e-05), ENSG00000176681(1.083e-66), ENSG00000214425(1.08e-05), ENSG00000228696(1.083e-66), ENSG00000267198(5.005e-08)	NA	NA	5_TxWk			LRRC37A, LRRC37A4P, ARL17B	NA	NA
chr17	44,227,623	chr17:44227623m	rs142920272, rs147317628	2.9e-07, 1.1e-06	ENSG00000267198(1.976e-05)	ENSG00000131484(1.08e-05), ENSG00000176681(1.083e-66), ENSG00000214425(1.08e-05), ENSG00000228696(1.083e-66), ENSG00000267198(5.005e-08)	NA	NA	5_TxWk			LRRC37A, LRRC37A4P, ARL17B	NA	NA
chr17	44,228,169	chr17:44228169	rs142920272, rs147317628	2.9e-07, 1.1e-06	ENSG00000267198(1.976e-05)	ENSG00000131484(1.08e-05), ENSG00000176681(1.083e-66), ENSG00000214425(1.08e-05), ENSG00000228696(1.083e-66), ENSG00000267198(5.005e-08)	NA	NA	5_TxWk			LRRC37A, LRRC37A4P, ARL17B	NA	NA
chr17	44,228,529	chr17:44228529	rs142920272, rs147317628	2.9e-07, 1.1e-06	ENSG00000267198(1.976e-05)	ENSG00000131484(1.08e-05), ENSG00000176681(1.083e-66), ENSG00000214425(1.08e-05), ENSG00000228696(1.083e-66), ENSG00000267198(5.005e-08)	NA	NA	5_TxWk			LRRC37A, LRRC37A4P, ARL17B	NA	NA
chr17	44,228,609	chr17:44228609	rs147317628	1.1e-06	ENSG00000267198(1.976e-05)	ENSG00000131484(1.08e-05), ENSG00000176681(1.083e-66), ENSG00000214425(1.08e-05), ENSG00000228696(1.083e-66), ENSG00000267198(5.005e-08)	NA	NA	5_TxWk			LRRC37A, LRRC37A4P, ARL17B	NA	NA
chr17	44,228,770	chr17:44228770	rs147317628	1.1e-06	ENSG00000267198(1.976e-05)	ENSG00000131484(1.08e-05), ENSG00000176681(1.083e-66), ENSG00000214425(1.08e-05), ENSG00000228696(1.083e-66), ENSG00000267198(5.005e-08)	NA	NA	5_TxWk			LRRC37A, LRRC37A4P, ARL17B	NA	NA
chr17	44,230,647	chr17:44230647	rs142920272, rs147317628	2.9e-07, 1.1e-06	ENSG00000073969(6.506e-16), ENSG00000176681(6.285e-64), ENSG00000228696(6.285e-64), ENSG00000262879(1.715e-07), ENSG00000263142(1.622e-06)	ENSG00000073969(3.809e-94), ENSG00000131484(1.089e-13), ENSG00000176681(8.213e-05), ENSG00000214425(1.089e-13), ENSG00000225190(2.05e-06), ENSG00000228696(8.213e-05), ENSG00000264225(2.05e-06), ENSG00000266918(1.089e-13)	NA	NA	5_TxWk		NSF, LRRC37A, ARL17B, LRRC37A17P	NSF, LRRC37A, LRRC37A4P, PLEKHM1, ARL17B, RN7SL730P	NA	NA
chr17	44,231,117	chr17:44231117	rs147317628	1.1e-06	ENSG00000073969(6.506e-16), ENSG00000176681(6.285e-64), ENSG00000228696(6.285e-64), ENSG00000262879(1.715e-07), ENSG00000263142(1.622e-06)	ENSG00000073969(3.809e-94), ENSG00000131484(1.089e-13), ENSG00000176681(8.213e-05), ENSG00000214425(1.089e-13), ENSG00000225190(2.05e-06), ENSG00000228696(8.213e-05), ENSG00000264225(2.05e-06), ENSG00000266918(1.089e-13)	NA	NA	5_TxWk	H3K4me1	NSF, LRRC37A, ARL17B, LRRC37A17P	NSF, LRRC37A, LRRC37A4P, PLEKHM1, ARL17B, RN7SL730P	NA	NA

Continues on the next page

Supplementary Table 16 – continued from previous page

CHR	BP	CredSNP	IndexSNP	Index P	ENSGID_CP	ENSGID_GZ	ENSGID Promoter	ENSGID functional	Chrom HMM	Histone	HGNC_CP	HGNC_GZ	HGNC Promoter	HGNC functional
chr17	44,231,295	chr17:44231295	rs142920272	2.9e-07	ENSG00000073969(6.506e-16), ENSG00000176681(6.285e-64), ENSG00000228696(6.285e-64), ENSG00000262879(1.715e-07), ENSG00000263142(1.622e-06)	ENSG00000073969(3.809e-94), ENSG00000131484(1.089e-13), ENSG00000176681(8.213e-05), ENSG00000214425(1.089e-13), ENSG00000225190(2.05e-06), ENSG00000228696(8.213e-05), ENSG00000264225(2.05e-06), ENSG00000266918(1.089e-13)	NA	NA	7_Enh	H3K4me1	NSF, LRRC37A, ARL17B, LRRC37A17P	NSF, LRRC37A, LRRC37A4P, PLEKHM1, ARL17B, RN7SL730P	NA	NA
chr17	44,231,326	chr17:44231326	rs147317628	1.1e-06	ENSG00000073969(6.506e-16), ENSG00000176681(6.285e-64), ENSG00000228696(6.285e-64), ENSG00000262879(1.715e-07), ENSG00000263142(1.622e-06)	ENSG00000073969(3.809e-94), ENSG00000131484(1.089e-13), ENSG00000176681(8.213e-05), ENSG00000214425(1.089e-13), ENSG00000225190(2.05e-06), ENSG00000228696(8.213e-05), ENSG00000264225(2.05e-06), ENSG00000266918(1.089e-13)	NA	NA	7_Enh		NSF, LRRC37A, ARL17B, LRRC37A17P	NSF, LRRC37A, LRRC37A4P, PLEKHM1, ARL17B, RN7SL730P	NA	NA
chr17	44,232,959	chr17:44232959	rs142920272, rs147317628	2.9e-07, 1.1e-06	ENSG00000073969(6.506e-16), ENSG00000176681(6.285e-64), ENSG00000228696(6.285e-64), ENSG00000262879(1.715e-07), ENSG00000263142(1.622e-06)	ENSG00000073969(3.809e-94), ENSG00000131484(1.089e-13), ENSG00000176681(8.213e-05), ENSG00000214425(1.089e-13), ENSG00000225190(2.05e-06), ENSG00000228696(8.213e-05), ENSG00000264225(2.05e-06), ENSG00000266918(1.089e-13)	NA	NA	5_TxWk		NSF, LRRC37A, ARL17B, LRRC37A17P	NSF, LRRC37A, LRRC37A4P, PLEKHM1, ARL17B, RN7SL730P	NA	NA
chr17	44,233,433	chr17:44233433	rs142920272	2.9e-07	ENSG00000073969(6.506e-16), ENSG00000176681(6.285e-64), ENSG00000228696(6.285e-64), ENSG00000262879(1.715e-07), ENSG00000263142(1.622e-06)	ENSG00000073969(3.809e-94), ENSG00000131484(1.089e-13), ENSG00000176681(8.213e-05), ENSG00000214425(1.089e-13), ENSG00000225190(2.05e-06), ENSG00000228696(8.213e-05), ENSG00000264225(2.05e-06), ENSG00000266918(1.089e-13)	NA	NA	5_TxWk		NSF, LRRC37A, ARL17B, LRRC37A17P	NSF, LRRC37A, LRRC37A4P, PLEKHM1, ARL17B, RN7SL730P	NA	NA
chr17	44,233,589	chr17:44233589	rs147317628	1.1e-06	ENSG00000073969(6.506e-16), ENSG00000176681(6.285e-64), ENSG00000228696(6.285e-64), ENSG00000262879(1.715e-07), ENSG00000263142(1.622e-06)	ENSG00000073969(3.809e-94), ENSG00000131484(1.089e-13), ENSG00000176681(8.213e-05), ENSG00000214425(1.089e-13), ENSG00000225190(2.05e-06), ENSG00000228696(8.213e-05), ENSG00000264225(2.05e-06), ENSG00000266918(1.089e-13)	NA	NA	5_TxWk		NSF, LRRC37A, ARL17B, LRRC37A17P	NSF, LRRC37A, LRRC37A4P, PLEKHM1, ARL17B, RN7SL730P	NA	NA
chr17	44,234,060	chr17:44234060	rs147317628	1.1e-06	ENSG00000073969(6.506e-16), ENSG00000176681(6.285e-64), ENSG00000228696(6.285e-64), ENSG00000262879(1.715e-07), ENSG00000263142(1.622e-06)	ENSG00000073969(3.809e-94), ENSG00000131484(1.089e-13), ENSG00000176681(8.213e-05), ENSG00000214425(1.089e-13), ENSG00000225190(2.05e-06), ENSG00000228696(8.213e-05), ENSG00000264225(2.05e-06), ENSG00000266918(1.089e-13)	NA	NA	5_TxWk		NSF, LRRC37A, ARL17B, LRRC37A17P	NSF, LRRC37A, LRRC37A4P, PLEKHM1, ARL17B, RN7SL730P	NA	NA
chr17	44,234,265	chr17:44234265	rs147317628	1.1e-06	ENSG00000073969(6.506e-16), ENSG00000176681(6.285e-64), ENSG00000228696(6.285e-64), ENSG00000262879(1.715e-07), ENSG00000263142(1.622e-06)	ENSG00000073969(3.809e-94), ENSG00000131484(1.089e-13), ENSG00000176681(8.213e-05), ENSG00000214425(1.089e-13), ENSG00000225190(2.05e-06), ENSG00000228696(8.213e-05), ENSG00000264225(2.05e-06), ENSG00000266918(1.089e-13)	NA	NA	5_TxWk		NSF, LRRC37A, ARL17B, LRRC37A17P	NSF, LRRC37A, LRRC37A4P, PLEKHM1, ARL17B, RN7SL730P	NA	NA
chr17	44,236,725	chr17:44236725	rs142920272, rs147317628	2.9e-07, 1.1e-06	ENSG00000073969(6.506e-16), ENSG00000176681(6.285e-64), ENSG00000228696(6.285e-64), ENSG00000262879(1.715e-07), ENSG00000263142(1.622e-06)	ENSG00000073969(3.809e-94), ENSG00000131484(1.089e-13), ENSG00000176681(8.213e-05), ENSG00000214425(1.089e-13), ENSG00000225190(2.05e-06), ENSG00000228696(8.213e-05), ENSG00000264225(2.05e-06), ENSG00000266918(1.089e-13)	NA	NA	5_TxWk		NSF, LRRC37A, ARL17B, LRRC37A17P	NSF, LRRC37A, LRRC37A4P, PLEKHM1, ARL17B, RN7SL730P	NA	NA
chr17	44,237,068	chr17:44237068	rs142920272	2.9e-07	ENSG00000073969(6.506e-16), ENSG00000176681(6.285e-64), ENSG00000228696(6.285e-64), ENSG00000262879(1.715e-07), ENSG00000263142(1.622e-06)	ENSG00000073969(3.809e-94), ENSG00000131484(1.089e-13), ENSG00000176681(8.213e-05), ENSG00000214425(1.089e-13), ENSG00000225190(2.05e-06), ENSG00000228696(8.213e-05), ENSG00000264225(2.05e-06), ENSG00000266918(1.089e-13)	NA	NA	5_TxWk		NSF, LRRC37A, ARL17B, LRRC37A17P	NSF, LRRC37A, LRRC37A4P, PLEKHM1, ARL17B, RN7SL730P	NA	NA

Continues on the next page

Supplementary Table 16 – continued from previous page

CHR	BP	CredSNP	IndexSNP	Index P	ENSGID_CP	ENSGID_GZ	ENSGID Promoter	ENSGID functional	Chrom HMM	Histone	HGNC_CP	HGNC_GZ	HGNC Promoter	HGNC functional
chr17	44,237,372	chr17:44237372	rs142920272	2.9e-07	ENSG00000073969(6.506e-16), ENSG00000176681(6.285e-64), ENSG00000228696(6.285e-64), ENSG00000262879(1.715e-07), ENSG00000263142(1.622e-06)	ENSG00000073969(3.809e-94), ENSG00000131484(1.089e-13), ENSG00000176681(8.213e-05), ENSG00000214425(1.089e-13), ENSG00000225190(2.05e-06), ENSG00000228696(8.213e-05), ENSG00000264225(2.05e-06), ENSG00000266918(1.089e-13)	NA	NA	5_TxWk		NSF, LRRC37A, ARL17B, LRRC37A17P	NSF, LRRC37A, LRRC37A4P, PLEKHM1, ARL17B, RN7SL730P	NA	NA
chr17	44,237,790	chr17:44237790	rs142920272, rs147317628	2.9e-07, 1.1e-06	ENSG00000073969(6.506e-16), ENSG00000176681(6.285e-64), ENSG00000228696(6.285e-64), ENSG00000262879(1.715e-07), ENSG00000263142(1.622e-06)	ENSG00000073969(3.809e-94), ENSG00000131484(1.089e-13), ENSG00000176681(8.213e-05), ENSG00000214425(1.089e-13), ENSG00000225190(2.05e-06), ENSG00000228696(8.213e-05), ENSG00000264225(2.05e-06), ENSG00000266918(1.089e-13)	NA	NA	5_TxWk		NSF, LRRC37A, ARL17B, LRRC37A17P	NSF, LRRC37A, LRRC37A4P, PLEKHM1, ARL17B, RN7SL730P	NA	NA
chr17	44,238,130	chr17:44238130	rs142920272, rs147317628	2.9e-07, 1.1e-06	ENSG00000073969(6.506e-16), ENSG00000176681(6.285e-64), ENSG00000228696(6.285e-64), ENSG00000262879(1.715e-07), ENSG00000263142(1.622e-06)	ENSG00000073969(3.809e-94), ENSG00000131484(1.089e-13), ENSG00000176681(8.213e-05), ENSG00000214425(1.089e-13), ENSG00000225190(2.05e-06), ENSG00000228696(8.213e-05), ENSG00000264225(2.05e-06), ENSG00000266918(1.089e-13)	NA	NA	5_TxWk		NSF, LRRC37A, ARL17B, LRRC37A17P	NSF, LRRC37A, LRRC37A4P, PLEKHM1, ARL17B, RN7SL730P	NA	NA
chr17	44,238,424	chr17:44238424	rs142920272, rs147317628	2.9e-07, 1.1e-06	ENSG00000073969(6.506e-16), ENSG00000176681(6.285e-64), ENSG00000228696(6.285e-64), ENSG00000262879(1.715e-07), ENSG00000263142(1.622e-06)	ENSG00000073969(3.809e-94), ENSG00000131484(1.089e-13), ENSG00000176681(8.213e-05), ENSG00000214425(1.089e-13), ENSG00000225190(2.05e-06), ENSG00000228696(8.213e-05), ENSG00000264225(2.05e-06), ENSG00000266918(1.089e-13)	NA	NA	5_TxWk		NSF, LRRC37A, ARL17B, LRRC37A17P	NSF, LRRC37A, LRRC37A4P, PLEKHM1, ARL17B, RN7SL730P	NA	NA
chr17	44,238,571	chr17:44238571	rs142920272, rs147317628	2.9e-07, 1.1e-06	ENSG00000073969(6.506e-16), ENSG00000176681(6.285e-64), ENSG00000228696(6.285e-64), ENSG00000262879(1.715e-07), ENSG00000263142(1.622e-06)	ENSG00000073969(3.809e-94), ENSG00000131484(1.089e-13), ENSG00000176681(8.213e-05), ENSG00000214425(1.089e-13), ENSG00000225190(2.05e-06), ENSG00000228696(8.213e-05), ENSG00000264225(2.05e-06), ENSG00000266918(1.089e-13)	NA	NA	5_TxWk		NSF, LRRC37A, ARL17B, LRRC37A17P	NSF, LRRC37A, LRRC37A4P, PLEKHM1, ARL17B, RN7SL730P	NA	NA
chr17	44,239,958	chr17:44239958	rs142920272	2.9e-07	ENSG00000073969(6.506e-16), ENSG00000176681(6.285e-64), ENSG00000228696(6.285e-64), ENSG00000262879(1.715e-07), ENSG00000263142(1.622e-06)	ENSG00000073969(3.809e-94), ENSG00000131484(1.089e-13), ENSG00000176681(8.213e-05), ENSG00000214425(1.089e-13), ENSG00000225190(2.05e-06), ENSG00000228696(8.213e-05), ENSG00000264225(2.05e-06), ENSG00000266918(1.089e-13)	NA	NA	5_TxWk		NSF, LRRC37A, ARL17B, LRRC37A17P	NSF, LRRC37A, LRRC37A4P, PLEKHM1, ARL17B, RN7SL730P	NA	NA
chr17	44,241,304	chr17:44241304	rs147317628	1.1e-06	ENSG00000176681(0), ENSG00000228696(0), ENSG00000260075(8.89e-10)	ENSG00000176681(2.828e-09), ENSG00000228696(2.597e-31), ENSG00000238083(1.646e-06), ENSG00000260075(3.47e-99), ENSG00000266497(1.646e-06)	NA	NA	5_TxWk		LRRC37A, ARL17B, NSFP1	LRRC37A, ARL17B, LRRC37A2, NSFP1	NA	NA
chr17	44,242,536	chr17:44242536	rs142920272, rs147317628	2.9e-07, 1.1e-06	ENSG00000176681(0), ENSG00000228696(0), ENSG00000260075(8.89e-10)	ENSG00000176681(2.828e-09), ENSG00000228696(2.597e-31), ENSG00000238083(1.646e-06), ENSG00000260075(3.47e-99), ENSG00000266497(1.646e-06)	NA	NA	5_TxWk		LRRC37A, ARL17B, NSFP1	LRRC37A, ARL17B, LRRC37A2, NSFP1	NA	NA
chr17	44,242,574	chr17:44242574	rs142920272, rs147317628	2.9e-07, 1.1e-06	ENSG00000176681(0), ENSG00000228696(0), ENSG00000260075(8.89e-10)	ENSG00000176681(2.828e-09), ENSG00000228696(2.597e-31), ENSG00000238083(1.646e-06), ENSG00000260075(3.47e-99), ENSG00000266497(1.646e-06)	NA	NA	5_TxWk		LRRC37A, ARL17B, NSFP1	LRRC37A, ARL17B, LRRC37A2, NSFP1	NA	NA
chr17	44,242,788	chr17:44242788	rs142920272, rs147317628	2.9e-07, 1.1e-06	ENSG00000176681(0), ENSG00000228696(0), ENSG00000260075(8.89e-10)	ENSG00000176681(2.828e-09), ENSG00000228696(2.597e-31), ENSG00000238083(1.646e-06), ENSG00000260075(3.47e-99), ENSG00000266497(1.646e-06)	NA	NA	5_TxWk		LRRC37A, ARL17B, NSFP1	LRRC37A, ARL17B, LRRC37A2, NSFP1	NA	NA

Continues on the next page

Supplementary Table 16 – continued from previous page

CHR	BP	CredSNP	IndexSNP	Index P	ENSGID_CP	ENSGID_GZ	ENSGID Promoter	ENSGID functional	Chrom HMM	Histone	HGNC_CP	HGNC_GZ	HGNC Promoter	HGNC functional
chr17	44,243,543	chr17:44243543	rs142920272, rs147317628	2.9e-07, 1.1e-06	ENSG00000176681(0), ENSG00000228696(0), ENSG00000260075(8.89e-10)	ENSG00000176681(2.828e-09), ENSG00000228696(2.597e-31), ENSG00000238083(1.646e-06), ENSG00000260075(3.47e-99), ENSG00000266497(1.646e-06)	NA	NA	5_TxWk		LRRC37A, ARL17B, NSFP1	LRRC37A, ARL17B, LRRC37A2, NSFP1	NA	NA
chr17	44,243,979	chr17:44243979	rs142920272	2.9e-07	ENSG00000176681(0), ENSG00000228696(0), ENSG00000260075(8.89e-10)	ENSG00000176681(2.828e-09), ENSG00000228696(2.597e-31), ENSG00000238083(1.646e-06), ENSG00000260075(3.47e-99), ENSG00000266497(1.646e-06)	NA	NA	7_Enh	H3K4me1	LRRC37A, ARL17B, NSFP1	LRRC37A, ARL17B, LRRC37A2, NSFP1	NA	NA
chr17	44,244,397	chr17:44244397	rs142920272	2.9e-07	ENSG00000176681(0), ENSG00000228696(0), ENSG00000260075(8.89e-10)	ENSG00000176681(2.828e-09), ENSG00000228696(2.597e-31), ENSG00000238083(1.646e-06), ENSG00000260075(3.47e-99), ENSG00000266497(1.646e-06)	NA	NA	7_Enh		LRRC37A, ARL17B, NSFP1	LRRC37A, ARL17B, LRRC37A2, NSFP1	NA	NA
chr17	44,244,581	chr17:44244581	rs147317628	1.1e-06	ENSG00000176681(0), ENSG00000228696(0), ENSG00000260075(8.89e-10)	ENSG00000176681(2.828e-09), ENSG00000228696(2.597e-31), ENSG00000238083(1.646e-06), ENSG00000260075(3.47e-99), ENSG00000266497(1.646e-06)	NA	NA	5_TxWk		LRRC37A, ARL17B, NSFP1	LRRC37A, ARL17B, LRRC37A2, NSFP1	NA	NA
chr17	44,245,766	chr17:44245766	rs142920272, rs147317628	2.9e-07, 1.1e-06	ENSG00000176681(0), ENSG00000228696(0), ENSG00000260075(8.89e-10)	ENSG00000176681(2.828e-09), ENSG00000228696(2.597e-31), ENSG00000238083(1.646e-06), ENSG00000260075(3.47e-99), ENSG00000266497(1.646e-06)	NA	NA	5_TxWk		LRRC37A, ARL17B, NSFP1	LRRC37A, ARL17B, LRRC37A2, NSFP1	NA	NA
chr17	44,245,876	chr17:44245876	rs147317628	1.1e-06	ENSG00000176681(0), ENSG00000228696(0), ENSG00000260075(8.89e-10)	ENSG00000176681(2.828e-09), ENSG00000228696(2.597e-31), ENSG00000238083(1.646e-06), ENSG00000260075(3.47e-99), ENSG00000266497(1.646e-06)	NA	NA	5_TxWk		LRRC37A, ARL17B, NSFP1	LRRC37A, ARL17B, LRRC37A2, NSFP1	NA	NA
chr17	44,246,405	chr17:44246405	rs142920272, rs147317628	2.9e-07, 1.1e-06	ENSG00000176681(0), ENSG00000228696(0), ENSG00000260075(8.89e-10)	ENSG00000176681(2.828e-09), ENSG00000228696(2.597e-31), ENSG00000238083(1.646e-06), ENSG00000260075(3.47e-99), ENSG00000266497(1.646e-06)	NA	NA	5_TxWk		LRRC37A, ARL17B, NSFP1	LRRC37A, ARL17B, LRRC37A2, NSFP1	NA	NA
chr17	44,246,997	chr17:44246997	rs142920272, rs147317628	2.9e-07, 1.1e-06	ENSG00000176681(0), ENSG00000228696(0), ENSG00000260075(8.89e-10)	ENSG00000176681(2.828e-09), ENSG00000228696(2.597e-31), ENSG00000238083(1.646e-06), ENSG00000260075(3.47e-99), ENSG00000266497(1.646e-06)	NA	NA	7_Enh		LRRC37A, ARL17B, NSFP1	LRRC37A, ARL17B, LRRC37A2, NSFP1	NA	NA
chr17	44,247,314	chr17:44247314	rs142920272, rs147317628	2.9e-07, 1.1e-06	ENSG00000176681(0), ENSG00000228696(0), ENSG00000260075(8.89e-10)	ENSG00000176681(2.828e-09), ENSG00000228696(2.597e-31), ENSG00000238083(1.646e-06), ENSG00000260075(3.47e-99), ENSG00000266497(1.646e-06)	NA	NA	7_Enh	H3K4me1	LRRC37A, ARL17B, NSFP1	LRRC37A, ARL17B, LRRC37A2, NSFP1	NA	NA
chr17	44,248,042	chr17:44248042	rs142920272, rs147317628	2.9e-07, 1.1e-06	ENSG00000176681(0), ENSG00000228696(0), ENSG00000260075(8.89e-10)	ENSG00000176681(2.828e-09), ENSG00000228696(2.597e-31), ENSG00000238083(1.646e-06), ENSG00000260075(3.47e-99), ENSG00000266497(1.646e-06)	NA	NA	6_EnhG	H3K36me3	LRRC37A, ARL17B, NSFP1	LRRC37A, ARL17B, LRRC37A2, NSFP1	NA	NA
chr17	44,248,814	chr17:44248814	rs142920272, rs147317628	2.9e-07, 1.1e-06			ENSG00000120071		5_TxWk				KANSL1	
chr17	44,249,800	chr17:44249800	rs142920272, rs147317628	2.9e-07, 1.1e-06			ENSG00000120071		5_TxWk	DHS:H3K4me1			KANSL1	
chr17	44,250,616	chr17:44250616	rs142920272	2.9e-07			ENSG00000120071		5_TxWk				KANSL1	
chr17	44,250,669	chr17:44250669	rs142920272, rs147317628	2.9e-07, 1.1e-06			ENSG00000120071		5_TxWk				KANSL1	
chr17	44,251,548	chr17:44251548	rs147317628	1.1e-06			ENSG00000120071		5_TxWk	H3K4me1			KANSL1	
chr17	44,251,582	chr17:44251582	rs142920272, rs147317628	2.9e-07, 1.1e-06			ENSG00000120071		5_TxWk	H3K4me1			KANSL1	
chr17	44,251,698	chr17:44251698	rs142920272	2.9e-07	ENSG00000004897(3.479e-05), ENSG00000214425(0), ENSG00000267198(0), ENSG00000267246(0)	ENSG00000073969(9.158e-12), ENSG00000120071(2.834e-05), ENSG00000131484(1.201e-19), ENSG00000186868(2.834e-05), ENSG00000214425(1.201e-19), ENSG00000228696(1.46e-32), ENSG00000260075(1.46e-32), ENSG00000266918(1.201e-19)	NA	NA	5_TxWk	H3K4me1	CDC27, LRRC37A4P	NSF, KANSL1, MAPT, LRRC37A4P, ARL17B, NSFP1	NA	NA

Continues on the next page

Supplementary Table 16 – continued from previous page

CHR	BP	CredSNP	IndexSNP	Index P	ENSGID_CP	ENSGID_GZ	ENSGID Promoter	ENSGID functional	Chrom HMM	Histone	HGNC_CP	HGNC_GZ	HGNC Promoter	HGNC functional
chr17	44,251,907	chr17:44251907	rs142920272, rs147317628	2.9e-07, 1.1e-06	ENSG00000004897(3.479e-05), ENSG00000214425(0), ENSG00000267198(0), ENSG00000267246(0)	ENSG00000073969(9.158e-12), ENSG00000120071(2.834e-05), ENSG00000131484(1.201e-19), ENSG00000186868(2.834e-05), ENSG00000214425(1.201e-19), ENSG00000228696(1.46e-32), ENSG00000260075(1.46e-32), ENSG00000266918(1.201e-19)	NA	NA	5_TxWk		CDC27, LRRC37A4P	NSF, KANSL1, MAPT, LRRC37A4P, ARL17B, NSFP1	NA	NA
chr17	44,251,972	chr17:44251972	rs142920272, rs147317628	2.9e-07, 1.1e-06	ENSG00000004897(3.479e-05), ENSG00000214425(0), ENSG00000267198(0), ENSG00000267246(0)	ENSG00000073969(9.158e-12), ENSG00000120071(2.834e-05), ENSG00000131484(1.201e-19), ENSG00000186868(2.834e-05), ENSG00000214425(1.201e-19), ENSG00000228696(1.46e-32), ENSG00000260075(1.46e-32), ENSG00000266918(1.201e-19)	NA	NA	5_TxWk		CDC27, LRRC37A4P	NSF, KANSL1, MAPT, LRRC37A4P, ARL17B, NSFP1	NA	NA
chr17	44,252,098	chr17:44252098	rs147317628	1.1e-06	ENSG00000004897(3.479e-05), ENSG00000214425(0), ENSG00000267198(0), ENSG00000267246(0)	ENSG00000073969(9.158e-12), ENSG00000120071(2.834e-05), ENSG00000131484(1.201e-19), ENSG00000186868(2.834e-05), ENSG00000214425(1.201e-19), ENSG00000228696(1.46e-32), ENSG00000260075(1.46e-32), ENSG00000266918(1.201e-19)	NA	NA	5_TxWk		CDC27, LRRC37A4P	NSF, KANSL1, MAPT, LRRC37A4P, ARL17B, NSFP1	NA	NA
chr17	44,252,197	chr17:44252197	rs147317628	1.1e-06	ENSG00000004897(3.479e-05), ENSG00000214425(0), ENSG00000267198(0), ENSG00000267246(0)	ENSG00000073969(9.158e-12), ENSG00000120071(2.834e-05), ENSG00000131484(1.201e-19), ENSG00000186868(2.834e-05), ENSG00000214425(1.201e-19), ENSG00000228696(1.46e-32), ENSG00000260075(1.46e-32), ENSG00000266918(1.201e-19)	NA	NA	5_TxWk		CDC27, LRRC37A4P	NSF, KANSL1, MAPT, LRRC37A4P, ARL17B, NSFP1	NA	NA
chr17	44,252,416	chr17:44252416	rs142920272, rs147317628	2.9e-07, 1.1e-06	ENSG00000004897(3.479e-05), ENSG00000214425(0), ENSG00000267198(0), ENSG00000267246(0)	ENSG00000073969(9.158e-12), ENSG00000120071(2.834e-05), ENSG00000131484(1.201e-19), ENSG00000186868(2.834e-05), ENSG00000214425(1.201e-19), ENSG00000228696(1.46e-32), ENSG00000260075(1.46e-32), ENSG00000266918(1.201e-19)	NA	NA	5_TxWk		CDC27, LRRC37A4P	NSF, KANSL1, MAPT, LRRC37A4P, ARL17B, NSFP1	NA	NA
chr17	44,253,203	chr17:44253203	rs142920272, rs147317628	2.9e-07, 1.1e-06	ENSG00000004897(3.479e-05), ENSG00000214425(0), ENSG00000267198(0), ENSG00000267246(0)	ENSG00000073969(9.158e-12), ENSG00000120071(2.834e-05), ENSG00000131484(1.201e-19), ENSG00000186868(2.834e-05), ENSG00000214425(1.201e-19), ENSG00000228696(1.46e-32), ENSG00000260075(1.46e-32), ENSG00000266918(1.201e-19)	NA	NA	5_TxWk		CDC27, LRRC37A4P	NSF, KANSL1, MAPT, LRRC37A4P, ARL17B, NSFP1	NA	NA
chr17	44,254,379	chr17:44254379	rs142920272	2.9e-07	ENSG00000004897(3.479e-05), ENSG00000214425(0), ENSG00000267198(0), ENSG00000267246(0)	ENSG00000073969(9.158e-12), ENSG00000120071(2.834e-05), ENSG00000131484(1.201e-19), ENSG00000186868(2.834e-05), ENSG00000214425(1.201e-19), ENSG00000228696(1.46e-32), ENSG00000260075(1.46e-32), ENSG00000266918(1.201e-19)	NA	NA	5_TxWk		CDC27, LRRC37A4P	NSF, KANSL1, MAPT, LRRC37A4P, ARL17B, NSFP1	NA	NA
chr17	44,254,494	chr17:44254494	rs147317628	1.1e-06	ENSG00000004897(3.479e-05), ENSG00000214425(0), ENSG00000267198(0), ENSG00000267246(0)	ENSG00000073969(9.158e-12), ENSG00000120071(2.834e-05), ENSG00000131484(1.201e-19), ENSG00000186868(2.834e-05), ENSG00000214425(1.201e-19), ENSG00000228696(1.46e-32), ENSG00000260075(1.46e-32), ENSG00000266918(1.201e-19)	NA	NA	5_TxWk		CDC27, LRRC37A4P	NSF, KANSL1, MAPT, LRRC37A4P, ARL17B, NSFP1	NA	NA
chr17	44,254,686	chr17:44254686	rs142920272, rs147317628	2.9e-07, 1.1e-06	ENSG00000004897(3.479e-05), ENSG00000214425(0), ENSG00000267198(0), ENSG00000267246(0)	ENSG00000073969(9.158e-12), ENSG00000120071(2.834e-05), ENSG00000131484(1.201e-19), ENSG00000186868(2.834e-05), ENSG00000214425(1.201e-19), ENSG00000228696(1.46e-32), ENSG00000260075(1.46e-32), ENSG00000266918(1.201e-19)	NA	NA	5_TxWk		CDC27, LRRC37A4P	NSF, KANSL1, MAPT, LRRC37A4P, ARL17B, NSFP1	NA	NA

Continues on the next page

Supplementary Table 16 – continued from previous page

CHR	BP	CredSNP	IndexSNP	Index P	ENSGID_CP	ENSGID_GZ	ENSGID Promoter	ENSGID functional	Chrom HMM	Histone	HGNC_CP	HGNC_GZ	HGNC Promoter	HGNC functional
chr17	44,254,993	chr17:44254993	rs142920272	2.9e-07	ENSG00000004897(3.479e-05), ENSG00000214425(0), ENSG00000267198(0), ENSG00000267246(0)	ENSG00000073969(9.158e-12), ENSG00000120071(2.834e-05), ENSG00000131484(1.201e-19), ENSG00000186868(2.834e-05), ENSG00000214425(1.201e-19), ENSG00000228696(1.46e-32), ENSG00000260075(1.46e-32), ENSG00000266918(1.201e-19)	NA	NA	5_TxWk		CDC27, LRRC37A4P	NSF, KANSL1, MAPT, LRRC37A4P, ARL17B, NSFP1	NA	NA
chr17	44,255,532	chr17:44255532	rs147317628	1.1e-06	ENSG00000004897(3.479e-05), ENSG00000214425(0), ENSG00000267198(0), ENSG00000267246(0)	ENSG00000073969(9.158e-12), ENSG00000120071(2.834e-05), ENSG00000131484(1.201e-19), ENSG00000186868(2.834e-05), ENSG00000214425(1.201e-19), ENSG00000228696(1.46e-32), ENSG00000260075(1.46e-32), ENSG00000266918(1.201e-19)	NA	NA	5_TxWk		CDC27, LRRC37A4P	NSF, KANSL1, MAPT, LRRC37A4P, ARL17B, NSFP1	NA	NA
chr17	44,255,777	chr17:44255777	rs142920272, rs147317628	2.9e-07, 1.1e-06	ENSG00000004897(3.479e-05), ENSG00000214425(0), ENSG00000267198(0), ENSG00000267246(0)	ENSG00000073969(9.158e-12), ENSG00000120071(2.834e-05), ENSG00000131484(1.201e-19), ENSG00000186868(2.834e-05), ENSG00000214425(1.201e-19), ENSG00000228696(1.46e-32), ENSG00000260075(1.46e-32), ENSG00000266918(1.201e-19)	NA	NA	5_TxWk		CDC27, LRRC37A4P	NSF, KANSL1, MAPT, LRRC37A4P, ARL17B, NSFP1	NA	NA
chr17	44,257,783	chr17:44257783	rs142920272	2.9e-07	ENSG00000004897(3.479e-05), ENSG00000214425(0), ENSG00000267198(0), ENSG00000267246(0)	ENSG00000073969(9.158e-12), ENSG00000120071(2.834e-05), ENSG00000131484(1.201e-19), ENSG00000186868(2.834e-05), ENSG00000214425(1.201e-19), ENSG00000228696(1.46e-32), ENSG00000260075(1.46e-32), ENSG00000266918(1.201e-19)	NA	NA	5_TxWk		CDC27, LRRC37A4P	NSF, KANSL1, MAPT, LRRC37A4P, ARL17B, NSFP1	NA	NA
chr17	44,257,788	chr17:44257788	rs147317628	1.1e-06	ENSG00000004897(3.479e-05), ENSG00000214425(0), ENSG00000267198(0), ENSG00000267246(0)	ENSG00000073969(9.158e-12), ENSG00000120071(2.834e-05), ENSG00000131484(1.201e-19), ENSG00000186868(2.834e-05), ENSG00000214425(1.201e-19), ENSG00000228696(1.46e-32), ENSG00000260075(1.46e-32), ENSG00000266918(1.201e-19)	NA	NA	5_TxWk		CDC27, LRRC37A4P	NSF, KANSL1, MAPT, LRRC37A4P, ARL17B, NSFP1	NA	NA
chr17	44,258,354	chr17:44258354	rs142920272, rs147317628	2.9e-07, 1.1e-06	ENSG00000004897(3.479e-05), ENSG00000214425(0), ENSG00000267198(0), ENSG00000267246(0)	ENSG00000073969(9.158e-12), ENSG00000120071(2.834e-05), ENSG00000131484(1.201e-19), ENSG00000186868(2.834e-05), ENSG00000214425(1.201e-19), ENSG00000228696(1.46e-32), ENSG00000260075(1.46e-32), ENSG00000266918(1.201e-19)	NA	NA	5_TxWk		CDC27, LRRC37A4P	NSF, KANSL1, MAPT, LRRC37A4P, ARL17B, NSFP1	NA	NA
chr17	44,258,422	chr17:44258422	rs142920272, rs147317628	2.9e-07, 1.1e-06	ENSG00000004897(3.479e-05), ENSG00000214425(0), ENSG00000267198(0), ENSG00000267246(0)	ENSG00000073969(9.158e-12), ENSG00000120071(2.834e-05), ENSG00000131484(1.201e-19), ENSG00000186868(2.834e-05), ENSG00000214425(1.201e-19), ENSG00000228696(1.46e-32), ENSG00000260075(1.46e-32), ENSG00000266918(1.201e-19)	NA	NA	5_TxWk		CDC27, LRRC37A4P	NSF, KANSL1, MAPT, LRRC37A4P, ARL17B, NSFP1	NA	NA
chr17	44,258,954	chr17:44258954	rs142920272, rs147317628	2.9e-07, 1.1e-06	ENSG00000004897(3.479e-05), ENSG00000214425(0), ENSG00000267198(0), ENSG00000267246(0)	ENSG00000073969(9.158e-12), ENSG00000120071(2.834e-05), ENSG00000131484(1.201e-19), ENSG00000186868(2.834e-05), ENSG00000214425(1.201e-19), ENSG00000228696(1.46e-32), ENSG00000260075(1.46e-32), ENSG00000266918(1.201e-19)	NA	NA	5_TxWk		CDC27, LRRC37A4P	NSF, KANSL1, MAPT, LRRC37A4P, ARL17B, NSFP1	NA	NA
chr17	44,259,040	chr17:44259040	rs142920272	2.9e-07	ENSG00000004897(3.479e-05), ENSG00000214425(0), ENSG00000267198(0), ENSG00000267246(0)	ENSG00000073969(9.158e-12), ENSG00000120071(2.834e-05), ENSG00000131484(1.201e-19), ENSG00000186868(2.834e-05), ENSG00000214425(1.201e-19), ENSG00000228696(1.46e-32), ENSG00000260075(1.46e-32), ENSG00000266918(1.201e-19)	NA	NA	5_TxWk		CDC27, LRRC37A4P	NSF, KANSL1, MAPT, LRRC37A4P, ARL17B, NSFP1	NA	NA

Continues on the next page

Supplementary Table 16 – continued from previous page

CHR	BP	CredSNP	IndexSNP	Index P	ENSGID_CP	ENSGID_GZ	ENSGID Promoter	ENSGID functional	Chrom HMM	Histone	HGNC_CP	HGNC_GZ	HGNC Promoter	HGNC functional
chr17	44,259,792	chr17:44259792	rs142920272, rs147317628	2.9e-07, 1.1e-06	ENSG00000004897(3.479e-05), ENSG00000214425(0), ENSG00000267198(0), ENSG00000267246(0)	ENSG00000073969(9.158e-12), ENSG00000120071(2.834e-05), ENSG00000131484(1.201e-19), ENSG00000186868(2.834e-05), ENSG00000214425(1.201e-19), ENSG00000228696(1.46e-32), ENSG00000260075(1.46e-32), ENSG00000266918(1.201e-19)	NA	NA	5_TxWk		CDC27, LRRC37A4P	NSF, KANSL1, MAPT, LRRC37A4P, ARL17B, NSFP1	NA	NA
chr17	44,260,416	chr17:44260416	rs142920272	2.9e-07	ENSG00000120071(9.613e-15), ENSG00000186868(1.943e-06), ENSG00000228696(1.763e-05), ENSG00000260075(1.763e-05), ENSG00000262372(2.229e-05)	ENSG00000131484(6.359e-16), ENSG00000176681(0), ENSG00000185829(4.033e-101), ENSG00000214425(6.359e-16), ENSG00000228696(0), ENSG00000238083(4.033e-101), ENSG00000262879(5.357e-06)	NA	NA	5_TxWk	H3K4me1	KANSL1, MAPT, ARL17B, NSFP1	LRRC37A, ARL17A, LRRC37A4P, ARL17B, LRRC37A2	NA	NA
chr17	44,260,939	chr17:44260939	rs147317628	1.1e-06	ENSG00000120071(9.613e-15), ENSG00000186868(1.943e-06), ENSG00000228696(1.763e-05), ENSG00000260075(1.763e-05), ENSG00000262372(2.229e-05)	ENSG00000131484(6.359e-16), ENSG00000176681(0), ENSG00000185829(4.033e-101), ENSG00000214425(6.359e-16), ENSG00000228696(0), ENSG00000238083(4.033e-101), ENSG00000262879(5.357e-06)	NA	NA	7_Enh	H3K4me1	KANSL1, MAPT, ARL17B, NSFP1	LRRC37A, ARL17A, LRRC37A4P, ARL17B, LRRC37A2	NA	NA
chr17	44,260,967	chr17:44260967	rs142920272, rs147317628	2.9e-07, 1.1e-06	ENSG00000120071(9.613e-15), ENSG00000186868(1.943e-06), ENSG00000228696(1.763e-05), ENSG00000260075(1.763e-05), ENSG00000262372(2.229e-05)	ENSG00000131484(6.359e-16), ENSG00000176681(0), ENSG00000185829(4.033e-101), ENSG00000214425(6.359e-16), ENSG00000228696(0), ENSG00000238083(4.033e-101), ENSG00000262879(5.357e-06)	NA	NA	7_Enh	H3K4me1	KANSL1, MAPT, ARL17B, NSFP1	LRRC37A, ARL17A, LRRC37A4P, ARL17B, LRRC37A2	NA	NA
chr17	44,261,613	chr17:44261613	rs142920272, rs147317628	2.9e-07, 1.1e-06	ENSG00000120071(9.613e-15), ENSG00000186868(1.943e-06), ENSG00000228696(1.763e-05), ENSG00000260075(1.763e-05), ENSG00000262372(2.229e-05)	ENSG00000131484(6.359e-16), ENSG00000176681(0), ENSG00000185829(4.033e-101), ENSG00000214425(6.359e-16), ENSG00000228696(0), ENSG00000238083(4.033e-101), ENSG00000262879(5.357e-06)	NA	NA	7_Enh	DHS	KANSL1, MAPT, ARL17B, NSFP1	LRRC37A, ARL17A, LRRC37A4P, ARL17B, LRRC37A2	NA	NA
chr17	44,261,753	chr17:44261753	rs147317628	1.1e-06	ENSG00000120071(9.613e-15), ENSG00000186868(1.943e-06), ENSG00000228696(1.763e-05), ENSG00000260075(1.763e-05), ENSG00000262372(2.229e-05)	ENSG00000131484(6.359e-16), ENSG00000176681(0), ENSG00000185829(4.033e-101), ENSG00000214425(6.359e-16), ENSG00000228696(0), ENSG00000238083(4.033e-101), ENSG00000262879(5.357e-06)	NA	NA	7_Enh		KANSL1, MAPT, ARL17B, NSFP1	LRRC37A, ARL17A, LRRC37A4P, ARL17B, LRRC37A2	NA	NA
chr17	44,262,203	chr17:44262203	rs142920272, rs147317628	2.9e-07, 1.1e-06	ENSG00000120071(9.613e-15), ENSG00000186868(1.943e-06), ENSG00000228696(1.763e-05), ENSG00000260075(1.763e-05), ENSG00000262372(2.229e-05)	ENSG00000131484(6.359e-16), ENSG00000176681(0), ENSG00000185829(4.033e-101), ENSG00000214425(6.359e-16), ENSG00000228696(0), ENSG00000238083(4.033e-101), ENSG00000262879(5.357e-06)	NA	NA	7_Enh	H3K4me1	KANSL1, MAPT, ARL17B, NSFP1	LRRC37A, ARL17A, LRRC37A4P, ARL17B, LRRC37A2	NA	NA
chr17	44,262,403	chr17:44262403	rs142920272, rs147317628	2.9e-07, 1.1e-06	ENSG00000120071(9.613e-15), ENSG00000186868(1.943e-06), ENSG00000228696(1.763e-05), ENSG00000260075(1.763e-05), ENSG00000262372(2.229e-05)	ENSG00000131484(6.359e-16), ENSG00000176681(0), ENSG00000185829(4.033e-101), ENSG00000214425(6.359e-16), ENSG00000228696(0), ENSG00000238083(4.033e-101), ENSG00000262879(5.357e-06)	NA	NA	7_Enh	H3K4me1	KANSL1, MAPT, ARL17B, NSFP1	LRRC37A, ARL17A, LRRC37A4P, ARL17B, LRRC37A2	NA	NA
chr17	44,262,418	chr17:44262418	rs142920272	2.9e-07	ENSG00000120071(9.613e-15), ENSG00000186868(1.943e-06), ENSG00000228696(1.763e-05), ENSG00000260075(1.763e-05), ENSG00000262372(2.229e-05)	ENSG00000131484(6.359e-16), ENSG00000176681(0), ENSG00000185829(4.033e-101), ENSG00000214425(6.359e-16), ENSG00000228696(0), ENSG00000238083(4.033e-101), ENSG00000262879(5.357e-06)	NA	NA	7_Enh	H3K4me1	KANSL1, MAPT, ARL17B, NSFP1	LRRC37A, ARL17A, LRRC37A4P, ARL17B, LRRC37A2	NA	NA
chr17	44,263,022	chr17:44263022	rs142920272	2.9e-07	ENSG00000120071(9.613e-15), ENSG00000186868(1.943e-06), ENSG00000228696(1.763e-05), ENSG00000260075(1.763e-05), ENSG00000262372(2.229e-05)	ENSG00000131484(6.359e-16), ENSG00000176681(0), ENSG00000185829(4.033e-101), ENSG00000214425(6.359e-16), ENSG00000228696(0), ENSG00000238083(4.033e-101), ENSG00000262879(5.357e-06)	NA	NA	7_Enh	H3K4me1	KANSL1, MAPT, ARL17B, NSFP1	LRRC37A, ARL17A, LRRC37A4P, ARL17B, LRRC37A2	NA	NA

Continues on the next page

Supplementary Table 16 – continued from previous page

CHR	BP	CredSNP	IndexSNP	Index P	ENSGID_CP	ENSGID_GZ	ENSGID Promoter	ENSGID functional	Chrom HMM	Histone	HGNC_CP	HGNC_GZ	HGNC Promoter	HGNC functional
chr17	44,263,341	chr17:44263341	rs142920272, rs147317628	2.9e-07, 1.1e-06	ENSG00000120071(9.613e-15), ENSG00000186868(1.943e-06), ENSG00000228696(1.763e-05), ENSG00000260075(1.763e-05), ENSG00000262372(2.229e-05)	ENSG00000131484(6.359e-16), ENSG00000176681(0), ENSG00000185829(4.033e-101), ENSG00000214425(6.359e-16), ENSG00000228696(0), ENSG00000238083(4.033e-101), ENSG00000262879(5.357e-06)	NA	NA	7_Enh	H3K4me1	KANSL1, MAPT, ARL17B, NSFP1	LRRC37A, ARL17A, LRRC37A4P, ARL17B, LRRC37A2	NA	NA
chr17	44,263,729	chr17:44263729	rs147317628	1.1e-06	ENSG00000120071(9.613e-15), ENSG00000186868(1.943e-06), ENSG00000228696(1.763e-05), ENSG00000260075(1.763e-05), ENSG00000262372(2.229e-05)	ENSG00000131484(6.359e-16), ENSG00000176681(0), ENSG00000185829(4.033e-101), ENSG00000214425(6.359e-16), ENSG00000228696(0), ENSG00000238083(4.033e-101), ENSG00000262879(5.357e-06)	NA	NA	7_Enh		KANSL1, MAPT, ARL17B, NSFP1	LRRC37A, ARL17A, LRRC37A4P, ARL17B, LRRC37A2	NA	NA
chr17	44,263,965	chr17:44263965	rs147317628	1.1e-06	ENSG00000120071(9.613e-15), ENSG00000186868(1.943e-06), ENSG00000228696(1.763e-05), ENSG00000260075(1.763e-05), ENSG00000262372(2.229e-05)	ENSG00000131484(6.359e-16), ENSG00000176681(0), ENSG00000185829(4.033e-101), ENSG00000214425(6.359e-16), ENSG00000228696(0), ENSG00000238083(4.033e-101), ENSG00000262879(5.357e-06)	NA	NA	7_Enh		KANSL1, MAPT, ARL17B, NSFP1	LRRC37A, ARL17A, LRRC37A4P, ARL17B, LRRC37A2	NA	NA
chr17	44,264,045	chr17:44264045	rs142920272, rs147317628	2.9e-07, 1.1e-06	ENSG00000120071(9.613e-15), ENSG00000186868(1.943e-06), ENSG00000228696(1.763e-05), ENSG00000260075(1.763e-05), ENSG00000262372(2.229e-05)	ENSG00000131484(6.359e-16), ENSG00000176681(0), ENSG00000185829(4.033e-101), ENSG00000214425(6.359e-16), ENSG00000228696(0), ENSG00000238083(4.033e-101), ENSG00000262879(5.357e-06)	NA	NA	7_Enh		KANSL1, MAPT, ARL17B, NSFP1	LRRC37A, ARL17A, LRRC37A4P, ARL17B, LRRC37A2	NA	NA
chr17	44,264,269	chr17:44264269	rs142920272, rs147317628	2.9e-07, 1.1e-06	ENSG00000120071(9.613e-15), ENSG00000186868(1.943e-06), ENSG00000228696(1.763e-05), ENSG00000260075(1.763e-05), ENSG00000262372(2.229e-05)	ENSG00000131484(6.359e-16), ENSG00000176681(0), ENSG00000185829(4.033e-101), ENSG00000214425(6.359e-16), ENSG00000228696(0), ENSG00000238083(4.033e-101), ENSG00000262879(5.357e-06)	NA	NA	7_Enh	H3K4me1	KANSL1, MAPT, ARL17B, NSFP1	LRRC37A, ARL17A, LRRC37A4P, ARL17B, LRRC37A2	NA	NA
chr17	44,264,717	chr17:44264717	rs142920272, rs147317628	2.9e-07, 1.1e-06	ENSG00000120071(9.613e-15), ENSG00000186868(1.943e-06), ENSG00000228696(1.763e-05), ENSG00000260075(1.763e-05), ENSG00000262372(2.229e-05)	ENSG00000131484(6.359e-16), ENSG00000176681(0), ENSG00000185829(4.033e-101), ENSG00000214425(6.359e-16), ENSG00000228696(0), ENSG00000238083(4.033e-101), ENSG00000262879(5.357e-06)	NA	NA	7_Enh	H3K4me1	KANSL1, MAPT, ARL17B, NSFP1	LRRC37A, ARL17A, LRRC37A4P, ARL17B, LRRC37A2	NA	NA
chr17	44,264,943	chr17:44264943	rs142920272, rs147317628	2.9e-07, 1.1e-06	ENSG00000120071(9.613e-15), ENSG00000186868(1.943e-06), ENSG00000228696(1.763e-05), ENSG00000260075(1.763e-05), ENSG00000262372(2.229e-05)	ENSG00000131484(6.359e-16), ENSG00000176681(0), ENSG00000185829(4.033e-101), ENSG00000214425(6.359e-16), ENSG00000228696(0), ENSG00000238083(4.033e-101), ENSG00000262879(5.357e-06)	NA	NA	7_Enh		KANSL1, MAPT, ARL17B, NSFP1	LRRC37A, ARL17A, LRRC37A4P, ARL17B, LRRC37A2	NA	NA
chr17	44,265,192	chr17:44265192	rs147317628	1.1e-06	ENSG00000120071(9.613e-15), ENSG00000186868(1.943e-06), ENSG00000228696(1.763e-05), ENSG00000260075(1.763e-05), ENSG00000262372(2.229e-05)	ENSG00000131484(6.359e-16), ENSG00000176681(0), ENSG00000185829(4.033e-101), ENSG00000214425(6.359e-16), ENSG00000228696(0), ENSG00000238083(4.033e-101), ENSG00000262879(5.357e-06)	NA	NA	7_Enh		KANSL1, MAPT, ARL17B, NSFP1	LRRC37A, ARL17A, LRRC37A4P, ARL17B, LRRC37A2	NA	NA
chr17	44,265,328	chr17:44265328	rs142920272, rs147317628	2.9e-07, 1.1e-06	ENSG00000120071(9.613e-15), ENSG00000186868(1.943e-06), ENSG00000228696(1.763e-05), ENSG00000260075(1.763e-05), ENSG00000262372(2.229e-05)	ENSG00000131484(6.359e-16), ENSG00000176681(0), ENSG00000185829(4.033e-101), ENSG00000214425(6.359e-16), ENSG00000228696(0), ENSG00000238083(4.033e-101), ENSG00000262879(5.357e-06)	NA	NA	7_Enh		KANSL1, MAPT, ARL17B, NSFP1	LRRC37A, ARL17A, LRRC37A4P, ARL17B, LRRC37A2	NA	NA
chr17	44,265,702	chr17:44265702	rs147317628	1.1e-06	ENSG00000120071(9.613e-15), ENSG00000186868(1.943e-06), ENSG00000228696(1.763e-05), ENSG00000260075(1.763e-05), ENSG00000262372(2.229e-05)	ENSG00000131484(6.359e-16), ENSG00000176681(0), ENSG00000185829(4.033e-101), ENSG00000214425(6.359e-16), ENSG00000228696(0), ENSG00000238083(4.033e-101), ENSG00000262879(5.357e-06)	NA	NA	2_TssAFlnk	H3K4me1	KANSL1, MAPT, ARL17B, NSFP1	LRRC37A, ARL17A, LRRC37A4P, ARL17B, LRRC37A2	NA	NA

Continues on the next page

Supplementary Table 16 – continued from previous page

CHR	BP	CredSNP	IndexSNP	Index P	ENSGID_CP	ENSGID_GZ	ENSGID Promoter	ENSGID functional	Chrom HMM	Histone	HGNC_CP	HGNC_GZ	HGNC Promoter	HGNC functional
chr17	44,266,022	chr17:44266022	rs142920272, rs147317628	2.9e-07, 1.1e-06	ENSG00000120071(9.613e-15), ENSG00000186868(1.943e-06), ENSG00000228696(1.763e-05), ENSG00000260075(1.763e-05), ENSG00000262372(2.229e-05)	ENSG00000131484(6.359e-16), ENSG00000176681(0), ENSG00000185829(4.033e-101), ENSG00000214425(6.359e-16), ENSG00000228696(0), ENSG00000238083(4.033e-101), ENSG00000262879(5.357e-06)	NA	NA	7_Enh		KANSL1, MAPT, ARL17B, NSFP1	LRRC37A, ARL17A, LRRC37A4P, ARL17B, LRRC37A2	NA	NA
chr17	44,266,972	chr17:44266972	rs147317628	1.1e-06	ENSG00000120071(9.613e-15), ENSG00000186868(1.943e-06), ENSG00000228696(1.763e-05), ENSG00000260075(1.763e-05), ENSG00000262372(2.229e-05)	ENSG00000131484(6.359e-16), ENSG00000176681(0), ENSG00000185829(4.033e-101), ENSG00000214425(6.359e-16), ENSG00000228696(0), ENSG00000238083(4.033e-101), ENSG00000262879(5.357e-06)	NA	NA	7_Enh	H3K4me1	KANSL1, MAPT, ARL17B, NSFP1	LRRC37A, ARL17A, LRRC37A4P, ARL17B, LRRC37A2	NA	NA
chr17	44,267,617	chr17:44267617	rs147317628	1.1e-06	ENSG00000120071(9.613e-15), ENSG00000186868(1.943e-06), ENSG00000228696(1.763e-05), ENSG00000260075(1.763e-05), ENSG00000262372(2.229e-05)	ENSG00000131484(6.359e-16), ENSG00000176681(0), ENSG00000185829(4.033e-101), ENSG00000214425(6.359e-16), ENSG00000228696(0), ENSG00000238083(4.033e-101), ENSG00000262879(5.357e-06)	NA	NA	2_TssAFlnk		KANSL1, MAPT, ARL17B, NSFP1	LRRC37A, ARL17A, LRRC37A4P, ARL17B, LRRC37A2	NA	NA
chr17	44,269,546	chr17:44269546	rs142920272, rs147317628	2.9e-07, 1.1e-06			ENSG00000214401		8_ZNF/Rpts	DHS:H3K4me3			KANSL1-AS1	
chr17	44,269,676	chr17:44269676	rs142920272, rs147317628	2.9e-07, 1.1e-06			ENSG00000214401		8_ZNF/Rpts	H3K4me3			KANSL1-AS1	
chr17	44,271,152	chr17:44271152	rs142920272, rs147317628	2.9e-07, 1.1e-06			ENSG00000120071		1_TssA	DHS:H3K4me3			KANSL1	
chr17	44,271,430	chr17:44271430	rs142920272, rs147317628	2.9e-07, 1.1e-06			ENSG00000120071, ENSG00000214401		1_TssA	DHS			KANSL1, KANSL1-AS1	
chr17	44,272,266	chr17:44272266	rs142920272	2.9e-07			ENSG00000120071, ENSG00000214401		5_TxWk				KANSL1, KANSL1-AS1	
chr17	44,272,552	chr17:44272552	rs142920272	2.9e-07			ENSG00000120071, ENSG00000214401		5_TxWk	DHS			KANSL1, KANSL1-AS1	
chr17	44,272,679	chr17:44272679	rs142920272, rs147317628	2.9e-07, 1.1e-06			ENSG00000120071, ENSG00000214401		5_TxWk				KANSL1, KANSL1-AS1	
chr17	44,272,928	chr17:44272928	rs142920272	2.9e-07			ENSG00000120071, ENSG00000214401		5_TxWk				KANSL1, KANSL1-AS1	
chr17	44,273,264	chr17:44273264	rs142920272	2.9e-07			ENSG00000214401		5_TxWk				KANSL1-AS1	
chr17	44,273,448	chr17:44273448	rs142920272, rs147317628	2.9e-07, 1.1e-06	ENSG00000120071(5.738e-08), ENSG00000228696(6.206e-181), ENSG00000260075(6.206e-181)	ENSG00000120071(8.6e-08), ENSG00000185829(0), ENSG00000238083(0), ENSG00000262500(1.699e-08)	NA	NA	5_TxWk		KANSL1, ARL17B, NSFP1	KANSL1, ARL17A, LRRC37A2	NA	NA
chr17	44,273,448	chr17:44273448m	rs142920272	2.9e-07	ENSG00000120071(5.738e-08), ENSG00000228696(6.206e-181), ENSG00000260075(6.206e-181)	ENSG00000120071(8.6e-08), ENSG00000185829(0), ENSG00000238083(0), ENSG00000262500(1.699e-08)	NA	NA	5_TxWk		KANSL1, ARL17B, NSFP1	KANSL1, ARL17A, LRRC37A2	NA	NA
chr17	44,275,172	chr17:44275172	rs142920272, rs147317628	2.9e-07, 1.1e-06	ENSG00000120071(5.738e-08), ENSG00000228696(6.206e-181), ENSG00000260075(6.206e-181)	ENSG00000120071(8.6e-08), ENSG00000185829(0), ENSG00000238083(0), ENSG00000262500(1.699e-08)	NA	NA	5_TxWk		KANSL1, ARL17B, NSFP1	KANSL1, ARL17A, LRRC37A2	NA	NA
chr17	44,275,619	chr17:44275619	rs147317628	1.1e-06	ENSG00000120071(5.738e-08), ENSG00000228696(6.206e-181), ENSG00000260075(6.206e-181)	ENSG00000120071(8.6e-08), ENSG00000185829(0), ENSG00000238083(0), ENSG00000262500(1.699e-08)	NA	NA	5_TxWk		KANSL1, ARL17B, NSFP1	KANSL1, ARL17A, LRRC37A2	NA	NA
chr17	44,276,578	chr17:44276578	rs147317628	1.1e-06	ENSG00000120071(5.738e-08), ENSG00000228696(6.206e-181), ENSG00000260075(6.206e-181)	ENSG00000120071(8.6e-08), ENSG00000185829(0), ENSG00000238083(0), ENSG00000262500(1.699e-08)	NA	NA	5_TxWk		KANSL1, ARL17B, NSFP1	KANSL1, ARL17A, LRRC37A2	NA	NA

Continues on the next page

Supplementary Table 16 – continued from previous page

CHR	BP	CredSNP	IndexSNP	Index P	ENSGID_CP	ENSGID_GZ	ENSGID Promoter	ENSGID functional	Chrom HMM	Histone	HGNC_CP	HGNC_GZ	HGNC Promoter	HGNC functional
chr17	44,276,618	chr17:44276618	rs142920272	2.9e-07	ENSG00000120071(5.738e-08), ENSG00000228696(6.206e-181), ENSG00000260075(6.206e-181)	ENSG00000120071(8.6e-08), ENSG00000185829(0), ENSG00000238083(0), ENSG00000262500(1.699e-08)	NA	NA	5_TxWk		KANSL1, ARL17B, NSFP1	KANSL1, ARL17A, LRRC37A2	NA	NA
chr17	44,276,821	chr17:44276821	rs142920272, rs147317628	2.9e-07, 1.1e-06	ENSG00000120071(5.738e-08), ENSG00000228696(6.206e-181), ENSG00000260075(6.206e-181)	ENSG00000120071(8.6e-08), ENSG00000185829(0), ENSG00000238083(0), ENSG00000262500(1.699e-08)	NA	NA	5_TxWk		KANSL1, ARL17B, NSFP1	KANSL1, ARL17A, LRRC37A2	NA	NA
chr17	44,277,691	chr17:44277691	rs142920272, rs147317628	2.9e-07, 1.1e-06	ENSG00000120071(5.738e-08), ENSG00000228696(6.206e-181), ENSG00000260075(6.206e-181)	ENSG00000120071(8.6e-08), ENSG00000185829(0), ENSG00000238083(0), ENSG00000262500(1.699e-08)	NA	NA	5_TxWk		KANSL1, ARL17B, NSFP1	KANSL1, ARL17A, LRRC37A2	NA	NA
chr17	44,277,818	chr17:44277818	rs147317628	1.1e-06	ENSG00000120071(5.738e-08), ENSG00000228696(6.206e-181), ENSG00000260075(6.206e-181)	ENSG00000120071(8.6e-08), ENSG00000185829(0), ENSG00000238083(0), ENSG00000262500(1.699e-08)	NA	NA	5_TxWk		KANSL1, ARL17B, NSFP1	KANSL1, ARL17A, LRRC37A2	NA	NA
chr17	44,277,923	chr17:44277923	rs142920272, rs147317628	2.9e-07, 1.1e-06	ENSG00000120071(5.738e-08), ENSG00000228696(6.206e-181), ENSG00000260075(6.206e-181)	ENSG00000120071(8.6e-08), ENSG00000185829(0), ENSG00000238083(0), ENSG00000262500(1.699e-08)	NA	NA	5_TxWk		KANSL1, ARL17B, NSFP1	KANSL1, ARL17A, LRRC37A2	NA	NA
chr17	44,281,452	chr17:44281452	rs147317628	1.1e-06	ENSG00000006062(7.889e-05), ENSG00000120071(6.771e-18), ENSG00000186868(4.302e-05), ENSG00000228696(8.171e-82), ENSG00000260075(8.171e-82), ENSG00000262500(4.334e-75)	ENSG00000120071(8.907e-09), ENSG00000131484(1.778e-10), ENSG00000176681(0), ENSG00000185829(2.706e-16), ENSG00000214425(1.778e-10), ENSG00000225190(1.778e-10), ENSG00000228696(0), ENSG00000238083(2.706e-16), ENSG00000262500(1.013e-28), ENSG00000262879(1.557e-07)	NA	NA	5_TxWk		MAP3K14, KANSL1, MAPT, ARL17B, NSFP1	KANSL1, LRRC37A, ARL17A, LRRC37A4P, PLEKHM1, ARL17B, LRRC37A2	NA	NA
chr17	44,283,139	chr17:44283139	rs147317628	1.1e-06	ENSG00000006062(7.889e-05), ENSG00000120071(6.771e-18), ENSG00000186868(4.302e-05), ENSG00000228696(8.171e-82), ENSG00000260075(8.171e-82), ENSG00000262500(4.334e-75)	ENSG00000120071(8.907e-09), ENSG00000131484(1.778e-10), ENSG00000176681(0), ENSG00000185829(2.706e-16), ENSG00000214425(1.778e-10), ENSG00000225190(1.778e-10), ENSG00000228696(0), ENSG00000238083(2.706e-16), ENSG00000262500(1.013e-28), ENSG00000262879(1.557e-07)	NA	NA	5_TxWk		MAP3K14, KANSL1, MAPT, ARL17B, NSFP1	KANSL1, LRRC37A, ARL17A, LRRC37A4P, PLEKHM1, ARL17B, LRRC37A2	NA	NA
chr17	44,283,479	chr17:44283479	rs142920272	2.9e-07	ENSG00000006062(7.889e-05), ENSG00000120071(6.771e-18), ENSG00000186868(4.302e-05), ENSG00000228696(8.171e-82), ENSG00000260075(8.171e-82), ENSG00000262500(4.334e-75)	ENSG00000120071(8.907e-09), ENSG00000131484(1.778e-10), ENSG00000176681(0), ENSG00000185829(2.706e-16), ENSG00000214425(1.778e-10), ENSG00000225190(1.778e-10), ENSG00000228696(0), ENSG00000238083(2.706e-16), ENSG00000262500(1.013e-28), ENSG00000262879(1.557e-07)	NA	NA	8_ZNF/Rpts		MAP3K14, KANSL1, MAPT, ARL17B, NSFP1	KANSL1, LRRC37A, ARL17A, LRRC37A4P, PLEKHM1, ARL17B, LRRC37A2	NA	NA
chr17	44,283,761	chr17:44283761	rs142920272, rs147317628	2.9e-07, 1.1e-06	ENSG00000006062(7.889e-05), ENSG00000120071(6.771e-18), ENSG00000186868(4.302e-05), ENSG00000228696(8.171e-82), ENSG00000260075(8.171e-82), ENSG00000262500(4.334e-75)	ENSG00000120071(8.907e-09), ENSG00000131484(1.778e-10), ENSG00000176681(0), ENSG00000185829(2.706e-16), ENSG00000214425(1.778e-10), ENSG00000225190(1.778e-10), ENSG00000228696(0), ENSG00000238083(2.706e-16), ENSG00000262500(1.013e-28), ENSG00000262879(1.557e-07)	NA	NA	8_ZNF/Rpts		MAP3K14, KANSL1, MAPT, ARL17B, NSFP1	KANSL1, LRRC37A, ARL17A, LRRC37A4P, PLEKHM1, ARL17B, LRRC37A2	NA	NA
chr17	44,284,542	chr17:44284542	rs142920272, rs147317628	2.9e-07, 1.1e-06	ENSG00000006062(7.889e-05), ENSG00000120071(6.771e-18), ENSG00000186868(4.302e-05), ENSG00000228696(8.171e-82), ENSG00000260075(8.171e-82), ENSG00000262500(4.334e-75)	ENSG00000120071(8.907e-09), ENSG00000131484(1.778e-10), ENSG00000176681(0), ENSG00000185829(2.706e-16), ENSG00000214425(1.778e-10), ENSG00000225190(1.778e-10), ENSG00000228696(0), ENSG00000238083(2.706e-16), ENSG00000262500(1.013e-28), ENSG00000262879(1.557e-07)	NA	NA	5_TxWk		MAP3K14, KANSL1, MAPT, ARL17B, NSFP1	KANSL1, LRRC37A, ARL17A, LRRC37A4P, PLEKHM1, ARL17B, LRRC37A2	NA	NA

Continues on the next page

Supplementary Table 16 – continued from previous page

CHR	BP	CredSNP	IndexSNP	Index P	ENSGID_CP	ENSGID_GZ	ENSGID Promoter	ENSGID functional	Chrom HMM	Histone	HGNC_CP	HGNC_GZ	HGNC Promoter	HGNC functional
chr17	44,285,142	chr17:44285142	rs142920272, rs147317628	2.9e-07, 1.1e-06	ENSG00000006062(7.889e-05), ENSG00000120071(6.771e-18), ENSG00000186868(4.302e-05), ENSG00000228696(8.171e-82), ENSG00000260075(8.171e-82), ENSG00000262500(4.334e-75)	ENSG00000120071(8.907e-09), ENSG00000131484(1.778e-10), ENSG00000176681(0), ENSG00000185829(2.706e-16), ENSG00000214425(1.778e-10), ENSG00000225190(1.778e-10), ENSG00000228696(0), ENSG00000238083(2.706e-16), ENSG00000262500(1.013e-28), ENSG00000262879(1.557e-07)	NA	NA	5_TxWk		MAP3K14, KANSL1, MAPT, ARL17B, NSFP1	KANSL1, LRRC37A, ARL17A, LRRC37A4P, PLEKHM1, ARL17B, LRRC37A2	NA	NA
chr17	44,285,531	chr17:44285531	rs142920272, rs147317628	2.9e-07, 1.1e-06	ENSG00000006062(7.889e-05), ENSG00000120071(6.771e-18), ENSG00000186868(4.302e-05), ENSG00000228696(8.171e-82), ENSG00000260075(8.171e-82), ENSG00000262500(4.334e-75)	ENSG00000120071(8.907e-09), ENSG00000131484(1.778e-10), ENSG00000176681(0), ENSG00000185829(2.706e-16), ENSG00000214425(1.778e-10), ENSG00000225190(1.778e-10), ENSG00000228696(0), ENSG00000238083(2.706e-16), ENSG00000262500(1.013e-28), ENSG00000262879(1.557e-07)	NA	NA	5_TxWk		MAP3K14, KANSL1, MAPT, ARL17B, NSFP1	KANSL1, LRRC37A, ARL17A, LRRC37A4P, PLEKHM1, ARL17B, LRRC37A2	NA	NA
chr17	44,286,089	chr17:44286089	rs142920272, rs147317628	2.9e-07, 1.1e-06	ENSG00000006062(7.889e-05), ENSG00000120071(6.771e-18), ENSG00000186868(4.302e-05), ENSG00000228696(8.171e-82), ENSG00000260075(8.171e-82), ENSG00000262500(4.334e-75)	ENSG00000120071(8.907e-09), ENSG00000131484(1.778e-10), ENSG00000176681(0), ENSG00000185829(2.706e-16), ENSG00000214425(1.778e-10), ENSG00000225190(1.778e-10), ENSG00000228696(0), ENSG00000238083(2.706e-16), ENSG00000262500(1.013e-28), ENSG00000262879(1.557e-07)	NA	NA	5_TxWk		MAP3K14, KANSL1, MAPT, ARL17B, NSFP1	KANSL1, LRRC37A, ARL17A, LRRC37A4P, PLEKHM1, ARL17B, LRRC37A2	NA	NA
chr17	44,286,128	chr17:44286128	rs142920272, rs147317628	2.9e-07, 1.1e-06	ENSG00000006062(7.889e-05), ENSG00000120071(6.771e-18), ENSG00000186868(4.302e-05), ENSG00000228696(8.171e-82), ENSG00000260075(8.171e-82), ENSG00000262500(4.334e-75)	ENSG00000120071(8.907e-09), ENSG00000131484(1.778e-10), ENSG00000176681(0), ENSG00000185829(2.706e-16), ENSG00000214425(1.778e-10), ENSG00000225190(1.778e-10), ENSG00000228696(0), ENSG00000238083(2.706e-16), ENSG00000262500(1.013e-28), ENSG00000262879(1.557e-07)	NA	NA	5_TxWk		MAP3K14, KANSL1, MAPT, ARL17B, NSFP1	KANSL1, LRRC37A, ARL17A, LRRC37A4P, PLEKHM1, ARL17B, LRRC37A2	NA	NA
chr17	44,286,198	chr17:44286198	rs142920272	2.9e-07	ENSG00000006062(7.889e-05), ENSG00000120071(6.771e-18), ENSG00000186868(4.302e-05), ENSG00000228696(8.171e-82), ENSG00000260075(8.171e-82), ENSG00000262500(4.334e-75)	ENSG00000120071(8.907e-09), ENSG00000131484(1.778e-10), ENSG00000176681(0), ENSG00000185829(2.706e-16), ENSG00000214425(1.778e-10), ENSG00000225190(1.778e-10), ENSG00000228696(0), ENSG00000238083(2.706e-16), ENSG00000262500(1.013e-28), ENSG00000262879(1.557e-07)	NA	NA	5_TxWk		MAP3K14, KANSL1, MAPT, ARL17B, NSFP1	KANSL1, LRRC37A, ARL17A, LRRC37A4P, PLEKHM1, ARL17B, LRRC37A2	NA	NA
chr17	44,287,310	chr17:44287310	rs147317628	1.1e-06	ENSG00000006062(7.889e-05), ENSG00000120071(6.771e-18), ENSG00000186868(4.302e-05), ENSG00000228696(8.171e-82), ENSG00000260075(8.171e-82), ENSG00000262500(4.334e-75)	ENSG00000120071(8.907e-09), ENSG00000131484(1.778e-10), ENSG00000176681(0), ENSG00000185829(2.706e-16), ENSG00000214425(1.778e-10), ENSG00000225190(1.778e-10), ENSG00000228696(0), ENSG00000238083(2.706e-16), ENSG00000262500(1.013e-28), ENSG00000262879(1.557e-07)	NA	NA	5_TxWk	H3K36me3	MAP3K14, KANSL1, MAPT, ARL17B, NSFP1	KANSL1, LRRC37A, ARL17A, LRRC37A4P, PLEKHM1, ARL17B, LRRC37A2	NA	NA
chr17	44,288,114	chr17:44288114	rs142920272, rs147317628	2.9e-07, 1.1e-06	ENSG00000006062(7.889e-05), ENSG00000120071(6.771e-18), ENSG00000186868(4.302e-05), ENSG00000228696(8.171e-82), ENSG00000260075(8.171e-82), ENSG00000262500(4.334e-75)	ENSG00000120071(8.907e-09), ENSG00000131484(1.778e-10), ENSG00000176681(0), ENSG00000185829(2.706e-16), ENSG00000214425(1.778e-10), ENSG00000225190(1.778e-10), ENSG00000228696(0), ENSG00000238083(2.706e-16), ENSG00000262500(1.013e-28), ENSG00000262879(1.557e-07)	NA	NA	5_TxWk		MAP3K14, KANSL1, MAPT, ARL17B, NSFP1	KANSL1, LRRC37A, ARL17A, LRRC37A4P, PLEKHM1, ARL17B, LRRC37A2	NA	NA

Continues on the next page

Supplementary Table 16 – continued from previous page

CHR	BP	CredSNP	IndexSNP	Index P	ENSGID_CP	ENSGID_GZ	ENSGID Promoter	ENSGID functional	Chrom HMM	Histone	HGNC_CP	HGNC_GZ	HGNC Promoter	HGNC functional
chr17	44,295,157	chr17:44295157	rs147317628	1.1e-06	ENSG00000108379(6.796e-05), ENSG00000120071(1.371e-15), ENSG00000158955(6.796e-05), ENSG00000186868(1.113e-08), ENSG00000225190(1.173e-17), ENSG00000262372(2.024e-10), ENSG00000262539(4.07e-09), ENSG00000264589(1.113e-08), ENSG00000266497(5.756e-25)	ENSG00000004897(3.849e-37), ENSG00000108379(1.454e-06), ENSG00000120071(1.453e-15), ENSG00000159314(1.815e-07), ENSG00000186868(7.968e-07), ENSG00000225190(2.236e-12), ENSG00000236234(2.236e-12), ENSG00000239291(8.887e-15), ENSG00000256762(7.075e-06), ENSG00000260075(1.26e-41), ENSG00000262265(8.887e-15), ENSG00000262372(1.283e-13), ENSG00000262879(1.357e-09), ENSG00000264038(3.203e-07), ENSG00000264225(2.236e-12), ENSG00000266497(9.576e-13)	NA	NA	5_TxWk		WNT3, KANSL1, WNT9B, MAPT, PLEKHM1, MAPT-AS1	CDC27, WNT3, KANSL1, ARHGAP27, MAPT, PLEKHM1, STH, NSFP1, RN7SL730P	NA	NA
chr17	44,298,102	chr17:44298102	rs142920272, rs147317628	2.9e-07, 1.1e-06	ENSG00000108379(6.796e-05), ENSG00000120071(1.371e-15), ENSG00000158955(6.796e-05), ENSG00000186868(1.113e-08), ENSG00000225190(1.173e-17), ENSG00000262372(2.024e-10), ENSG00000262539(4.07e-09), ENSG00000264589(1.113e-08), ENSG00000266497(5.756e-25)	ENSG00000004897(3.849e-37), ENSG00000108379(1.454e-06), ENSG00000120071(1.453e-15), ENSG00000159314(1.815e-07), ENSG00000186868(7.968e-07), ENSG00000225190(2.236e-12), ENSG00000236234(2.236e-12), ENSG00000239291(8.887e-15), ENSG00000256762(7.075e-06), ENSG00000260075(1.26e-41), ENSG00000262265(8.887e-15), ENSG00000262372(1.283e-13), ENSG00000262879(1.357e-09), ENSG00000264038(3.203e-07), ENSG00000264225(2.236e-12), ENSG00000266497(9.576e-13)	NA	NA	5_TxWk		WNT3, KANSL1, WNT9B, MAPT, PLEKHM1, MAPT-AS1	CDC27, WNT3, KANSL1, ARHGAP27, MAPT, PLEKHM1, STH, NSFP1, RN7SL730P	NA	NA
chr17	44,298,209	chr17:44298209	rs147317628	1.1e-06	ENSG00000108379(6.796e-05), ENSG00000120071(1.371e-15), ENSG00000158955(6.796e-05), ENSG00000186868(1.113e-08), ENSG00000225190(1.173e-17), ENSG00000262372(2.024e-10), ENSG00000262539(4.07e-09), ENSG00000264589(1.113e-08), ENSG00000266497(5.756e-25)	ENSG00000004897(3.849e-37), ENSG00000108379(1.454e-06), ENSG00000120071(1.453e-15), ENSG00000159314(1.815e-07), ENSG00000186868(7.968e-07), ENSG00000225190(2.236e-12), ENSG00000236234(2.236e-12), ENSG00000239291(8.887e-15), ENSG00000256762(7.075e-06), ENSG00000260075(1.26e-41), ENSG00000262265(8.887e-15), ENSG00000262372(1.283e-13), ENSG00000262879(1.357e-09), ENSG00000264038(3.203e-07), ENSG00000264225(2.236e-12), ENSG00000266497(9.576e-13)	NA	NA	7_Enh		WNT3, KANSL1, WNT9B, MAPT, PLEKHM1, MAPT-AS1	CDC27, WNT3, KANSL1, ARHGAP27, MAPT, PLEKHM1, STH, NSFP1, RN7SL730P	NA	NA
chr17	44,302,881	chr17:44302881	rs147317628	1.1e-06			ENSG00000120071		9_Het	DHS:H3K4me3			KANSL1	
chr17	44,305,689	chr17:44305689	rs147317628	1.1e-06	ENSG00000120071(6.42e-18), ENSG00000186868(5.937e-08), ENSG00000225190(1.552e-14), ENSG00000262372(3.52e-09), ENSG00000264589(5.937e-08), ENSG00000266497(1.564e-21)	ENSG00000004897(1.111e-36), ENSG00000108379(2.723e-06), ENSG00000120071(5.97e-15), ENSG00000159314(1.602e-07), ENSG00000186868(1.111e-06), ENSG00000225190(2.259e-11), ENSG00000236234(2.259e-11), ENSG00000239291(4.569e-13), ENSG00000256762(5.986e-06), ENSG00000260075(1.762e-39), ENSG00000262265(4.569e-13), ENSG00000262372(1.069e-12), ENSG00000262879(4.408e-09), ENSG00000264038(8.752e-07), ENSG00000264225(2.259e-11), ENSG00000266497(7.218e-12)	NA	NA	15_Quies		KANSL1, MAPT, PLEKHM1, MAPT-AS1	CDC27, WNT3, KANSL1, ARHGAP27, MAPT, PLEKHM1, STH, NSFP1, RN7SL730P	NA	NA

Continues on the next page

CHR	BP	CredSNP	IndexSNP	Index P	ENSGID_CP	ENSGID_GZ	ENSGID Promoter	ENSGID functional	Chrom HMM	Histone	HGNC_CP	HGNC_GZ	HGNC Promoter	HGNC functional
chr17	44,311,099	chr17:44311099	rs147317628	1.1e-06	ENSG00000120071(1.001e-75), ENSG00000186868(4.221e-08), ENSG00000225190(1.513e-15), ENSG00000262372(1.712e-09), ENSG00000264589(4.221e-08), ENSG00000266497(2.367e-21)	ENSG00000004897(5.898e-35), ENSG00000108379(3.433e-06), ENSG00000120071(6.373e-29), ENSG00000159314(2.318e-07), ENSG00000186868(5.531e-07), ENSG00000214401(1.613e-08), ENSG00000225190(2.693e-11), ENSG00000236234(2.693e-11), ENSG00000239291(2.76e-13), ENSG00000256762(5.458e-06), ENSG00000260075(2.959e-37), ENSG00000262265(2.76e-13), ENSG00000262372(5.801e-12), ENSG00000262879(1.682e-08), ENSG00000264038(1.084e-06), ENSG00000264225(2.693e-11), ENSG00000266497(1.002e-11)	NA	NA	15_Quies		KANSL1, MAPT, PLEKHM1, MAPT-AS1	CDC27, WNT3, KANSL1, ARHGAP27, MAPT, KANSL1-AS1, PLEKHM1, STH, NSFP1, RN7SL730P	NA	NA
chr20	21,117,240	chr20:21117240	rs6047270	7.7e-08	NA	NA	NA	NA	15_Quies		NA	NA	NA	NA
chr2	159,384,735	chr2:159384735	rs59566011	9.3e-07	ENSG00000153237(3.184e-05), ENSG00000227480(3.184e-05)	NA	NA	NA	15_Quies		CCDC148, CCDC148-AS1	NA	NA	NA
chr5	168,173,526	chr5:168173526	chr5:168173526	1.3e-06	NA	NA	NA	NA	14_ReprPCWk		NA	NA	NA	NA
chr6	98,584,711	chr6:98584711	rs72934503	5.9e-07	NA	NA	NA	NA	15_Quies		NA	NA	NA	NA
chr8	10,575,786	chr8:10575786	rs10099100	1.1e-08	NA	ENSG00000171056(9.841e-05), ENSG00000171060(1.154e-09), ENSG00000183638(1.154e-09), ENSG00000212433(1.154e-09), ENSG00000252565(9.841e-05), ENSG00000254093(9.841e-05), ENSG00000258724(9.841e-05)	NA	NA	14_ReprPCWk		NA	SOX7, C8orf74, RP1L1, RNA5SP252, PINX1	NA	NA
chr17	44,212,310	rs10221243	rs142920272, rs147317628	2.9e-07, 1.1e-06	ENSG00000120071(1.173e-15), ENSG00000159314(3.167e-06), ENSG00000225190(3.167e-06), ENSG00000238723(1.173e-15), ENSG00000260075(3.877e-18), ENSG00000262500(4.273e-15), ENSG00000262879(3.174e-29), ENSG00000263142(3.174e-29)	ENSG00000131484(6.934e-14), ENSG00000159314(2.906e-07), ENSG00000176681(0), ENSG00000214425(6.934e-14), ENSG00000225190(1.09e-11), ENSG00000228696(0), ENSG00000236234(1.09e-11)	NA	NA	5_TxWk		KANSL1, ARHGAP27, PLEKHM1, NSFP1, LRRC37A17P	ARHGAP27, LRRC37A, LRRC37A4P, PLEKHM1, ARL17B	NA	NA
chr8	53,374,007	rs1036715	rs10666089m	1.0e-06			ENSG00000147488		15_Quies				ST18	
chr6	98,572,120	rs10457441	rs72934503	5.9e-07	NA	NA	NA	NA	15_Quies		NA	NA	NA	NA
chr1	104,791,770	rs10625106	rs11185408	7.0e-07	NA	NA	NA	NA	15_Quies		NA	NA	NA	NA
chr20	21,258,707	rs10627346	rs910805	2.0e-09	NA	NA	NA	NA	14_ReprPCWk		NA	NA	NA	NA
chr8	53,341,258	rs10666089	rs10666089m	1.0e-06	NA	NA	NA	NA	15_Quies		NA	NA	NA	NA
chr8	53,341,258	rs10666089m	rs10666089m	1.0e-06	NA	NA	NA	NA	15_Quies		NA	NA	NA	NA
chr20	21,151,377	rs1072271	rs6047270	7.7e-08	NA	NA	NA	NA	15_Quies		NA	NA	NA	NA
chr1	96,961,107	rs11165656	rs2391769	1.1e-07	NA	NA	NA	NA	15_Quies		NA	NA	NA	NA
chr1	104,792,257	rs11185408	rs11185408	7.0e-07	NA	NA	NA	NA	15_Quies		NA	NA	NA	NA
chr18	55,882,032	rs111876941	rs292441	1.1e-06	NA	ENSG00000049759(3.605e-07)	NA	NA	7_Enh	H3K4me1	NA	NEDD4L	NA	NA
chr7	104,744,219	rs111931861	rs111931861	1.1e-07				ENSG00000005483	5_TxWk					KMT2E
chr14	94,838,142	rs112635299	rs112635299	3.0e-07	NA	NA	NA	NA	14_ReprPCWk		NA	NA	NA	NA
chr20	21,272,136	rs112777342	rs910805	2.0e-09	NA	NA	NA	NA	14_ReprPCWk		NA	NA	NA	NA
chr17	44,256,811	rs113089855	rs147317628	1.1e-06	ENSG00000004897(3.479e-05), ENSG00000214425(0), ENSG00000267198(0), ENSG00000267246(0)	ENSG00000073969(9.158e-12), ENSG00000120071(2.834e-05), ENSG00000131484(1.201e-19), ENSG00000186868(2.834e-05), ENSG00000214425(1.201e-19), ENSG00000228696(1.46e-32), ENSG00000260075(1.46e-32), ENSG00000266918(1.201e-19)	NA	NA	5_TxWk		CDC27, LRRC37A4P	NSF, KANSL1, MAPT, LRRC37A4P, ARL17B, NSFP1	NA	NA
chr17	44,270,809	rs113417378	rs142920272, rs147317628	2.9e-07, 1.1e-06			ENSG00000120071, ENSG00000214401		5_TxWk	DHS			KANSL1, KANSL1-AS1	
chr8	53,372,983	rs11452991	rs10666089m	1.0e-06	NA	NA	NA	NA	15_Quies		NA	NA	NA	NA
chr20	21,145,353	rs11475262	rs6047270	7.7e-08			ENSG00000228604		5_TxWk					

Continues on the next page

Supplementary Table 16 – continued from previous page

CHR	BP	CredSNP	IndexSNP	Index P	ENSGID_CP	ENSGID_GZ	ENSGID Promoter	ENSGID functional	Chrom HMM	Histone	HGNC_CP	HGNC_GZ	HGNC Promoter	HGNC functional
chr20	14,822,173	rs11481126	rs11481126	1.3e-07	NA	NA	NA	NA	15_Quies		NA	NA	NA	NA
chr20	21,136,056	rs11483719	rs6047270	7.7e-08	NA	NA	NA	NA	5_TxWk		NA	NA	NA	NA
chr2	159,377,277	rs11675009	rs59566011	9.3e-07				ENSG00000144283	15_Quies					PKP4
chr2	159,376,514	rs11695939	rs59566011	9.3e-07				ENSG00000144283	15_Quies					PKP4
chr11	106,827,977	rs117603308	rs117603308π	1.4e-06	ENSG00000254580(9.283e-05)	NA	NA	NA	5_TxWk			NA	NA	NA
chr11	106,827,977	rs117603308m	rs117603308m	1.4e-06	ENSG00000254580(9.283e-05)	NA	NA	NA	5_TxWk			NA	NA	NA
chr17	44,298,631	rs117662214	rs142920272, rs147317628	2.9e-07, 1.1e-06	ENSG00000108379(6.796e-05), ENSG00000120071(1.371e-15), ENSG00000158955(6.796e-05), ENSG00000186868(1.113e-08), ENSG00000225190(1.173e-17), ENSG00000262372(2.024e-10), ENSG00000262539(4.07e-09), ENSG00000264589(1.113e-08), ENSG00000266497(5.756e-25)	ENSG00000004897(3.849e-37), ENSG00000108379(1.454e-06), ENSG00000120071(1.453e-15), ENSG00000159314(1.815e-07), ENSG00000186868(7.968e-07), ENSG00000225190(2.236e-12), ENSG00000236234(2.236e-12), ENSG00000239291(8.887e-15), ENSG00000256762(7.075e-06), ENSG00000260075(1.26e-41), ENSG00000262265(8.887e-15), ENSG00000262372(1.283e-13), ENSG00000262879(1.357e-09), ENSG00000264038(3.203e-07), ENSG00000264225(2.236e-12), ENSG00000266497(9.576e-13)	NA	NA	15_Quies		WNT3, KANSL1, WNT9B, MAPT, PLEKHM1, MAPT-AS1	CDC27, WNT3, KANSL1, ARHGAP27, MAPT, PLEKHM1, STH, NSFP1, RN7SL730P	NA	NA
chr1	104,790,871	rs11806291	rs11185408	7.0e-07	NA	NA	NA	NA	15_Quies		NA	NA	NA	NA
chr1	96,586,426	rs12089599	rs201910565	3.4e-07	NA	NA	NA	NA	15_Quies		NA	NA	NA	NA
chr6	98,576,223	rs12202969	rs72934503	5.9e-07	NA	NA	NA	NA	5_TxWk	DHS	NA	NA	NA	NA
chr6	98,579,481	rs12204181	rs72934503	5.9e-07	NA	NA	NA	NA	7_Enh	H3K4me1	NA	NA	NA	NA
chr6	98,582,900	rs12206087	rs72934503	5.9e-07	NA	NA	NA	NA	15_Quies		NA	NA	NA	NA
chr1	96,602,440	rs1222063	rs1222063	2.6e-07	NA	NA	NA	NA	15_Quies		NA	NA	NA	NA
chr20	21,130,707	rs13041255	rs6047270	7.7e-08	NA	NA	NA	NA	5_TxWk		NA	NA	NA	NA
chr8	53,333,088	rs1365880	rs10666089m	1.0e-06	ENSG00000147485(8.966e-05), ENSG00000147488(5.221e-11)	ENSG00000147488(7.94e-08), ENSG00000253844(9.555e-06)	NA	NA	5_TxWk		PXDNL, ST18	ST18	NA	NA
chr6	98,583,487	rs138027849	rs72934503	5.9e-07	NA	NA	NA	NA	15_Quies		NA	NA	NA	NA
chr19	37,439,641	rs138867053	rs138867053	1.2e-07	NA	NA	NA	NA	4_Tx		NA	NA	NA	NA
chr20	21,263,168	rs139520783	rs910805	2.0e-09	NA	NA	NA	NA	14_ReprPCWk		NA	NA	NA	NA
chr10	72,749,057	rs140093403	rs78827416	9.0e-07	NA	NA	NA	NA	15_Quies		NA	NA	NA	NA
chr17	44,305,817	rs140256385	rs147317628	1.1e-06	ENSG00000120071(6.42e-18), ENSG00000186868(5.937e-08), ENSG00000225190(1.552e-14), ENSG00000262372(3.52e-09), ENSG00000264589(5.937e-08), ENSG00000266497(1.564e-21)	ENSG00000004897(1.111e-36), ENSG00000108379(2.723e-06), ENSG00000120071(5.97e-15), ENSG00000159314(1.602e-07), ENSG00000186868(1.111e-06), ENSG00000225190(2.259e-11), ENSG00000236234(2.259e-11), ENSG00000239291(4.569e-13), ENSG00000256762(5.986e-06), ENSG00000260075(1.762e-39), ENSG00000262265(4.569e-13), ENSG00000262372(1.069e-12), ENSG00000262879(4.408e-09), ENSG00000264038(8.752e-07), ENSG00000264225(2.259e-11), ENSG00000266497(7.218e-12)	NA	NA	15_Quies		KANSL1, MAPT, PLEKHM1, MAPT-AS1	CDC27, WNT3, KANSL1, ARHGAP27, MAPT, PLEKHM1, STH, NSFP1, RN7SL730P	NA	NA
chr17	44,019,083	rs141455452	rs141455452	8.9e-07				ENSG00000186868	7_Enh	H3K4me1				MAPT

Continues on the next page

Supplementary Table 16 – continued from previous page

CHR	BP	CredSNP	IndexSNP	Index P	ENSGID_CP	ENSGID_GZ	ENSGID Promoter	ENSGID functional	Chrom HMM	Histone	HGNC_CP	HGNC_GZ	HGNC Promoter	HGNC functional
chr17	44,325,593	rs142380704	rs147317628	1.1e-06	ENSG00000120071(4.406e-45), ENSG00000225190(1.681e-08), ENSG00000262372(6.759e-07), ENSG00000266497(1.582e-08)	ENSG00000004897(2.896e-17), ENSG00000073969(2.982e-90), ENSG00000120071(4.184e-10), ENSG00000159314(0.0001098), ENSG00000186868(5.377e-07), ENSG00000225190(5.302e-06), ENSG00000236234(5.302e-06), ENSG00000239291(1.338e-06), ENSG00000256762(0.0001159), ENSG00000260075(3.06e-13), ENSG00000262265(1.338e-06), ENSG00000262372(7.016e-07), ENSG00000264038(0.0001098), ENSG00000264070(2.942e-32), ENSG00000264225(5.302e-06)	NA	NA	15_Quies		KANSL1, PLEKHM1	CDC27, NSF, KANSL1, ARHGAP27, MAPT, PLEKHM1, STH, NSFP1, DND1P1, RN7SL730P	NA	NA
chr17	44,301,840	rs142920272	rs142920272, rs147317628	2.9e-07, 1.1e-06			ENSG00000120071		15_Quies				KANSL1	
chr17	44,296,523	rs144416125	rs142920272	2.9e-07	ENSG00000108379(6.796e-05), ENSG00000120071(1.371e-15), ENSG00000158955(6.796e-05), ENSG00000186868(1.113e-08), ENSG00000225190(1.173e-17), ENSG00000262372(2.024e-10), ENSG00000262539(4.07e-09), ENSG00000264589(1.113e-08), ENSG00000266497(5.756e-25)	ENSG00000004897(3.849e-37), ENSG00000108379(1.454e-06), ENSG00000120071(1.453e-15), ENSG00000159314(1.815e-07), ENSG00000186868(7.968e-07), ENSG00000225190(2.236e-12), ENSG00000236234(2.236e-12), ENSG00000239291(8.887e-15), ENSG00000256762(7.075e-06), ENSG00000260075(1.26e-41), ENSG00000262265(8.887e-15), ENSG00000262372(1.283e-13), ENSG00000262879(1.357e-09), ENSG00000264038(3.203e-07), ENSG00000264225(2.236e-12), ENSG00000266497(9.576e-13)	NA	NA	5_TxWk		WNT3, KANSL1, WNT9B, MAPT, PLEKHM1, MAPT-AS1	CDC27, WNT3, KANSL1, ARHGAP27, MAPT, PLEKHM1, STH, NSFP1, RN7SL730P	NA	NA
chr3	62,481,063	rs1452075	rs1452075	2.1e-07	NA	ENSG00000153266(1.642e-05), ENSG00000241472(1.642e-05)	NA	NA	15_Quies		NA	FEZF2, PTPRG-AS1	NA	NA
chr17	44,277,476	rs147317628	rs142920272, rs147317628	2.9e-07, 1.1e-06	ENSG00000120071(5.738e-08), ENSG00000228696(6.206e-181), ENSG00000260075(6.206e-181)	ENSG00000120071(8.6e-08), ENSG00000185829(0), ENSG00000238083(0), ENSG00000262500(1.699e-08)	NA	NA	5_TxWk		KANSL1, ARL17B, NSFP1	KANSL1, ARL17A, LRRC37A2	NA	NA
chr6	98,553,894	rs1487441	rs72934503	5.9e-07	ENSG00000187472(2.472e-05)	ENSG00000236920(6.072e-05), ENSG00000271860(6.072e-05)	NA	NA	15_Quies				NA	NA
chr6	98,565,211	rs1487445	rs72934503	5.9e-07	NA	NA	NA	NA	7_Enh		NA	NA	NA	NA
chr17	44,285,982	rs149187563	rs147317628	1.1e-06	ENSG00000006062(7.889e-05), ENSG00000120071(6.771e-18), ENSG00000186868(4.302e-05), ENSG00000228696(8.171e-82), ENSG00000260075(8.171e-82), ENSG00000262500(4.334e-75)	ENSG00000120071(8.907e-09), ENSG00000131484(1.778e-10), ENSG00000176681(0), ENSG00000185829(2.706e-16), ENSG00000214425(1.778e-10), ENSG00000225190(1.778e-10), ENSG00000228696(0), ENSG00000238083(2.706e-16), ENSG00000262500(1.013e-28), ENSG00000262879(1.557e-07)	NA	NA	5_TxWk		MAP3K14, KANSL1, MAPT, ARL17B, NSFP1	KANSL1, LRRC37A, ARL17A, LRRC37A4P, PLEKHM1, ARL17B, LRRC37A2	NA	NA
chr19	37,980,494	rs149923766	rs138867053	1.2e-07	NA	NA	NA	NA	9_Het		NA	NA	NA	NA
chr8	48,402,014	rs150271817	rs183563276n	1.9e-07				ENSG00000164808	15_Quies					SPIDR
chr1	96,543,995	rs150859	rs201910565	3.4e-07	NA	NA	NA	NA	15_Quies		NA	NA	NA	NA
chr8	53,367,501	rs1582846	rs10666089m	1.0e-06	NA	NA	NA	NA	15_Quies		NA	NA	NA	NA
chr8	53,371,160	rs1627458	rs10666089m	1.0e-06	NA	NA	NA	NA	15_Quies		NA	NA	NA	NA
chr8	53,367,337	rs1660550	rs10666089m	1.0e-06	NA	NA	NA	NA	15_Quies		NA	NA	NA	NA
chr8	53,343,969	rs1660554	rs10666089m	1.0e-06	NA	NA	NA	NA	15_Quies	H3K4me1	NA	NA	NA	NA
chr17	44,186,063	rs16940904	rs147317628	1.1e-06	ENSG00000131484(6.16e-22), ENSG00000176681(4.632e-15), ENSG00000214425(6.16e-22), ENSG00000228696(4.28e-59), ENSG00000238083(1.129e-08), ENSG00000260075(4.28e-59), ENSG00000266497(1.129e-08), ENSG00000266918(6.16e-22)	ENSG00000120071(3.253e-05), ENSG00000238723(3.253e-05), ENSG00000262500(3.755e-05)	NA	NA	15_Quies		LRRC37A, LRRC37A4P, ARL17B, LRRC37A2, NSFP1	KANSL1	NA	NA

Continues on the next page

Supplementary Table 16 – continued from previous page

CHR	BP	CredSNP	IndexSNP	Index P	ENSGID_CP	ENSGID_GZ	ENSGID Promoter	ENSGID functional	Chrom HMM	Histone	HGNC_CP	HGNC_GZ	HGNC Promoter	HGNC functional
chr8	53,365,864	rs176184	rs10666089m	1.0e-06	NA	NA	NA	NA	15_Quies		NA	NA	NA	NA
chr17	44,196,015	rs17661141	rs147317628	1.1e-06	ENSG00000108433(1.024e-12), ENSG00000238083(1.869e-07), ENSG00000262633(1.024e-12), ENSG00000262879(1.024e-12), ENSG00000263142(1.024e-12), ENSG00000264070(2.525e-10), ENSG00000266497(1.869e-07)	ENSG00000262633(7.751e-14), ENSG00000262879(7.751e-14), ENSG00000263142(7.751e-14)	NA	NA	15_Quies	H3K4me1	GOSR2, LRRC37A2, LRRC37A17P, DND1P1	LRRC37A17P	NA	NA
chr6	98,585,502	rs17814604	rs72934503	5.9e-07	NA	NA	NA	NA	15_Quies	DHS	NA	NA	NA	NA
chr8	53,346,704	rs182262	rs10666089m	1.0e-06	NA	NA	NA	NA	15_Quies		NA	NA	NA	NA
chr8	48,036,474	rs183563276	rs183563276m	1.9e-07	ENSG00000188873(7.505e-06), ENSG00000248347(7.505e-06), ENSG00000248498(2.381e-05), ENSG00000251470(7.116e-08)	ENSG00000164808(4.108e-06), ENSG00000251470(6.413e-14)	NA	NA	15_Quies		RPL10AP2, ASNSP1, ASNSP4	SPIDR, ASNSP4	NA	NA
chr8	48,036,474	rs183563276m	rs183563276m	1.9e-07	ENSG00000188873(7.505e-06), ENSG00000248347(7.505e-06), ENSG00000248498(2.381e-05), ENSG00000251470(7.116e-08)	ENSG00000164808(4.108e-06), ENSG00000251470(6.413e-14)	NA	NA	15_Quies		RPL10AP2, ASNSP1, ASNSP4	SPIDR, ASNSP4	NA	NA
chr6	98,576,688	rs1872841	rs72934503	5.9e-07	NA	NA	NA	NA	5_TxWk		NA	NA	NA	NA
chr8	53,365,524	rs188209	rs10666089m	1.0e-06	NA	NA	NA	NA	15_Quies		NA	NA	NA	NA
chr20	21,128,127	rs1884763	rs6047270	7.7e-08	NA	NA	NA	NA	5_TxWk		NA	NA	NA	NA
chr17	44,299,864	rs201443147	rs142920272, rs147317628	2.9e-07, 1.1e-06	ENSG00000108379(6.796e-05), ENSG00000120071(1.371e-15), ENSG00000158955(6.796e-05), ENSG00000186868(1.113e-08), ENSG00000225190(1.173e-17), ENSG00000262372(2.024e-10), ENSG00000262539(4.07e-09), ENSG00000264589(1.113e-08), ENSG00000266497(5.756e-25)	ENSG00000004897(3.849e-37), ENSG00000108379(1.454e-06), ENSG00000120071(1.453e-15), ENSG00000159314(1.815e-07), ENSG00000186868(7.968e-07), ENSG00000225190(2.236e-12), ENSG00000236234(2.236e-12), ENSG00000239291(8.887e-15), ENSG00000256762(7.075e-06), ENSG00000260075(1.26e-41), ENSG00000262265(8.887e-15), ENSG00000262372(1.283e-13), ENSG00000262879(1.357e-09), ENSG00000264038(3.203e-07), ENSG00000264225(2.236e-12), ENSG00000266497(9.576e-13)	NA	NA	15_Quies		WNT3, KANSL1, WNT9B, MAPT, PLEKHM1, MAPT-AS1	CDC27, WNT3, KANSL1, ARHGAP27, MAPT, PLEKHM1, STH, NSFP1, RN7SL730P	NA	NA
chr20	21,298,446	rs202829	rs910805	2.0e-09	ENSG00000188559(5.21e-05)	ENSG00000088930(8.115e-07)	NA	NA	15_Quies		RALGAPA2	XRN2	NA	NA
chr20	21,312,288	rs202837	rs910805	2.0e-09	NA	NA	NA	NA	4_Tx		NA	NA	NA	NA
chr17	44,155,732	rs2066899	rs142920272, rs147317628	2.9e-07, 1.1e-06	ENSG00000108433(1.738e-17), ENSG00000120071(9.114e-05), ENSG00000176681(2.996e-19), ENSG00000214401(9.114e-05), ENSG00000228696(2.996e-19), ENSG00000260075(7.901e-08), ENSG00000262633(1.738e-17), ENSG00000262879(1.738e-17), ENSG00000263142(1.738e-17)	ENSG00000073969(0), ENSG00000225190(2.979e-06)	NA	NA	15_Quies		GOSR2, KANSL1, LRRC37A, KANSL1-AS1, ARL17B, NSFP1, LRRC37A17P	NSF, PLEKHM1	NA	NA
chr20	21,140,342	rs2093069	rs6047270	7.7e-08			ENSG00000228604		5_TxWk					
chr17	44,168,677	rs2097760	rs142920272	2.9e-07	ENSG00000120071(1.319e-14), ENSG00000214401(1.319e-14), ENSG00000260075(9.54e-06)	ENSG00000073969(1.964e-37), ENSG00000120071(1.862e-09), ENSG00000176681(5.414e-10), ENSG00000228696(5.414e-10), ENSG00000238723(1.862e-09), ENSG00000262500(1.094e-09)	NA	NA	15_Quies		KANSL1, KANSL1-AS1, NSFP1	NSF, KANSL1, LRRC37A, ARL17B	NA	NA
chr20	21,156,960	rs2103976	rs6047270	7.7e-08	NA	NA	NA	NA	15_Quies		NA	NA	NA	NA
chr6	11,731,999	rs210894	rs210894m	4.9e-07				ENSG00000111863	7_Enh					ADTRP
chr6	11,731,999	rs210894m	rs210894m	4.9e-07				ENSG00000111863	7_Enh					ADTRP
chr5	104,013,782	rs21126	rs325485	3.3e-07	NA	ENSG00000251574(2.86e-08), ENSG00000253584(2.86e-08)	NA	NA	15_Quies		NA		NA	NA

Continues on the next page

Supplementary Table 16 – continued from previous page

CHR	BP	CredSNP	IndexSNP	Index P	ENSGID_CP	ENSGID_GZ	ENSGID Promoter	ENSGID functional	Chrom HMM	Histone	HGNC_CP	HGNC_GZ	HGNC Promoter	HGNC functional
chr17	44,268,488	rs2141298	rs142920272, rs147317628	2.9e-07, 1.1e-06	ENSG00000120071(9.613e-15), ENSG00000186868(1.943e-06), ENSG00000228696(1.763e-05), ENSG00000260075(1.763e-05), ENSG00000262372(2.229e-05)	ENSG00000131484(6.359e-16), ENSG00000176681(0), ENSG00000185829(4.033e-101), ENSG00000214425(6.359e-16), ENSG00000228696(0), ENSG00000238083(4.033e-101), ENSG00000262879(5.357e-06)	NA	NA	1_TssA		KANSL1, MAPT, ARL17B, NSFP1	LRRC37A, ARL17A, LRRC37A4P, ARL17B, LRRC37A2	NA	NA
chr20	21,151,852	rs2180581	rs6047270	7.7e-08	NA	NA	NA	NA	15_Quies		NA	NA	NA	NA
chr20	14,766,216	rs2224275	rs11481126	1.3e-07	NA	NA	NA	NA	15_Quies		NA	NA	NA	NA
chr1	96,526,728	rs222887	rs201910565	3.4e-07	NA	ENSG00000117569(4.103e-05)	NA	NA	15_Quies		NA	PTBP2	NA	NA
chr1	96,525,762	rs222888	rs201910565	3.4e-07	NA	ENSG00000117569(4.103e-05)	NA	NA	15_Quies		NA	PTBP2	NA	NA
chr1	96,508,040	rs222901	rs201910565	3.4e-07	NA	NA	NA	NA	15_Quies		NA	NA	NA	NA
chr1	96,552,025	rs223245	rs201910565	3.4e-07	NA	NA	NA	NA	15_Quies		NA	NA	NA	NA
chr1	96,522,970	rs223250	rs201910565	3.4e-07	NA	ENSG00000117569(4.103e-05)	NA	NA	15_Quies		NA	PTBP2	NA	NA
chr20	21,142,813	rs2236178	rs6047270	7.7e-08	NA	NA	NA	NA	5_TxWk		NA	NA	NA	NA
chr17	44,294,786	rs2266497	rs147317628	1.1e-06	ENSG00000108379(6.796e-05), ENSG00000120071(1.371e-15), ENSG00000158955(6.796e-05), ENSG00000186868(1.113e-08), ENSG00000225190(1.173e-17), ENSG00000262372(2.024e-10), ENSG00000262539(4.07e-09), ENSG00000264589(1.113e-08), ENSG00000266497(5.756e-25)	ENSG00000004897(3.849e-37), ENSG00000108379(1.454e-06), ENSG00000120071(1.453e-15), ENSG00000159314(1.815e-07), ENSG00000186868(7.968e-07), ENSG00000225190(2.236e-12), ENSG00000236234(2.236e-12), ENSG00000239291(8.887e-15), ENSG00000256762(7.075e-06), ENSG00000260075(1.26e-41), ENSG00000262265(8.887e-15), ENSG00000262372(1.283e-13), ENSG00000262879(1.357e-09), ENSG00000264038(3.203e-07), ENSG00000264225(2.236e-12), ENSG00000266497(9.576e-13)	NA	NA	5_TxWk		WNT3, KANSL1, WNT9B, MAPT, PLEKHM1, MAPT-AS1	CDC27, WNT3, KANSL1, ARHGAP27, MAPT, PLEKHM1, STH, NSFP1, RN7SL730P	NA	NA
chr1	104,789,431	rs2317081	rs11185408	7.0e-07	NA	NA	NA	NA	15_Quies		NA	NA	NA	NA
chr20	21,153,138	rs2328608	rs6047270	7.7e-08	NA	NA	NA	NA	15_Quies		NA	NA	NA	NA
chr20	21,156,578	rs2328609	rs6047270	7.7e-08	NA	NA	NA	NA	15_Quies		NA	NA	NA	NA
chr1	96,978,961	rs2391769	rs2391769	1.1e-07	NA	NA	NA	NA	7_Enh	DHS	NA	NA	NA	NA
chr17	44,293,963	rs2458204	rs142920272, rs147317628	2.9e-07, 1.1e-06			ENSG00000238723		5_TxWk					
chr17	44,273,218	rs2532233	rs142920272, rs147317628	2.9e-07, 1.1e-06			ENSG00000120071, ENSG00000214401		5_TxWk	H3K4me1			KANSL1, KANSL1-AS1	
chr17	44,266,227	rs2532239	rs142920272, rs147317628	2.9e-07, 1.1e-06	ENSG00000120071(9.613e-15), ENSG00000186868(1.943e-06), ENSG00000228696(1.763e-05), ENSG00000260075(1.763e-05), ENSG00000262372(2.229e-05)	ENSG00000131484(6.359e-16), ENSG00000176681(0), ENSG00000185829(4.033e-101), ENSG00000214425(6.359e-16), ENSG00000228696(0), ENSG00000238083(4.033e-101), ENSG00000262879(5.357e-06)	NA	NA	7_Enh	H3K4me1	KANSL1, MAPT, ARL17B, NSFP1	LRRC37A, ARL17A, LRRC37A4P, ARL17B, LRRC37A2	NA	NA
chr17	44,246,624	rs2532276	rs142920272, rs147317628	2.9e-07, 1.1e-06	ENSG00000176681(0), ENSG00000228696(0), ENSG00000260075(8.89e-10)	ENSG00000176681(2.828e-09), ENSG00000228696(2.597e-31), ENSG00000238083(1.646e-06), ENSG00000260075(3.47e-99), ENSG00000266497(1.646e-06)	NA	NA	5_TxWk		LRRC37A, ARL17B, NSFP1	LRRC37A, ARL17B, LRRC37A2, NSFP1	NA	NA

Continues on the next page

Supplementary Table 16 – continued from previous page

CHR	BP	CredSNP	IndexSNP	Index P	ENSGID_CP	ENSGID_GZ	ENSGID Promoter	ENSGID functional	Chrom HMM	Histone	HGNC_CP	HGNC_GZ	HGNC Promoter	HGNC functional
chr17	44,307,193	rs2532395	rs147317628	1.1e-06	ENSG00000120071(6.42e-18), ENSG00000186868(5.937e-08), ENSG00000225190(1.552e-14), ENSG00000262372(3.52e-09), ENSG00000264589(5.937e-08), ENSG00000266497(1.564e-21)	ENSG00000004897(1.111e-36), ENSG00000108379(2.723e-06), ENSG00000120071(5.97e-15), ENSG00000159314(1.602e-07), ENSG00000186868(1.111e-06), ENSG00000225190(2.259e-11), ENSG00000236234(2.259e-11), ENSG00000239291(4.569e-13), ENSG00000256762(5.986e-06), ENSG00000260075(1.762e-39), ENSG00000262265(4.569e-13), ENSG00000262372(1.069e-12), ENSG00000262879(4.408e-09), ENSG00000264038(8.752e-07), ENSG00000264225(2.259e-11), ENSG00000266497(7.218e-12)	NA	NA	15_Quies		KANSL1, MAPT, PLEKHM1, MAPT-AS1	CDC27, WNT3, KANSL1, ARHGAP27, MAPT, PLEKHM1, STH, NSFP1, RN7SL730P	NA	NA
chr17	44,294,983	rs2532413	rs142920272, rs147317628	2.9e-07, 1.1e-06	ENSG00000108379(6.796e-05), ENSG00000120071(1.371e-15), ENSG00000158955(6.796e-05), ENSG00000186868(1.113e-08), ENSG00000225190(1.173e-17), ENSG00000262372(2.024e-10), ENSG00000262539(4.07e-09), ENSG00000264589(1.113e-08), ENSG00000266497(5.756e-25)	ENSG00000004897(3.849e-37), ENSG00000108379(1.454e-06), ENSG00000120071(1.453e-15), ENSG00000159314(1.815e-07), ENSG00000186868(7.968e-07), ENSG00000225190(2.236e-12), ENSG00000236234(2.236e-12), ENSG00000239291(8.887e-15), ENSG00000256762(7.075e-06), ENSG00000260075(1.26e-41), ENSG00000262265(8.887e-15), ENSG00000262372(1.283e-13), ENSG00000262879(1.357e-09), ENSG00000264038(3.203e-07), ENSG00000264225(2.236e-12), ENSG00000266497(9.576e-13)	NA	NA	5_TxWk		WNT3, KANSL1, WNT9B, MAPT, PLEKHM1, MAPT-AS1	CDC27, WNT3, KANSL1, ARHGAP27, MAPT, PLEKHM1, STH, NSFP1, RN7SL730P	NA	NA
chr17	44,289,220	rs2532417	rs142920272, rs147317628	2.9e-07, 1.1e-06	ENSG00000006062(7.889e-05), ENSG00000120071(6.771e-18), ENSG00000186868(4.302e-05), ENSG00000228696(8.171e-82), ENSG00000260075(8.171e-82), ENSG00000262500(4.334e-75)	ENSG00000120071(8.907e-09), ENSG00000131484(1.778e-10), ENSG00000176681(0), ENSG00000185829(2.706e-16), ENSG00000214425(1.778e-10), ENSG00000225190(1.778e-10), ENSG00000228696(0), ENSG00000238083(2.706e-16), ENSG00000262500(1.013e-28), ENSG00000262879(1.557e-07)	NA	NA	5_TxWk		MAP3K14, KANSL1, MAPT, ARL17B, NSFP1	KANSL1, LRRC37A, ARL17A, LRRC37A4P, PLEKHM1, ARL17B, LRRC37A2	NA	NA
chr17	44,288,579	rs2532418	rs142920272, rs147317628	2.9e-07, 1.1e-06	ENSG00000006062(7.889e-05), ENSG00000120071(6.771e-18), ENSG00000186868(4.302e-05), ENSG00000228696(8.171e-82), ENSG00000260075(8.171e-82), ENSG00000262500(4.334e-75)	ENSG00000120071(8.907e-09), ENSG00000131484(1.778e-10), ENSG00000176681(0), ENSG00000185829(2.706e-16), ENSG00000214425(1.778e-10), ENSG00000225190(1.778e-10), ENSG00000228696(0), ENSG00000238083(2.706e-16), ENSG00000262500(1.013e-28), ENSG00000262879(1.557e-07)	NA	NA	5_TxWk		MAP3K14, KANSL1, MAPT, ARL17B, NSFP1	KANSL1, LRRC37A, ARL17A, LRRC37A4P, PLEKHM1, ARL17B, LRRC37A2	NA	NA
chr17	44,285,952	rs2532423	rs147317628	1.1e-06	ENSG00000006062(7.889e-05), ENSG00000120071(6.771e-18), ENSG00000186868(4.302e-05), ENSG00000228696(8.171e-82), ENSG00000260075(8.171e-82), ENSG00000262500(4.334e-75)	ENSG00000120071(8.907e-09), ENSG00000131484(1.778e-10), ENSG00000176681(0), ENSG00000185829(2.706e-16), ENSG00000214425(1.778e-10), ENSG00000225190(1.778e-10), ENSG00000228696(0), ENSG00000238083(2.706e-16), ENSG00000262500(1.013e-28), ENSG00000262879(1.557e-07)	NA	NA	5_TxWk		MAP3K14, KANSL1, MAPT, ARL17B, NSFP1	KANSL1, LRRC37A, ARL17A, LRRC37A4P, PLEKHM1, ARL17B, LRRC37A2	NA	NA
chr8	53,373,448	rs2582639	rs10666089m	1.0e-06	NA	NA	NA	NA	15_Quies		NA	NA	NA	NA

Continues on the next page

Supplementary Table 16 – continued from previous page

CHR	BP	CredSNP	IndexSNP	Index P	ENSGID_CP	ENSGID_GZ	ENSGID Promoter	ENSGID functional	Chrom HMM	Histone	HGNC_CP	HGNC_GZ	HGNC Promoter	HGNC functional
chr17	44,324,539	rs2668639	rs147317628	1.1e-06	ENSG00000120071(4.406e-45), ENSG00000225190(1.681e-08), ENSG00000262372(6.759e-07), ENSG00000266497(1.582e-08)	ENSG00000004897(2.896e-17), ENSG00000073969(2.982e-90), ENSG00000120071(4.184e-10), ENSG00000159314(0.0001098), ENSG00000186868(5.377e-07), ENSG00000225190(5.302e-06), ENSG00000236234(5.302e-06), ENSG00000239291(1.338e-06), ENSG00000256762(0.0001159), ENSG00000260075(3.06e-13), ENSG00000262265(1.338e-06), ENSG00000262372(7.016e-07), ENSG00000264038(0.0001098), ENSG00000264070(2.942e-32), ENSG00000264225(5.302e-06)	NA	NA	15_Quies		KANSL1, PLEKHM1	CDC27, NSF, KANSL1, ARHGAP27, MAPT, PLEKHM1, STH, NSFP1, DND1P1, RN7SL730P	NA	NA
chr17	44,288,640	rs2668645	rs142920272	2.9e-07	ENSG00000006062(7.889e-05), ENSG00000120071(6.771e-18), ENSG00000186868(4.302e-05), ENSG00000228696(8.171e-82), ENSG00000260075(8.171e-82), ENSG00000262500(4.334e-75)	ENSG00000120071(8.907e-09), ENSG00000131484(1.778e-10), ENSG00000176681(0), ENSG00000185829(2.706e-16), ENSG00000214425(1.778e-10), ENSG00000225190(1.778e-10), ENSG00000228696(0), ENSG00000238083(2.706e-16), ENSG00000262500(1.013e-28), ENSG00000262879(1.557e-07)	NA	NA	5_TxWk		MAP3K14, KANSL1, MAPT, ARL17B, NSFP1	KANSL1, LRRC37A, ARL17A, LRRC37A4P, PLEKHM1, ARL17B, LRRC37A2	NA	NA
chr17	44,288,156	rs2668653	rs142920272, rs147317628	2.9e-07, 1.1e-06	ENSG00000006062(7.889e-05), ENSG00000120071(6.771e-18), ENSG00000186868(4.302e-05), ENSG00000228696(8.171e-82), ENSG00000260075(8.171e-82), ENSG00000262500(4.334e-75)	ENSG00000120071(8.907e-09), ENSG00000131484(1.778e-10), ENSG00000176681(0), ENSG00000185829(2.706e-16), ENSG00000214425(1.778e-10), ENSG00000225190(1.778e-10), ENSG00000228696(0), ENSG00000238083(2.706e-16), ENSG00000262500(1.013e-28), ENSG00000262879(1.557e-07)	NA	NA	5_TxWk		MAP3K14, KANSL1, MAPT, ARL17B, NSFP1	KANSL1, LRRC37A, ARL17A, LRRC37A4P, PLEKHM1, ARL17B, LRRC37A2	NA	NA
chr17	44,290,759	rs2668662	rs142920272, rs147317628	2.9e-07, 1.1e-06	ENSG00000108379(6.796e-05), ENSG00000120071(1.371e-15), ENSG00000158955(6.796e-05), ENSG00000186868(1.113e-08), ENSG00000225190(1.173e-17), ENSG00000262372(2.024e-10), ENSG00000262539(4.07e-09), ENSG00000264589(1.113e-08), ENSG00000266497(5.756e-25)	ENSG00000004897(3.849e-37), ENSG00000108379(1.454e-06), ENSG00000120071(1.453e-15), ENSG00000159314(1.815e-07), ENSG00000186868(7.968e-07), ENSG00000225190(2.236e-12), ENSG00000236234(2.236e-12), ENSG00000239291(8.887e-15), ENSG00000256762(7.075e-06), ENSG00000260075(1.26e-41), ENSG00000262265(8.887e-15), ENSG00000262372(1.283e-13), ENSG00000262879(1.357e-09), ENSG00000264038(3.203e-07), ENSG00000264225(2.236e-12), ENSG00000266497(9.576e-13)	NA	NA	5_TxWk		WNT3, KANSL1, WNT9B, MAPT, PLEKHM1, MAPT-AS1	CDC27, WNT3, KANSL1, ARHGAP27, MAPT, PLEKHM1, STH, NSFP1, RN7SL730P	NA	NA
chr17	44,290,047	rs2668665	rs142920272, rs147317628	2.9e-07, 1.1e-06	ENSG00000108379(6.796e-05), ENSG00000120071(1.371e-15), ENSG00000158955(6.796e-05), ENSG00000186868(1.113e-08), ENSG00000225190(1.173e-17), ENSG00000262372(2.024e-10), ENSG00000262539(4.07e-09), ENSG00000264589(1.113e-08), ENSG00000266497(5.756e-25)	ENSG00000004897(3.849e-37), ENSG00000108379(1.454e-06), ENSG00000120071(1.453e-15), ENSG00000159314(1.815e-07), ENSG00000186868(7.968e-07), ENSG00000225190(2.236e-12), ENSG00000236234(2.236e-12), ENSG00000239291(8.887e-15), ENSG00000256762(7.075e-06), ENSG00000260075(1.26e-41), ENSG00000262265(8.887e-15), ENSG00000262372(1.283e-13), ENSG00000262879(1.357e-09), ENSG00000264038(3.203e-07), ENSG00000264225(2.236e-12), ENSG00000266497(9.576e-13)	NA	NA	5_TxWk		WNT3, KANSL1, WNT9B, MAPT, PLEKHM1, MAPT-AS1	CDC27, WNT3, KANSL1, ARHGAP27, MAPT, PLEKHM1, STH, NSFP1, RN7SL730P	NA	NA

Continues on the next page

Supplementary Table 16 – continued from previous page

CHR	BP	CredSNP	IndexSNP	Index P	ENSGID_CP	ENSGID_GZ	ENSGID Promoter	ENSGID functional	Chrom HMM	Histone	HGNC_CP	HGNC_GZ	HGNC Promoter	HGNC functional
chr17	44,289,628	rs2668670	rs147317628	1.1e-06	ENSG00000006062(7.889e-05), ENSG00000120071(6.771e-18), ENSG00000186868(4.302e-05), ENSG00000228696(8.171e-82), ENSG00000260075(8.171e-82), ENSG00000262500(4.334e-75)	ENSG00000120071(8.907e-09), ENSG00000131484(1.778e-10), ENSG00000176681(0), ENSG00000185829(2.706e-16), ENSG00000214425(1.778e-10), ENSG00000225190(1.778e-10), ENSG00000228696(0), ENSG00000238083(2.706e-16), ENSG00000262500(1.013e-28), ENSG00000262879(1.557e-07)	NA	NA	5_TxWk		MAP3K14, KANSL1, MAPT, ARL17B, NSFP1	KANSL1, LRRC37A, ARL17A, LRRC37A4P, PLEKHM1, ARL17B, LRRC37A2	NA	NA
chr17	44,292,319	rs2668694	rs147317628	1.1e-06	ENSG00000108379(6.796e-05), ENSG00000120071(1.371e-15), ENSG00000158955(6.796e-05), ENSG00000186868(1.113e-08), ENSG00000225190(1.173e-17), ENSG00000262372(2.024e-10), ENSG00000262539(4.07e-09), ENSG00000264589(1.113e-08), ENSG00000266497(5.756e-25)	ENSG00000004897(3.849e-37), ENSG00000108379(1.454e-06), ENSG00000120071(1.453e-15), ENSG00000159314(1.815e-07), ENSG00000186868(7.968e-07), ENSG00000225190(2.236e-12), ENSG00000236234(2.236e-12), ENSG00000239291(8.887e-15), ENSG00000256762(7.075e-06), ENSG00000260075(1.26e-41), ENSG00000262265(8.887e-15), ENSG00000262372(1.283e-13), ENSG00000262879(1.357e-09), ENSG00000264038(3.203e-07), ENSG00000264225(2.236e-12), ENSG00000266497(9.576e-13)	NA	NA	5_TxWk	H3K36me3	WNT3, KANSL1, WNT9B, MAPT, PLEKHM1, MAPT-AS1	CDC27, WNT3, KANSL1, ARHGAP27, MAPT, PLEKHM1, STH, NSFP1, RN7SL730P	NA	NA
chr17	44,266,531	rs2696566	rs142920272, rs147317628	2.9e-07, 1.1e-06	ENSG00000120071(9.613e-15), ENSG00000186868(1.943e-06), ENSG00000228696(1.763e-05), ENSG00000260075(1.763e-05), ENSG00000262372(2.229e-05)	ENSG00000131484(6.359e-16), ENSG00000176681(0), ENSG00000185829(4.033e-101), ENSG00000214425(6.359e-16), ENSG00000228696(0), ENSG00000238083(4.033e-101), ENSG00000262879(5.357e-06)	NA	NA	7_Enh	H3K4me1	KANSL1, MAPT, ARL17B, NSFP1	LRRC37A, ARL17A, LRRC37A4P, ARL17B, LRRC37A2	NA	NA
chr17	44,266,342	rs2696568	rs142920272, rs147317628	2.9e-07, 1.1e-06	ENSG00000120071(9.613e-15), ENSG00000186868(1.943e-06), ENSG00000228696(1.763e-05), ENSG00000260075(1.763e-05), ENSG00000262372(2.229e-05)	ENSG00000131484(6.359e-16), ENSG00000176681(0), ENSG00000185829(4.033e-101), ENSG00000214425(6.359e-16), ENSG00000228696(0), ENSG00000238083(4.033e-101), ENSG00000262879(5.357e-06)	NA	NA	7_Enh	H3K4me1	KANSL1, MAPT, ARL17B, NSFP1	LRRC37A, ARL17A, LRRC37A4P, ARL17B, LRRC37A2	NA	NA
chr17	44,293,205	rs2696609	rs142920272	2.9e-07			ENSG00000238723		5_TxWk					
chr17	44,270,059	rs2696633	rs147317628	1.1e-06			ENSG00000214401		8_ZNF/Rpts	DHS:H3K4me3			KANSL1-AS1	
chr17	44,291,479	rs2732601	rs142920272	2.9e-07	ENSG00000108379(6.796e-05), ENSG00000120071(1.371e-15), ENSG00000158955(6.796e-05), ENSG00000186868(1.113e-08), ENSG00000225190(1.173e-17), ENSG00000262372(2.024e-10), ENSG00000262539(4.07e-09), ENSG00000264589(1.113e-08), ENSG00000266497(5.756e-25)	ENSG00000004897(3.849e-37), ENSG00000108379(1.454e-06), ENSG00000120071(1.453e-15), ENSG00000159314(1.815e-07), ENSG00000186868(7.968e-07), ENSG00000225190(2.236e-12), ENSG00000236234(2.236e-12), ENSG00000239291(8.887e-15), ENSG00000256762(7.075e-06), ENSG00000260075(1.26e-41), ENSG00000262265(8.887e-15), ENSG00000262372(1.283e-13), ENSG00000262879(1.357e-09), ENSG00000264038(3.203e-07), ENSG00000264225(2.236e-12), ENSG00000266497(9.576e-13)	NA	NA	5_TxWk		WNT3, KANSL1, WNT9B, MAPT, PLEKHM1, MAPT-AS1	CDC27, WNT3, KANSL1, ARHGAP27, MAPT, PLEKHM1, STH, NSFP1, RN7SL730P	NA	NA

Continues on the next page

Supplementary Table 16 – continued from previous page

CHR	BP	CredSNP	IndexSNP	Index P	ENSGID_CP	ENSGID_GZ	ENSGID Promoter	ENSGID functional	Chrom HMM	Histone	HGNC_CP	HGNC_GZ	HGNC Promoter	HGNC functional
chr17	44,291,365	rs2732606	rs142920272	2.9e-07	ENSG00000108379(6.796e-05), ENSG00000120071(1.371e-15), ENSG00000158955(6.796e-05), ENSG00000186868(1.113e-08), ENSG00000225190(1.173e-17), ENSG00000262372(2.024e-10), ENSG00000262539(4.07e-09), ENSG00000264589(1.113e-08), ENSG00000266497(5.756e-25)	ENSG00000004897(3.849e-37), ENSG00000108379(1.454e-06), ENSG00000120071(1.453e-15), ENSG00000159314(1.815e-07), ENSG00000186868(7.968e-07), ENSG00000225190(2.236e-12), ENSG00000236234(2.236e-12), ENSG00000239291(8.887e-15), ENSG00000256762(7.075e-06), ENSG00000260075(1.26e-41), ENSG00000262265(8.887e-15), ENSG00000262372(1.283e-13), ENSG00000262879(1.357e-09), ENSG00000264038(3.203e-07), ENSG00000264225(2.236e-12), ENSG00000266497(9.576e-13)	NA	NA	5_TxWk		WNT3, KANSL1, WNT9B, MAPT, PLEKHM1, MAPT-AS1	CDC27, WNT3, KANSL1, ARHGAP27, MAPT, PLEKHM1, STH, NSFP1, RN7SL730P	NA	NA
chr17	44,289,101	rs2732629	rs147317628	1.1e-06	ENSG00000006062(7.889e-05), ENSG00000120071(6.771e-18), ENSG00000186868(4.302e-05), ENSG00000228696(8.171e-82), ENSG00000260075(8.171e-82), ENSG00000262500(4.334e-75)	ENSG00000120071(8.907e-09), ENSG00000131484(1.778e-10), ENSG00000176681(0), ENSG00000185829(2.706e-16), ENSG00000214425(1.778e-10), ENSG00000225190(1.778e-10), ENSG00000228696(0), ENSG00000238083(2.706e-16), ENSG00000262500(1.013e-28), ENSG00000262879(1.557e-07)	NA	NA	5_TxWk		MAP3K14, KANSL1, MAPT, ARL17B, NSFP1	KANSL1, LRRC37A, ARL17A, LRRC37A4P, PLEKHM1, ARL17B, LRRC37A2	NA	NA
chr17	44,289,232	rs2732631	rs142920272, rs147317628	2.9e-07, 1.1e-06	ENSG00000006062(7.889e-05), ENSG00000120071(6.771e-18), ENSG00000186868(4.302e-05), ENSG00000228696(8.171e-82), ENSG00000260075(8.171e-82), ENSG00000262500(4.334e-75)	ENSG00000120071(8.907e-09), ENSG00000131484(1.778e-10), ENSG00000176681(0), ENSG00000185829(2.706e-16), ENSG00000214425(1.778e-10), ENSG00000225190(1.778e-10), ENSG00000228696(0), ENSG00000238083(2.706e-16), ENSG00000262500(1.013e-28), ENSG00000262879(1.557e-07)	NA	NA	5_TxWk		MAP3K14, KANSL1, MAPT, ARL17B, NSFP1	KANSL1, LRRC37A, ARL17A, LRRC37A4P, PLEKHM1, ARL17B, LRRC37A2	NA	NA
chr8	53,351,137	rs284800	rs10666089m	1.0e-06	ENSG00000147488(7.9e-07)	NA	NA	NA	15_Quies		ST18	NA	NA	NA
chr8	53,348,475	rs284801	rs10666089m	1.0e-06	NA	NA	NA	NA	15_Quies		NA	NA	NA	NA
chr8	53,368,585	rs284803	rs10666089m	1.0e-06	NA	NA	NA	NA	15_Quies		NA	NA	NA	NA
chr8	53,343,063	rs284810	rs10666089m	1.0e-06	NA	NA	NA	NA	15_Quies		NA	NA	NA	NA
chr8	53,338,714	rs284813	rs10666089m	1.0e-06	ENSG00000147485(8.966e-05), ENSG00000147488(5.221e-11)	ENSG00000147488(7.94e-08), ENSG00000253844(9.555e-06)	NA	NA	15_Quies		PXDNL, ST18	ST18	NA	NA
chr8	53,360,144	rs284814	rs10666089m	1.0e-06	NA	NA	NA	NA	15_Quies		NA	NA	NA	NA
chr8	53,361,934	rs284815	rs10666089m	1.0e-06	NA	NA	NA	NA	15_Quies		NA	NA	NA	NA
chr8	53,364,500	rs284819	rs10666089m	1.0e-06	NA	NA	NA	NA	15_Quies		NA	NA	NA	NA
chr20	21,158,371	rs2876596	rs6047270	7.7e-08	NA	NA	NA	NA	15_Quies		NA	NA	NA	NA
chr14	94,844,947	rs28929474	rs112635299	3.0e-07				ENSG00000197249	14_ReprPCWk					SERPINA1
chr18	55,888,468	rs292453	rs292441	1.1e-06			ENSG00000049759		5_TxWk				NEDD4L	
chr5	103,995,368	rs325485	rs325485	3.3e-07	NA	NA	NA	NA	15_Quies		NA	NA	NA	NA
chr5	104,007,433	rs325501	rs325485	3.3e-07	NA	NA	NA	NA	15_Quies		NA	NA	NA	NA
chr5	104,012,303	rs325506	rs325485	3.3e-07	NA	ENSG00000251574(2.86e-08), ENSG00000253584(2.86e-08)	NA	NA	15_Quies		NA		NA	NA
chr8	53,336,933	rs34006528	rs10666089m	1.0e-06	ENSG00000147485(8.966e-05), ENSG00000147488(5.221e-11)	ENSG00000147488(7.94e-08), ENSG00000253844(9.555e-06)	NA	NA	15_Quies	DHS	PXDNL, ST18	ST18	NA	NA
chr6	98,591,074	rs34645063	rs72934503	5.9e-07	NA	NA	NA	NA	9_Het		NA	NA	NA	NA
chr17	44,288,672	rs34898647	rs142920272, rs147317628	2.9e-07, 1.1e-06	ENSG00000006062(7.889e-05), ENSG00000120071(6.771e-18), ENSG00000186868(4.302e-05), ENSG00000228696(8.171e-82), ENSG00000260075(8.171e-82), ENSG00000262500(4.334e-75)	ENSG00000120071(8.907e-09), ENSG00000131484(1.778e-10), ENSG00000176681(0), ENSG00000185829(2.706e-16), ENSG00000214425(1.778e-10), ENSG00000225190(1.778e-10), ENSG00000228696(0), ENSG00000238083(2.706e-16), ENSG00000262500(1.013e-28), ENSG00000262879(1.557e-07)	NA	NA	5_TxWk		MAP3K14, KANSL1, MAPT, ARL17B, NSFP1	KANSL1, LRRC37A, ARL17A, LRRC37A4P, PLEKHM1, ARL17B, LRRC37A2	NA	NA

Continues on the next page

Supplementary Table 16 – continued from previous page

CHR	BP	CredSNP	IndexSNP	Index P	ENSGID_CP	ENSGID_GZ	ENSGID Promoter	ENSGID functional	Chrom HMM	Histone	HGNC_CP	HGNC_GZ	HGNC Promoter	HGNC functional
chr8	53,353,660	rs366249	rs10666089m	1.0e-06	ENSG00000147488(7.9e-07)	NA	NA	NA	15_Quies		ST18	NA	NA	NA
chr6	98,584,720	rs368928614	rs72934503	5.9e-07	NA	NA	NA	NA	15_Quies		NA	NA	NA	NA
chr17	44,311,200	rs373392968	rs147317628	1.1e-06	ENSG00000120071(1.001e-75), ENSG00000186868(4.221e-08), ENSG00000225190(1.513e-15), ENSG00000262372(1.712e-09), ENSG00000264589(4.221e-08), ENSG00000266497(2.367e-21)	ENSG00000004897(5.898e-35), ENSG00000108379(3.433e-06), ENSG00000120071(6.373e-29), ENSG00000159314(2.318e-07), ENSG00000186868(5.531e-07), ENSG00000214401(1.613e-08), ENSG00000225190(2.693e-11), ENSG00000236234(2.693e-11), ENSG00000239291(2.76e-13), ENSG00000256762(5.458e-06), ENSG00000260075(2.959e-37), ENSG00000262265(2.76e-13), ENSG00000262372(5.801e-12), ENSG00000262879(1.682e-08), ENSG00000264038(1.084e-06), ENSG00000264225(2.693e-11), ENSG00000266497(1.002e-11)	NA	NA	15_Quies		KANSL1, MAPT, PLEKHM1, MAPT-AS1	CDC27, WNT3, KANSL1, ARHGAP27, MAPT, KANSL1-AS1, PLEKHM1, STH, NSFP1, RN7SL730P	NA	NA
chr20	21,343,944	rs3848794	rs910805	2.0e-09	ENSG00000225803(2.479e-05)	ENSG00000088930(1.351e-06)	NA	NA	4_Tx		MRPS11P1	XRN2	NA	NA
chr1	96,984,894	rs3851274	rs2391769	1.1e-07	NA	NA	NA	NA	5_TxWk		NA	NA	NA	NA
chr20	14,832,798	rs386257	rs11481126	1.3e-07	NA	NA	NA	NA	15_Quies		NA	NA	NA	NA
chr17	44,165,169	rs3865315	rs142920272, rs147317628	2.9e-07, 1.1e-06	ENSG00000120071(1.319e-14), ENSG00000214401(1.319e-14), ENSG00000260075(9.54e-06)	ENSG00000073969(1.964e-37), ENSG00000120071(1.862e-09), ENSG00000176681(5.414e-10), ENSG00000228696(5.414e-10), ENSG00000238723(1.862e-09), ENSG00000262500(1.094e-09)	NA	NA	15_Quies		KANSL1, KANSL1-AS1, NSFP1	NSF, KANSL1, LRRC37A, ARL17B	NA	NA
chr20	14,817,453	rs389171	rs11481126	1.3e-07	NA	NA	NA	NA	15_Quies		NA	NA	NA	NA
chr20	14,825,067	rs447564	rs11481126	1.3e-07	NA	NA	NA	NA	15_Quies		NA	NA	NA	NA
chr10	16,691,399	rs45595836	rs45595836	3.1e-07	NA	ENSG00000148484(8.329e-05)	NA	NA	15_Quies		NA	RSU1	NA	NA
chr17	44,110,670	rs4597358	rs142920272, rs147317628	2.9e-07, 1.1e-06			ENSG00000120071		4_Tx	H3K36me3			KANSL1	
chr20	21,147,968	rs4625995	rs6047270	7.7e-08			ENSG00000214535		5_TxWk				RPS15AP1	
chr6	11,729,460	rs4713834	rs210894m	4.9e-07				ENSG00000111863	15_Quies					ADTRP
chr10	130,488,026	rs4750990	rs4750990	1.4e-06	NA	NA	NA	NA	14_ReprPCWk		NA	NA	NA	NA
chr18	55,880,518	rs477257	rs292441	1.1e-06	NA	ENSG00000049759(3.605e-07)	NA	NA	7_Enh		NA	NEDD4L	NA	NA
chr18	55,881,771	rs479865	rs292441	1.1e-06	NA	ENSG00000049759(3.605e-07)	NA	NA	7_Enh		NA	NEDD4L	NA	NA
chr20	21,133,212	rs4813414	rs6047270	7.7e-08	NA	NA	NA	NA	5_TxWk		NA	NA	NA	NA
chr20	21,124,872	rs4815022	rs6047270	7.7e-08			ENSG00000088970		15_Quies				PLK1S1	
chr20	21,138,367	rs4815024	rs6047270	7.7e-08	NA	NA	NA	NA	5_TxWk		NA	NA	NA	NA
chr20	21,149,971	rs4815027	rs6047270	7.7e-08	NA	NA	NA	NA	15_Quies		NA	NA	NA	NA
chr20	21,344,454	rs4815040	rs910805	2.0e-09	ENSG00000225803(2.479e-05)	ENSG00000088930(1.351e-06)	NA	NA	5_TxWk		MRPS11P1	XRN2	NA	NA
chr18	55,881,103	rs482805	rs292441	1.1e-06	NA	ENSG00000049759(3.605e-07)	NA	NA	7_Enh		NA	NEDD4L	NA	NA
chr18	55,877,856	rs526730	rs292441	1.1e-06	ENSG00000198796(4.493e-05), ENSG00000267579(4.493e-05)	NA	NA	NA	5_TxWk		ALPK2	NA	NA	NA
chr18	55,880,322	rs535188	rs292441	1.1e-06	NA	ENSG00000049759(3.605e-07)	NA	NA	5_TxWk		NA	NEDD4L	NA	NA
chr17	44,316,076	rs55653937	rs147317628	1.1e-06	ENSG00000120071(1.001e-75), ENSG00000186868(4.221e-08), ENSG00000225190(1.513e-15), ENSG00000262372(1.712e-09), ENSG00000264589(4.221e-08), ENSG00000266497(2.367e-21)	ENSG00000004897(5.898e-35), ENSG00000108379(3.433e-06), ENSG00000120071(6.373e-29), ENSG00000159314(2.318e-07), ENSG00000186868(5.531e-07), ENSG00000214401(1.613e-08), ENSG00000225190(2.693e-11), ENSG00000236234(2.693e-11), ENSG00000239291(2.76e-13), ENSG00000256762(5.458e-06), ENSG00000260075(2.959e-37), ENSG00000262265(2.76e-13), ENSG00000262372(5.801e-12), ENSG00000262879(1.682e-08), ENSG00000264038(1.084e-06), ENSG00000264225(2.693e-11), ENSG00000266497(1.002e-11)	NA	NA	15_Quies		KANSL1, MAPT, PLEKHM1, MAPT-AS1	CDC27, WNT3, KANSL1, ARHGAP27, MAPT, KANSL1-AS1, PLEKHM1, STH, NSFP1, RN7SL730P	NA	NA

Continues on the next page

Supplementary Table 16 – continued from previous page

CHR	BP	CredSNP	IndexSNP	Index P	ENSGID_CP	ENSGID_GZ	ENSGID Promoter	ENSGID functional	Chrom HMM	Histone	HGNC_CP	HGNC_GZ	HGNC Promoter	HGNC functional
chr20	21,242,161	rs55962189	rs55962189	3.0e-07	NA	ENSG00000226405(8.388e-08)	NA	NA	15_Quies		NA		NA	NA
chr18	55,879,203	rs566343	rs292441	1.1e-06	ENSG00000198796(4.493e-05), ENSG00000267579(4.493e-05)	NA	NA	NA	5_TxWk		ALPK2	NA	NA	NA
chr18	55,872,566	rs56724831	rs292441	1.1e-06	ENSG00000198796(4.493e-05), ENSG00000267579(4.493e-05)	NA	NA	NA	7_Enh	H3K4me1	ALPK2	NA	NA	NA
chr18	55,882,192	rs574626	rs292441	1.1e-06	NA	ENSG00000049759(3.605e-07)	NA	NA	7_Enh	H3K4me1	NA	NEDD4L	NA	NA
chr18	55,877,842	rs576451	rs292441	1.1e-06	ENSG00000198796(4.493e-05), ENSG00000267579(4.493e-05)	NA	NA	NA	5_TxWk		ALPK2	NA	NA	NA
chr20	21,401,057	rs57976745	rs910805	2.0e-09	NA	NA	NA	NA	13_ReprPC	H3K27me3:H3K9	NA	NA	NA	NA
chr1	96,588,432	rs58752701	rs201910565	3.4e-07	NA	NA	NA	NA	15_Quies		NA	NA	NA	NA
chr1	96,588,438	rs60135683	rs201910565	3.4e-07	NA	NA	NA	NA	15_Quies		NA	NA	NA	NA
chr19	37,284,873	rs60288454	rs138867053	1.2e-07	ENSG00000120784(1.563e-05), ENSG00000171817(1.563e-05)	ENSG00000120784(2.492e-05), ENSG00000171817(2.492e-05), ENSG00000226686(4.354e-05), ENSG00000232677(1.903e-05), ENSG00000267053(1.903e-05), ENSG00000267605(4.354e-05)	NA	NA	9_Het		ZFP30, ZNF540	ZFP30, ZNF540, LINC00665	NA	NA
chr20	21,121,739	rs6035788	rs6047270	7.7e-08	NA	NA	NA	NA	15_Quies		NA	NA	NA	NA
chr20	21,135,718	rs6035791	rs6047270	7.7e-08	NA	NA	NA	NA	5_TxWk		NA	NA	NA	NA
chr20	21,138,989	rs6035792	rs6047270	7.7e-08	NA	NA	NA	NA	5_TxWk		NA	NA	NA	NA
chr20	21,139,252	rs6035793	rs6047270	7.7e-08	NA	NA	NA	NA	5_TxWk		NA	NA	NA	NA
chr20	21,145,885	rs6035795	rs6047270	7.7e-08	NA	NA	NA	NA	5_TxWk		NA	NA	NA	NA
chr20	21,151,348	rs6035800	rs6047270	7.7e-08	NA	NA	NA	NA	15_Quies		NA	NA	NA	NA
chr20	21,153,782	rs6035803	rs6047270	7.7e-08	NA	NA	NA	NA	15_Quies		NA	NA	NA	NA
chr20	21,243,293	rs6035821	rs910805	2.0e-09	NA	ENSG00000226405(8.388e-08)	NA	NA	15_Quies		NA		NA	NA
chr20	21,332,449	rs6035852	rs910805	2.0e-09	NA	ENSG00000235065(1.844e-05)	NA	NA	5_TxWk		NA	RPL24P2	NA	NA
chr8	10,572,617	rs60410697	rs10099100	1.1e-08	NA	ENSG00000171056(9.841e-05), ENSG00000171060(1.154e-09), ENSG00000183638(1.154e-09), ENSG00000212433(1.154e-09), ENSG00000252565(9.841e-05), ENSG00000254093(9.841e-05), ENSG00000258724(9.841e-05)	NA	NA	14_ReprPCWk		NA	SOX7, C8orf74, RP1L1, RNA5SP252, PINX1	NA	NA
chr20	21,126,194	rs6047271	rs6047270	7.7e-08			ENSG00000088970		15_Quies				PLK1S1	
chr20	21,134,799	rs6047273	rs6047270	7.7e-08	NA	NA	NA	NA	5_TxWk		NA	NA	NA	NA
chr20	21,139,382	rs6047278	rs6047270	7.7e-08			ENSG00000228604		5_TxWk					
chr20	21,143,935	rs6047280	rs6047270	7.7e-08			ENSG00000228604		5_TxWk					
chr20	21,146,468	rs6047282	rs6047270	7.7e-08	NA	NA	NA	NA	5_TxWk		NA	NA	NA	NA
chr20	21,147,009	rs6047283	rs6047270	7.7e-08	NA	NA	NA	NA	5_TxWk		NA	NA	NA	NA
chr20	21,151,324	rs6047288	rs6047270	7.7e-08	NA	NA	NA	NA	15_Quies		NA	NA	NA	NA
chr20	21,158,239	rs6047296	rs6047270	7.7e-08	NA	NA	NA	NA	15_Quies		NA	NA	NA	NA
chr20	21,331,541	rs6047396	rs910805	2.0e-09	NA	ENSG00000235065(1.844e-05)	NA	NA	5_TxWk	H3K36me3	NA	RPL24P2	NA	NA
chr20	21,152,231	rs6082338	rs6047270	7.7e-08	NA	NA	NA	NA	15_Quies		NA	NA	NA	NA
chr20	21,348,430	rs6082397	rs910805	2.0e-09	ENSG00000225803(2.479e-05)	ENSG00000088930(1.351e-06)	NA	NA	5_TxWk		MRPS11P1	XRN2	NA	NA
chr20	14,761,232	rs6110430	rs11481126	1.3e-07	NA	NA	NA	NA	15_Quies		NA	NA	NA	NA
chr20	21,150,267	rs6132402	rs6047270	7.7e-08	NA	NA	NA	NA	15_Quies		NA	NA	NA	NA
chr20	21,146,816	rs6137276	rs6047270	7.7e-08	NA	NA	NA	NA	5_TxWk		NA	NA	NA	NA
chr17	44,185,431	rs62061820	rs142920272, rs147317628	2.9e-07, 1.1e-06	ENSG00000131484(6.16e-22), ENSG00000176681(4.632e-15), ENSG00000214425(6.16e-22), ENSG00000228696(4.28e-59), ENSG00000238083(1.129e-08), ENSG00000260075(4.28e-59), ENSG00000266497(1.129e-08), ENSG00000266918(6.16e-22)	ENSG00000120071(3.253e-05), ENSG00000238723(3.253e-05), ENSG00000262500(3.755e-05)	NA	NA	15_Quies		LRRC37A, LRRC37A4P, ARL17B, LRRC37A2, NSFP1	KANSL1	NA	NA

Continues on the next page

Supplementary Table 16 – continued from previous page

CHR	BP	CredSNP	IndexSNP	Index P	ENSGID_CP	ENSGID_GZ	ENSGID Promoter	ENSGID functional	Chrom HMM	Histone	HGNC_CP	HGNC_GZ	HGNC Promoter	HGNC functional
chr17	44,096,541	rs62062287	rs147317628	1.1e-06	ENSG00000131484(4.629e-14), ENSG00000176681(2.617e-38), ENSG00000214425(4.629e-14), ENSG00000228696(2.617e-38), ENSG00000266918(4.629e-14)	ENSG00000120071(7.247e-07), ENSG00000228696(1.262e-09), ENSG00000238723(7.247e-07), ENSG00000262500(4.782e-07), ENSG00000262539(1.124e-06)	NA	NA	5_TxWk		LRRC37A, LRRC37A4P, ARL17B	KANSL1, ARL17B	NA	NA
chr17	44,096,541	rs62062287m	rs147317628	1.1e-06	ENSG00000131484(4.629e-14), ENSG00000176681(2.617e-38), ENSG00000214425(4.629e-14), ENSG00000228696(2.617e-38), ENSG00000266918(4.629e-14)	ENSG00000120071(7.247e-07), ENSG00000228696(1.262e-09), ENSG00000238723(7.247e-07), ENSG00000262500(4.782e-07), ENSG00000262539(1.124e-06)	NA	NA	5_TxWk		LRRC37A, LRRC37A4P, ARL17B	KANSL1, ARL17B	NA	NA
chr17	44,096,553	rs62062288	rs142920272, rs147317628	2.9e-07, 1.1e-06	ENSG00000131484(4.629e-14), ENSG00000176681(2.617e-38), ENSG00000214425(4.629e-14), ENSG00000228696(2.617e-38), ENSG00000266918(4.629e-14)	ENSG00000120071(7.247e-07), ENSG00000228696(1.262e-09), ENSG00000238723(7.247e-07), ENSG00000262500(4.782e-07), ENSG00000262539(1.124e-06)	NA	NA	5_TxWk		LRRC37A, LRRC37A4P, ARL17B	KANSL1, ARL17B	NA	NA
chr1	96,549,641	rs638729	rs201910565	3.4e-07	NA	NA	NA	NA	15_Quies		NA	NA	NA	NA
chr17	44,208,312	rs6503457	rs142920272, rs147317628	2.9e-07, 1.1e-06	ENSG00000185829(6.167e-37), ENSG00000238083(6.167e-37), ENSG00000262633(3.592e-08), ENSG00000262879(3.592e-08), ENSG00000263142(3.592e-08), ENSG00000263650(3.592e-08), ENSG00000265315(7.022e-29), ENSG00000266497(2.372e-25)	ENSG00000073969(2.084e-07), ENSG00000228696(1.23e-44), ENSG00000260075(1.23e-44), ENSG00000266497(2.657e-06)	NA	NA	7_Enh	H3K4me1	ARL17A, LRRC37A2, LRRC37A17P, RN7SL270P, RN7SL199P	NSF, ARL17B, NSFP1	NA	NA
chr17	44,278,110	rs66498281	rs147317628	1.1e-06	ENSG00000120071(5.738e-08), ENSG00000228696(6.206e-181), ENSG00000260075(6.206e-181)	ENSG00000120071(8.6e-08), ENSG00000185829(0), ENSG00000238083(0), ENSG00000262500(1.699e-08)	NA	NA	5_TxWk		KANSL1, ARL17B, NSFP1	KANSL1, ARL17A, LRRC37A2	NA	NA
chr1	96,511,272	rs66512	rs201910565	3.4e-07	NA	NA	NA	NA	15_Quies		NA	NA	NA	NA
chr1	96,522,935	rs6682371	rs201910565	3.4e-07	NA	ENSG00000117569(4.103e-05)	NA	NA	15_Quies		NA	PTBP2	NA	NA
chr1	99,092,784	rs6701243	rs6701243	3.1e-07	NA	NA	NA	NA	15_Quies		NA	NA	NA	NA
chr2	159,379,244	rs6734020	rs59566011	9.3e-07				ENSG00000144283	15_Quies					PKP4
chr2	159,378,458	rs6743102	rs59566011	9.3e-07				ENSG00000144283	15_Quies					PKP4
chr20	21,139,624	rs68145616	rs6047270	7.7e-08			ENSG00000228604		5_TxWk					
chr20	21,139,623	rs68145616mm	rs6047270	7.7e-08			ENSG00000228604		5_TxWk					
chr20	14,836,243	rs71190156	rs71190156	2.8e-08	NA	NA	NA	NA	15_Quies		NA	NA	NA	NA
chr6	98,561,749	rs71806471	rs72934503	5.9e-07	NA	NA	NA	NA	5_TxWk		NA	NA	NA	NA
chr17	44,210,933	rs7207582	rs142920272	2.9e-07	ENSG00000120071(1.173e-15), ENSG00000159314(3.167e-06), ENSG00000225190(3.167e-06), ENSG00000238723(1.173e-15), ENSG00000260075(3.877e-18), ENSG00000262500(4.273e-15), ENSG00000262879(3.174e-29), ENSG00000263142(3.174e-29)	ENSG00000131484(6.934e-14), ENSG00000159314(2.906e-07), ENSG00000176681(0), ENSG00000214425(6.934e-14), ENSG00000225190(1.09e-11), ENSG00000228696(0), ENSG00000236234(1.09e-11)	NA	NA	5_TxWk		KANSL1, ARHGAP27, PLEKHM1, NSFP1, LRRC37A17P	ARHGAP27, LRRC37A, LRRC37A4P, PLEKHM1, ARL17B	NA	NA
chr20	21,140,171	rs721785	rs6047270	7.7e-08			ENSG00000228604		5_TxWk					
chr17	44,126,365	rs7218319	rs142920272, rs147317628	2.9e-07, 1.1e-06	ENSG00000108433(7.417e-05), ENSG00000120071(2.093e-15), ENSG00000176681(4.187e-13), ENSG00000214401(7.753e-08), ENSG00000228696(4.187e-13), ENSG00000238723(2.093e-15), ENSG00000262500(1.238e-14), ENSG00000262633(7.417e-05), ENSG00000262879(7.417e-05), ENSG00000263142(7.417e-05)	ENSG00000108433(4.841e-06), ENSG00000120071(1.708e-15), ENSG00000176681(1.036e-29), ENSG00000214401(8.406e-08), ENSG00000228696(1.036e-29), ENSG00000238723(1.708e-15), ENSG00000262500(5.602e-15), ENSG00000262633(4.841e-06), ENSG00000262879(4.841e-06), ENSG00000263142(4.841e-06), ENSG00000266497(2.301e-06)	NA	NA	5_TxWk		GOSR2, KANSL1, LRRC37A, KANSL1-AS1, ARL17B, LRRC37A17P	GOSR2, KANSL1, LRRC37A, KANSL1-AS1, ARL17B, LRRC37A17P	NA	NA
chr17	44,138,201	rs7220752	rs147317628	1.1e-06	ENSG00000073969(8.129e-26), ENSG00000108433(8.236e-05), ENSG00000176681(6.545e-66), ENSG00000228696(6.545e-66), ENSG00000262633(8.236e-05)	ENSG00000176681(2.694e-19), ENSG00000185829(3.87e-268), ENSG00000228696(2.694e-19), ENSG00000238083(3.87e-268), ENSG00000265315(6.759e-53), ENSG00000266497(7.335e-05)	NA	NA	5_TxWk		NSF, GOSR2, LRRC37A, ARL17B	LRRC37A, ARL17A, ARL17B, LRRC37A2, RN7SL199P	NA	NA
chr17	44,116,950	rs7221390	rs142920272	2.9e-07			ENSG00000120071		5_TxWk				KANSL1	
chr20	21,267,360	rs726025	rs910805	2.0e-09	NA	NA	NA	NA	14_ReprPCWk		NA	NA	NA	NA

Continues on the next page

Supplementary Table 16 – continued from previous page

CHR	BP	CredSNP	IndexSNP	Index P	ENSGID_CP	ENSGID_GZ	ENSGID Promoter	ENSGID functional	Chrom HMM	Histone	HGNC_CP	HGNC_GZ	HGNC Promoter	HGNC functional
chr6	98,583,488	rs72934503	rs72934503	5.9e-07	NA	NA	NA	NA	15_Quies		NA	NA	NA	NA
chr20	21,277,361	rs73128960	rs910805	2.0e-09	NA	NA	NA	NA	13_ReprPC	H3K27me3	NA	NA	NA	NA
chr20	21,279,983	rs73128966	rs910805	2.0e-09	NA	NA	NA	NA	14_ReprPCWk		NA	NA	NA	NA
chr17	44,110,271	rs7350980	rs142920272, rs147317628	2.9e-07, 1.1e-06			ENSG00000120071		5_TxWk				KANSL1	
chr2	159,379,571	rs7421094	rs59566011	9.3e-07				ENSG00000144283	15_Quies					PKP4
chr17	44,290,849	rs76475191	rs142920272	2.9e-07	ENSG00000108379(6.796e-05), ENSG00000120071(1.371e-15), ENSG00000158955(6.796e-05), ENSG00000186868(1.113e-08), ENSG00000225190(1.173e-17), ENSG00000262372(2.024e-10), ENSG00000262539(4.07e-09), ENSG00000264589(1.113e-08), ENSG00000266497(5.756e-25)	ENSG00000004897(3.849e-37), ENSG00000108379(1.454e-06), ENSG00000120071(1.453e-15), ENSG00000159314(1.815e-07), ENSG00000186868(7.968e-07), ENSG00000225190(2.236e-12), ENSG00000236234(2.236e-12), ENSG00000239291(8.887e-15), ENSG00000256762(7.075e-06), ENSG00000260075(1.26e-41), ENSG00000262265(8.887e-15), ENSG00000262372(1.283e-13), ENSG00000262879(1.357e-09), ENSG00000264038(3.203e-07), ENSG00000264225(2.236e-12), ENSG00000266497(9.576e-13)	NA	NA	5_TxWk		WNT3, KANSL1, WNT9B, MAPT, PLEKHM1, MAPT-AS1	CDC27, WNT3, KANSL1, ARHGAP27, MAPT, PLEKHM1, STH, NSFP1, RN7SL730P	NA	NA
chr1	96,968,232	rs76504869	rs2391769	1.1e-07	NA	NA	NA	NA	15_Quies		NA	NA	NA	NA
chr18	55,881,169	rs76747718	rs292441	1.1e-06	NA	ENSG00000049759(3.605e-07)	NA	NA	7_Enh		NA	NEDD4L	NA	NA
chr6	98,566,506	rs77910749	rs72934503	5.9e-07	NA	NA	NA	NA	14_ReprPCWk	DHS	NA	NA	NA	NA
chr8	10,573,702	rs7820334	rs10099100	1.1e-08	NA	ENSG00000171056(9.841e-05), ENSG00000171060(1.154e-09), ENSG00000183638(1.154e-09), ENSG00000212433(1.154e-09), ENSG00000252565(9.841e-05), ENSG00000254093(9.841e-05), ENSG00000258724(9.841e-05)	NA	NA	14_ReprPCWk		NA	SOX7, C8orf74, RP1L1, RNA5SP252, PINX1	NA	NA
chr17	44,296,230	rs78358711	rs142920272, rs147317628	2.9e-07, 1.1e-06	ENSG00000108379(6.796e-05), ENSG00000120071(1.371e-15), ENSG00000158955(6.796e-05), ENSG00000186868(1.113e-08), ENSG00000225190(1.173e-17), ENSG00000262372(2.024e-10), ENSG00000262539(4.07e-09), ENSG00000264589(1.113e-08), ENSG00000266497(5.756e-25)	ENSG00000004897(3.849e-37), ENSG00000108379(1.454e-06), ENSG00000120071(1.453e-15), ENSG00000159314(1.815e-07), ENSG00000186868(7.968e-07), ENSG00000225190(2.236e-12), ENSG00000236234(2.236e-12), ENSG00000239291(8.887e-15), ENSG00000256762(7.075e-06), ENSG00000260075(1.26e-41), ENSG00000262265(8.887e-15), ENSG00000262372(1.283e-13), ENSG00000262879(1.357e-09), ENSG00000264038(3.203e-07), ENSG00000264225(2.236e-12), ENSG00000266497(9.576e-13)	NA	NA	5_TxWk		WNT3, KANSL1, WNT9B, MAPT, PLEKHM1, MAPT-AS1	CDC27, WNT3, KANSL1, ARHGAP27, MAPT, PLEKHM1, STH, NSFP1, RN7SL730P	NA	NA
chr19	37,621,419	rs78410150	rs138867053	1.2e-07				ENSG00000196967	8_ZNF/Rpts					ZNF585A
chr8	48,504,452	rs78611701	rs183563276π	1.9e-07				ENSG00000272972	15_Quies					NA
chr10	72,749,037	rs78827416	rs78827416	9.0e-07	NA	NA	NA	NA	15_Quies		NA	NA	NA	NA
chr2	159,375,792	rs78932389	rs59566011	9.3e-07				ENSG00000144283	15_Quies					PKP4
chr1	104,791,770	rs79783584	rs11185408	7.0e-07	NA	NA	NA	NA	15_Quies		NA	NA	NA	NA

Continues on the next page

Supplementary Table 16 – continued from previous page

CHR	BP	CredSNP	IndexSNP	Index P	ENSGID_CP	ENSGID_GZ	ENSGID Promoter	ENSGID functional	Chrom HMM	Histone	HGNC_CP	HGNC_GZ	HGNC Promoter	HGNC functional
chr17	44,290,910	rs79861768	rs147317628	1.1e-06	ENSG00000108379(6.796e-05), ENSG00000120071(1.371e-15), ENSG00000158955(6.796e-05), ENSG00000186868(1.113e-08), ENSG00000225190(1.173e-17), ENSG00000262372(2.024e-10), ENSG00000262539(4.07e-09), ENSG00000264589(1.113e-08), ENSG00000266497(5.756e-25)	ENSG00000004897(3.849e-37), ENSG00000108379(1.454e-06), ENSG00000120071(1.453e-15), ENSG00000159314(1.815e-07), ENSG00000186868(7.968e-07), ENSG00000225190(2.236e-12), ENSG00000236234(2.236e-12), ENSG00000239291(8.887e-15), ENSG00000256762(7.075e-06), ENSG00000260075(1.26e-41), ENSG00000262265(8.887e-15), ENSG00000262372(1.283e-13), ENSG00000262879(1.357e-09), ENSG00000264038(3.203e-07), ENSG00000264225(2.236e-12), ENSG00000266497(9.576e-13)	NA	NA	5_TxWk		WNT3, KANSL1, WNT9B, MAPT, PLEKHM1, MAPT-AS1	CDC27, WNT3, KANSL1, ARHGAP27, MAPT, PLEKHM1, STH, NSFP1, RN7SL730P	NA	NA
chr17	44,208,674	rs8070942	rs147317628	1.1e-06	ENSG00000185829(6.167e-37), ENSG00000238083(6.167e-37), ENSG00000262633(3.592e-08), ENSG00000262879(3.592e-08), ENSG00000263142(3.592e-08), ENSG00000263650(3.592e-08), ENSG00000265315(7.022e-29), ENSG00000266497(2.372e-25)	ENSG00000073969(2.084e-07), ENSG00000228696(1.23e-44), ENSG00000260075(1.23e-44), ENSG00000266497(2.657e-06)	NA	NA	7_Enh	H3K4me1	ARL17A, LRRC37A2, LRRC37A17P, RN7SL270P, RN7SL199P	NSF, ARL17B, NSFP1	NA	NA
chr17	44,115,440	rs8077487	rs142920272, rs147317628	2.9e-07, 1.1e-06	ENSG00000120071(2.025e-10), ENSG00000131484(3.196e-08), ENSG00000176681(5.016e-43), ENSG00000214401(2.347e-05), ENSG00000214425(3.196e-08), ENSG00000228696(5.016e-43), ENSG00000238723(2.025e-10), ENSG00000260075(8.608e-13), ENSG00000262500(1.634e-09), ENSG00000266918(3.196e-08)	ENSG00000120071(1.235e-13), ENSG00000176681(8.657e-28), ENSG00000214425(1.962e-99), ENSG00000228696(8.657e-28), ENSG00000238723(1.235e-13), ENSG00000260075(2.132e-197), ENSG00000262500(4.59e-12), ENSG00000267198(1.962e-99), ENSG00000267246(1.962e-99)	NA	NA	5_TxWk		KANSL1, LRRC37A, KANSL1-AS1, LRRC37A4P, ARL17B, NSFP1	KANSL1, LRRC37A, LRRC37A4P, ARL17B, NSFP1	NA	NA
chr17	44,162,597	rs8080583	rs147317628	1.1e-06	ENSG00000120071(1.319e-14), ENSG00000214401(1.319e-14), ENSG00000260075(9.54e-06)	ENSG00000073969(1.964e-37), ENSG00000120071(1.862e-09), ENSG00000176681(5.414e-10), ENSG00000228696(5.414e-10), ENSG00000238723(1.862e-09), ENSG00000262500(1.094e-09)	NA	NA	15_Quies		KANSL1, KANSL1-AS1, NSFP1	NSF, KANSL1, LRRC37A, ARL17B	NA	NA
chr20	21,168,395	rs8120293	rs6047270	7.7e-08	NA	NA	NA	NA	14_ReprPCWk		NA	NA	NA	NA
chr20	21,248,116	rs910805	rs910805	2.0e-09	NA	ENSG00000226405(8.388e-08)	NA	NA	14_ReprPCWk		NA		NA	NA
chr17	44,187,257	rs9303525	rs142920272, rs147317628	2.9e-07, 1.1e-06	ENSG00000131484(6.16e-22), ENSG00000176681(4.632e-15), ENSG00000214425(6.16e-22), ENSG00000228696(4.28e-59), ENSG00000238083(1.129e-08), ENSG00000260075(4.28e-59), ENSG00000266497(1.129e-08), ENSG00000266918(6.16e-22)	ENSG00000120071(3.253e-05), ENSG00000238723(3.253e-05), ENSG00000262500(3.755e-05)	NA	NA	15_Quies		LRRC37A, LRRC37A4P, ARL17B, LRRC37A2, NSFP1	KANSL1	NA	NA
chr3	62,478,786	rs9311841	rs1452075	2.1e-07			ENSG00000163618		15_Quies				CADPS	
chr6	11,730,878	rs9366877	rs210894m	4.9e-07				ENSG00000111863	15_Quies					ADTRP
chr6	98,577,689	rs9372734	rs72934503	5.9e-07	NA	NA	NA	NA	5_TxWk		NA	NA	NA	NA
chr6	98,575,726	rs9388171	rs72934503	5.9e-07	NA	NA	NA	NA	5_TxWk		NA	NA	NA	NA
chr6	98,549,801	rs9401593	rs72934503	5.9e-07	NA	NA	NA	NA	15_Quies		NA	NA	NA	NA
chr6	98,574,560	rs968050	rs72934503	5.9e-07	NA	NA	NA	NA	5_TxWk		NA	NA	NA	NA
chr1	96,968,371	rs9804071	rs2391769	1.1e-07	NA	NA	NA	NA	15_Quies		NA	NA	NA	NA
chr17	44,091,886	rs9891103	rs147317628	1.1e-06	ENSG00000131484(4.629e-14), ENSG00000176681(2.617e-38), ENSG00000214425(4.629e-14), ENSG00000228696(2.617e-38), ENSG00000266918(4.629e-14)	ENSG00000120071(7.247e-07), ENSG00000228696(1.262e-09), ENSG00000238723(7.247e-07), ENSG00000262500(4.782e-07), ENSG00000262539(1.124e-06)	NA	NA	5_TxWk		LRRC37A, LRRC37A4P, ARL17B	KANSL1, ARL17B	NA	NA

Continues on the next page

Supplementary Table 16 – continued from previous page

CHR	BP	CredSNP	IndexSNP	Index P	ENSGID_CP	ENSGID_GZ	ENSGID Promoter	ENSGID functional	Chrom HMM	Histone	HGNC_CP	HGNC_GZ	HGNC Promoter	HGNC functional
chr17	44,151,546	rs9907738	rs142920272, rs147317628	2.9e-07, 1.1e-06	ENSG00000108433(1.738e-17), ENSG00000120071(9.114e-05), ENSG00000176681(2.996e-19), ENSG00000214401(9.114e-05), ENSG00000228696(2.996e-19), ENSG00000260075(7.901e-08), ENSG00000262633(1.738e-17), ENSG00000262879(1.738e-17), ENSG00000263142(1.738e-17)	ENSG00000073969(0), ENSG00000225190(2.979e-06)	NA	NA	15_Quies		GOSR2, KANSL1, LRRC37A, KANSL1-AS1, ARL17B, NSFP1, LRRC37A17P	NSF, PLEKHM1	NA	NA
chr17	44,212,782	rs9915547	rs142920272, rs147317628	2.9e-07, 1.1e-06	ENSG00000120071(1.173e-15), ENSG00000159314(3.167e-06), ENSG00000225190(3.167e-06), ENSG00000238723(1.173e-15), ENSG00000260075(3.877e-18), ENSG00000262500(4.273e-15), ENSG00000262879(3.174e-29), ENSG00000263142(3.174e-29)	ENSG00000131484(6.934e-14), ENSG00000159314(2.906e-07), ENSG00000176681(0), ENSG00000214425(6.934e-14), ENSG00000225190(1.09e-11), ENSG00000228696(0), ENSG00000236234(1.09e-11)	NA	NA	5_TxWk		KANSL1, ARHGAP27, PLEKHM1, NSFP1, LRRC37A17P	ARHGAP27, LRRC37A, LRRC37A4P, PLEKHM1, ARL17B	NA	NA
chr3	62,471,282	rs9968060	rs1452075	2.1e-07	ENSG00000163618(1.026e-06)	ENSG00000153266(9.164e-05), ENSG00000163618(6.154e-05), ENSG00000241472(9.164e-05)	NA	NA	5_TxWk		CADPS	FEZF2, CADPS, PTPRG-AS1	NA	NA

Supplementary figures

List of Supplementary Figures

4.1 GWAS

4.1.1 Qq plots

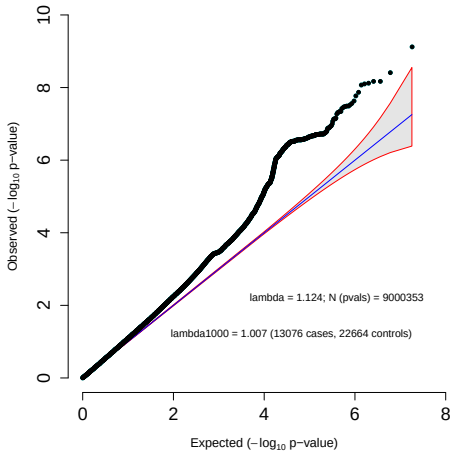

Supplementary Figure 1: Qq (quantile-quantile) plot for the 13 076 cases and 22 664 controls in the iPSYCH ASD GWAS. Association quantiles of the $-\log_{10}$ p-values (achieved from z-score from logistic regression in genotyping waves and subsequent inverse variant weighted meta-analysis across waves) are plotted against the quantiles expected under the null. The shading indicates 95%-confidence region under the null. The genomic inflation factor, lambda, is the observed median χ^2 test statistic divided by the median expected χ^2 test statistic under the null hypothesis, lambda1000 estimates what lambda would be equivalent to in a sample of 500 cases and 500 controls.

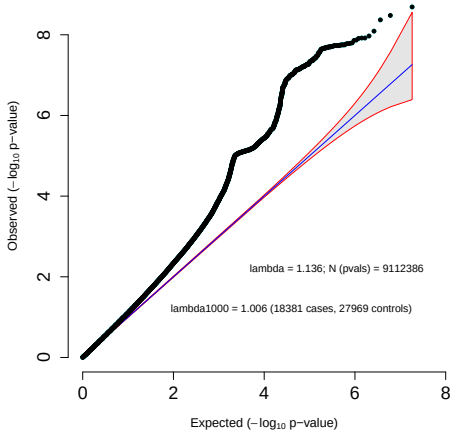

Supplementary Figure 2: Qq (quantile-quantile) plot for the iPSYCH-PGC meta analysis composed of 18 381 cases and 27 969 controls. Association quantiles of the p-values (achieved from z-score from logistic regression in genotyping waves and subsequent inverse variant weighted meta-analysis across waves) are plotted against the quantiles expected under the null. The shading indicates 95%-confidence region under the null. The genomic inflation factor, lambda, is the observed median χ^2 test statistic divided by the median expected χ^2 test statistic under the null hypothesis, lambda1000 estimates what lambda would be equivalent to in a sample of 500 cases and 500 controls.

4.1.2 Forest plots

In figures 3–25 we provide the forest plots for the top signals of the iPSYCH-PGC meta analysis.

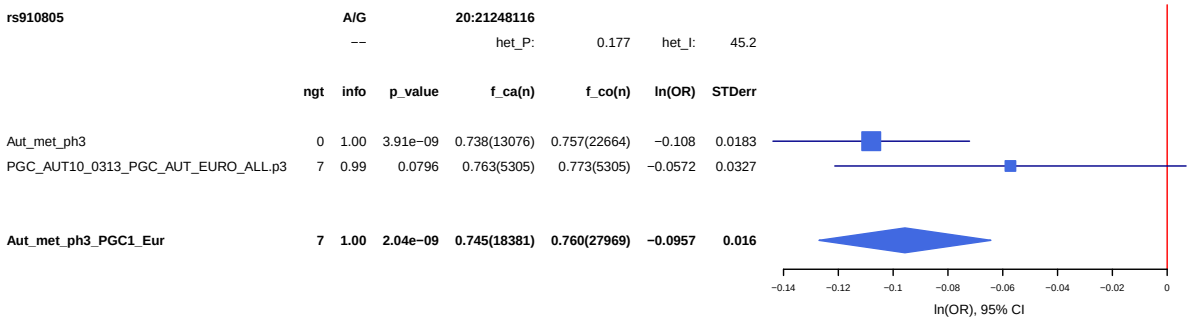

Supplementary Figure 3: Forest plot for rs910805 for meta analysis of iPSYCH ASD GWAS (13 076 cases and 22 664 controls) and the PGC ASD GWAS (5 305 cases and 5 305 pseudo-controls). The plot shows the effect estimate with 95%-confidence interval for rs910805 in the iPSYCH sample (Aut_met_ph3), PGC (PGC_AUT10_0313_PGC_AUT_EURO_ALL.p3) and the the inverse variance weighted meta analysis (Aut_met_ph3_PGC1_Eur).

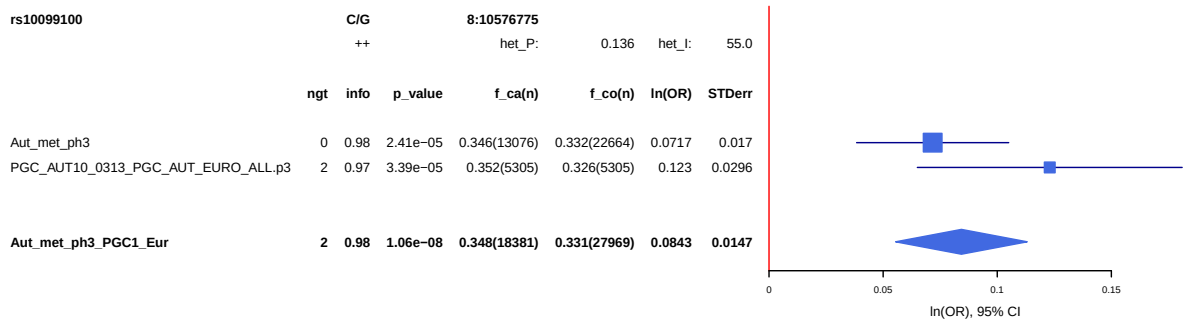

Supplementary Figure 4: Forest plot for rs10099100 for meta analysis of iPSYCH ASD GWAS (13 076 cases and 22 664 controls) and the PGC ASD GWAS (5 305 cases and 5 305 pseudo-controls). The plot shows the effect estimate with 95%-confidence interval for rs10099100 in the iPSYCH sample (Aut_met_ph3), PGC (PGC_AUT10_0313_PGC_AUT_EURO_ALL.p3) and the the inverse variance weighted meta analysis (Aut_met_ph3_PGC1_Eur).

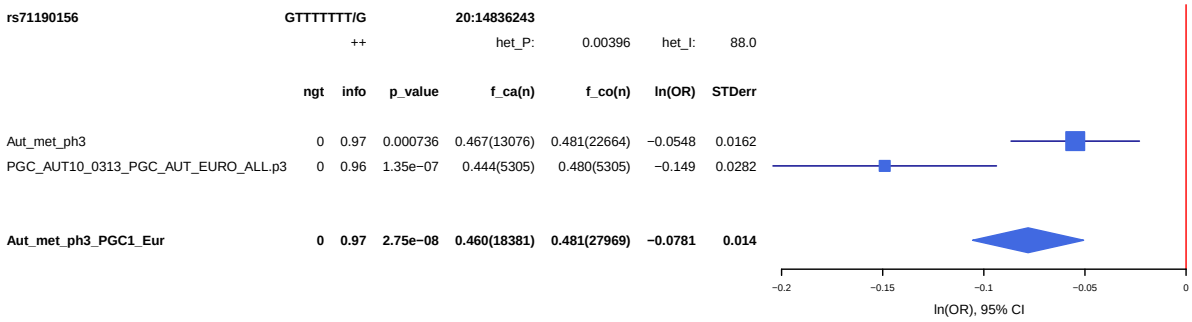

Supplementary Figure 5: Forest plot for rs71190156 for meta analysis of iPSYCH ASD GWAS (13 076 cases and 22 664 controls) and the PGC ASD GWAS (5 305 cases and 5 305 pseudo-controls). The plot shows the effect estimate with 95%-confidence interval for rs71190156 in the iPSYCH sample (Aut_met_ph3), PGC (PGC_AUT10_0313_PGC_AUT_EURO_ALL.p3) and the the inverse variance weighted meta analysis (Aut_met_ph3_PGC1_Eur).

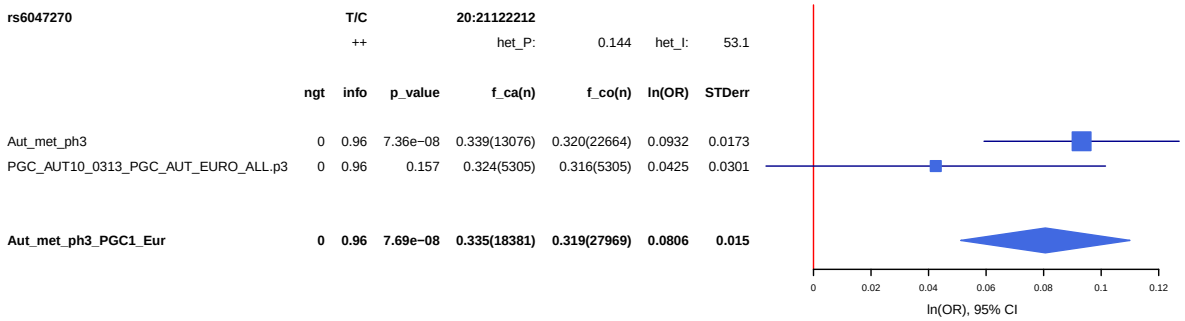

Supplementary Figure 6: Forest plot for rs6047270 for meta analysis of iPSYCH ASD GWAS (13 076 cases and 22 664 controls) and the PGC ASD GWAS (5 305 cases and 5 305 pseudo-controls). The plot shows the effect estimate with 95%-confidence interval for rs6047270 in the iPSYCH sample (Aut_met_ph3), PGC (PGC_AUT10_0313_PGC_AUT_EURO_ALL.p3) and the the inverse variance weighted meta analysis (Aut_met_ph3_PGC1_Eur).

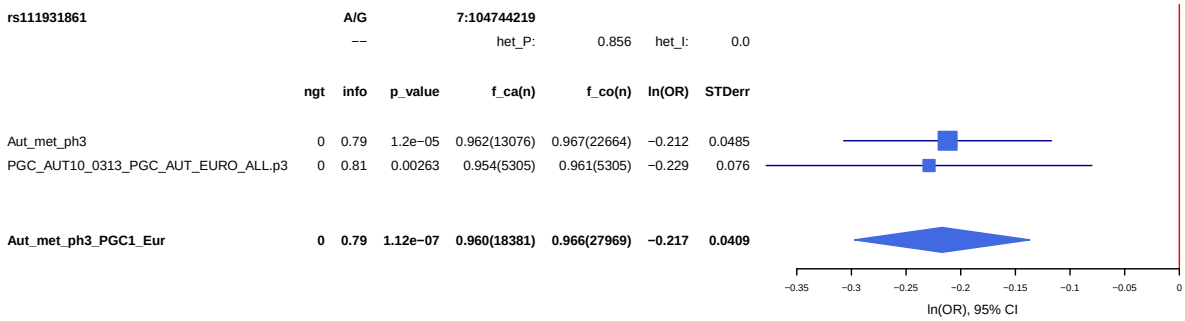

Supplementary Figure 7: Forest plot for rs111931861 for meta analysis of iPSYCH ASD GWAS (13 076 cases and 22 664 controls) and the PGC ASD GWAS (5 305 cases and 5 305 pseudo-controls). The plot shows the effect estimate with 95%-confidence interval for rs111931861 in the iPSYCH sample (Aut_met_ph3), PGC (PGC_AUT10_0313_PGC_AUT_EURO_ALL.p3) and the the inverse variance weighted meta analysis (Aut_met_ph3_PGC1_Eur).

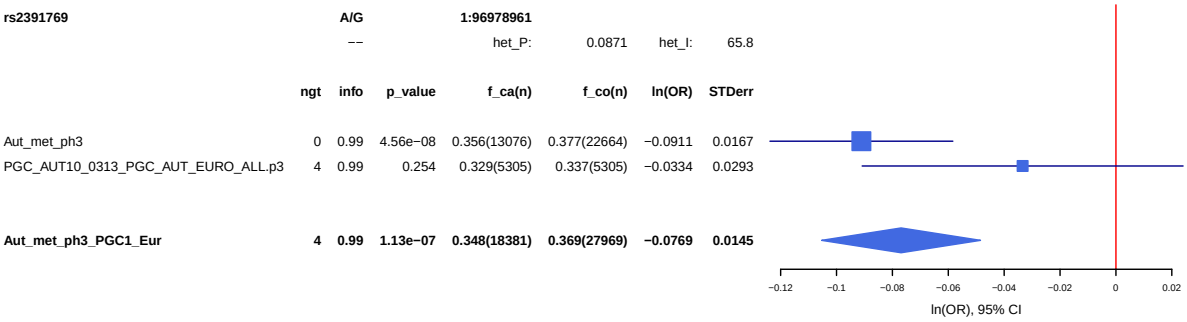

Supplementary Figure 8: Forest plot for rs2391769 for meta analysis of iPSYCH ASD GWAS (13 076 cases and 22 664 controls) and the PGC ASD GWAS (5 305 cases and 5 305 pseudo-controls). The plot shows the effect estimate with 95%-confidence interval for rs2391769 in the iPSYCH sample (Aut_met_ph3), PGC (PGC_AUT10_0313_PGC_AUT_EURO_ALL.p3) and the the inverse variance weighted meta analysis (Aut_met_ph3_PGC1_Eur).

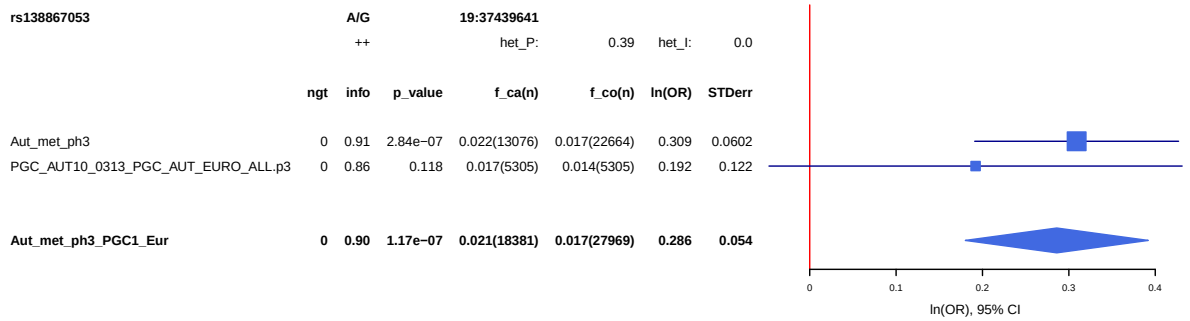

Supplementary Figure 9: Forest plot for rs138867053 for meta analysis of iPSYCH ASD GWAS (13 076 cases and 22 664 controls) and the PGC ASD GWAS (5 305 cases and 5 305 pseudo-controls). The plot shows the effect estimate with 95%-confidence interval for rs138867053 in the iPSYCH sample (Aut_met_ph3), PGC (PGC_AUT10_0313_PGC_AUT_EURO_ALL.p3) and the the inverse variance weighted meta analysis (Aut_met_ph3_PGC1_Eur).

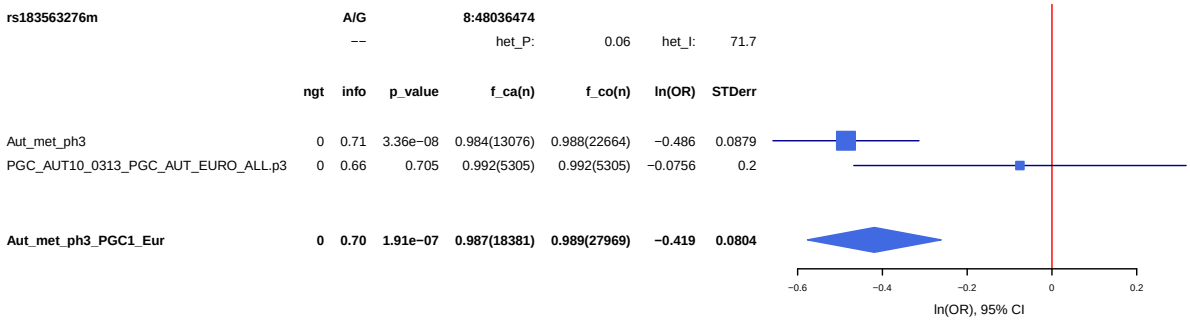

Supplementary Figure 10: Forest plot for rs183563276m for meta analysis of iPSYCH ASD GWAS (13 076 cases and 22 664 controls) and the PGC ASD GWAS (5 305 cases and 5 305 pseudo-controls). The plot shows the effect estimate with 95%-confidence interval for rs183563276m in the iPSYCH sample (Aut_met_ph3), PGC (PGC_AUT10_0313_PGC_AUT_EURO_ALL.p3) and the the inverse variance weighted meta analysis (Aut_met_ph3_PGC1_Eur).

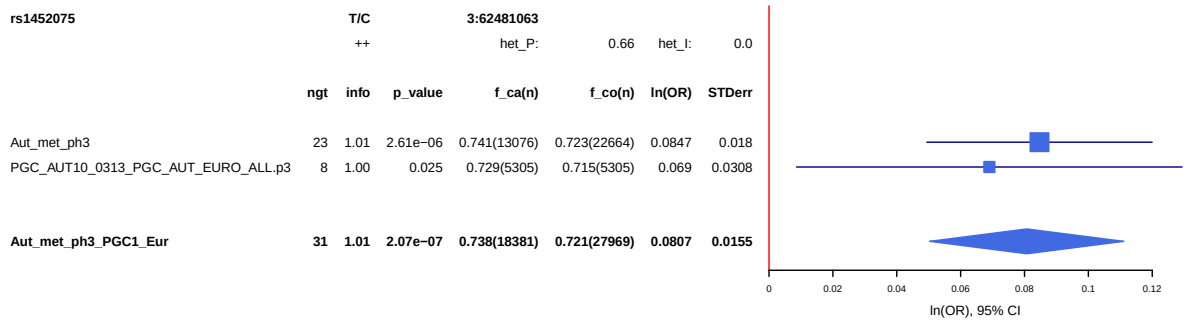

Supplementary Figure 11: Forest plot for rs1452075 for meta analysis of iPSYCH ASD GWAS (13 076 cases and 22 664 controls) and the PGC ASD GWAS (5 305 cases and 5 305 pseudo-controls). The plot shows the effect estimate with 95%-confidence interval for rs1452075 in the iPSYCH sample (Aut_met_ph3), PGC (PGC_AUT10_0313_PGC_AUT_EURO_ALL.p3) and the the inverse variance weighted meta analysis (Aut_met_ph3_PGC1_Eur).

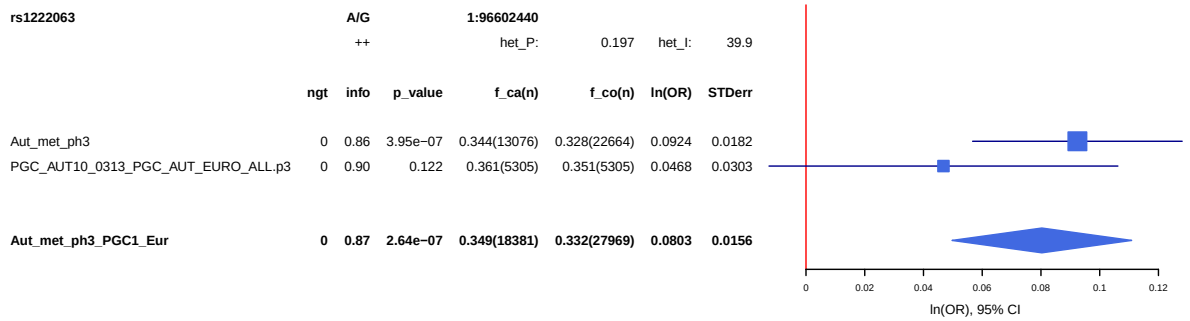

Supplementary Figure 12: Forest plot for rs1222063 for meta analysis of iPSYCH ASD GWAS (13 076 cases and 22 664 controls) and the PGC ASD GWAS (5 305 cases and 5 305 pseudo-controls). The plot shows the effect estimate with 95%-confidence interval for rs1222063 in the iPSYCH sample (Aut_met_ph3), PGC (PGC_AUT10_0313_PGC_AUT_EURO_ALL.p3) and the the inverse variance weighted meta analysis (Aut_met_ph3_PGC1_Eur).

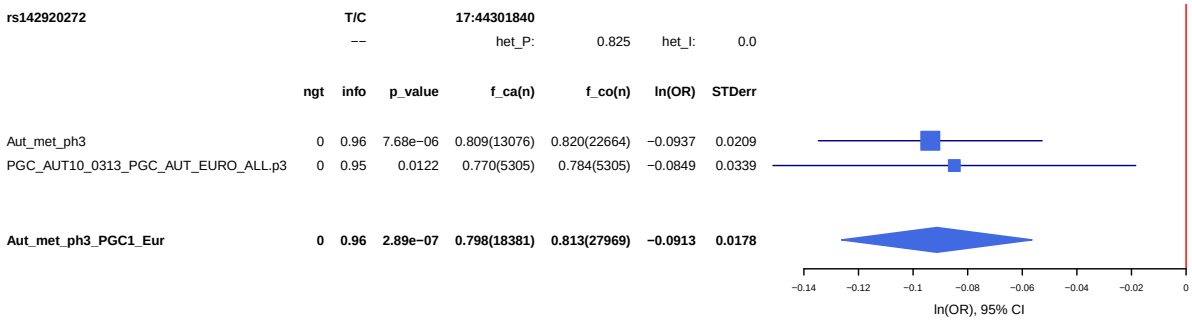

Supplementary Figure 13: Forest plot for rs142920272 for meta analysis of iPSYCH ASD GWAS (13 076 cases and 22 664 controls) and the PGC ASD GWAS (5 305 cases and 5 305 pseudo-controls). The plot shows the effect estimate with 95%-confidence interval for rs142920272 in the iPSYCH sample (Aut_met_ph3), PGC (PGC_AUT10_0313_PGC_AUT_EURO_ALL.p3) and the the inverse variance weighted meta analysis (Aut_met_ph3_PGC1_Eur).

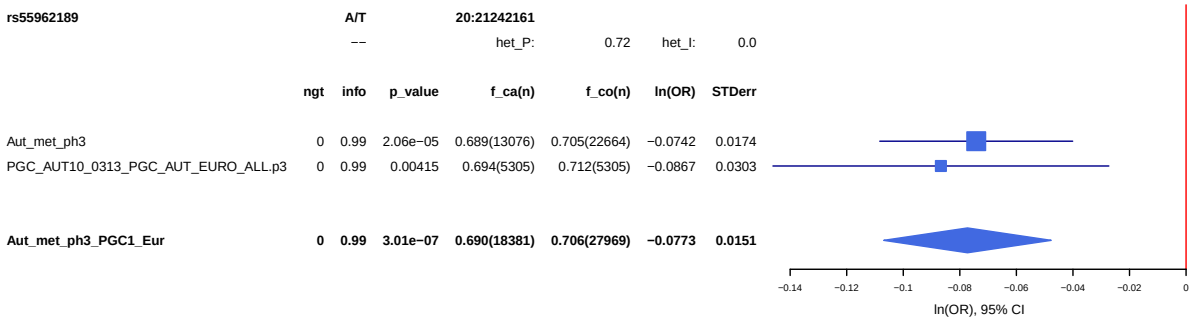

Supplementary Figure 14: Forest plot for rs55962189 for meta analysis of iPSYCH ASD GWAS (13 076 cases and 22 664 controls) and the PGC ASD GWAS (5 305 cases and 5 305 pseudo-controls). The plot shows the effect estimate with 95%-confidence interval for rs55962189 in the iPSYCH sample (Aut_met_ph3), PGC (PGC_AUT10_0313_PGC_AUT_EURO_ALL.p3) and the the inverse variance weighted meta analysis (Aut_met_ph3_PGC1_Eur).

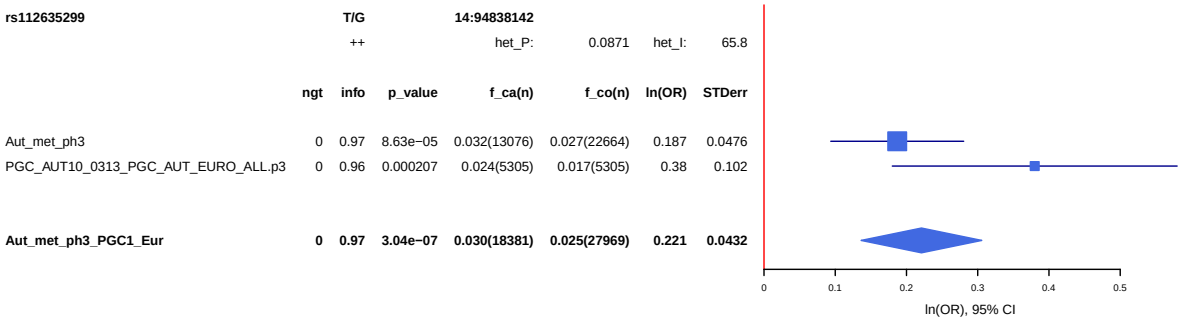

Supplementary Figure 15: Forest plot for rs112635299 for meta analysis of iPSYCH ASD GWAS (13 076 cases and 22 664 controls) and the PGC ASD GWAS (5 305 cases and 5 305 pseudo-controls). The plot shows the effect estimate with 95%-confidence interval for rs112635299 in the iPSYCH sample (Aut_met_ph3), PGC (PGC_AUT10_0313_PGC_AUT_EURO_ALL.p3) and the the inverse variance weighted meta analysis (Aut_met_ph3_PGC1_Eur).

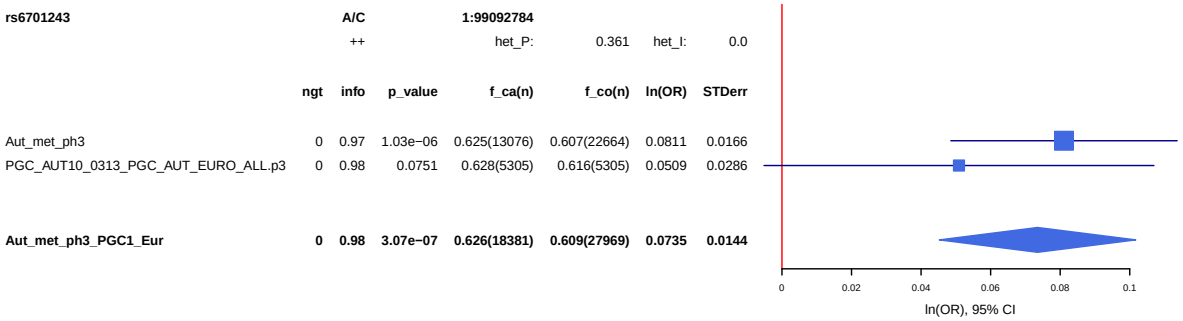

Supplementary Figure 16: Forest plot for rs6701243 for meta analysis of iPSYCH ASD GWAS (13 076 cases and 22 664 controls) and the PGC ASD GWAS (5 305 cases and 5 305 pseudo-controls). The plot shows the effect estimate with 95%-confidence interval for rs6701243 in the iPSYCH sample (Aut_met_ph3), PGC (PGC_AUT10_0313_PGC_AUT_EURO_ALL.p3) and the the inverse variance weighted meta analysis (Aut_met_ph3_PGC1_Eur).

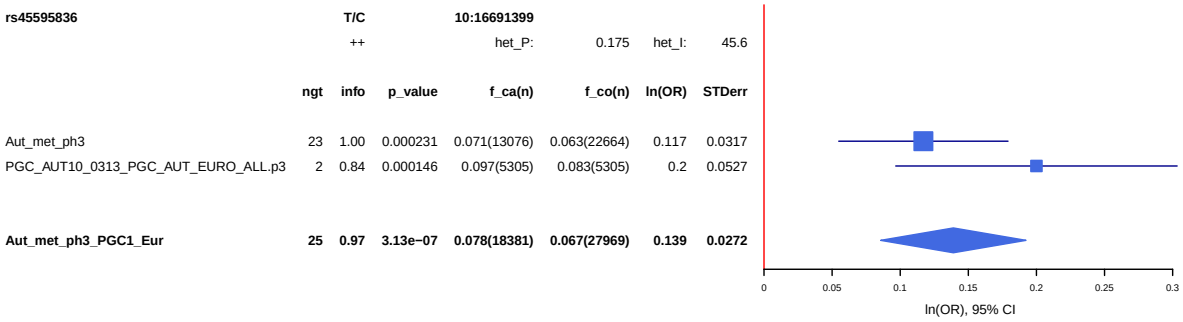

Supplementary Figure 17: Forest plot for rs45595836 for meta analysis of iPSYCH ASD GWAS (13 076 cases and 22 664 controls) and the PGC ASD GWAS (5 305 cases and 5 305 pseudo-controls). The plot shows the effect estimate with 95%-confidence interval for rs45595836 in the iPSYCH sample (Aut_met_ph3), PGC (PGC_AUT10_0313_PGC_AUT_EURO_ALL.p3) and the the inverse variance weighted meta analysis (Aut_met_ph3_PGC1_Eur).

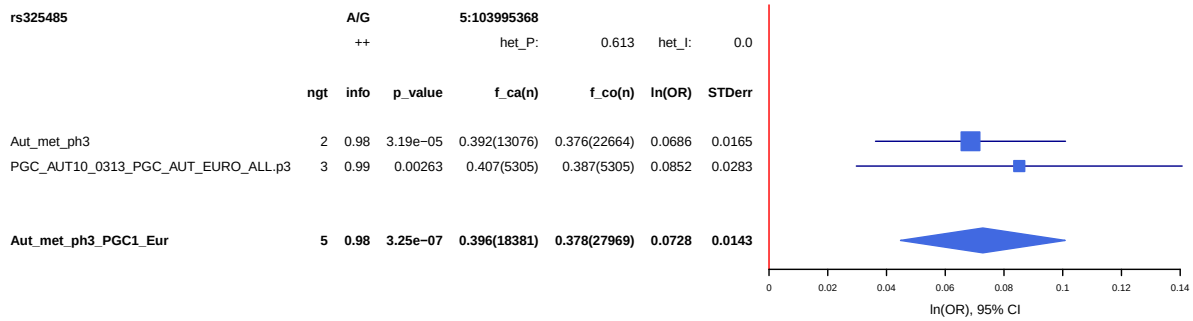

Supplementary Figure 18: Forest plot for rs325485 for meta analysis of iPSYCH ASD GWAS (13 076 cases and 22 664 controls) and the PGC ASD GWAS (5 305 cases and 5 305 pseudo-controls). The plot shows the effect estimate with 95%-confidence interval for rs325485 in the iPSYCH sample (Aut_met_ph3), PGC (PGC_AUT10_0313_PGC_AUT_EURO_ALL.p3) and the the inverse variance weighted meta analysis (Aut_met_ph3_PGC1_Eur).

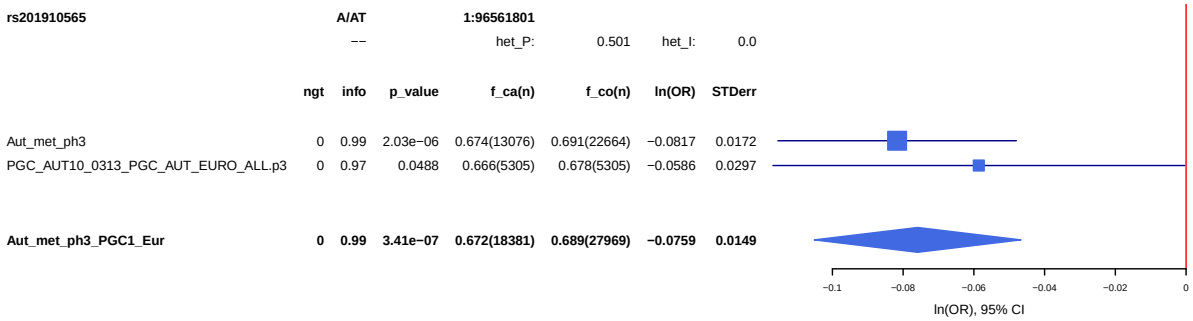

Supplementary Figure 19: Forest plot for rs201910565 for meta analysis of iPSYCH ASD GWAS (13 076 cases and 22 664 controls) and the PGC ASD GWAS (5 305 cases and 5 305 pseudo-controls). The plot shows the effect estimate with 95%-confidence interval for rs201910565 in the iPSYCH sample (Aut_met_ph3), PGC (PGC_AUT10_0313_PGC_AUT_EURO_ALL.p3) and the the inverse variance weighted meta analysis (Aut_met_ph3_PGC1_Eur).

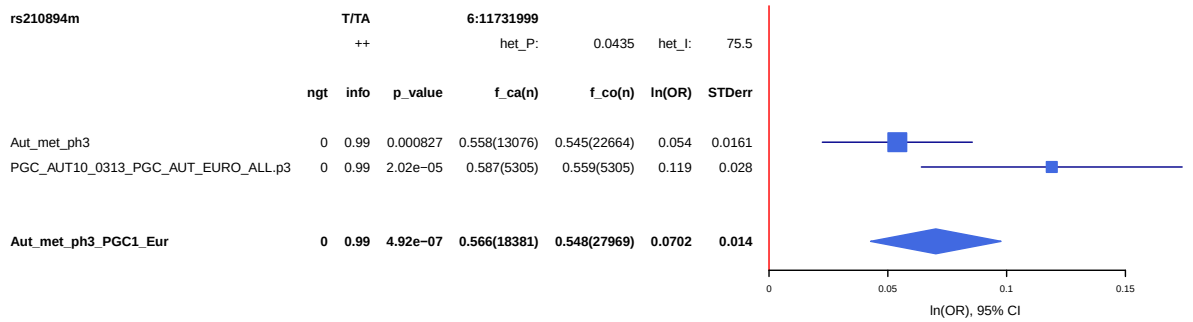

Supplementary Figure 20: Forest plot for rs210894m for meta analysis of iPSYCH ASD GWAS (13 076 cases and 22 664 controls) and the PGC ASD GWAS (5 305 cases and 5 305 pseudo-controls). The plot shows the effect estimate with 95%-confidence interval for rs210894m in the iPSYCH sample (Aut_met_ph3), PGC (PGC_AUT10_0313_PGC_AUT_EURO_ALL.p3) and the the inverse variance weighted meta analysis (Aut_met_ph3_PGC1_Eur).

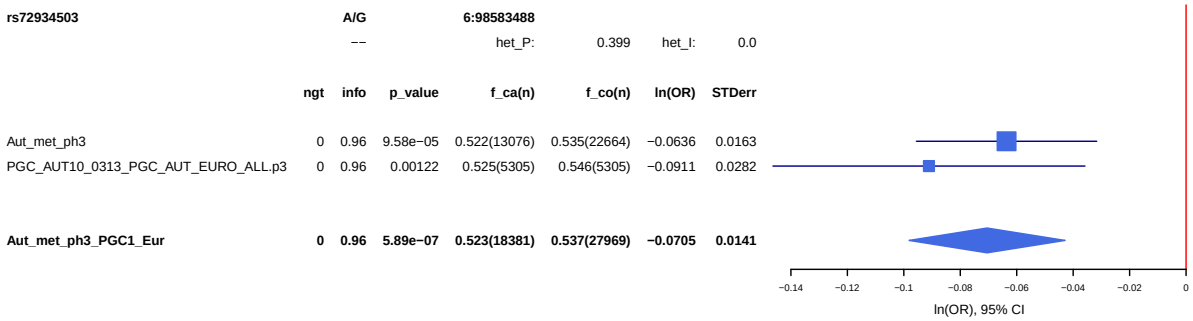

Supplementary Figure 21: Forest plot for rs72934503 for meta analysis of iPSYCH ASD GWAS (13 076 cases and 22 664 controls) and the PGC ASD GWAS (5 305 cases and 5 305 pseudo-controls). The plot shows the effect estimate with 95%-confidence interval for rs72934503 in the iPSYCH sample (Aut_met_ph3), PGC (PGC_AUT10_0313_PGC_AUT_EURO_ALL.p3) and the the inverse variance weighted meta analysis (Aut_met_ph3_PGC1_Eur).

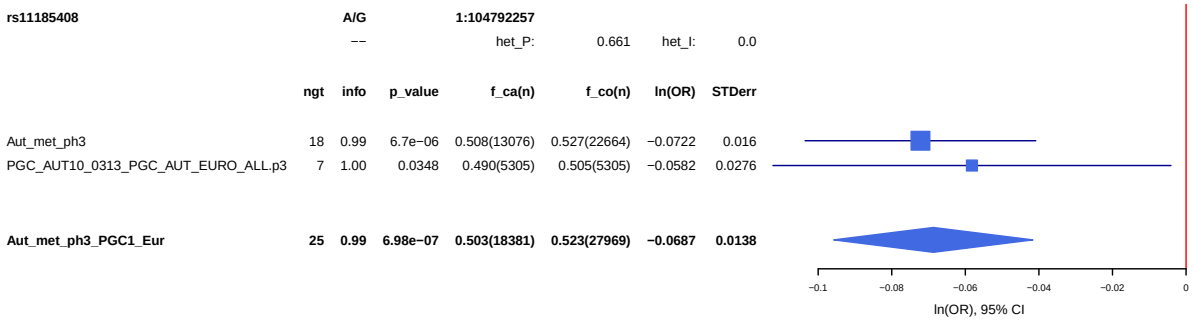

Supplementary Figure 22: Forest plot for rs11185408 for meta analysis of iPSYCH ASD GWAS (13 076 cases and 22 664 controls) and the PGC ASD GWAS (5 305 cases and 5 305 pseudo-controls). The plot shows the effect estimate with 95%-confidence interval for rs11185408 in the iPSYCH sample (Aut_met_ph3), PGC (PGC_AUT10_0313_PGC_AUT_EURO_ALL.p3) and the the inverse variance weighted meta analysis (Aut_met_ph3_PGC1_Eur).

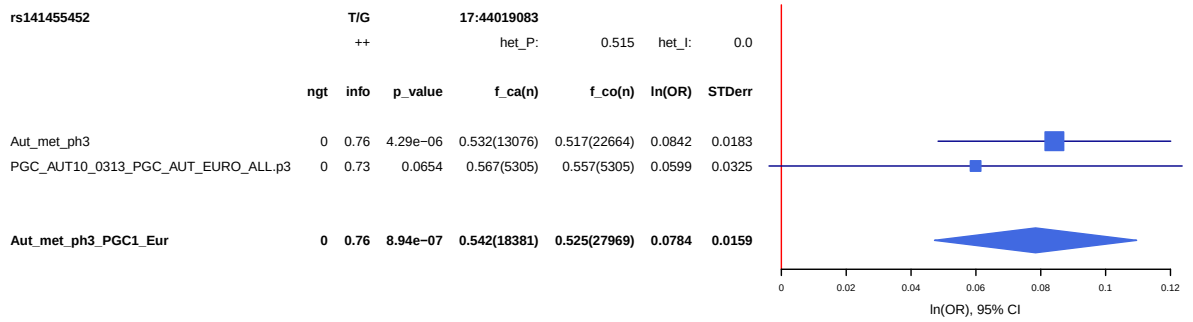

Supplementary Figure 23: Forest plot for rs141455452 for meta analysis of iPSYCH ASD GWAS (13 076 cases and 22 664 controls) and the PGC ASD GWAS (5 305 cases and 5 305 pseudo-controls). The plot shows the effect estimate with 95%-confidence interval for rs141455452 in the iPSYCH sample (Aut_met_ph3), PGC (PGC_AUT10_0313_PGC_AUT_EURO_ALL.p3) and the the inverse variance weighted meta analysis (Aut_met_ph3_PGC1_Eur).

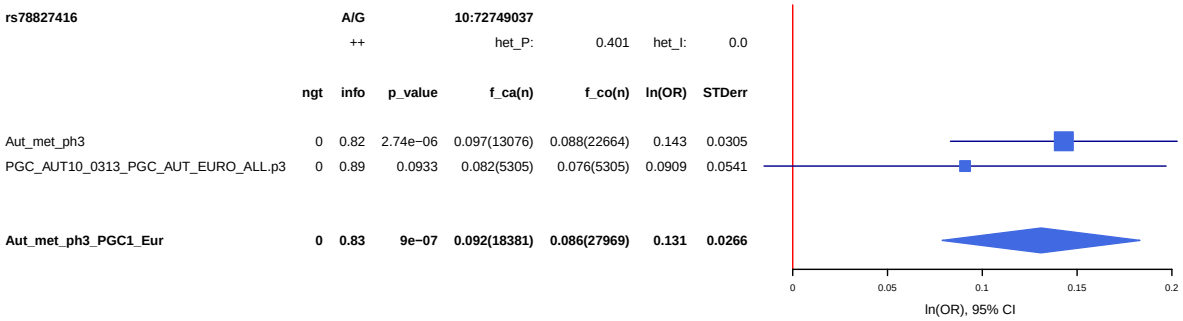

Supplementary Figure 24: Forest plot for rs78827416 for meta analysis of iPSYCH ASD GWAS (13 076 cases and 22 664 controls) and the PGC ASD GWAS (5 305 cases and 5 305 pseudo-controls). The plot shows the effect estimate with 95%-confidence interval for rs78827416 in the iPSYCH sample (Aut_met_ph3), PGC (PGC_AUT10_0313_PGC_AUT_EURO_ALL.p3) and the the inverse variance weighted meta analysis (Aut_met_ph3_PGC1_Eur).

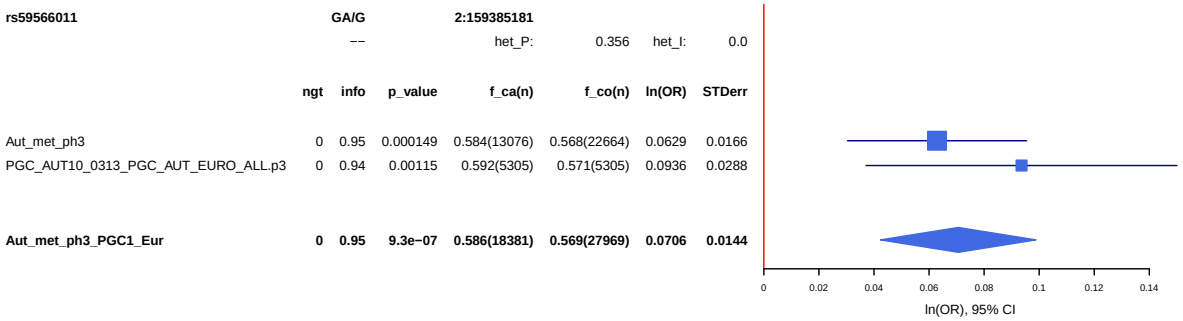

Supplementary Figure 25: Forest plot for rs59566011 for meta analysis of iPSYCH ASD GWAS (13 076 cases and 22 664 controls) and the PGC ASD GWAS (5 305 cases and 5 305 pseudo-controls). The plot shows the effect estimate with 95%-confidence interval for rs59566011 in the iPSYCH sample (Aut_met_ph3), PGC (PGC_AUT10_0313_PGC_AUT_EURO_ALL.p3) and the the inverse variance weighted meta analysis (Aut_met_ph3_PGC1_Eur).

4.1.3 Regional plots

In figures 26–44 we show the regional Manhattan plots for the top signals of the iPSYCH-PGC meta analysis.

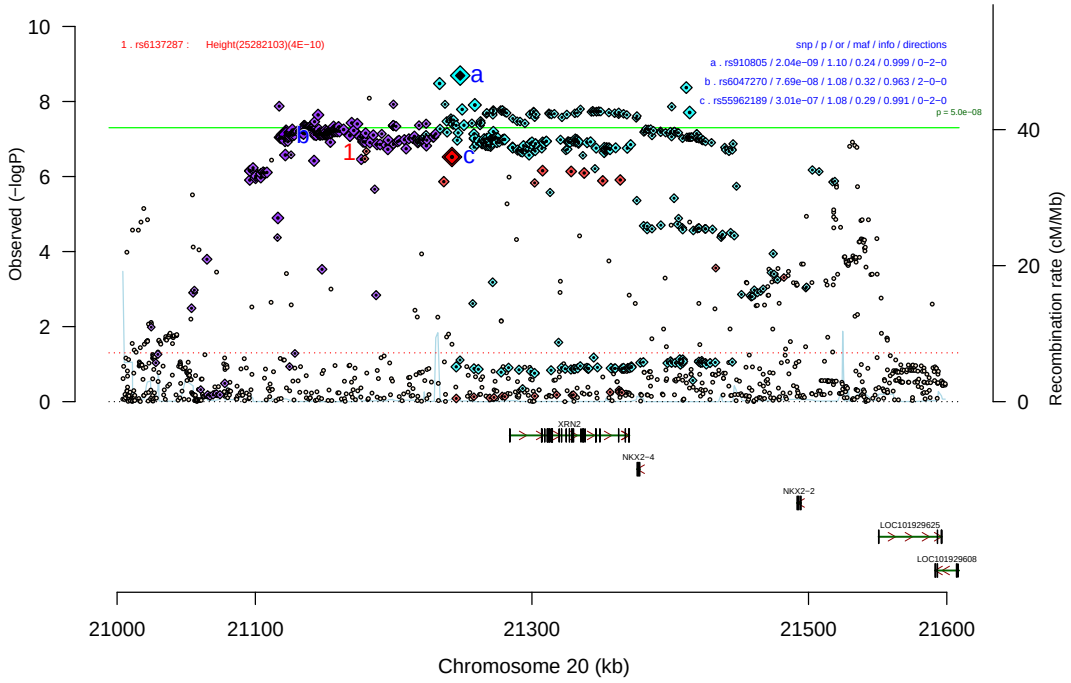

Supplementary Figure 26: Regional association plot around rs910805, rs6047270 & rs55962189 for iPSYCH-PGC meta analysis (18 381 cases and 27 969 controls). Chromosomal position is on the horizontal axis in kb, The significance of the association expressed as $-\log_{10}(\mathrm{P})$ (from z-test) is plotted vertically (left axis) and the recombination rate from HapMap is shown as light blue curve (right axis). The dot size is proportional to LD between the plotted SNP and the index SNP defining the associated region. Index SNPs are marked by diamonds and labelled with letters. As this locus contains multiple independent index SNPs, each index SNP is denoted by a different colour. LD to each index SNP is denoted by the intensity of that colour. A black centre indicates that the markers is present in the 1000 Genomes Project but not in HapMap3. The green line shows the genome-wide significance level ($5 \cdot 10^{-8}$). The upper right corner show details of the index SNPs (marker name/association p-value/odds ratio for the minor allele/minor allele frequency/imputation quality/direction of effect in the two studies (N one direction - N other direction- N missing)). Loci listed in the GWAS Catalogue for other phenotypes are shown in the upper left corner (capped at 10). The green lines in the lower half show genes (based on UCSC) with black vertical lines indicating exons. Arrow heads show the direction of transcription.

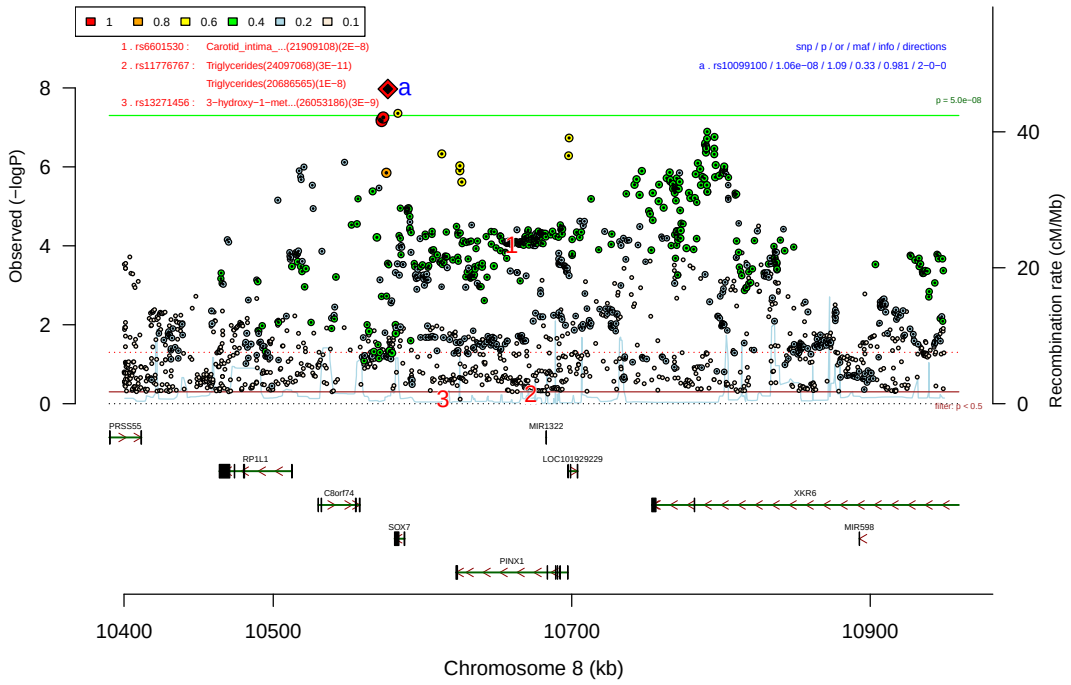

Supplementary Figure 27: Regional association plot around rs10099100 for iPSYCH-PGC meta analysis (18 381 cases and 27 969 controls). Chromosomal position is on the horizontal axis in kb, The significance of the association expressed as $-\log_{10}(P)$ (from z-test) is plotted vertically (left axis) and the recombination rate from HapMap is shown as light blue curve (right axis). The dot size is proportional to LD between the plotted SNP and the index SNP defining the associated region. Index SNPs are marked by diamonds and labelled with letters. As there is only a single index SNP in this region, colouring is based on degree of LD to that SNP as represented by r^2 (legend for r^2 is in the upper left corner). A black centre indicates that the markers is present in the 1000 Genomes Project but not in HapMap3. The green line shows the genome-wide significance level ($5 \cdot 10^{-8}$). The upper right corner show details of the index SNPs (marker name/association p-value/odds ratio for the minor allele/minor allele frequency/imputation quality/direction of effect in the two studies (N one direction - N other direction- N missing)). Loci listed in the GWAS Catalogue for other phenotypes are shown in the upper left corner (capped at 10). The green lines in the lower half show genes (based on UCSC) with black vertical lines indicating exons. Arrow heads show the direction of transcription.

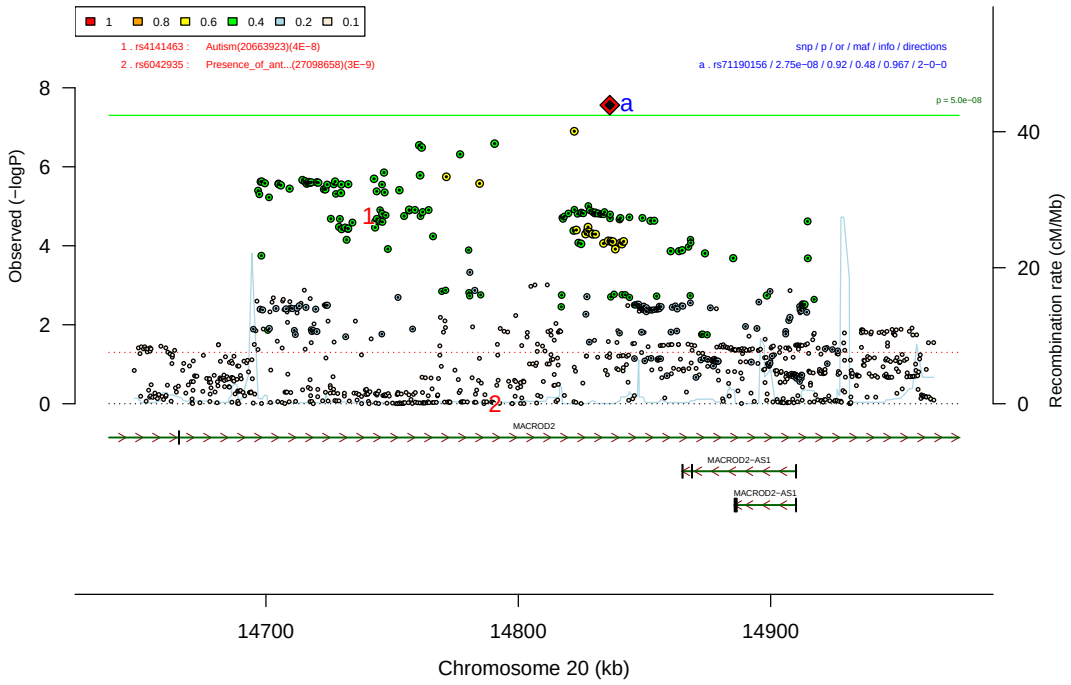

Supplementary Figure 28: Regional association plot around rs71190156 for iPSYCH-PGC meta analysis (18 381 cases and 27 969 controls). Chromosomal position is on the horizontal axis in kb, The significance of the association expressed as $-\log_{10}(\mathrm{P})$ (from z-test) is plotted vertically (left axis) and the recombination rate from HapMap is shown as light blue curve (right axis). The dot size is proportional to LD between the plotted SNP and the index SNP defining the associated region. Index SNPs are marked by diamonds and labelled with letters. As there is only a single index SNP in this region, colouring is based on degree of LD to that SNP as represented by r^2 (legend for r^2 is in the upper left corner). A black centre indicates that the markers is present in the 1000 Genomes Project but not in HapMap3. The green line shows the genome-wide significance level ($5 \cdot 10^{-8}$). The upper right corner show details of the index SNPs (marker name/association p-value/odds ratio for the minor allele/minor allele frequency/imputation quality/direction of effect in the two studies (N one direction - N other direction- N missing)). Loci listed in the GWAS Catalogue for other phenotypes are shown in the upper left corner (capped at 10). The green lines in the lower half show genes (based on UCSC) with black vertical lines indicating exons. Arrow heads show the direction of transcription.

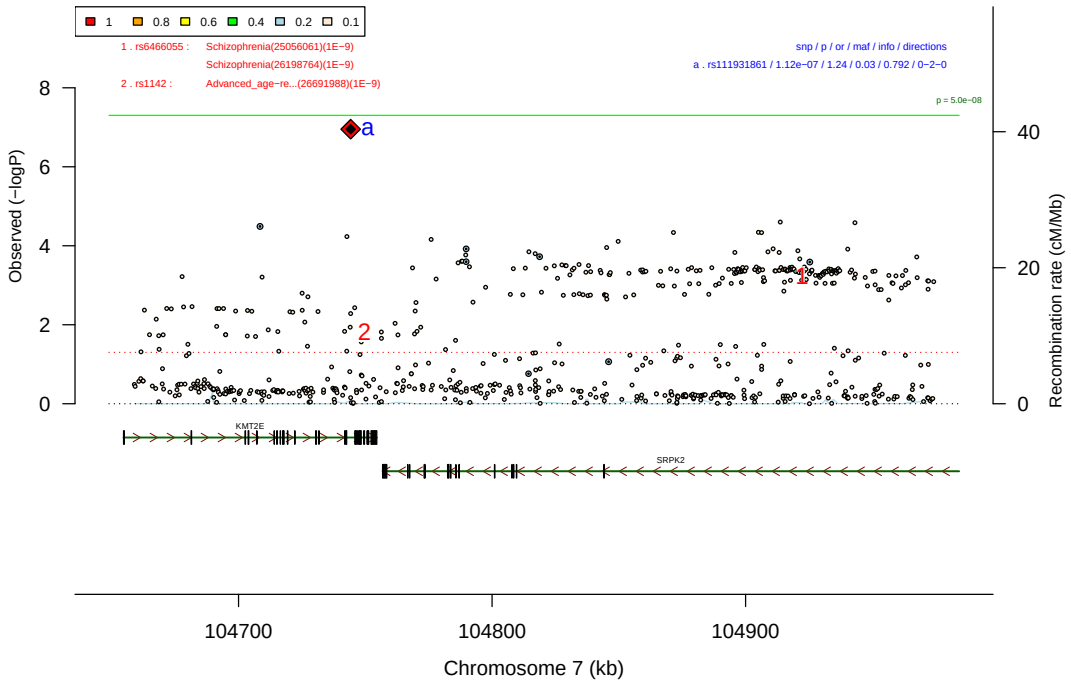

Supplementary Figure 29: Regional association plot around rs111931861 for iPSYCH-PGC meta analysis (18 381 cases and 27 969 controls). Chromosomal position is on the horizontal axis in kb, The significance of the association expressed as $-\log_{10}(P)$ (from z-test) is plotted vertically (left axis) and the recombination rate from HapMap is shown as light blue curve (right axis). The dot size is proportional to LD between the plotted SNP and the index SNP defining the associated region. Index SNPs are marked by diamonds and labelled with letters. As there is only a single index SNP in this region, colouring is based on degree of LD to that SNP as represented by r^2 (legend for r^2 is in the upper left corner). A black centre indicates that the markers is present in the 1000 Genomes Project but not in HapMap3. The green line shows the genome-wide significance level ($5 \cdot 10^{-8}$). The upper right corner show details of the index SNPs (marker name/association p-value/odds ratio for the minor allele/minor allele frequency/imputation quality/direction of effect in the two studies (N one direction - N other direction- N missing)). Loci listed in the GWAS Catalogue for other phenotypes are shown in the upper left corner (capped at 10). The green lines in the lower half show genes (based on UCSC) with black vertical lines indicating exons. Arrow heads show the direction of transcription.

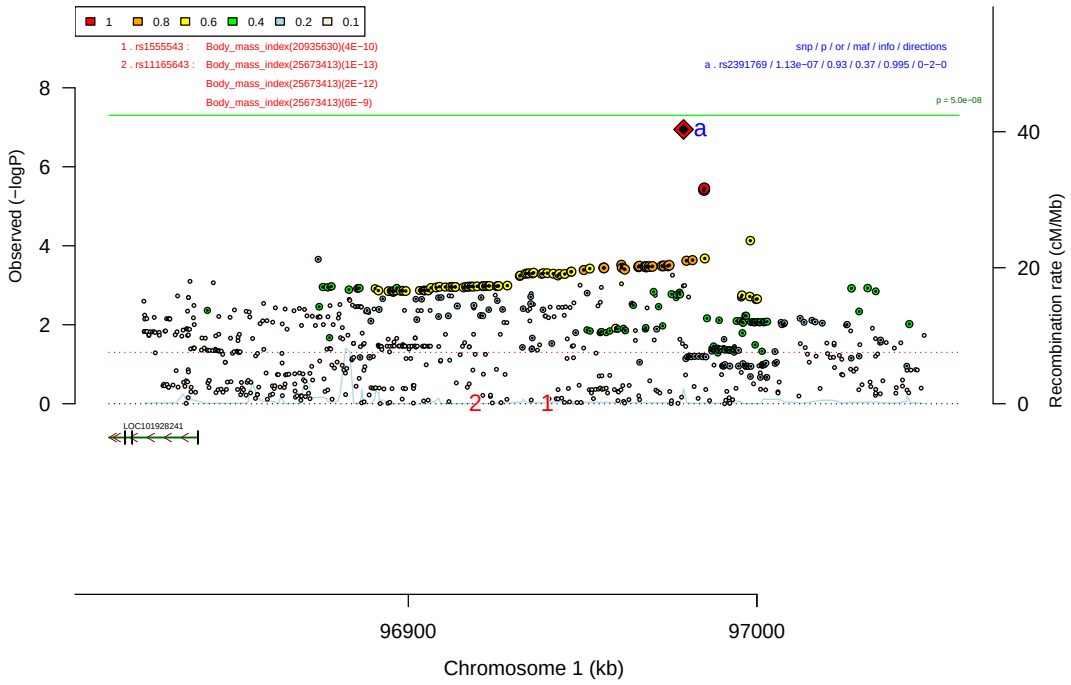

Supplementary Figure 30: Regional association plot around rs2391769 for iPSYCH-PGC meta analysis (18 381 cases and 27 969 controls). Chromosomal position is on the horizontal axis in kb, The significance of the association expressed as $-\log_{10}(P)$ (from z-test) is plotted vertically (left axis) and the recombination rate from HapMap is shown as light blue curve (right axis). The dot size is proportional to LD between the plotted SNP and the index SNP defining the associated region. Index SNPs are marked by diamonds and labelled with letters. As there is only a single index SNP in this region, colouring is based on degree of LD to that SNP as represented by r^2 (legend for r^2 is in the upper left corner). A black centre indicates that the markers is present in the 1000 Genomes Project but not in HapMap3. The green line shows the genome-wide significance level ($5 \cdot 10^{-8}$). The upper right corner show details of the index SNPs (marker name/association p-value/odds ratio for the minor allele/minor allele frequency/imputation quality/direction of effect in the two studies (N one direction - N other direction- N missing)). Loci listed in the GWAS Catalogue for other phenotypes are shown in the upper left corner (capped at 10). The green lines in the lower half show genes (based on UCSC) with black vertical lines indicating exons. Arrow heads show the direction of transcription.

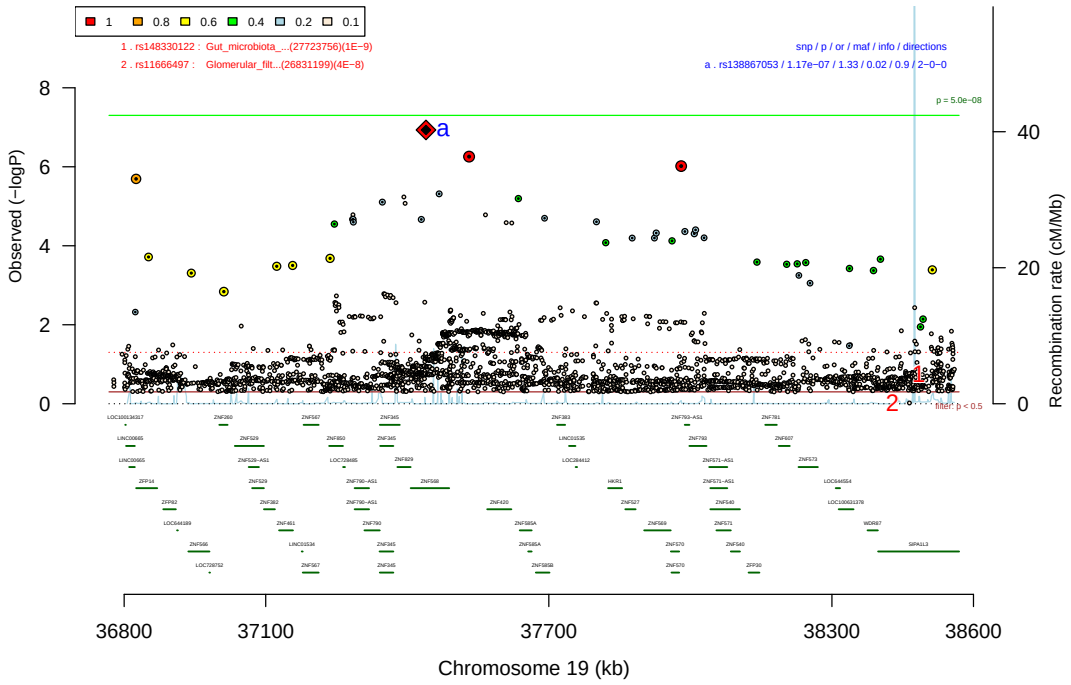

Supplementary Figure 31: Regional association plot around rs138867053 for iPSYCH-PGC meta analysis (18 381 cases and 27 969 controls). Chromosomal position is on the horizontal axis in kb, The significance of the association expressed as $-\log_{10}(P)$ (from z-test) is plotted vertically (left axis) and the recombination rate from HapMap is shown as light blue curve (right axis). The dot size is proportional to LD between the plotted SNP and the index SNP defining the associated region. Index SNPs are marked by diamonds and labelled with letters. As there is only a single index SNP in this region, colouring is based on degree of LD to that SNP as represented by r^2 (legend for r^2 is in the upper left corner). A black centre indicates that the markers is present in the 1000 Genomes Project but not in HapMap3. The green line shows the genome-wide significance level ($5 \cdot 10^{-8}$). The upper right corner show details of the index SNPs (marker name/association p-value/odds ratio for the minor allele/minor allele frequency/imputation quality/direction of effect in the two studies (N one direction - N other direction- N missing)). Loci listed in the GWAS Catalogue for other phenotypes are shown in the upper left corner (capped at 10). The green lines in the lower half show genes (based on UCSC) with black vertical lines indicating exons. Arrow heads show the direction of transcription.

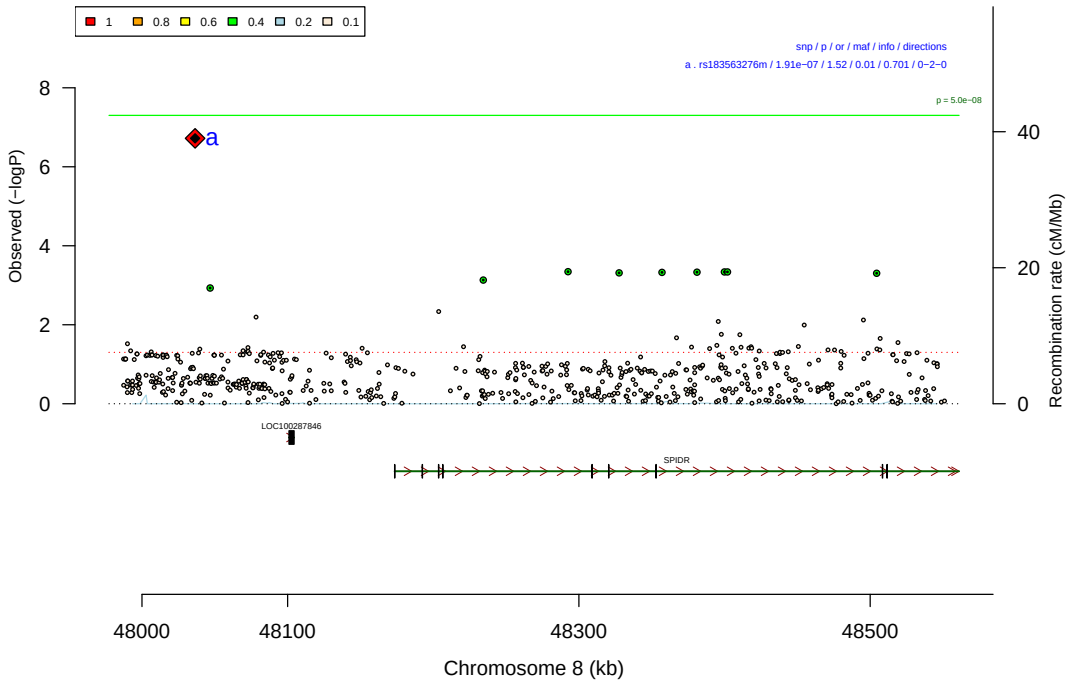

Supplementary Figure 32: Regional association plot around rs183563276m for iPSYCH-PGC meta analysis (18 381 cases and 27 969 controls). Chromosomal position is on the horizontal axis in kb, The significance of the association expressed as $-\log_{10}(P)$ (from z-test) is plotted vertically (left axis) and the recombination rate from HapMap is shown as light blue curve (right axis). The dot size is proportional to LD between the plotted SNP and the index SNP defining the associated region. Index SNPs are marked by diamonds and labelled with letters. As there is only a single index SNP in this region, colouring is based on degree of LD to that SNP as represented by r^2 (legend for r^2 is in the upper left corner). A black centre indicates that the markers is present in the 1000 Genomes Project but not in HapMap3. The green line shows the genome-wide significance level ($5 \cdot 10^{-8}$). The upper right corner show details of the index SNPs (marker name/association p-value/odds ratio for the minor allele/minor allele frequency/imputation quality/direction of effect in the two studies (N one direction - N other direction- N missing)). The green lines in the lower half show genes (based on UCSC) with black vertical lines indicating exons. Arrow heads show the direction of transcription.

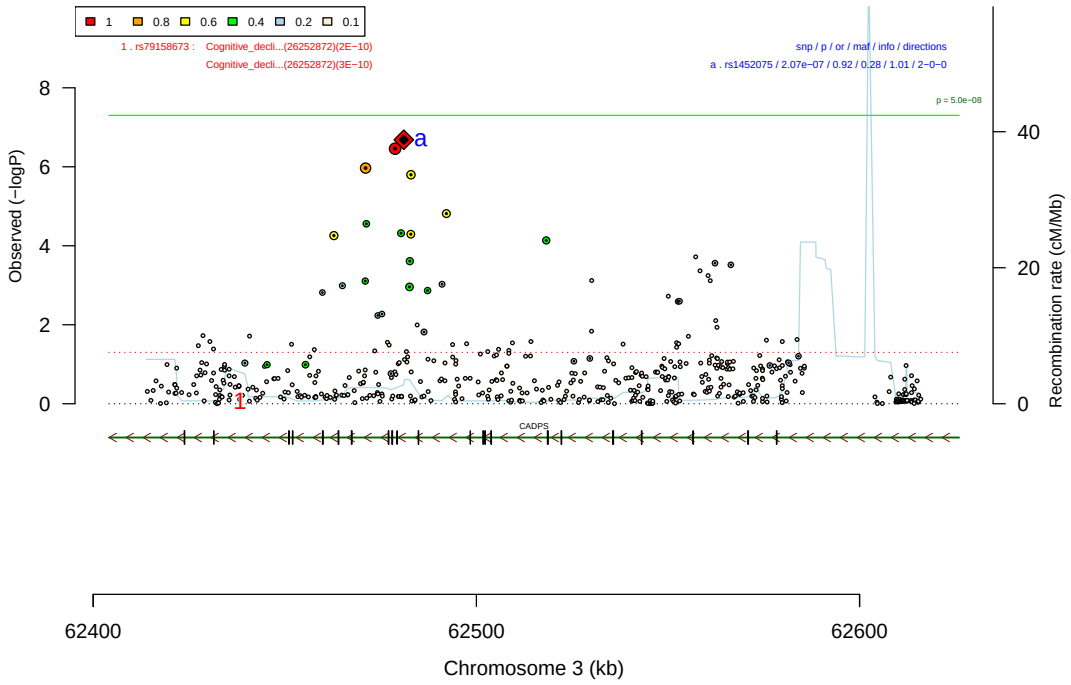

Supplementary Figure 33: Regional association plot around rs1452075 for iPSYCH-PGC meta analysis (18 381 cases and 27 969 controls). Chromosomal position is on the horizontal axis in kb, The significance of the association expressed as $-\log_{10}(\mathrm{P})$ (from z-test) is plotted vertically (left axis) and the recombination rate from HapMap is shown as light blue curve (right axis). The dot size is proportional to LD between the plotted SNP and the index SNP defining the associated region. Index SNPs are marked by diamonds and labelled with letters. As there is only a single index SNP in this region, colouring is based on degree of LD to that SNP as represented by r^2 (legend for r^2 is in the upper left corner). A black centre indicates that the markers is present in the 1000 Genomes Project but not in HapMap3. The green line shows the genome-wide significance level ($5 \cdot 10^{-8}$). The upper right corner show details of the index SNPs (marker name/association p-value/odds ratio for the minor allele/minor allele frequency/imputation quality/direction of effect in the two studies (N one direction - N other direction- N missing)). Loci listed in the GWAS Catalogue for other phenotypes are shown in the upper left corner (capped at 10). The green lines in the lower half show genes (based on UCSC) with black vertical lines indicating exons. Arrow heads show the direction of transcription.

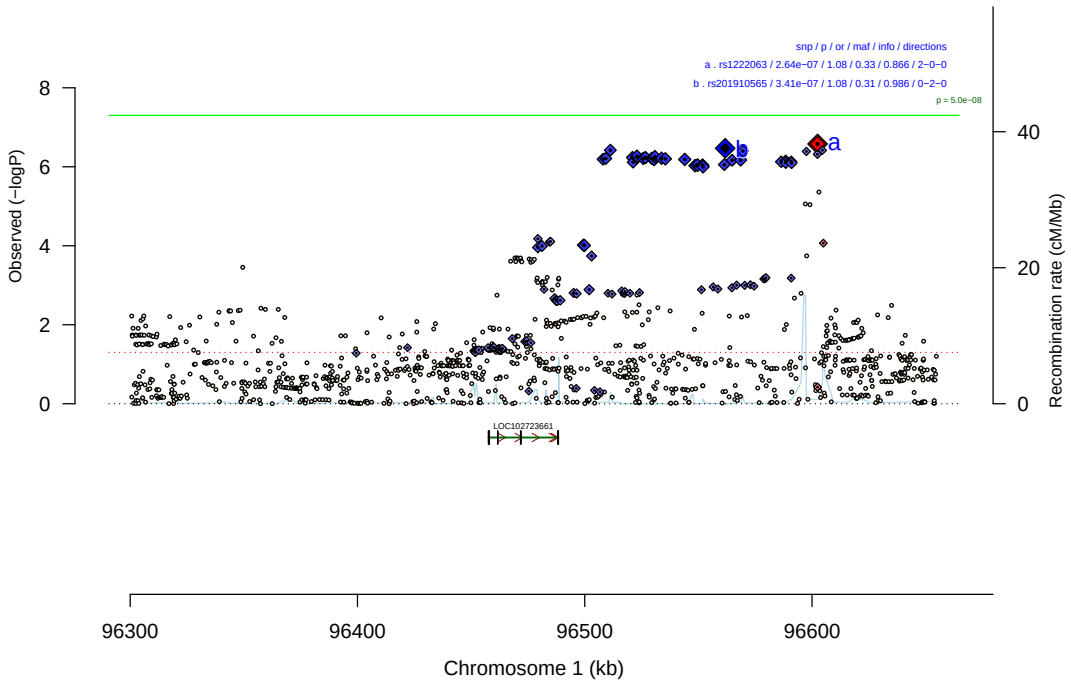

Supplementary Figure 34: Regional association plot around rs1222063 & rs201910565 for iPSYCH-PGC meta analysis (18 381 cases and 27 969 controls). Chromosomal position is on the horizontal axis in kb, The significance of the association expressed as $-\log_{10}(P)$ (from z-test) is plotted vertically (left axis) and the recombination rate from HapMap is shown as light blue curve (right axis). The dot size is proportional to LD between the plotted SNP and the index SNP defining the associated region. Index SNPs are marked by diamonds and labelled with letters. As this locus contains multiple independent index SNPs, each index SNP is denoted by a different colour. LD to each index SNP is denoted by the intensity of that colour. A black centre indicates that the markers is present in the 1000 Genomes Project but not in HapMap3. The green line shows the genome-wide significance level ($5 \cdot 10^{-8}$). The upper right corner show details of the index SNPs (marker name/association p-value/odds ratio for the minor allele/minor allele frequency/imputation quality/direction of effect in the two studies (N one direction - N other direction- N missing)). The green lines in the lower half show genes (based on UCSC) with black vertical lines indicating exons. Arrow heads show the direction of transcription.

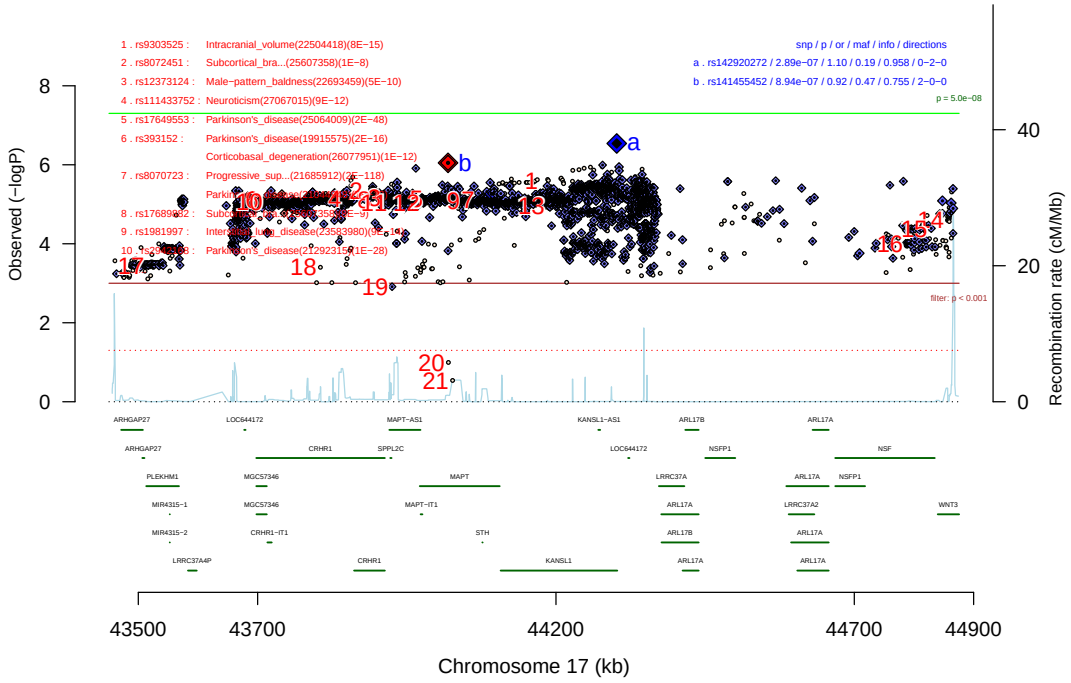

Supplementary Figure 35: Regional association plot around rs142920272 & rs141455452 for iPSYCH-PGC meta analysis (18 381 cases and 27 969 controls). Chromosomal position is on the horizontal axis in kb, The significance of the association expressed as $-\log_{10}(P)$ (from z-test) is plotted vertically (left axis) and the recombination rate from HapMap is shown as light blue curve (right axis). The dot size is proportional to LD between the plotted SNP and the index SNP defining the associated region. Index SNPs are marked by diamonds and labelled with letters. As this locus contains multiple independent index SNPs, each index SNP is denoted by a different colour. LD to each index SNP is denoted by the intensity of that colour. A black centre indicates that the markers is present in the 1000 Genomes Project but not in HapMap3. The green line shows the genome-wide significance level ($5 \cdot 10^{-8}$). The upper right corner show details of the index SNPs (marker name/association p-value/odds ratio for the minor allele/minor allele frequency/imputation quality/direction of effect in the two studies (N one direction - N other direction- N missing)). Loci listed in the GWAS Catalogue for other phenotypes are shown in the upper left corner (capped at 10). The green lines in the lower half show genes (based on UCSC) with black vertical lines indicating exons. Arrow heads show the direction of transcription.

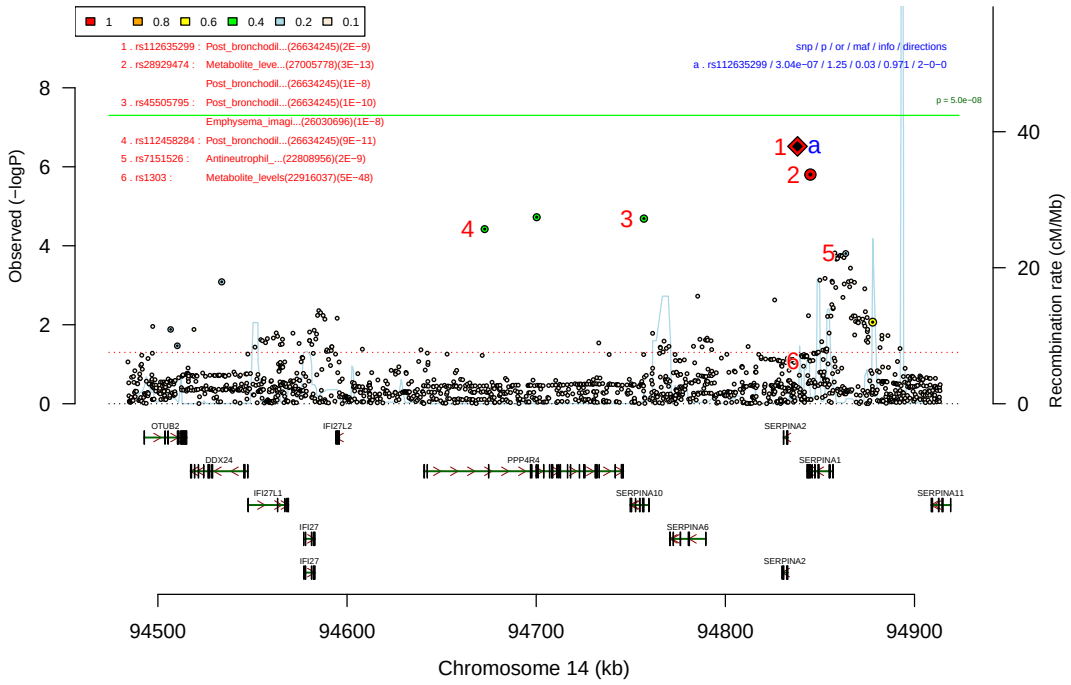

Supplementary Figure 36: Regional association plot around rs112635299 for iPSYCH-PGC meta analysis (18 381 cases and 27 969 controls). Chromosomal position is on the horizontal axis in kb, The significance of the association expressed as $-\log_{10}(P)$ (from z-test) is plotted vertically (left axis) and the recombination rate from HapMap is shown as light blue curve (right axis). The dot size is proportional to LD between the plotted SNP and the index SNP defining the associated region. Index SNPs are marked by diamonds and labelled with letters. As there is only a single index SNP in this region, colouring is based on degree of LD to that SNP as represented by r^2 (legend for r^2 is in the upper left corner). A black centre indicates that the markers is present in the 1000 Genomes Project but not in HapMap3. The green line shows the genome-wide significance level ($5 \cdot 10^{-8}$). The upper right corner show details of the index SNPs (marker name/association p-value/odds ratio for the minor allele/minor allele frequency/imputation quality/direction of effect in the two studies (N one direction - N other direction- N missing)). Loci listed in the GWAS Catalogue for other phenotypes are shown in the upper left corner (capped at 10). The green lines in the lower half show genes (based on UCSC) with black vertical lines indicating exons. Arrow heads show the direction of transcription.

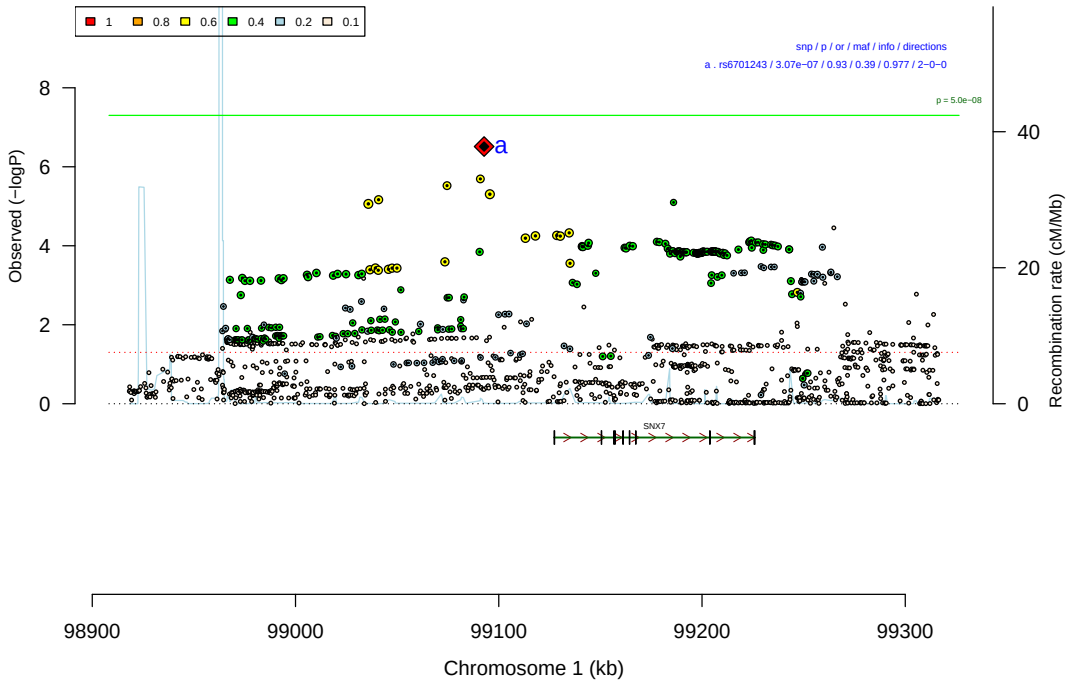

Supplementary Figure 37: Regional association plot around rs6701243 for iPSYCH-PGC meta analysis (18 381 cases and 27 969 controls). Chromosomal position is on the horizontal axis in kb, The significance of the association expressed as $-\log_{10}(P)$ (from z-test) is plotted vertically (left axis) and the recombination rate from HapMap is shown as light blue curve (right axis). The dot size is proportional to LD between the plotted SNP and the index SNP defining the associated region. Index SNPs are marked by diamonds and labelled with letters. As there is only a single index SNP in this region, colouring is based on degree of LD to that SNP as represented by r^2 (legend for r^2 is in the upper left corner). A black centre indicates that the markers is present in the 1000 Genomes Project but not in HapMap3. The green line shows the genome-wide significance level ($5 \cdot 10^{-8}$). The upper right corner show details of the index SNPs (marker name/association p-value/odds ratio for the minor allele/minor allele frequency/imputation quality/direction of effect in the two studies (N one direction - N other direction- N missing)). The green lines in the lower half show genes (based on UCSC) with black vertical lines indicating exons. Arrow heads show the direction of transcription.

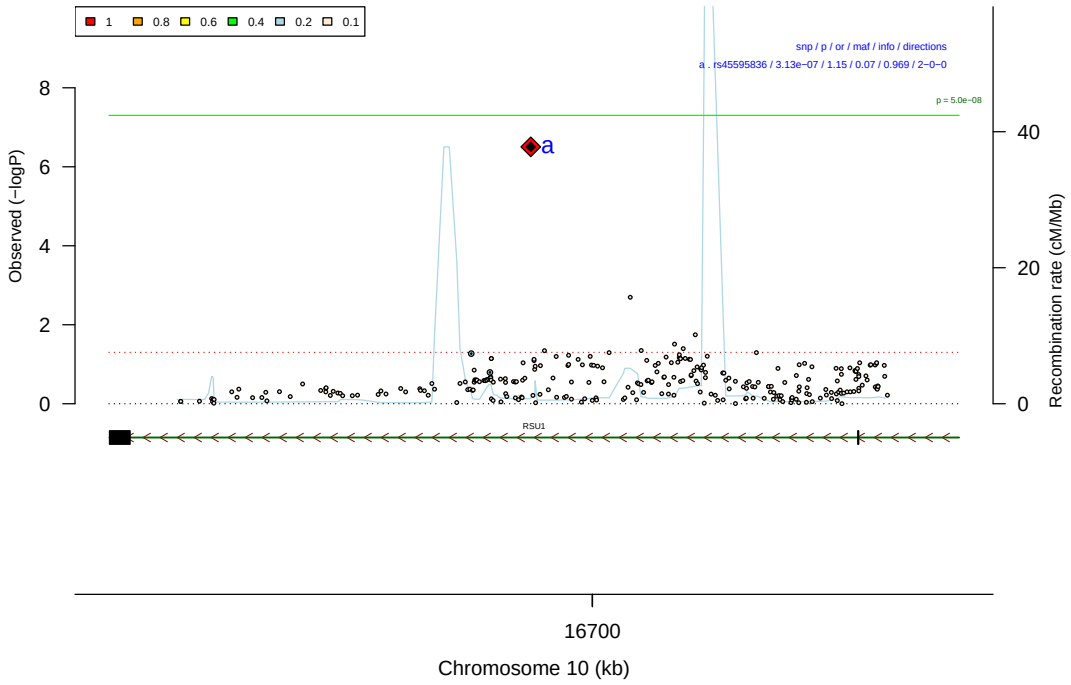

Supplementary Figure 38: Regional association plot around rs45595836 for iPSYCH-PGC meta analysis (18 381 cases and 27 969 controls). Chromosomal position is on the horizontal axis in kb, The significance of the association expressed as $-\log_{10}(P)$ (from z-test) is plotted vertically (left axis) and the recombination rate from HapMap is shown as light blue curve (right axis). The dot size is proportional to LD between the plotted SNP and the index SNP defining the associated region. Index SNPs are marked by diamonds and labelled with letters. As there is only a single index SNP in this region, colouring is based on degree of LD to that SNP as represented by r^2 (legend for r^2 is in the upper left corner). A black centre indicates that the markers is present in the 1000 Genomes Project but not in HapMap3. The green line shows the genome-wide significance level ($5 \cdot 10^{-8}$). The upper right corner show details of the index SNPs (marker name/association p-value/odds ratio for the minor allele/minor allele frequency/imputation quality/direction of effect in the two studies (N one direction - N other direction- N missing)). The green lines in the lower half show genes (based on UCSC) with black vertical lines indicating exons. Arrow heads show the direction of transcription.

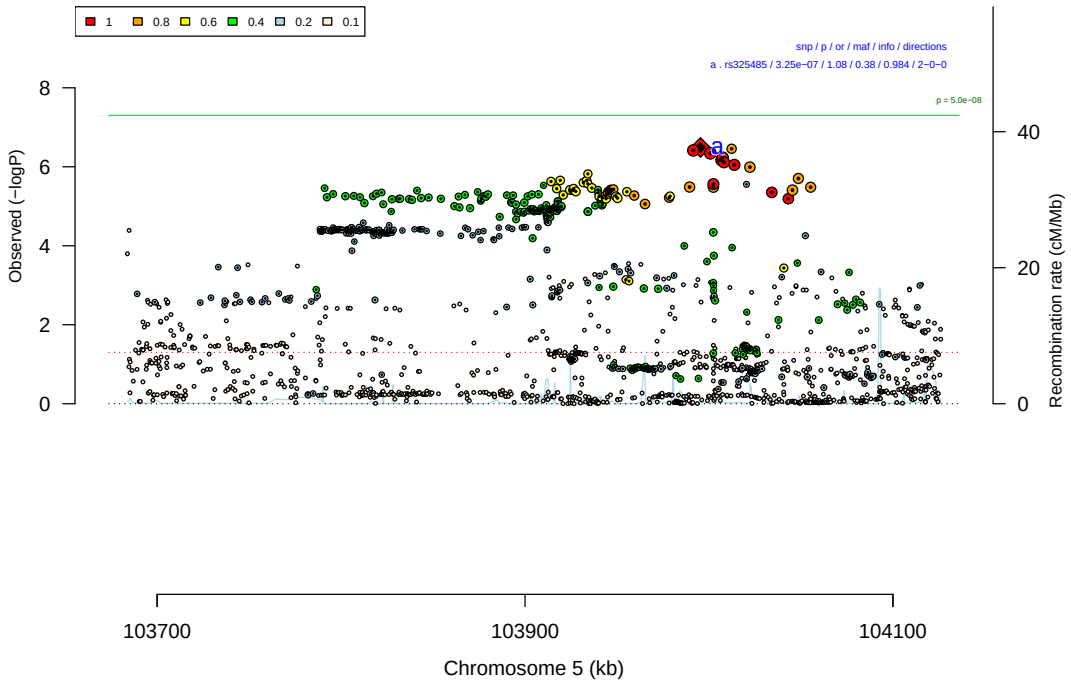

Supplementary Figure 39: Regional association plot around rs325485 for iPSYCH-PGC meta analysis (18 381 cases and 27 969 controls). Chromosomal position is on the horizontal axis in kb, The significance of the association expressed as $-\log_{10}(P)$ (from z-test) is plotted vertically (left axis) and the recombination rate from HapMap is shown as light blue curve (right axis). The dot size is proportional to LD between the plotted SNP and the index SNP defining the associated region. Index SNPs are marked by diamonds and labelled with letters. As there is only a single index SNP in this region, colouring is based on degree of LD to that SNP as represented by r^2 (legend for r^2 is in the upper left corner). A black centre indicates that the markers is present in the 1000 Genomes Project but not in HapMap3. The green line shows the genome-wide significance level ($5 \cdot 10^{-8}$). The upper right corner show details of the index SNPs (marker name/association p-value/odds ratio for the minor allele/minor allele frequency/imputation quality/direction of effect in the two studies (N one direction - N other direction- N missing)).

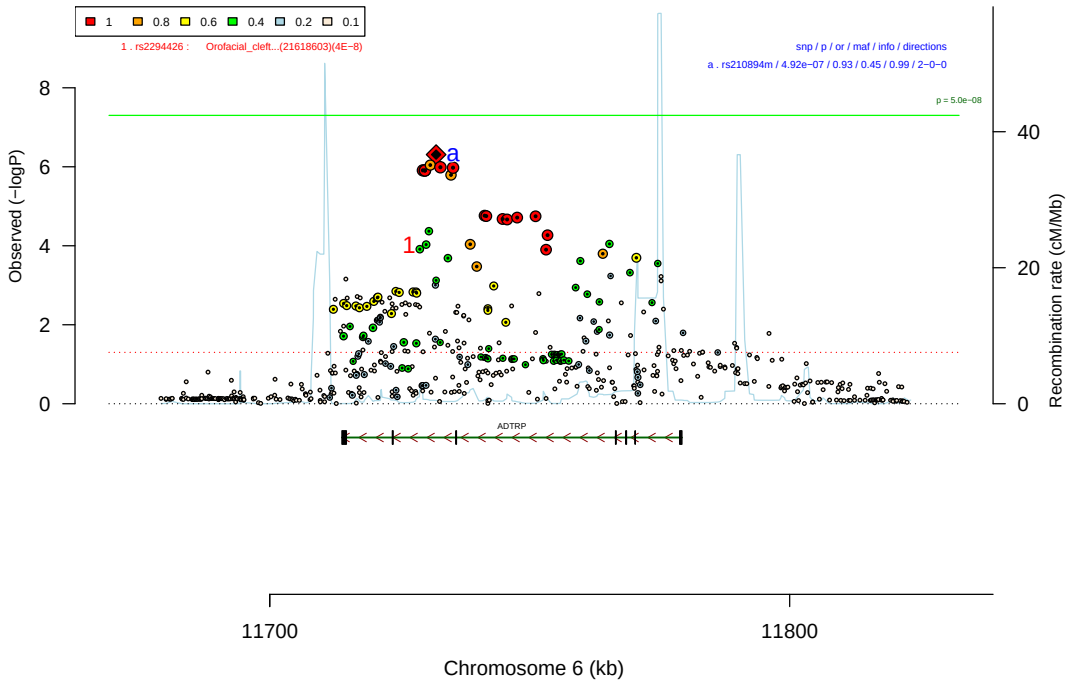

Supplementary Figure 40: Regional association plot around rs210894m for iPSYCH-PGC meta analysis (18 381 cases and 27 969 controls). Chromosomal position is on the horizontal axis in kb, The significance of the association expressed as $-\log_{10}(P)$ (from z-test) is plotted vertically (left axis) and the recombination rate from HapMap is shown as light blue curve (right axis). The dot size is proportional to LD between the plotted SNP and the index SNP defining the associated region. Index SNPs are marked by diamonds and labelled with letters. As there is only a single index SNP in this region, colouring is based on degree of LD to that SNP as represented by r^2 (legend for r^2 is in the upper left corner). A black centre indicates that the markers is present in the 1000 Genomes Project but not in HapMap3. The green line shows the genome-wide significance level ($5 \cdot 10^{-8}$). The upper right corner show details of the index SNPs (marker name/association p-value/odds ratio for the minor allele/minor allele frequency/imputation quality/direction of effect in the two studies (N one direction - N other direction- N missing)). Loci listed in the GWAS Catalogue for other phenotypes are shown in the upper left corner (capped at 10). The green lines in the lower half show genes (based on UCSC) with black vertical lines indicating exons. Arrow heads show the direction of transcription.

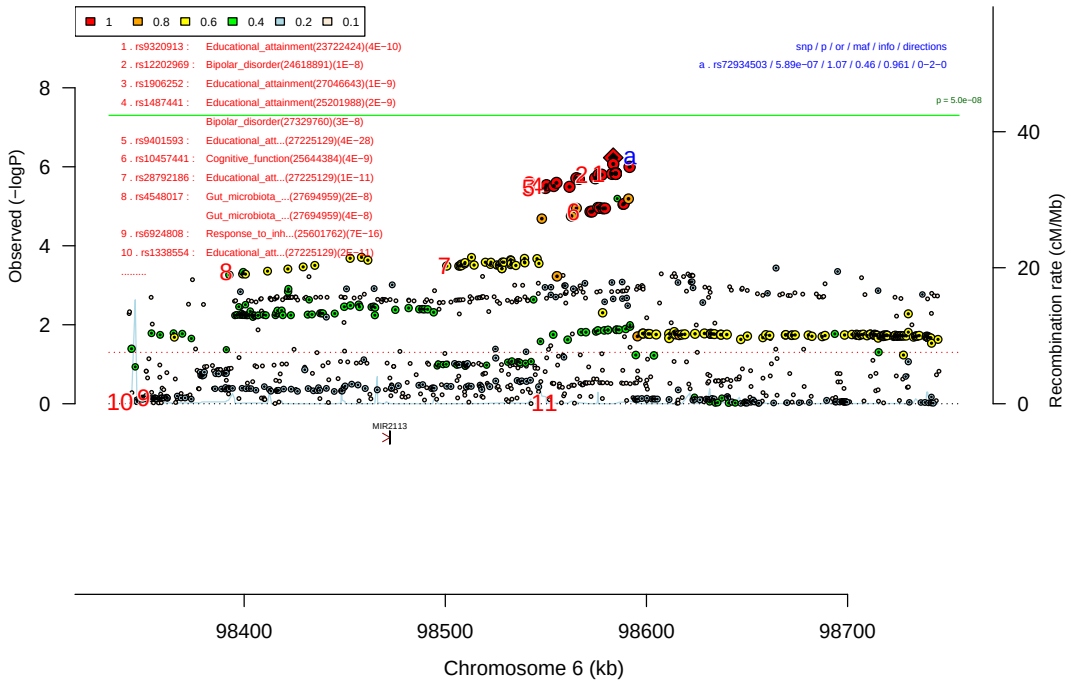

Supplementary Figure 41: Regional association plot around rs72934503 for iPSYCH-PGC meta analysis (18 381 cases and 27 969 controls). Chromosomal position is on the horizontal axis in kb, The significance of the association expressed as $-\log_{10}(P)$ (from z-test) is plotted vertically (left axis) and the recombination rate from HapMap is shown as light blue curve (right axis). The dot size is proportional to LD between the plotted SNP and the index SNP defining the associated region. Index SNPs are marked by diamonds and labelled with letters. As there is only a single index SNP in this region, colouring is based on degree of LD to that SNP as represented by r^2 (legend for r^2 is in the upper left corner). A black centre indicates that the markers is present in the 1000 Genomes Project but not in HapMap3. The green line shows the genome-wide significance level ($5 \cdot 10^{-8}$). The upper right corner show details of the index SNPs (marker name/association p-value/odds ratio for the minor allele/minor allele frequency/imputation quality/direction of effect in the two studies (N one direction - N other direction- N missing)). Loci listed in the GWAS Catalogue for other phenotypes are shown in the upper left corner (capped at 10). The green lines in the lower half show genes (based on UCSC) with black vertical lines indicating exons. Arrow heads show the direction of transcription.

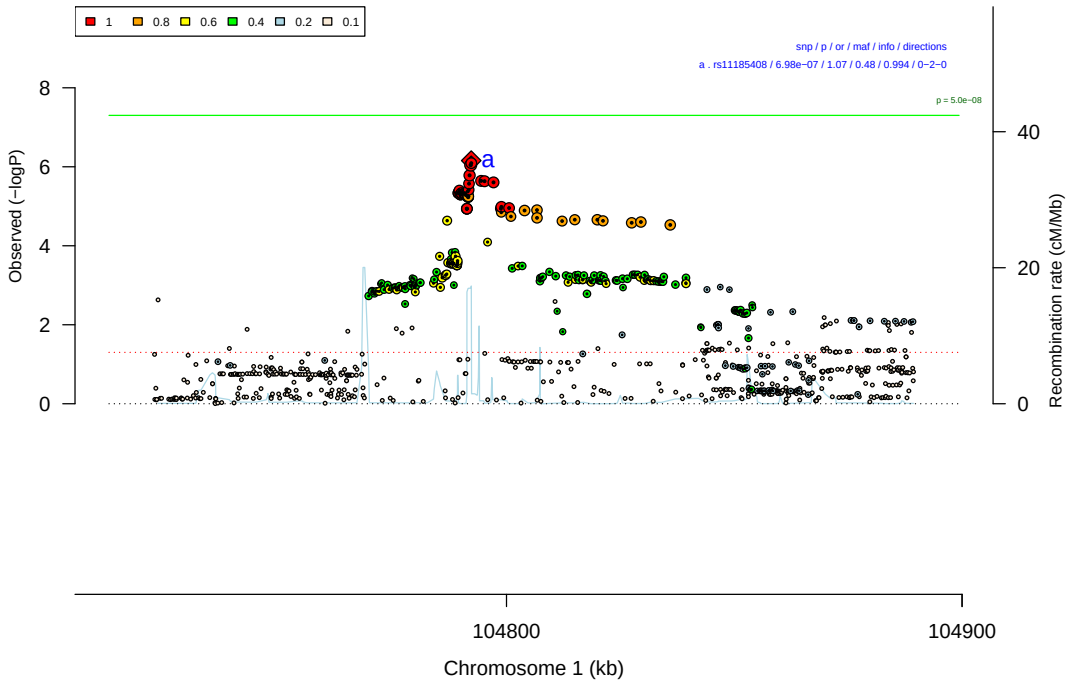

Supplementary Figure 42: Regional association plot around rs11185408 for iPSYCH-PGC meta analysis (18 381 cases and 27 969 controls). Chromosomal position is on the horizontal axis in kb, The significance of the association expressed as $-\log_{10}(P)$ (from z-test) is plotted vertically (left axis) and the recombination rate from HapMap is shown as light blue curve (right axis). The dot size is proportional to LD between the plotted SNP and the index SNP defining the associated region. Index SNPs are marked by diamonds and labelled with letters. As there is only a single index SNP in this region, colouring is based on degree of LD to that SNP as represented by r^2 (legend for r^2 is in the upper left corner). A black centre indicates that the markers is present in the 1000 Genomes Project but not in HapMap3. The green line shows the genome-wide significance level ($5 \cdot 10^{-8}$). The upper right corner show details of the index SNPs (marker name/association p-value/odds ratio for the minor allele/minor allele frequency/imputation quality/direction of effect in the two studies (N one direction - N other direction- N missing)).

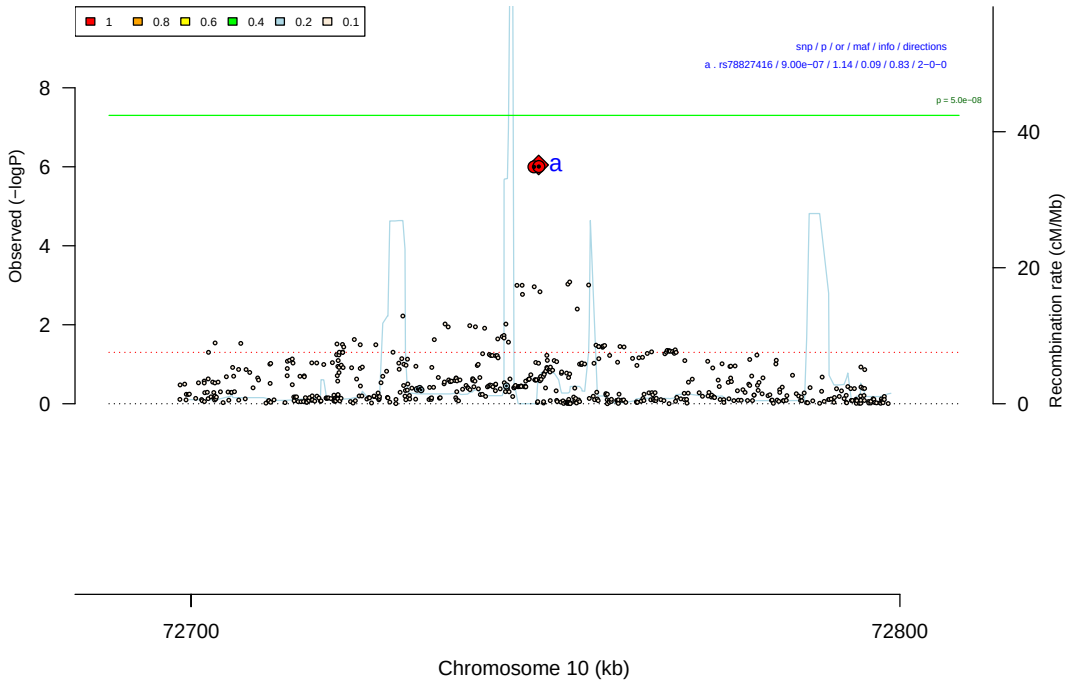

Supplementary Figure 43: Regional association plot around rs78827416 for iPSYCH-PGC meta analysis (18 381 cases and 27 969 controls). Chromosomal position is on the horizontal axis in kb, The significance of the association expressed as $-\log_{10}(P)$ (from z-test) is plotted vertically (left axis) and the recombination rate from HapMap is shown as light blue curve (right axis). The dot size is proportional to LD between the plotted SNP and the index SNP defining the associated region. Index SNPs are marked by diamonds and labelled with letters. As there is only a single index SNP in this region, colouring is based on degree of LD to that SNP as represented by r^2 (legend for r^2 is in the upper left corner). A black centre indicates that the markers is present in the 1000 Genomes Project but not in HapMap3. The green line shows the genome-wide significance level ($5 \cdot 10^{-8}$). The upper right corner show details of the index SNPs (marker name/association p-value/odds ratio for the minor allele/minor allele frequency/imputation quality/direction of effect in the two studies (N one direction - N other direction- N missing)).

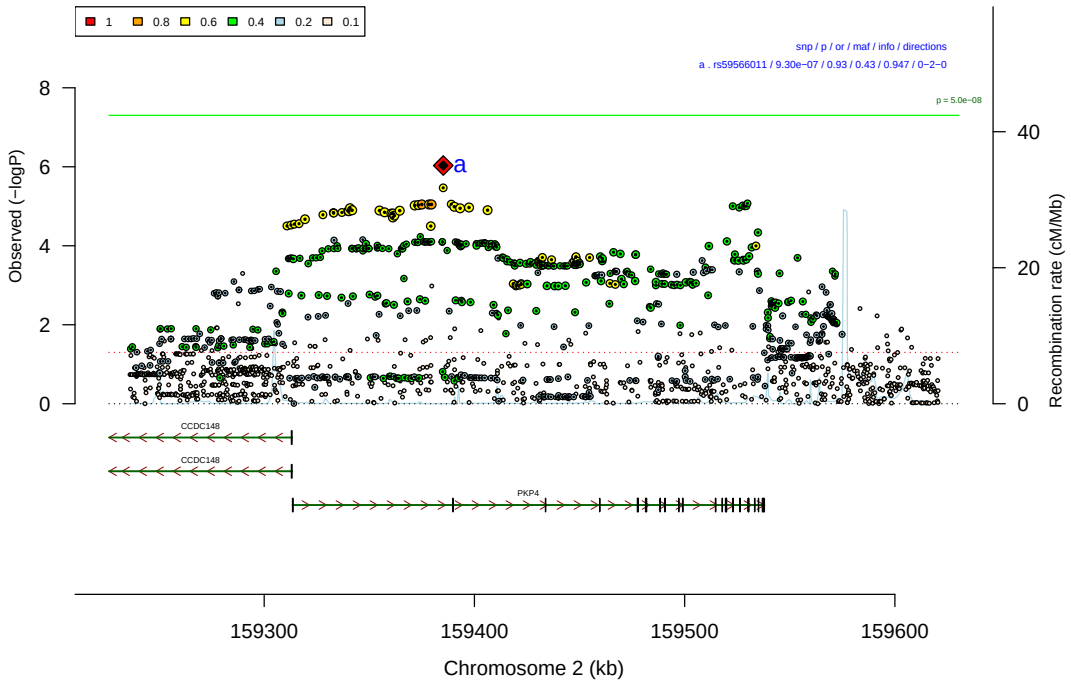

Supplementary Figure 44: Regional association plot around rs59566011 for iPSYCH-PGC meta analysis (18 381 cases and 27 969 controls). Chromosomal position is on the horizontal axis in kb, The significance of the association expressed as $-\log_{10}(P)$ (from z-test) is plotted vertically (left axis) and the recombination rate from HapMap is shown as light blue curve (right axis). The dot size is proportional to LD between the plotted SNP and the index SNP defining the associated region. Index SNPs are marked by diamonds and labelled with letters. As there is only a single index SNP in this region, colouring is based on degree of LD to that SNP as represented by r^2 (legend for r^2 is in the upper left corner). A black centre indicates that the markers is present in the 1000 Genomes Project but not in HapMap3. The green line shows the genome-wide significance level ($5 \cdot 10^{-8}$). The upper right corner show details of the index SNPs (marker name/association p-value/odds ratio for the minor allele/minor allele frequency/imputation quality/direction of effect in the two studies (N one direction - N other direction- N missing)). The green lines in the lower half show genes (based on UCSC) with black vertical lines indicating exons. Arrow heads show the direction of transcription.

4.1.4 MTAG analyses

In this section we show the full size version of the Manhattan plots drawn as sub-panels in figure 1 of the main manuscript, Figures 45–48, and regional plots of the 7 top loci, Figures 49–55. Each Manhattan plot is drawn on a background of a composite analysis corresponding to the minimal p-value at each marker achieved in each of the analyses main scan (iPSYCH+PGC), meta-analysis with replication sample, MTAG with schizophrenia[8], MTAG with educational attainment[50], and MTAG of major depression[48]. The regional plot are arranged with three panels showing the local plots for the input GWAS of ASD and the scondary phenotype as well as the resulting MTAG analysis.

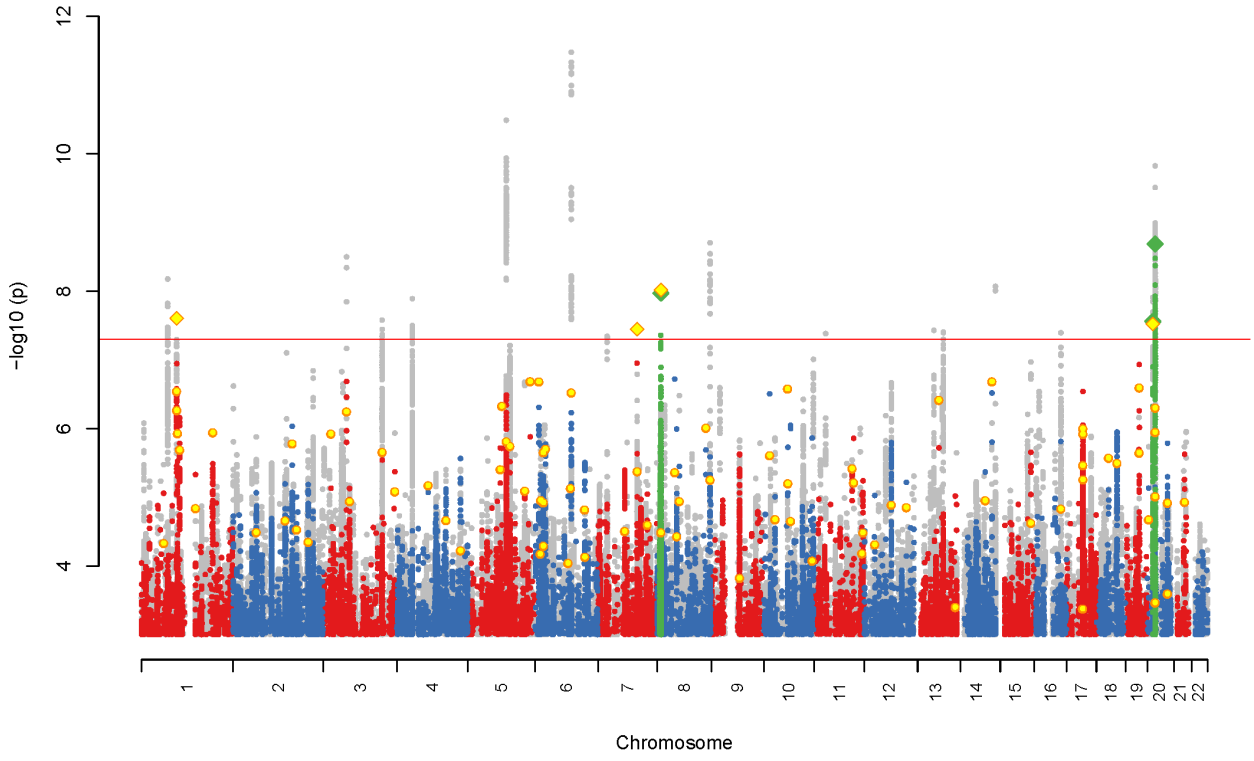

Supplementary Figure 45: Manhattan plot of ASD GWAS (18,381 cases and 27,969 controls) on composite MTAG background. The x axis shows genomic position (chromosomes 1–22) and the y axis the statistical significance as –log10 (P) of z statistics. Yellow marks show results from the meta-analysis with the follow-up samples (2,119 cases and 142,379 controls). Diamonds indicate the index SNP of genome wide significant clumps (at $5 \cdot 10^{-8}$) and genome wide significant clumps are painted green. The grey MTAG composit consists of the maximum at each locus of the results from the main scan, combined with follow-up, and three MTAG analyses.

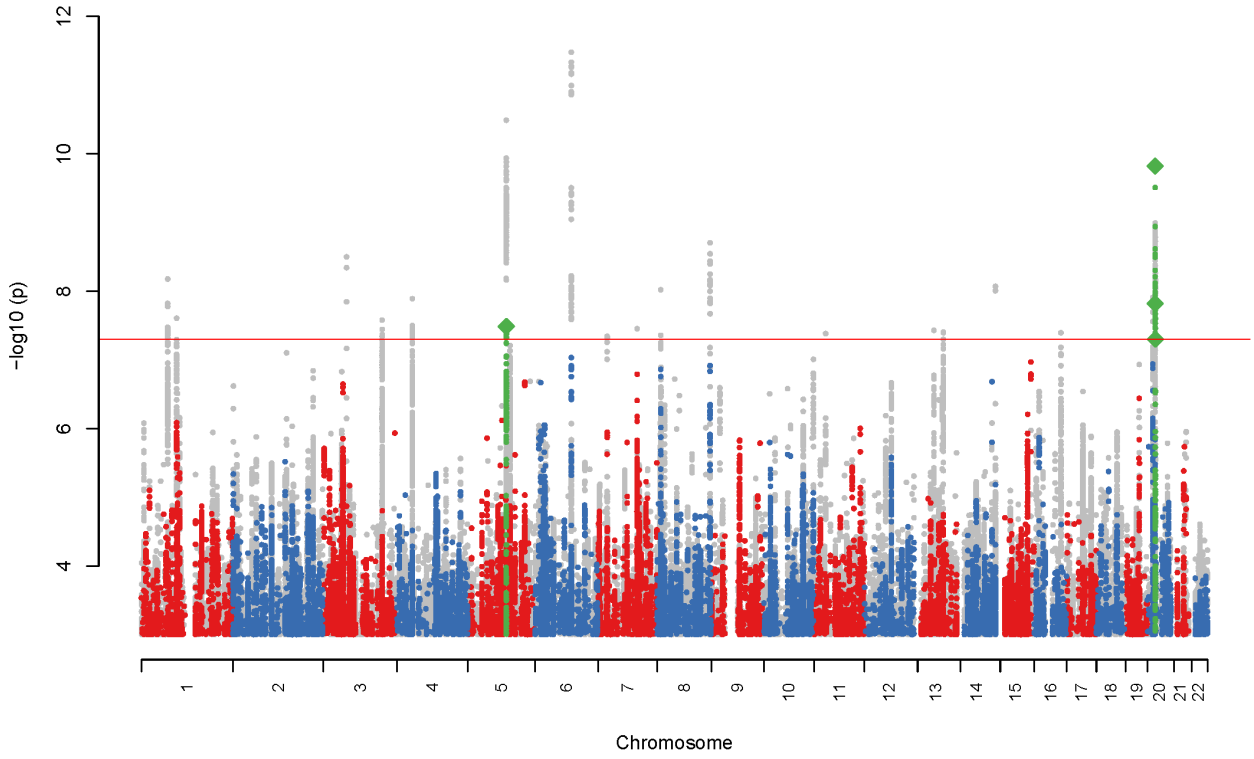

Supplementary Figure 46: Manhattan plot of MTAG analysis of ASD (18 381 cases, 27 969 controls and mean $\chi^2 = 1.201$) and schizophrenia[8] (without the Danish samples, 34 129 cases, 45 512 controls, and mean $\chi^2 = 1.804$) drawn on composite MTAG background. MTAG gives schizophrenia a weight of 0.27. The x axis shows genomic position (chromosomes 1–22) and the y axis the statistical significance as –log10 (P) of z statistics. Diamonds indicate the index SNP of genome wide significant clumps (at $5 \cdot 10^{-8}/3$) which in turn are painted green. The grey MTAG composit consists of the maximum at each locus of the results from the main scan, combined with follow-up, and three MTAG analyses.

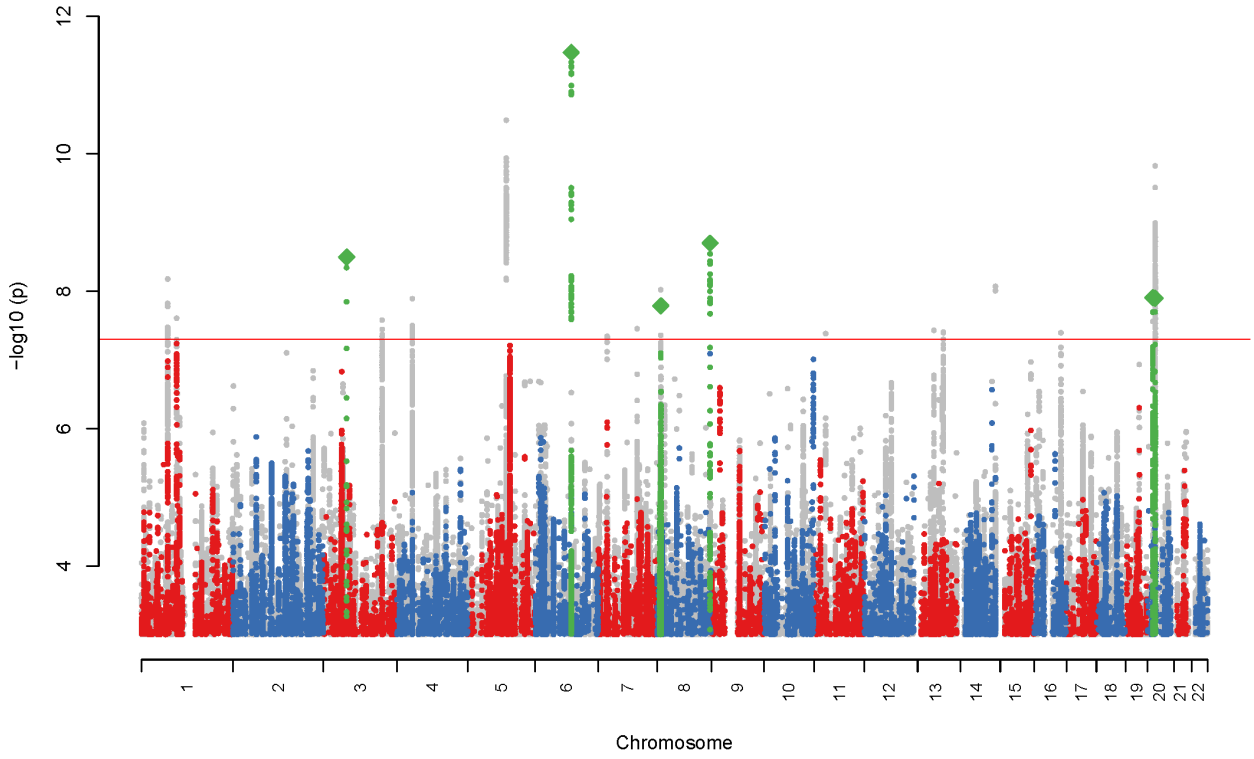

Supplementary Figure 47: Manhattan plot of MTAG analysis of ASD (18 381 cases, 27 969 controls and mean χ^2 = 1.201) and educational attainment[50] (328 917 samples and mean χ^2 = 1.648) drawn on composite MTAG background. MTAG gives educational attainment a weight of 0.11. The x axis shows genomic position (chromosomes 1–22) and the y axis the statistical significance as –log10 (P) of z statistics. Diamonds indicate the index SNP of genome wide significant clumps (at $5 \cdot 10^{-8}/3$) which in turn are painted green. The grey MTAG composit consists of the maximum at each locus of the results from the main scan, combined with follow-up, and three MTAG analyses.

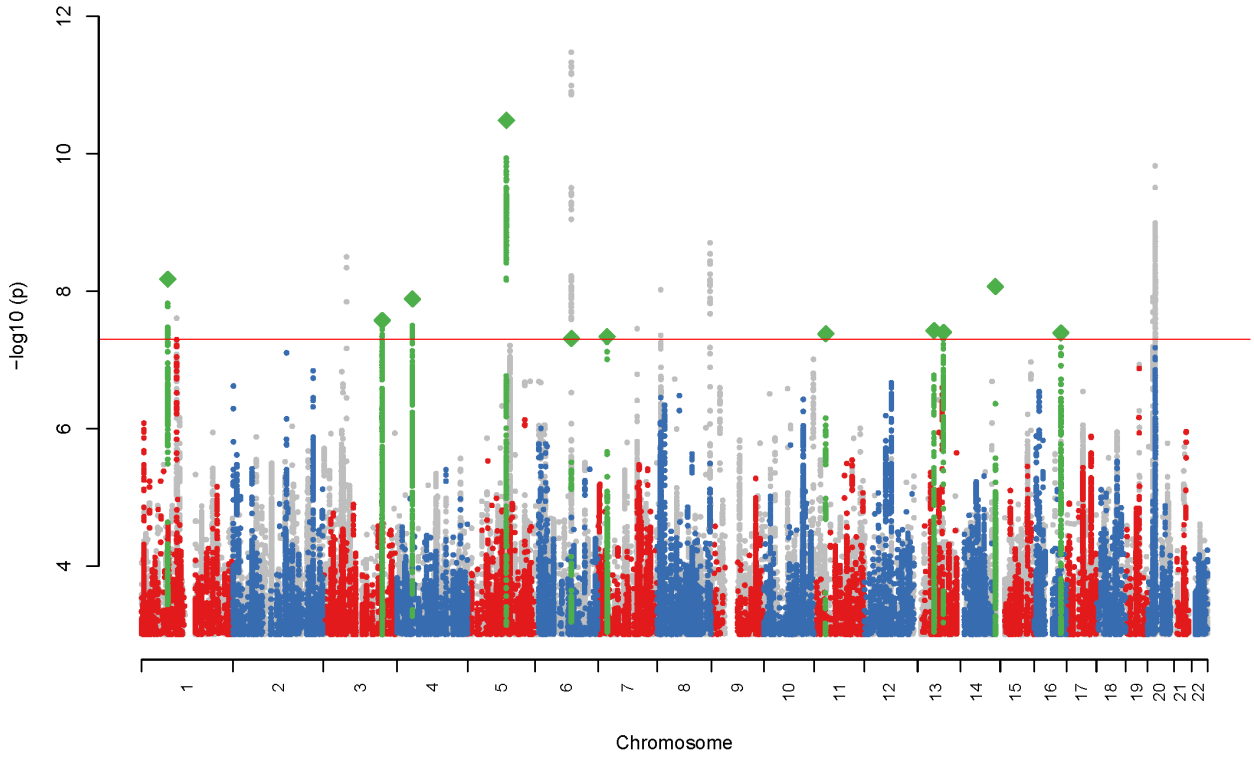

Supplementary Figure 48: Manhattan plot of MTAG analysis of ASD (18 381 cases, 27 969 controls and mean χ^2 = 1.201) and major depression (including the results from 23andMe[49], but excluding the Danish samples, 111 902 cases, 312 113 controls, and mean χ^2 = 1.477) drawn on composite MTAG background. MTAG gives major depression a weight of 0.24. The x axis shows genomic position (chromosomes 1–22) and the y axis the statistical significance as –log10 (P) of z statistics. Diamonds indicate the index SNP of genome wide significant clumps (at $5 \cdot 10^{-8}/3$) which in turn are painted green. The grey MTAG composit consists of the maximum at each locus of the results from the main scan, combined with follow-up, and three MTAG analyses.

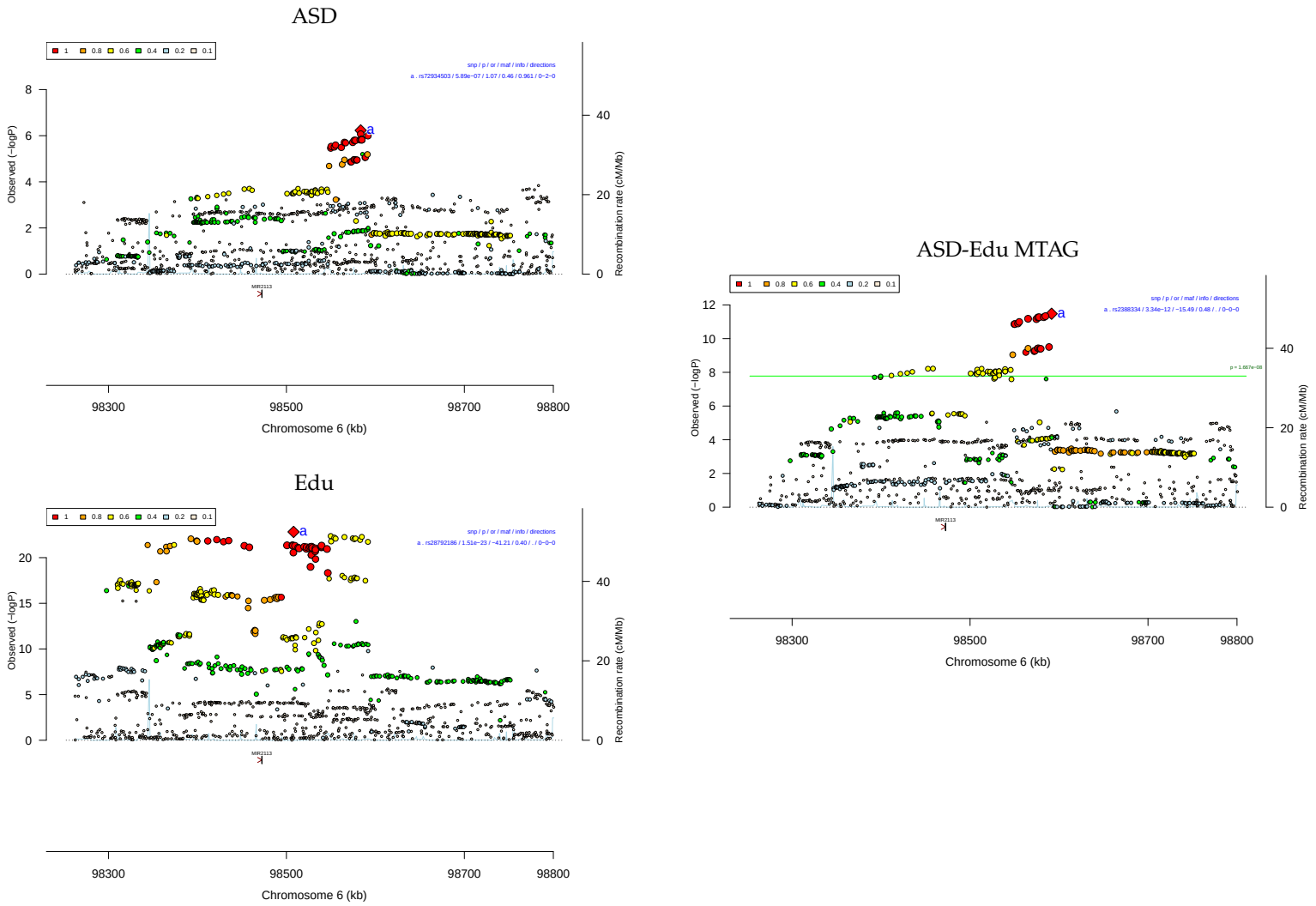

Supplementary Figure 49: Regional association plot around rs2388334 on chr 6 for ASD-Edu MTAG analysis. The left panels shows the regional plots for the ASD GWAS (18 381 cases and 27 969 controls) and the Edu GWAS (328 917 samples), and the right panel is the regional plot for the resulting MTAG analysis of ASD and Edu. Plots show very similar patterns with ASD having less power. Horizontal axis show chromosomal position in kb, Significance of the association expressed as $-\log_{10}(\mathrm{P})$ (from z-test) is plotted vertically (left axis) and the recombination rate from HapMap is shown as light blue curve (right axis). The dot size is proportional to LD between the plotted SNP and the index SNP defining the associated region. Index SNPs are marked by diamonds and labelled with letters. Colouring is based on degree of LD to that SNP as represented by r^2 (legend for r^2 is in the upper left corner). A black centre indicates that the markers is in the 1000 Genomes Project but not in HapMap3. The green line in the right panel shows the MTAG analysis significance level ($1.667 \cdot 10^{-8}$). Details of the index SNPs is in the upper right corner show (marker name/association p-value/odds ratio for the minor allele/minor allele frequency/imputation quality/direction of effect in the included studies (info only avialable for ASD)). The green lines in the lower half show genes (based on UCSC) with black vertical lines indicating exons. Arrow heads show the direction of transcription.

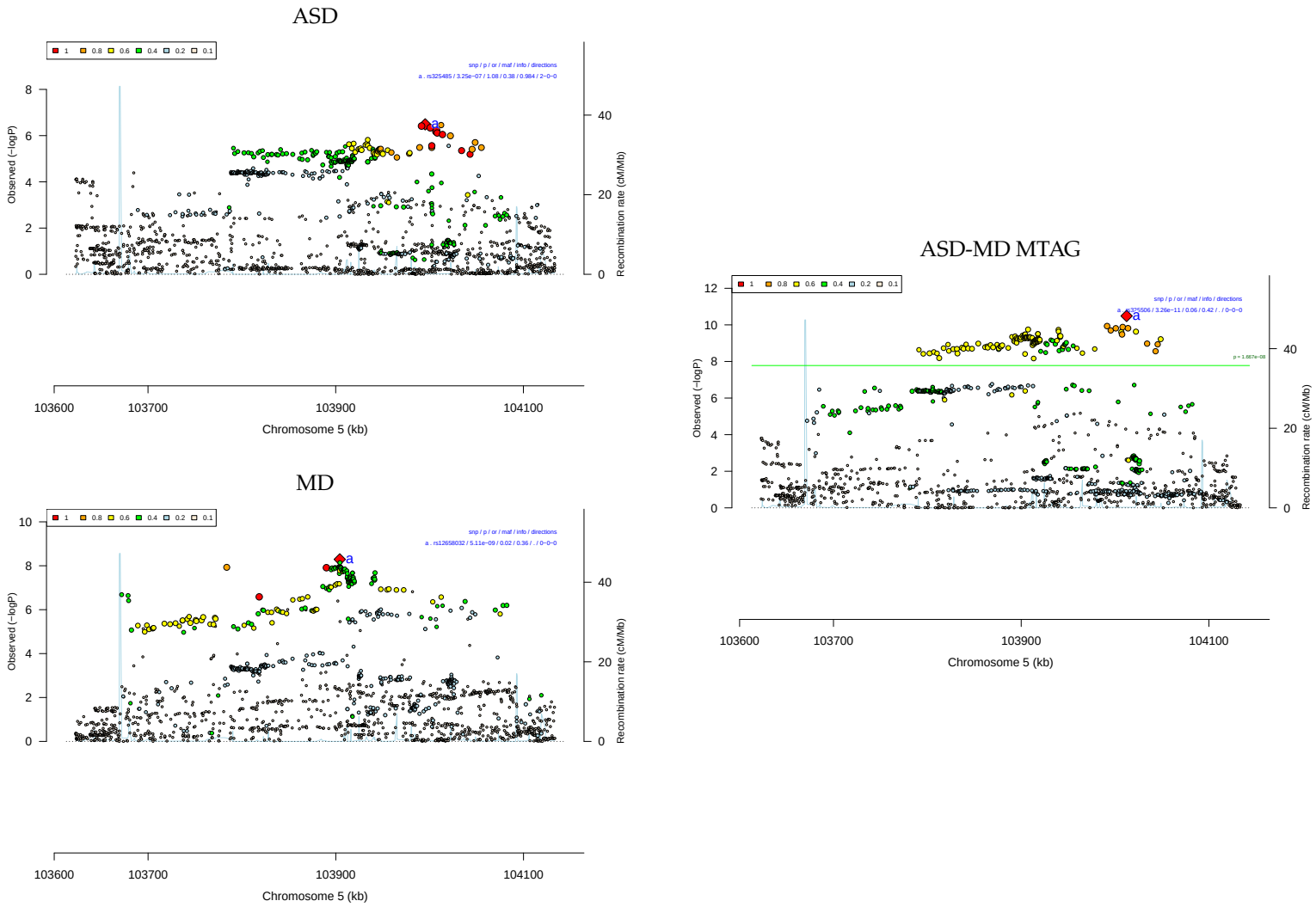

Supplementary Figure 50: Regional association plot around rs325506 on chr 5 for ASD-MD MTAG analysis. The left panels shows the regional plots for the ASD GWAS (18 381 cases and 27 969 controls) and the MD GWAS (111 902 cases and 312 113 controls), and the right panel is the regional plot for the resulting MTAG analysis of ASD and MD. Plots show very similar patterns with ASD having less power. Horizontal axis show chromosomal position in kb, Significance of the association expressed as $-\log_{10}(\mathrm{P})$ (from z-test) is plotted vertically (left axis) and the recombination rate from HapMap is shown as light blue curve (right axis). The dot size is proportional to LD between the plotted SNP and the index SNP defining the associated region. Index SNPs are marked by diamonds and labelled with letters. Colouring is based on degree of LD to that SNP as represented by r^2 (legend for r^2 is in the upper left corner). A black centre indicates that the markers is in the 1000 Genomes Project but not in HapMap3. The green line in the right panel shows the MTAG analysis significance level ($1.667 \cdot 10^{-8}$). Details of the index SNPs is in the upper right corner show (marker name/association p-value/odds ratio for the minor allele/minor allele frequency/imputation quality/direction of effect in the included studies (info only avialable for ASD)).

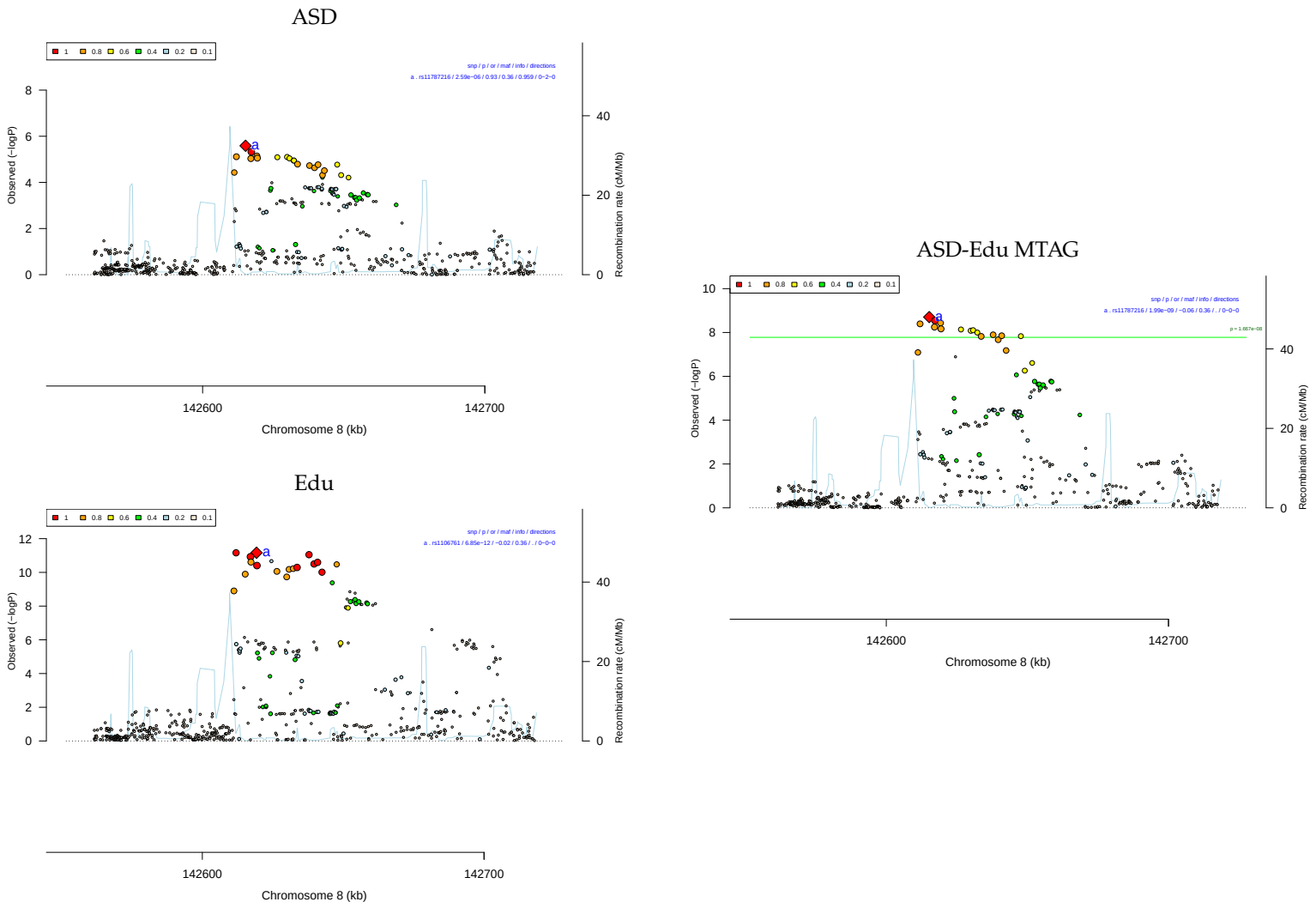

Supplementary Figure 51: Regional association plot around rs11787216 on chr 8 for ASD-Edu MTAG analysis. The left panels shows the regional plots for the ASD GWAS (18 381 cases and 27 969 controls) and the Edu GWAS (328 917 samples), and the right panel is the regional plot for the resulting MTAG analysis of ASD and Edu. Plots show very similar patterns with ASD having less power. Horizontal axis show chromosomal position in kb, Significance of the association expressed as $-\log_{10}(\mathrm{P})$ (from z-test) is plotted vertically (left axis) and the recombination rate from HapMap is shown as light blue curve (right axis). The dot size is proportional to LD between the plotted SNP and the index SNP defining the associated region. Index SNPs are marked by diamonds and labelled with letters. Colouring is based on degree of LD to that SNP as represented by r^2 (legend for r^2 is in the upper left corner). A black centre indicates that the markers is in the 1000 Genomes Project but not in HapMap3. The green line in the right panel shows the MTAG analysis significance level ($1.667 \cdot 10^{-8}$). Details of the index SNPs is in the upper right corner show (marker name/association p-value/odds ratio for the minor allele/minor allele frequency/imputation quality/direction of effect in the included studies (info only avialable for ASD)).

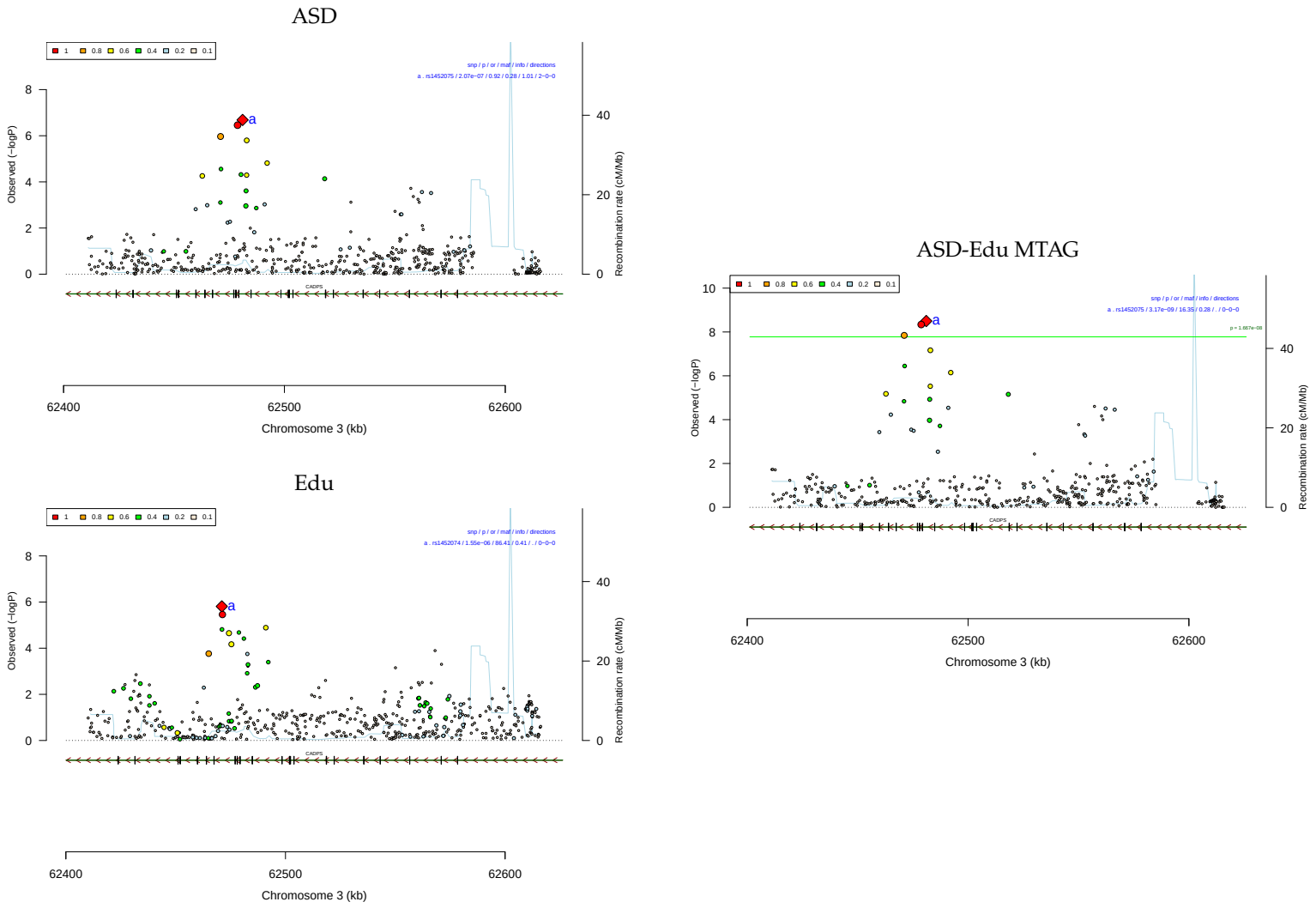

Supplementary Figure 52: Regional association plot around rs1452075 on chr 3 for ASD-Edu MTAG analysis. The left panels shows the regional plots for the ASD GWAS (18 381 cases and 27 969 controls) and the Edu GWAS (328 917 samples), and the right panel is the regional plot for the resulting MTAG analysis of ASD and Edu. Plots show very similar patterns with ASD having less power. Horizontal axis show chromosomal position in kb, Significance of the association expressed as $-\log_{10}(\mathrm{P})$ (from z-test) is plotted vertically (left axis) and the recombination rate from HapMap is shown as light blue curve (right axis). The dot size is proportional to LD between the plotted SNP and the index SNP defining the associated region. Index SNPs are marked by diamonds and labelled with letters. Colouring is based on degree of LD to that SNP as represented by r^2 (legend for r^2 is in the upper left corner). A black centre indicates that the markers is in the 1000 Genomes Project but not in HapMap3. The green line in the right panel shows the MTAG analysis significance level ($1.667 \cdot 10^{-8}$). Details of the index SNPs is in the upper right corner show (marker name/association p-value/odds ratio for the minor allele/minor allele frequency/imputation quality/direction of effect in the included studies (info only avialable for ASD)). The green lines in the lower half show genes (based on UCSC) with black vertical lines indicating exons. Arrow heads show the direction of transcription.

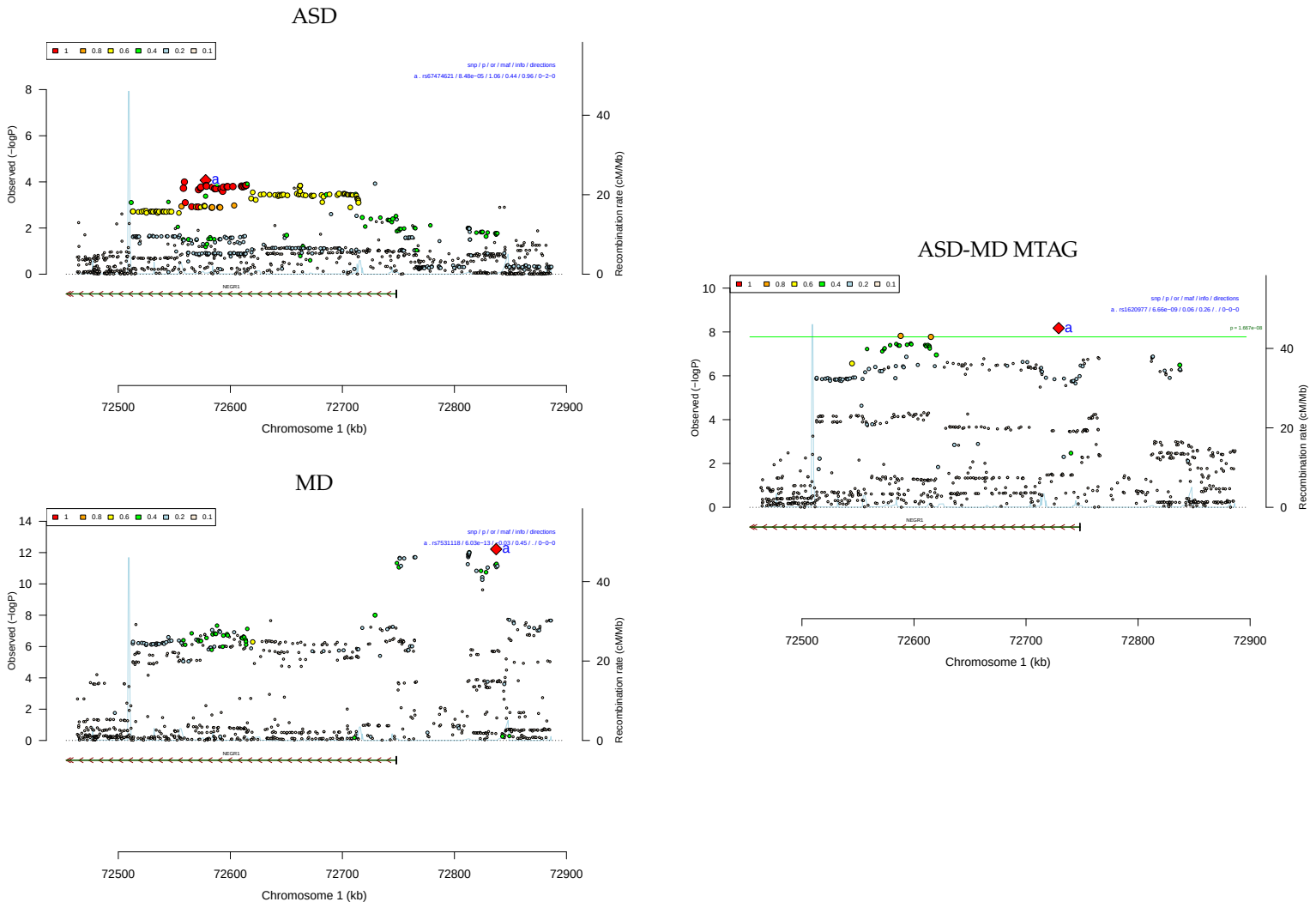

Supplementary Figure 53: Regional association plot around rs1620977 on chr 1 for ASD-MD MTAG analysis. The left panels shows the regional plots for the ASD GWAS (18 381 cases and 27 969 controls) and the MD GWAS (111 902 cases and 312 113 controls), and the right panel is the regional plot for the resulting MTAG analysis of ASD and MD. Plots show very similar patterns with ASD having less power and the index SNP shifted. Horizontal axis show chromosomal position in kb, Significance of the association expressed as $-\log_{10}(P)$ (from z-test) is plotted vertically (left axis) and the recombination rate from HapMap is shown as light blue curve (right axis). The dot size is proportional to LD between the plotted SNP and the index SNP defining the associated region. Index SNPs are marked by diamonds and labelled with letters. Colouring is based on degree of LD to that SNP as represented by r^2 (legend for r^2 is in the upper left corner). A black centre indicates that the markers is in the 1000 Genomes Project but not in HapMap3. The green line in the right panel shows the MTAG analysis significance level ($1.667 \cdot 10^{-8}$). Details of the index SNPs is in the upper right corner show (marker name/association p-value/odds ratio for the minor allele/minor allele frequency/imputation quality/direction of effect in the included studies (info only avialable for ASD)). The green lines in the lower half show genes (based on UCSC) with black vertical lines indicating exons. Arrow heads show the direction of transcription.

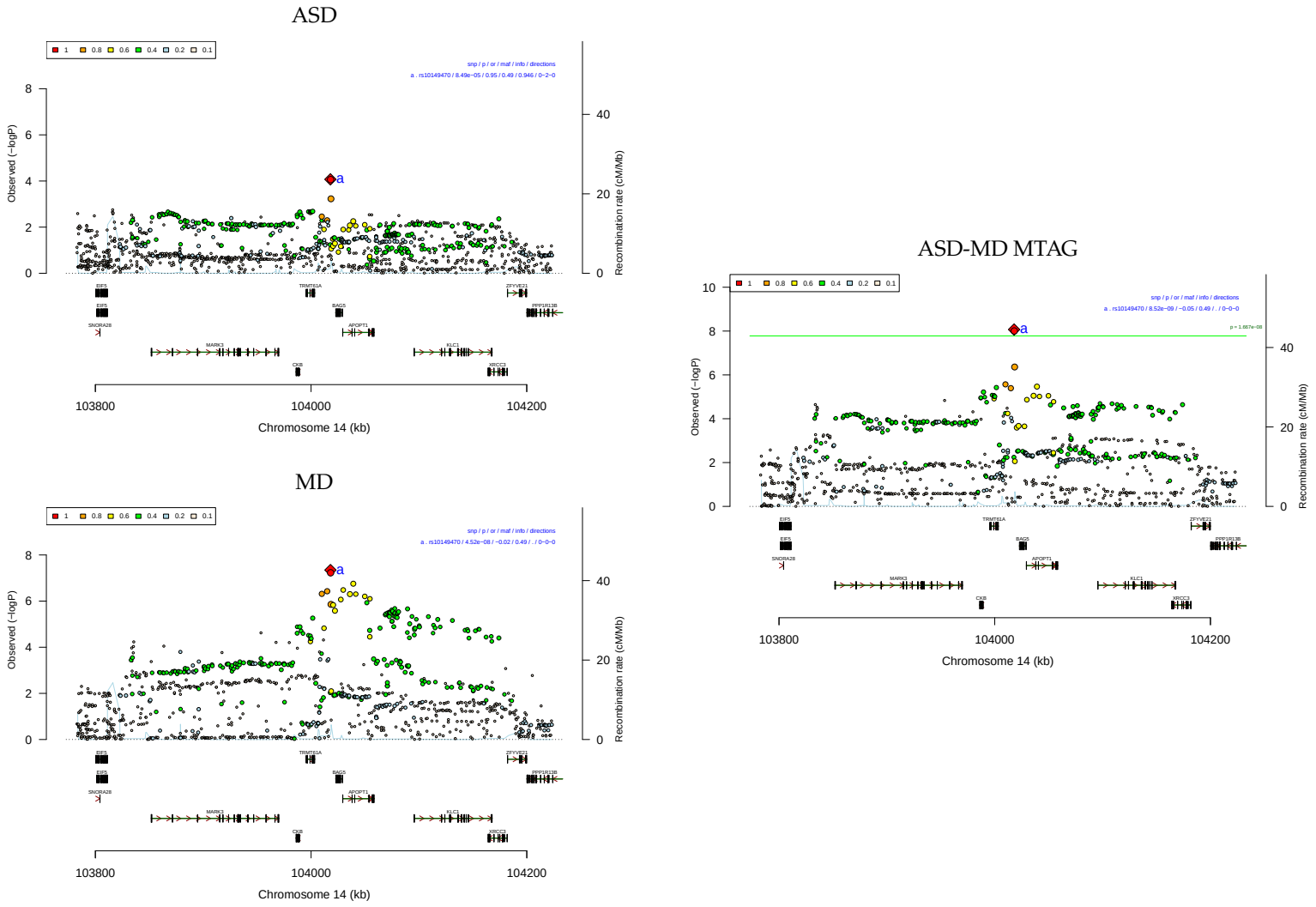

Supplementary Figure 54: Regional association plot around rs10149470 on chr 14 for ASD-MD MTAG analysis. The left panels shows the regional plots for the ASD GWAS (18 381 cases and 27 969 controls) and the MD GWAS (111 902 cases and 312 113 controls), and the right panel is the regional plot for the resulting MTAG analysis of ASD and MD. Plots show very similar patterns with ASD having less power. Horizontal axis show chromosomal position in kb, Significance of the association expressed as $-\log_{10}(\mathrm{P})$ (from z-test) is plotted vertically (left axis) and the recombination rate from HapMap is shown as light blue curve (right axis). The dot size is proportional to LD between the plotted SNP and the index SNP defining the associated region. Index SNPs are marked by diamonds and labelled with letters. Colouring is based on degree of LD to that SNP as represented by r^2 (legend for r^2 is in the upper left corner). A black centre indicates that the markers is in the 1000 Genomes Project but not in HapMap3. The green line in the right panel shows the MTAG analysis significance level ($1.667 \cdot 10^{-8}$). Details of the index SNPs is in the upper right corner show (marker name/association p-value/odds ratio for the minor allele/minor allele frequency/imputation quality/direction of effect in the included studies (info only avialable for ASD)). The green lines in the lower half show genes (based on UCSC) with black vertical lines indicating exons. Arrow heads show the direction of transcription.

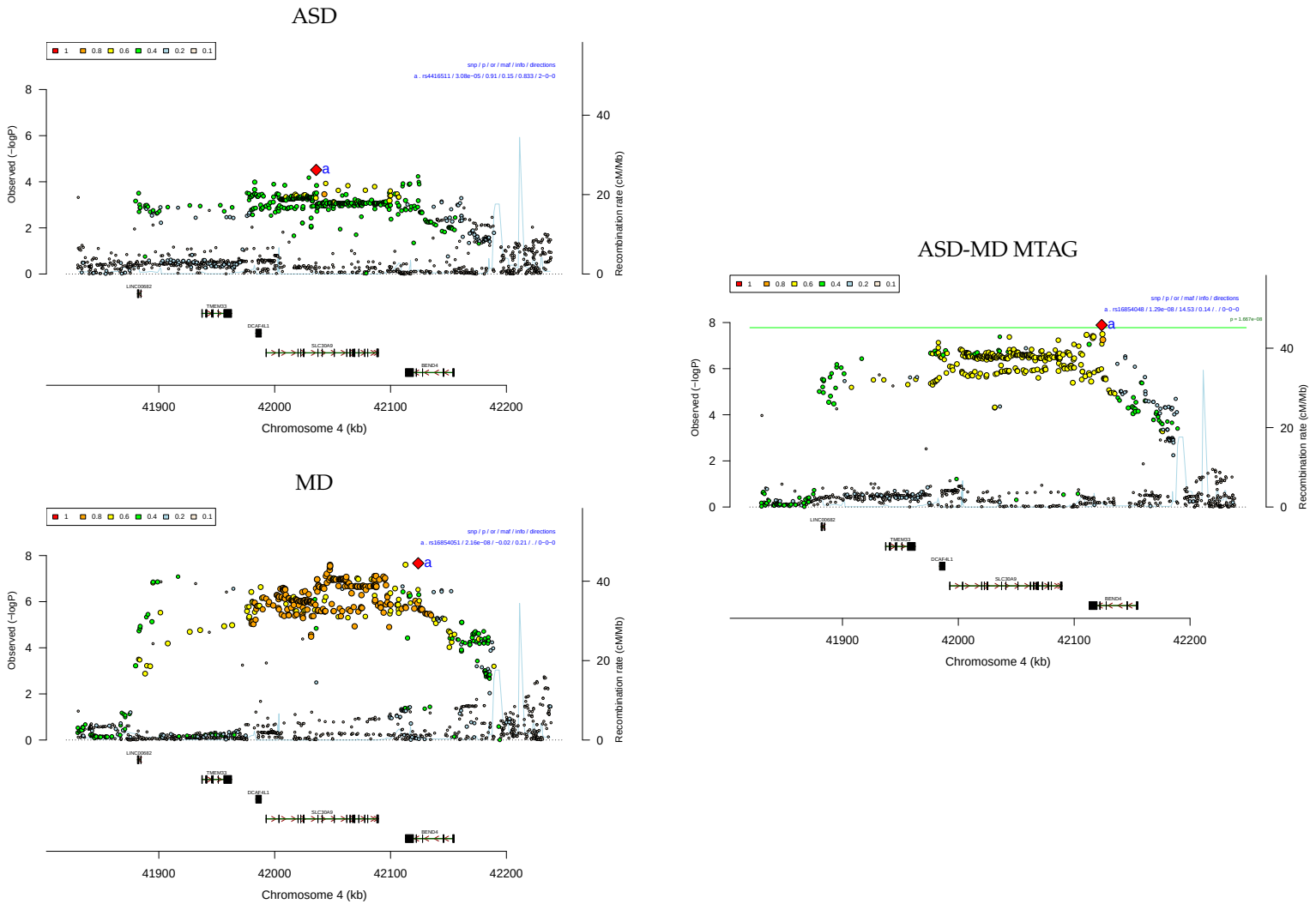

Supplementary Figure 55: Regional association plot around rs16854048 on chr 4 for ASD-MD MTAG analysis. The left panels shows the regional plots for the ASD GWAS (18 381 cases and 27 969 controls) and the MD GWAS (111 902 cases and 312 113 controls), and the right panel is the regional plot for the resulting MTAG analysis of ASD and MD. Plots show very similar patterns with ASD having less power and the index SNP shifted. Horizontal axis show chromosomal position in kb, Significance of the association expressed as $-\log_{10}(P)$ (from z-test) is plotted vertically (left axis) and the recombination rate from HapMap is shown as light blue curve (right axis). The dot size is proportional to LD between the plotted SNP and the index SNP defining the associated region. Index SNPs are marked by diamonds and labelled with letters. Colouring is based on degree of LD to that SNP as represented by r^2 (legend for r^2 is in the upper left corner). A black centre indicates that the markers is in the 1000 Genomes Project but not in HapMap3. The green line in the right panel shows the MTAG analysis significance level ($1.667 \cdot 10^{-8}$). Details of the index SNPs is in the upper right corner show (marker name/association p-value/odds ratio for the minor allele/minor allele frequency/imputation quality/direction of effect in the included studies (info only avialable for ASD)). The green lines in the lower half show genes (based on UCSC) with black vertical lines indicating exons. Arrow heads show the direction of transcription.

4.1.5 Gene-based association

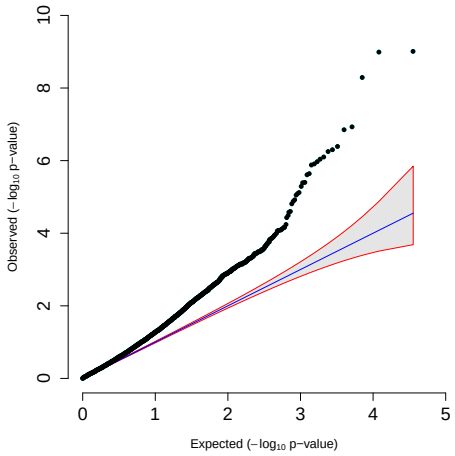

Supplementary Figure 56: Qq plot for gene-based analysis by MAGMA on the combined iPSYCH-PGC GWAS composed of 18 381 cases and 27 969 controls. Association quantiles of the p-values (achieved from z-score) are plotted against the quantiles expected under the null. The shading indicates 95%-confidence region under the null. The genomic inflation factor, lambda, is the observed median χ^2 test statistic divided by the median expected χ^2 test statistic under the null hypothesis, lambda1000 estimates what lambda would be equivalent to in a sample of 500 cases and 500 controls..

The figures 57–81 we show the regional Manhattan plots the individual markers around the areas of the top signals of the iPSYCH-PGC meta MAGMA analysis.

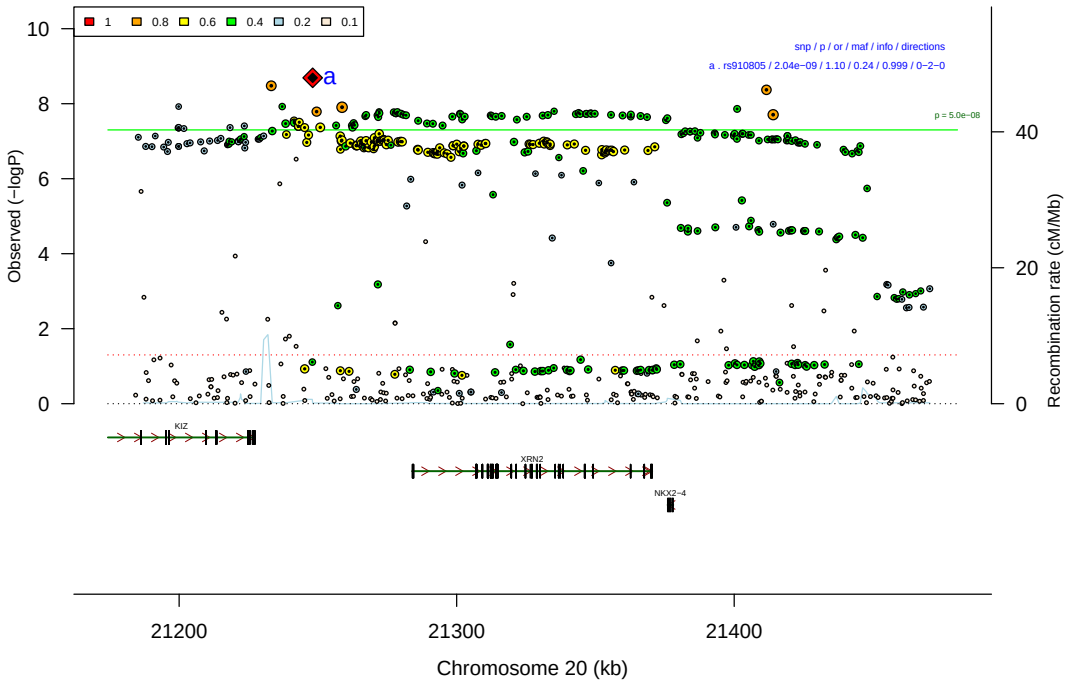

Supplementary Figure 57: Regional plot around *XRN2* for gene-based MAGMA analysis of iPSYCH-PGC meta (18 381 cases and 27 969 controls). Chromosomal position is on the horizontal axis in kb, The significance of the association expressed as $-\log_{10}(P)$ (from z-test) is plotted vertically (left axis) and the recombination rate from HapMap is shown as light blue curve (right axis). The dot size is proportional to LD between the plotted SNP and the index SNP defining the associated region. Index SNPs are marked by diamonds and labelled with letters. Colouring is based on degree of LD to that SNP as represented by r^2 (legend for r^2 is in the upper left corner). A black centre indicates that the markers is present in the 1000 Genomes Project but not in HapMap3. The green line shows the genome-wide significance level ($5 \cdot 10^{-8}$). The upper right corner show details of the index SNPs (marker name/association p-value/odds ratio for the minor allele/minor allele frequency/imputation quality/direction of effect in the two studies (N one direction - N other direction- N missing)). The green lines in the lower half show genes (based on UCSC) with black vertical lines indicating exons. Arrow heads show the direction of transcription.

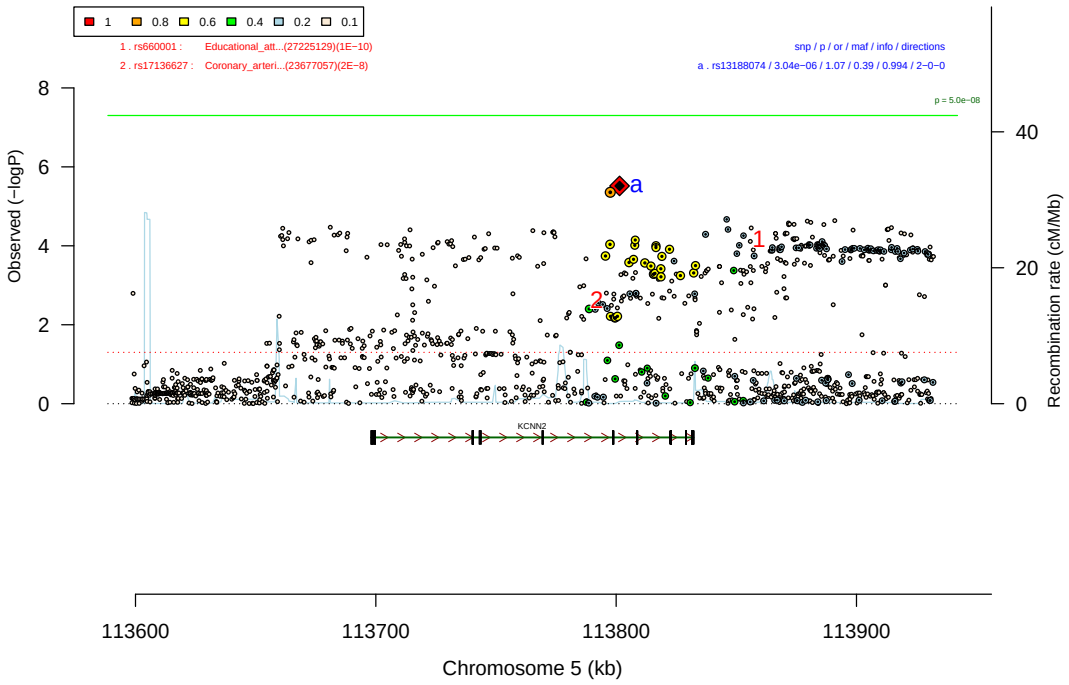

Supplementary Figure 58: Regional plot around *KCNN2* for gene-based MAGMA analysis of iPSYCH-PGC meta (18 381 cases and 27 969 controls). Chromosomal position is on the horizontal axis in kb, The significance of the association expressed as $-\log_{10}(P)$ (from z-test) is plotted vertically (left axis) and the recombination rate from HapMap is shown as light blue curve (right axis). The dot size is proportional to LD between the plotted SNP and the index SNP defining the associated region. Index SNPs are marked by diamonds and labelled with letters. Colouring is based on degree of LD to that SNP as represented by r^2 (legend for r^2 is in the upper left corner). A black centre indicates that the markers is present in the 1000 Genomes Project but not in HapMap3. The green line shows the genome-wide significance level ($5 \cdot 10^{-8}$). The upper right corner show details of the index SNPs (marker name/association p-value/odds ratio for the minor allele/minor allele frequency/imputation quality/direction of effect in the two studies (N one direction - N other direction- N missing)). Loci listed in the GWAS Catalogue for other phenotypes are shown in the upper left corner (capped at 10). The green lines in the lower half show genes (based on UCSC) with black vertical lines indicating exons. Arrow heads show the direction of transcription.

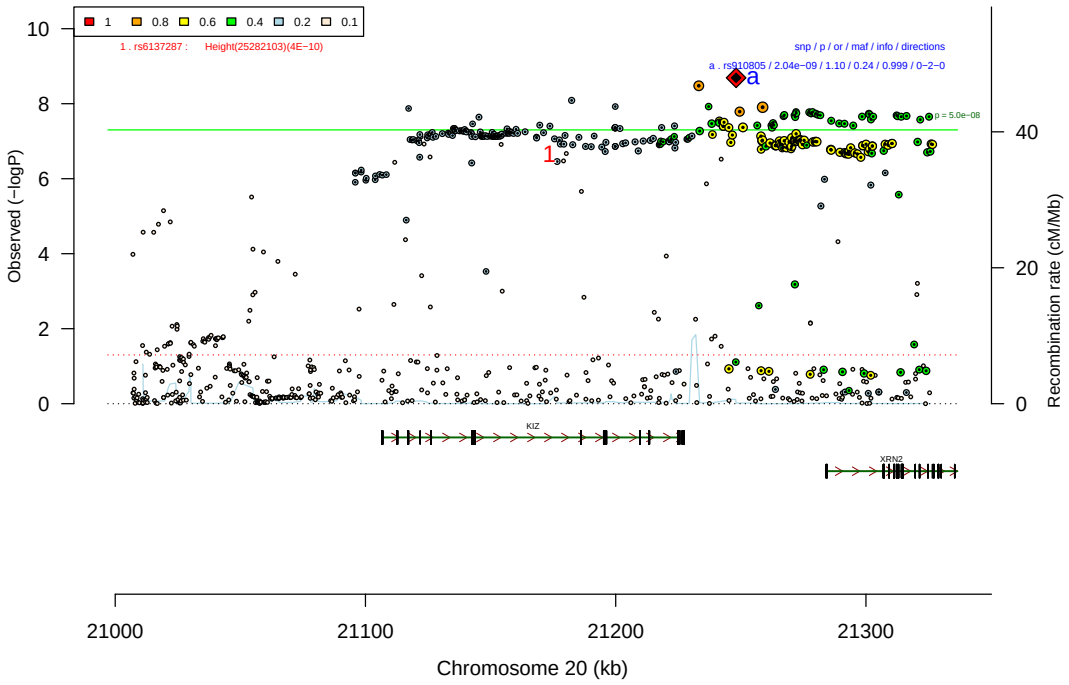

Supplementary Figure 59: Regional plot around *KIZ* for gene-based MAGMA analysis of iPSYCH-PGC meta (18 381 cases and 27 969 controls). Chromosomal position is on the horizontal axis in kb, The significance of the association expressed as $-\log_{10}(P)$ (from z-test) is plotted vertically (left axis) and the recombination rate from HapMap is shown as light blue curve (right axis). The dot size is proportional to LD between the plotted SNP and the index SNP defining the associated region. Index SNPs are marked by diamonds and labelled with letters. Colouring is based on degree of LD to that SNP as represented by r^2 (legend for r^2 is in the upper left corner). A black centre indicates that the markers is present in the 1000 Genomes Project but not in HapMap3. The green line shows the genome-wide significance level ($5 \cdot 10^{-8}$). The upper right corner show details of the index SNPs (marker name/association p-value/odds ratio for the minor allele/minor allele frequency/imputation quality/direction of effect in the two studies (N one direction - N other direction- N missing)). Loci listed in the GWAS Catalogue for other phenotypes are shown in the upper left corner (capped at 10). The green lines in the lower half show genes (based on UCSC) with black vertical lines indicating exons. Arrow heads show the direction of transcription.

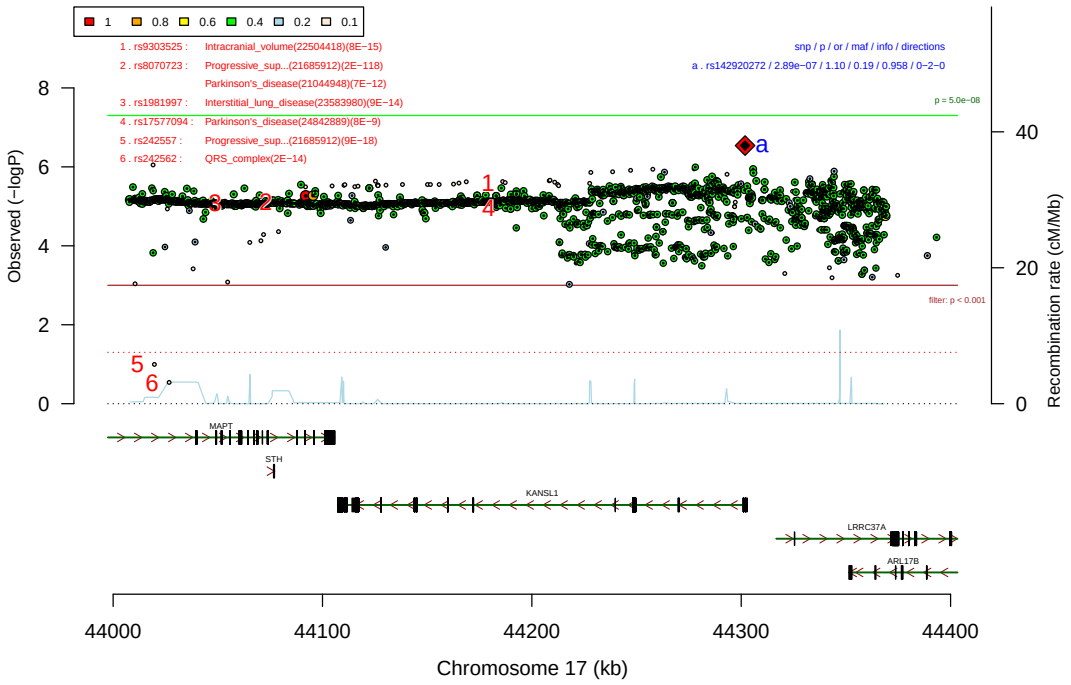

Supplementary Figure 60: Regional plot around *KANSL1* for gene-based MAGMA analysis of iPSYCH-PGC meta (18 381 cases and 27 969 controls). Chromosomal position is on the horizontal axis in kb, The significance of the association expressed as $-\log_{10}(P)$ (from z-test) is plotted vertically (left axis) and the recombination rate from HapMap is shown as light blue curve (right axis). The dot size is proportional to LD between the plotted SNP and the index SNP defining the associated region. Index SNPs are marked by diamonds and labelled with letters. Colouring is based on degree of LD to that SNP as represented by r^2 (legend for r^2 is in the upper left corner). A black centre indicates that the markers is present in the 1000 Genomes Project but not in HapMap3. The green line shows the genome-wide significance level ($5 \cdot 10^{-8}$). The upper right corner show details of the index SNPs (marker name/association p-value/odds ratio for the minor allele/minor allele frequency/imputation quality/direction of effect in the two studies (N one direction - N other direction- N missing)). Loci listed in the GWAS Catalogue for other phenotypes are shown in the upper left corner (capped at 10). The green lines in the lower half show genes (based on UCSC) with black vertical lines indicating exons. Arrow heads show the direction of transcription.

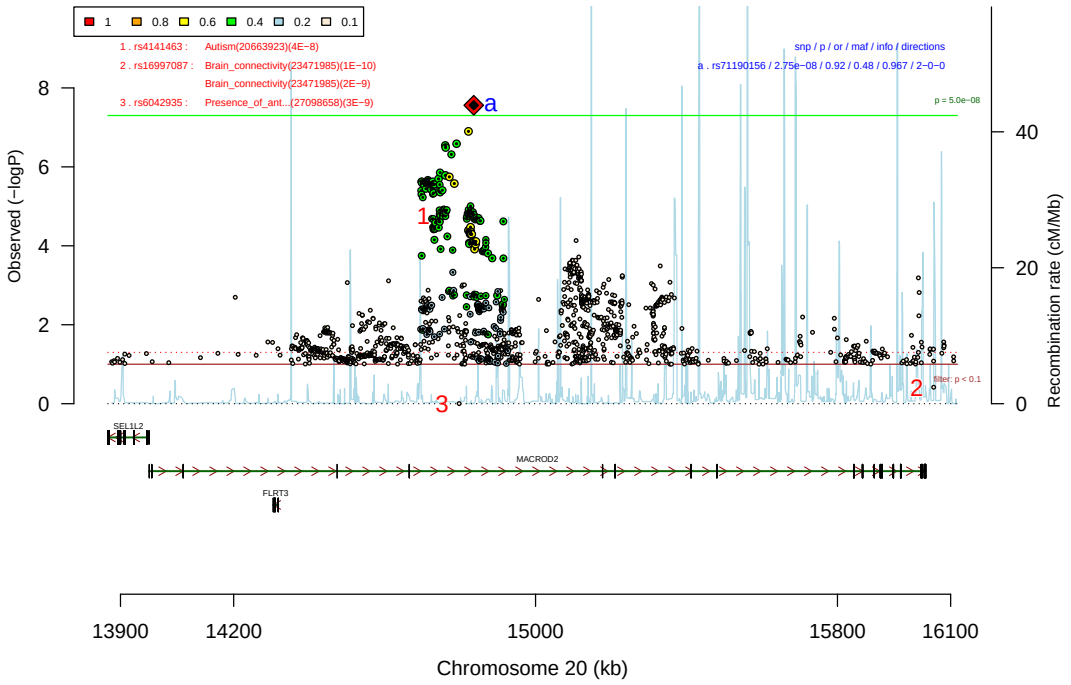

Supplementary Figure 61: Regional plot around *MACROD2* for gene-based MAGMA analysis of iPSYCH-PGC meta (18 381 cases and 27 969 controls). Chromosomal position is on the horizontal axis in kb, The significance of the association expressed as $-\log_{10}(P)$ (from z-test) is plotted vertically (left axis) and the recombination rate from HapMap is shown as light blue curve (right axis). The dot size is proportional to LD between the plotted SNP and the index SNP defining the associated region. Index SNPs are marked by diamonds and labelled with letters. Colouring is based on degree of LD to that SNP as represented by r^2 (legend for r^2 is in the upper left corner). A black centre indicates that the markers is present in the 1000 Genomes Project but not in HapMap3. The green line shows the genome-wide significance level ($5 \cdot 10^{-8}$). The upper right corner show details of the index SNPs (marker name/association p-value/odds ratio for the minor allele/minor allele frequency/imputation quality/direction of effect in the two studies (N one direction - N other direction- N missing)). Loci listed in the GWAS Catalogue for other phenotypes are shown in the upper left corner (capped at 10). The green lines in the lower half show genes (based on UCSC) with black vertical lines indicating exons. Arrow heads show the direction of transcription.

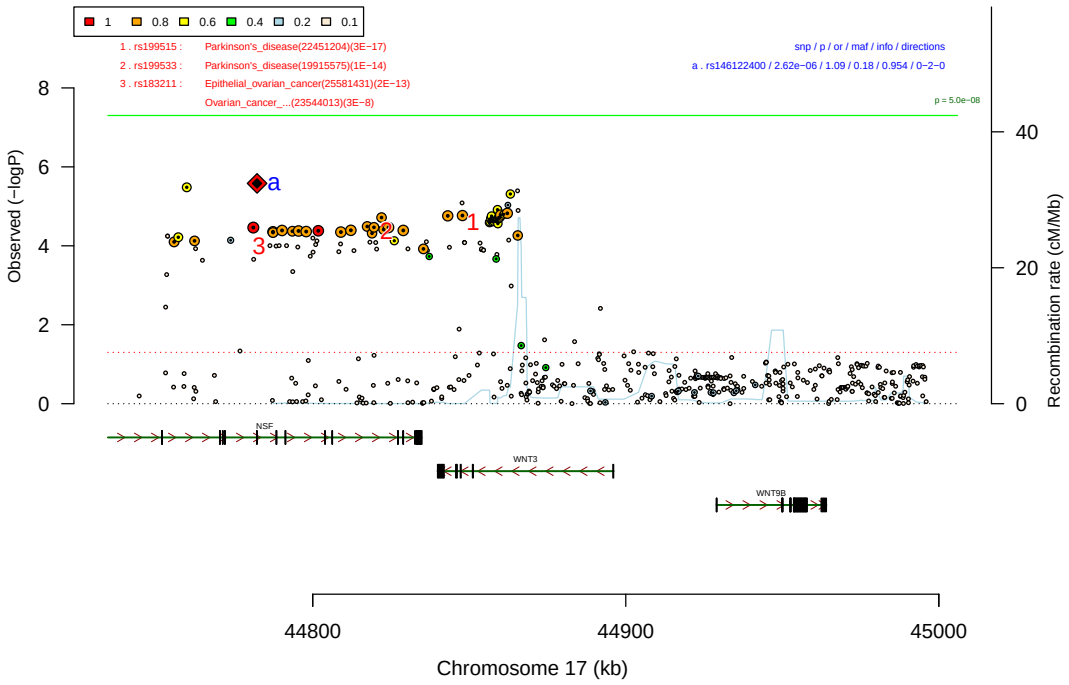

Supplementary Figure 62: Regional plot around *WNT3* for gene-based MAGMA analysis of iPSYCH-PGC meta (18 381 cases and 27 969 controls). Chromosomal position is on the horizontal axis in kb, The significance of the association expressed as $-\log_{10}(P)$ (from z-test) is plotted vertically (left axis) and the recombination rate from HapMap is shown as light blue curve (right axis). The dot size is proportional to LD between the plotted SNP and the index SNP defining the associated region. Index SNPs are marked by diamonds and labelled with letters. Colouring is based on degree of LD to that SNP as represented by r^2 (legend for r^2 is in the upper left corner). A black centre indicates that the markers is present in the 1000 Genomes Project but not in HapMap3. The green line shows the genome-wide significance level ($5 \cdot 10^{-8}$). The upper right corner show details of the index SNPs (marker name/association p-value/odds ratio for the minor allele/minor allele frequency/imputation quality/direction of effect in the two studies (N one direction - N other direction- N missing)). Loci listed in the GWAS Catalogue for other phenotypes are shown in the upper left corner (capped at 10). The green lines in the lower half show genes (based on UCSC) with black vertical lines indicating exons. Arrow heads show the direction of transcription.

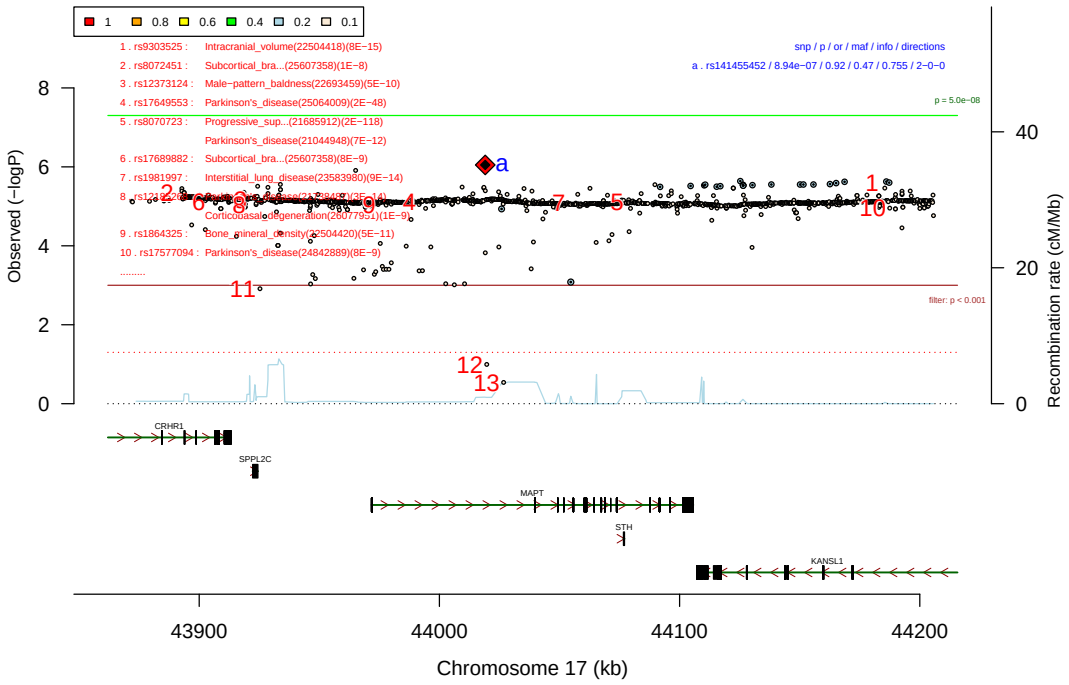

Supplementary Figure 63: Regional plot around *MAPT* for gene-based MAGMA analysis of iPSYCH-PGC meta (18 381 cases and 27 969 controls). Chromosomal position is on the horizontal axis in kb, The significance of the association expressed as $-\log_{10}(\mathrm{P})$ (from z-test) is plotted vertically (left axis) and the recombination rate from HapMap is shown as light blue curve (right axis). The dot size is proportional to LD between the plotted SNP and the index SNP defining the associated region. Index SNPs are marked by diamonds and labelled with letters. Colouring is based on degree of LD to that SNP as represented by r^2 (legend for r^2 is in the upper left corner). A black centre indicates that the markers is present in the 1000 Genomes Project but not in HapMap3. The green line shows the genome-wide significance level ($5 \cdot 10^{-8}$). The upper right corner show details of the index SNPs (marker name/association p-value/odds ratio for the minor allele/minor allele frequency/imputation quality/direction of effect in the two studies (N one direction - N other direction- N missing)). Loci listed in the GWAS Catalogue for other phenotypes are shown in the upper left corner (capped at 10). The green lines in the lower half show genes (based on UCSC) with black vertical lines indicating exons. Arrow heads show the direction of transcription.

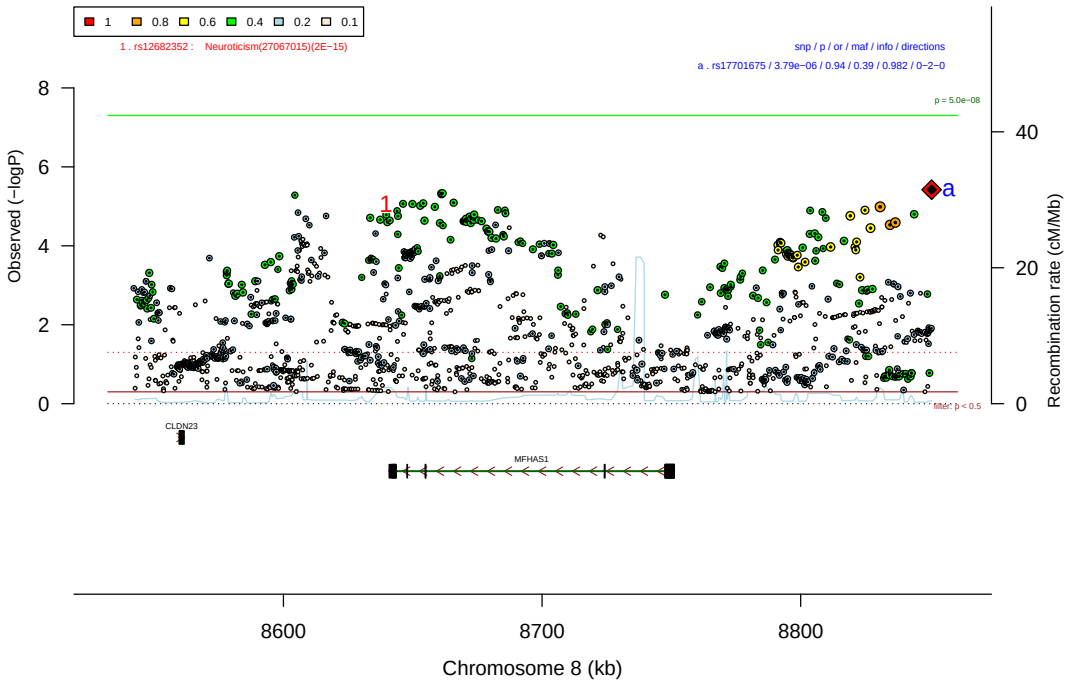

Supplementary Figure 64: Regional plot around *MFHAS1* for gene-based MAGMA analysis of iPSYCH-PGC meta (18 381 cases and 27 969 controls). Chromosomal position is on the horizontal axis in kb, The significance of the association expressed as $-\log_{10}(P)$ (from z-test) is plotted vertically (left axis) and the recombination rate from HapMap is shown as light blue curve (right axis). The dot size is proportional to LD between the plotted SNP and the index SNP defining the associated region. Index SNPs are marked by diamonds and labelled with letters. Colouring is based on degree of LD to that SNP as represented by r^2 (legend for r^2 is in the upper left corner). A black centre indicates that the markers is present in the 1000 Genomes Project but not in HapMap3. The green line shows the genome-wide significance level ($5 \cdot 10^{-8}$). The upper right corner show details of the index SNPs (marker name/association p-value/odds ratio for the minor allele/minor allele frequency/imputation quality/direction of effect in the two studies (N one direction - N other direction- N missing)). Loci listed in the GWAS Catalogue for other phenotypes are shown in the upper left corner (capped at 10). The green lines in the lower half show genes (based on UCSC) with black vertical lines indicating exons. Arrow heads show the direction of transcription.

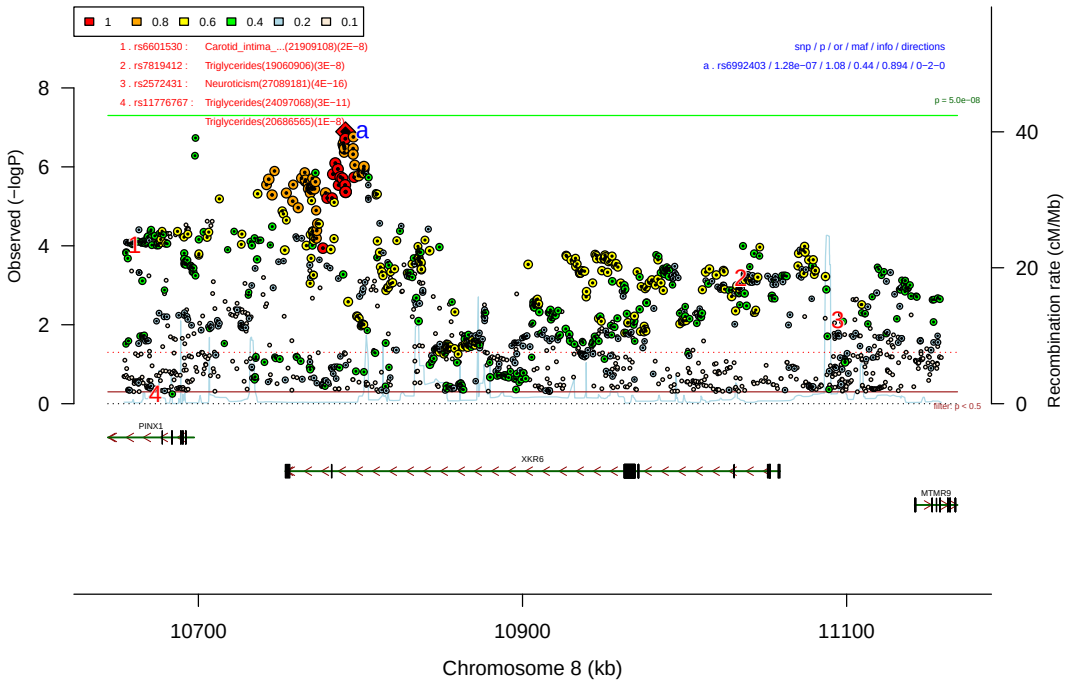

Supplementary Figure 65: Regional plot around *XKR6* for gene-based MAGMA analysis of iPSYCH-PGC meta (18 381 cases and 27 969 controls). Chromosomal position is on the horizontal axis in kb, The significance of the association expressed as $-\log_{10}(P)$ (from z-test) is plotted vertically (left axis) and the recombination rate from HapMap is shown as light blue curve (right axis). The dot size is proportional to LD between the plotted SNP and the index SNP defining the associated region. Index SNPs are marked by diamonds and labelled with letters. Colouring is based on degree of LD to that SNP as represented by r^2 (legend for r^2 is in the upper left corner). A black centre indicates that the markers is present in the 1000 Genomes Project but not in HapMap3. The green line shows the genome-wide significance level ($5 \cdot 10^{-8}$). The upper right corner show details of the index SNPs (marker name/association p-value/odds ratio for the minor allele/minor allele frequency/imputation quality/direction of effect in the two studies (N one direction - N other direction- N missing)). Loci listed in the GWAS Catalogue for other phenotypes are shown in the upper left corner (capped at 10). The green lines in the lower half show genes (based on UCSC) with black vertical lines indicating exons. Arrow heads show the direction of transcription.

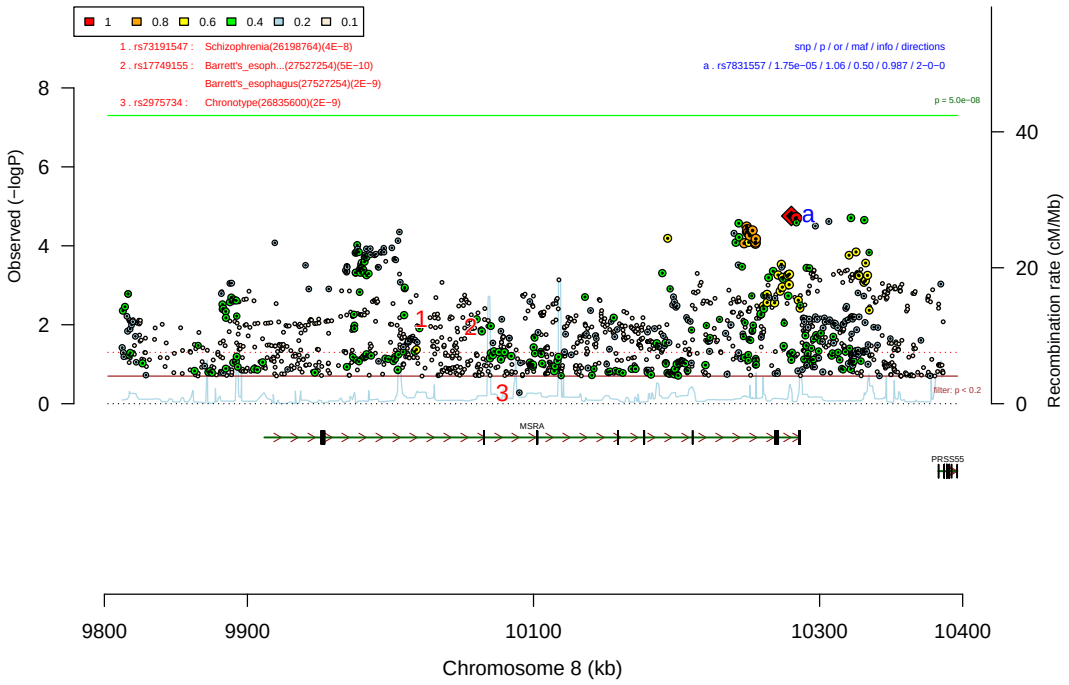

Supplementary Figure 66: Regional plot around *MSRA* for gene-based MAGMA analysis of iPSYCH-PGC meta (18 381 cases and 27 969 controls). Chromosomal position is on the horizontal axis in kb, The significance of the association expressed as $-\log_{10}(P)$ (from z-test) is plotted vertically (left axis) and the recombination rate from HapMap is shown as light blue curve (right axis). The dot size is proportional to LD between the plotted SNP and the index SNP defining the associated region. Index SNPs are marked by diamonds and labelled with letters. Colouring is based on degree of LD to that SNP as represented by r^2 (legend for r^2 is in the upper left corner). A black centre indicates that the markers is present in the 1000 Genomes Project but not in HapMap3. The green line shows the genome-wide significance level ($5 \cdot 10^{-8}$). The upper right corner show details of the index SNPs (marker name/association p-value/odds ratio for the minor allele/minor allele frequency/imputation quality/direction of effect in the two studies (N one direction - N other direction- N missing)). Loci listed in the GWAS Catalogue for other phenotypes are shown in the upper left corner (capped at 10). The green lines in the lower half show genes (based on UCSC) with black vertical lines indicating exons. Arrow heads show the direction of transcription.

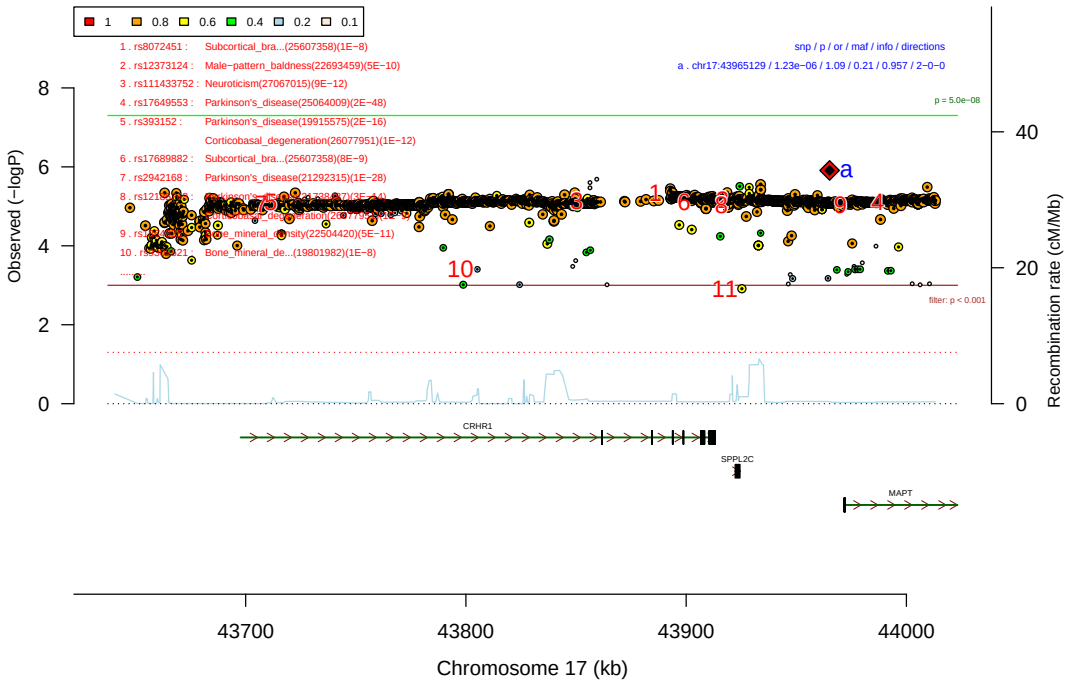

Supplementary Figure 67: Regional plot around *CRHR*1 for gene-based MAGMA analysis of iPSYCH-PGC meta (18 381 cases and 27 969 controls). Chromosomal position is on the horizontal axis in kb, The significance of the association expressed as $-\log_{10}(P)$ (from z-test) is plotted vertically (left axis) and the recombination rate from HapMap is shown as light blue curve (right axis). The dot size is proportional to LD between the plotted SNP and the index SNP defining the associated region. Index SNPs are marked by diamonds and labelled with letters. Colouring is based on degree of LD to that SNP as represented by r^2 (legend for r^2 is in the upper left corner). A black centre indicates that the markers is present in the 1000 Genomes Project but not in HapMap3. The green line shows the genome-wide significance level ($5 \cdot 10^{-8}$). The upper right corner show details of the index SNPs (marker name/association p-value/odds ratio for the minor allele/minor allele frequency/imputation quality/direction of effect in the two studies (N one direction - N other direction- N missing)). Loci listed in the GWAS Catalogue for other phenotypes are shown in the upper left corner (capped at 10). The green lines in the lower half show genes (based on UCSC) with black vertical lines indicating exons. Arrow heads show the direction of transcription.

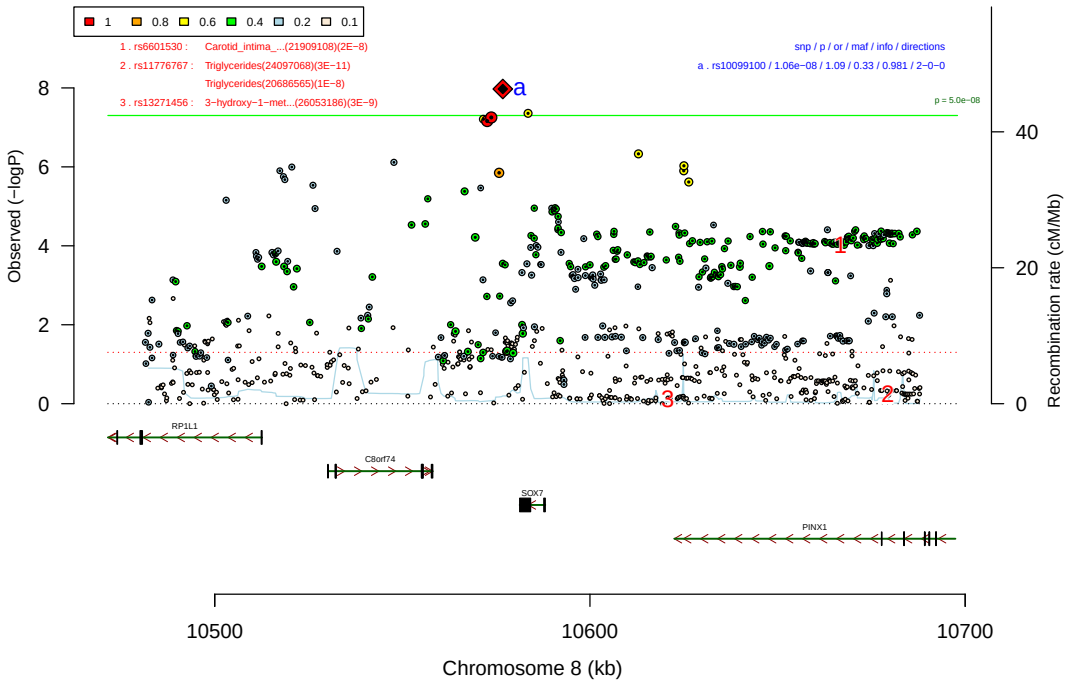

Supplementary Figure 68: Regional plot around *SOX7* for gene-based MAGMA analysis of iPSYCH-PGC meta (18 381 cases and 27 969 controls). Chromosomal position is on the horizontal axis in kb, The significance of the association expressed as $-\log_{10}(P)$ (from z-test) is plotted vertically (left axis) and the recombination rate from HapMap is shown as light blue curve (right axis). The dot size is proportional to LD between the plotted SNP and the index SNP defining the associated region. Index SNPs are marked by diamonds and labelled with letters. Colouring is based on degree of LD to that SNP as represented by r^2 (legend for r^2 is in the upper left corner). A black centre indicates that the markers is present in the 1000 Genomes Project but not in HapMap3. The green line shows the genome-wide significance level ($5 \cdot 10^{-8}$). The upper right corner show details of the index SNPs (marker name/association p-value/odds ratio for the minor allele/minor allele frequency/imputation quality/direction of effect in the two studies (N one direction - N other direction- N missing)). Loci listed in the GWAS Catalogue for other phenotypes are shown in the upper left corner (capped at 10). The green lines in the lower half show genes (based on UCSC) with black vertical lines indicating exons. Arrow heads show the direction of transcription.

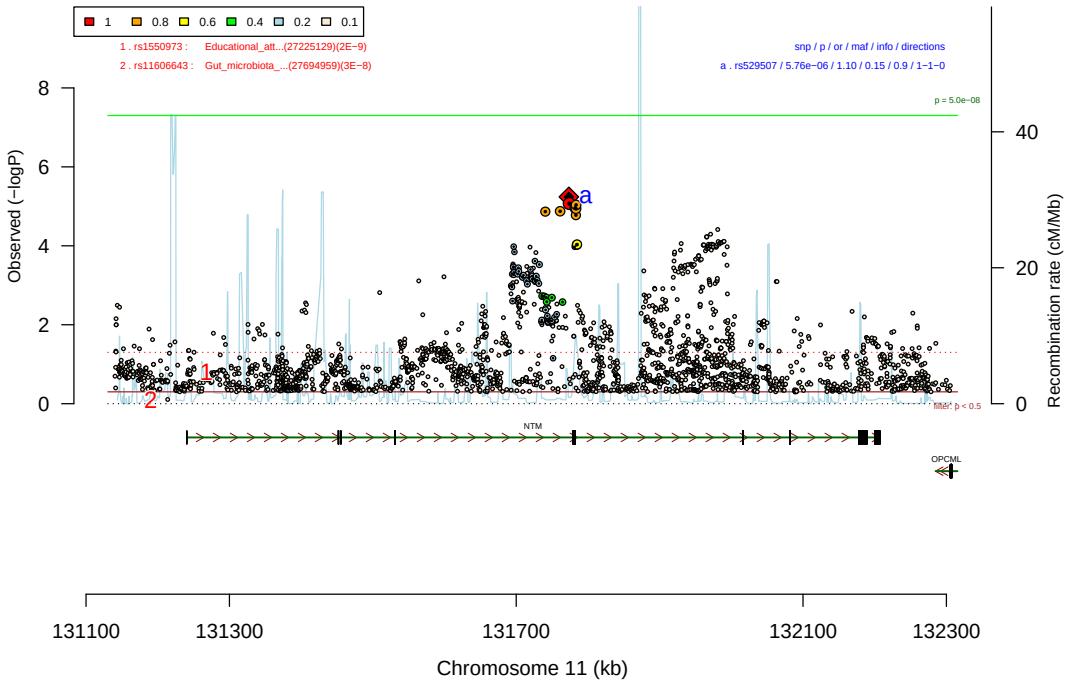

Supplementary Figure 69: Regional plot around *NTM* for gene-based MAGMA analysis of iPSYCH-PGC meta (18 381 cases and 27 969 controls). Chromosomal position is on the horizontal axis in kb, The significance of the association expressed as $-\log_{10}(P)$ (from z-test) is plotted vertically (left axis) and the recombination rate from HapMap is shown as light blue curve (right axis). The dot size is proportional to LD between the plotted SNP and the index SNP defining the associated region. Index SNPs are marked by diamonds and labelled with letters. Colouring is based on degree of LD to that SNP as represented by r^2 (legend for r^2 is in the upper left corner). A black centre indicates that the markers is present in the 1000 Genomes Project but not in HapMap3. The green line shows the genome-wide significance level ($5 \cdot 10^{-8}$). The upper right corner show details of the index SNPs (marker name/association p-value/odds ratio for the minor allele/minor allele frequency/imputation quality/direction of effect in the two studies (N one direction - N other direction- N missing)). Loci listed in the GWAS Catalogue for other phenotypes are shown in the upper left corner (capped at 10). The green lines in the lower half show genes (based on UCSC) with black vertical lines indicating exons. Arrow heads show the direction of transcription.

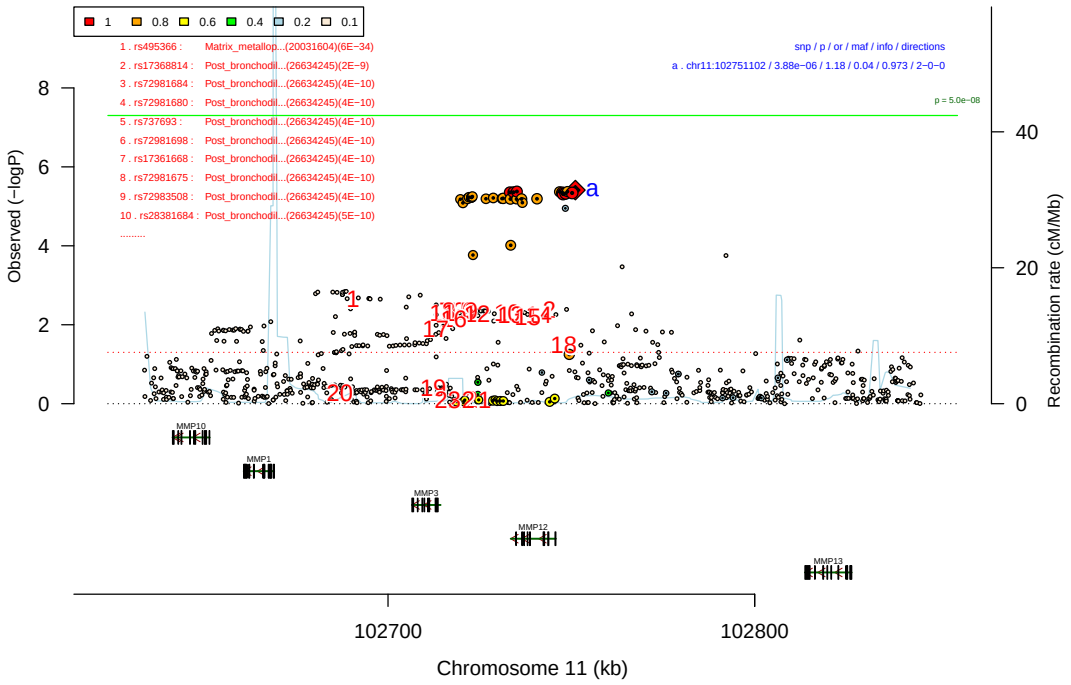

Supplementary Figure 70: Regional plot around *MMP*12 for gene-based MAGMA analysis of iPSYCH-PGC meta (18 381 cases and 27 969 controls). Chromosomal position is on the horizontal axis in kb, The significance of the association expressed as $-\log_{10}(P)$ (from z-test) is plotted vertically (left axis) and the recombination rate from HapMap is shown as light blue curve (right axis). The dot size is proportional to LD between the plotted SNP and the index SNP defining the associated region. Index SNPs are marked by diamonds and labelled with letters. Colouring is based on degree of LD to that SNP as represented by r^2 (legend for r^2 is in the upper left corner). A black centre indicates that the markers is present in the 1000 Genomes Project but not in HapMap3. The green line shows the genome-wide significance level ($5 \cdot 10^{-8}$). The upper right corner show details of the index SNPs (marker name/association p-value/odds ratio for the minor allele/minor allele frequency/imputation quality/direction of effect in the two studies (N one direction - N other direction- N missing)). Loci listed in the GWAS Catalogue for other phenotypes are shown in the upper left corner (capped at 10). The green lines in the lower half show genes (based on UCSC) with black vertical lines indicating exons. Arrow heads show the direction of transcription.

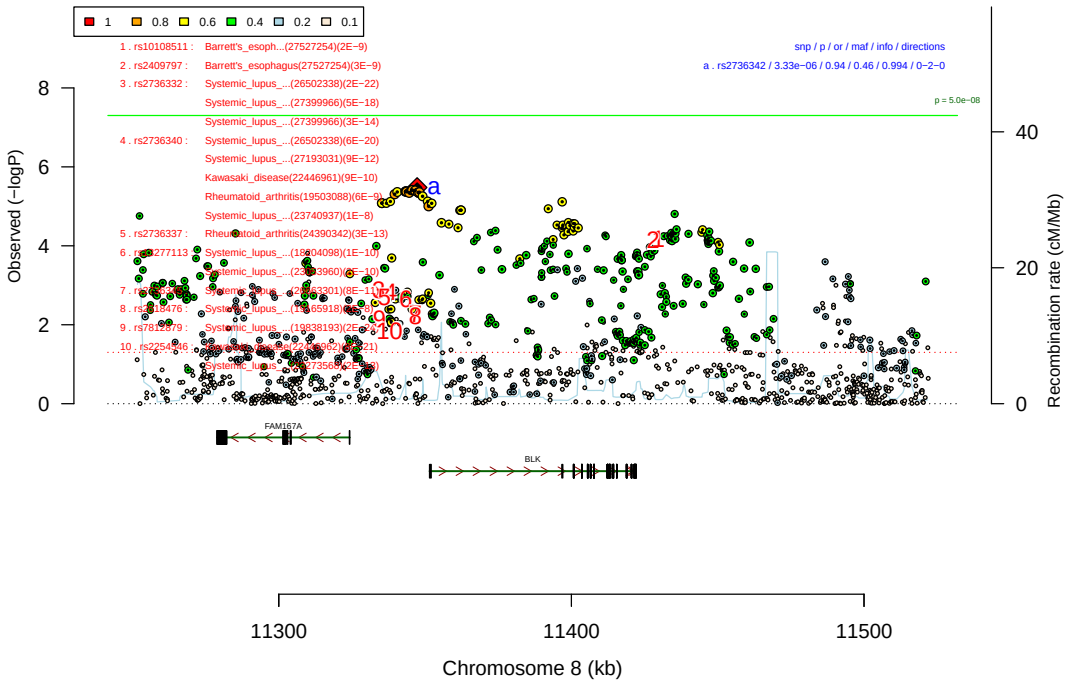

Supplementary Figure 71: Regional plot around *BLK* for gene-based MAGMA analysis of iPSYCH-PGC meta (18 381 cases and 27 969 controls). Chromosomal position is on the horizontal axis in kb, The significance of the association expressed as $-\log_{10}(P)$ (from z-test) is plotted vertically (left axis) and the recombination rate from HapMap is shown as light blue curve (right axis). The dot size is proportional to LD between the plotted SNP and the index SNP defining the associated region. Index SNPs are marked by diamonds and labelled with letters. Colouring is based on degree of LD to that SNP as represented by r^2 (legend for r^2 is in the upper left corner). A black centre indicates that the markers is present in the 1000 Genomes Project but not in HapMap3. The green line shows the genome-wide significance level ($5 \cdot 10^{-8}$). The upper right corner show details of the index SNPs (marker name/association p-value/odds ratio for the minor allele/minor allele frequency/imputation quality/direction of effect in the two studies (N one direction - N other direction- N missing)). Loci listed in the GWAS Catalogue for other phenotypes are shown in the upper left corner (capped at 10). The green lines in the lower half show genes (based on UCSC) with black vertical lines indicating exons. Arrow heads show the direction of transcription.

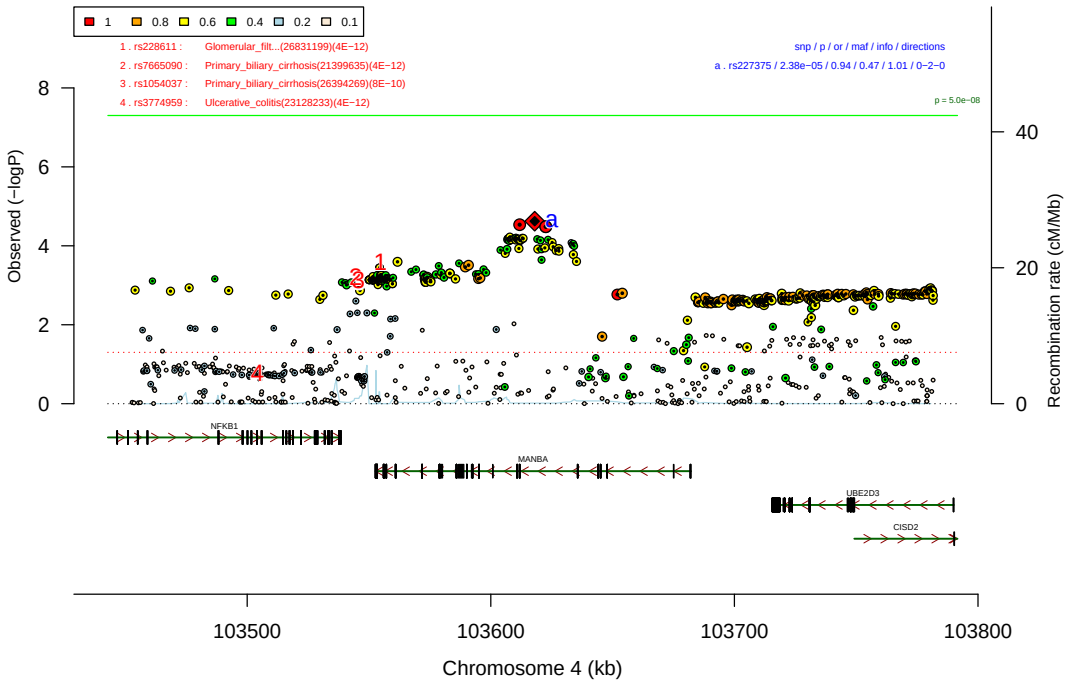

Supplementary Figure 72: Regional plot around *MANBA* for gene-based MAGMA analysis of iPSYCH-PGC meta (18 381 cases and 27 969 controls). Chromosomal position is on the horizontal axis in kb, The significance of the association expressed as $-\log_{10}(P)$ (from z-test) is plotted vertically (left axis) and the recombination rate from HapMap is shown as light blue curve (right axis). The dot size is proportional to LD between the plotted SNP and the index SNP defining the associated region. Index SNPs are marked by diamonds and labelled with letters. Colouring is based on degree of LD to that SNP as represented by r^2 (legend for r^2 is in the upper left corner). A black centre indicates that the markers is present in the 1000 Genomes Project but not in HapMap3. The green line shows the genome-wide significance level ($5 \cdot 10^{-8}$). The upper right corner show details of the index SNPs (marker name/association p-value/odds ratio for the minor allele/minor allele frequency/imputation quality/direction of effect in the two studies (N one direction - N other direction- N missing)). Loci listed in the GWAS Catalogue for other phenotypes are shown in the upper left corner (capped at 10). The green lines in the lower half show genes (based on UCSC) with black vertical lines indicating exons. Arrow heads show the direction of transcription.

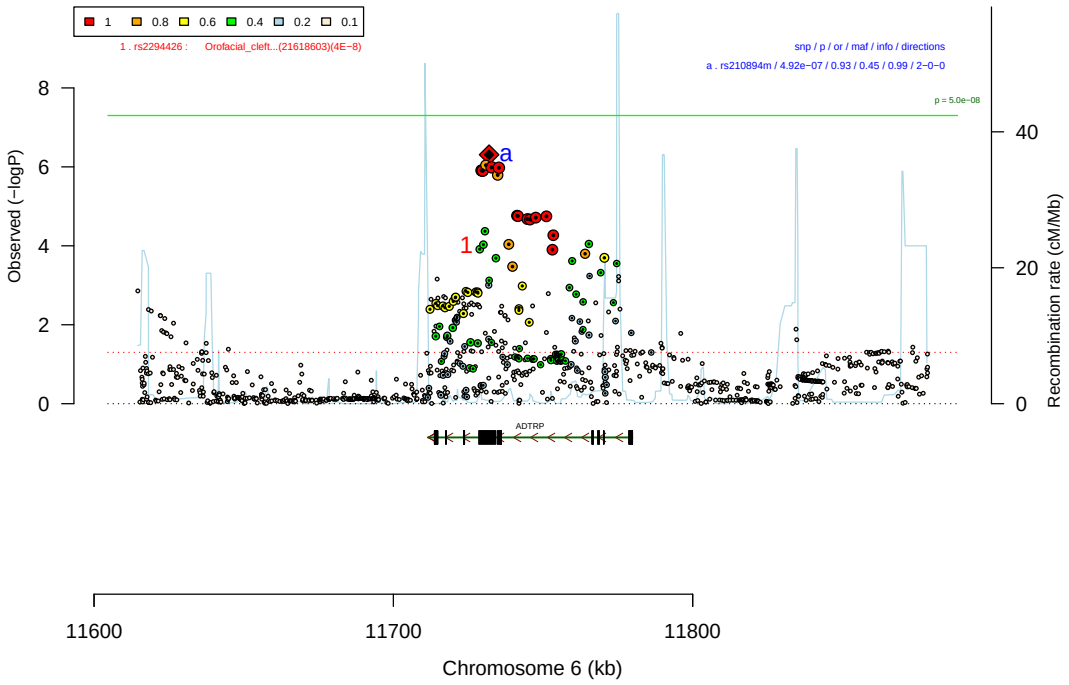

Supplementary Figure 73: Regional plot around *ADTRP* for gene-based MAGMA analysis of iPSYCH-PGC meta (18 381 cases and 27 969 controls). Chromosomal position is on the horizontal axis in kb, The significance of the association expressed as $-\log_{10}(P)$ (from z-test) is plotted vertically (left axis) and the recombination rate from HapMap is shown as light blue curve (right axis). The dot size is proportional to LD between the plotted SNP and the index SNP defining the associated region. Index SNPs are marked by diamonds and labelled with letters. Colouring is based on degree of LD to that SNP as represented by r^2 (legend for r^2 is in the upper left corner). A black centre indicates that the markers is present in the 1000 Genomes Project but not in HapMap3. The green line shows the genome-wide significance level ($5 \cdot 10^{-8}$). The upper right corner show details of the index SNPs (marker name/association p-value/odds ratio for the minor allele/minor allele frequency/imputation quality/direction of effect in the two studies (N one direction - N other direction- N missing)). Loci listed in the GWAS Catalogue for other phenotypes are shown in the upper left corner (capped at 10). The green lines in the lower half show genes (based on UCSC) with black vertical lines indicating exons. Arrow heads show the direction of transcription.

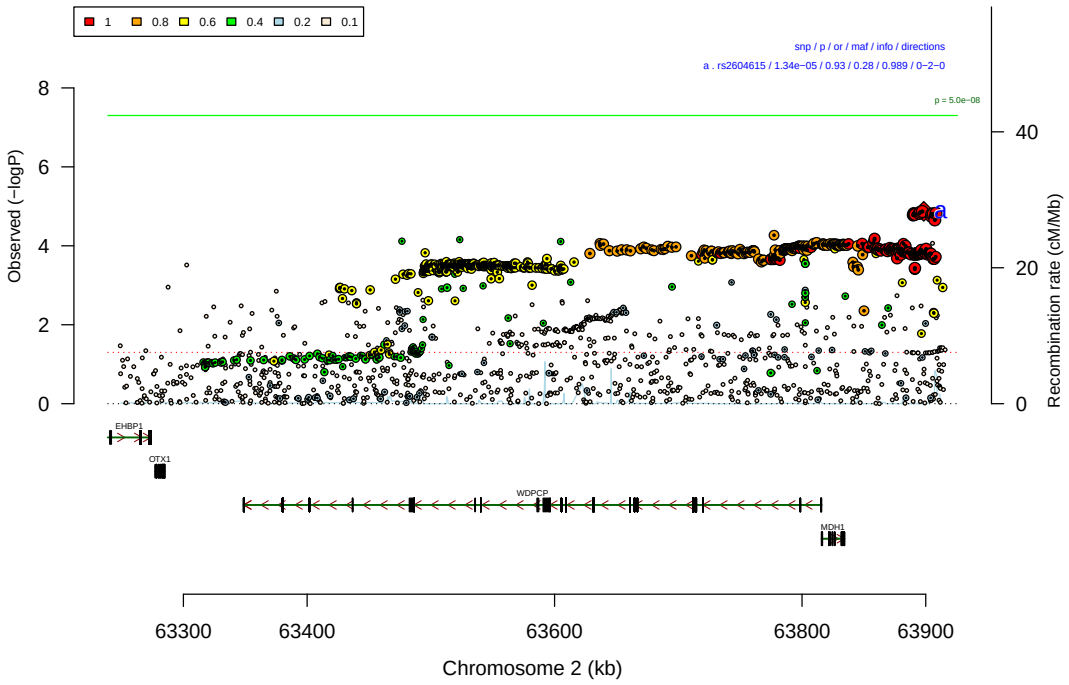

Supplementary Figure 74: Regional plot around *WDPCP* for gene-based MAGMA analysis of iPSYCH-PGC meta (18 381 cases and 27 969 controls). Chromosomal position is on the horizontal axis in kb, The significance of the association expressed as $-\log_{10}(P)$ (from z-test) is plotted vertically (left axis) and the recombination rate from HapMap is shown as light blue curve (right axis). The dot size is proportional to LD between the plotted SNP and the index SNP defining the associated region. Index SNPs are marked by diamonds and labelled with letters. Colouring is based on degree of LD to that SNP as represented by r^2 (legend for r^2 is in the upper left corner). A black centre indicates that the markers is present in the 1000 Genomes Project but not in HapMap3. The green line shows the genome-wide significance level ($5 \cdot 10^{-8}$). The upper right corner show details of the index SNPs (marker name/association p-value/odds ratio for the minor allele/minor allele frequency/imputation quality/direction of effect in the two studies (N one direction - N other direction- N missing)). The green lines in the lower half show genes (based on UCSC) with black vertical lines indicating exons. Arrow heads show the direction of transcription.

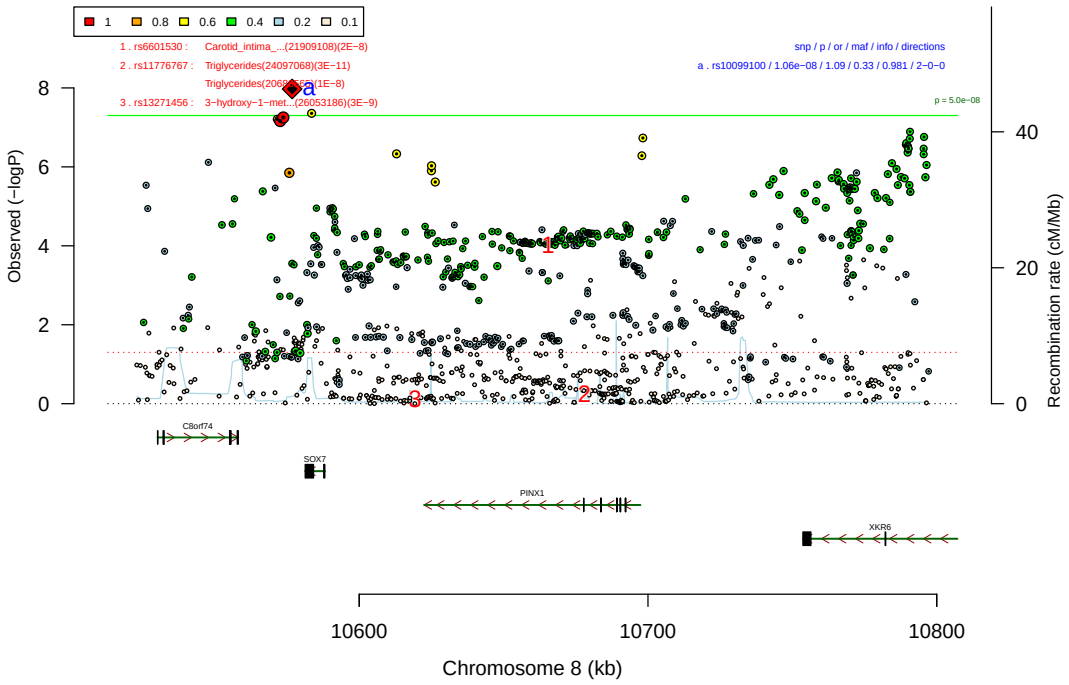

Supplementary Figure 75: Regional plot around *PINX*1 for gene-based MAGMA analysis of iPSYCH-PGC meta (18 381 cases and 27 969 controls). Chromosomal position is on the horizontal axis in kb, The significance of the association expressed as $-\log_{10}(\mathrm{P})$ (from z-test) is plotted vertically (left axis) and the recombination rate from HapMap is shown as light blue curve (right axis). The dot size is proportional to LD between the plotted SNP and the index SNP defining the associated region. Index SNPs are marked by diamonds and labelled with letters. Colouring is based on degree of LD to that SNP as represented by r^2 (legend for r^2 is in the upper left corner). A black centre indicates that the markers is present in the 1000 Genomes Project but not in HapMap3. The green line shows the genome-wide significance level ($5 \cdot 10^{-8}$). The upper right corner show details of the index SNPs (marker name/association p-value/odds ratio for the minor allele/minor allele frequency/imputation quality/direction of effect in the two studies (N one direction - N other direction- N missing)). Loci listed in the GWAS Catalogue for other phenotypes are shown in the upper left corner (capped at 10). The green lines in the lower half show genes (based on UCSC) with black vertical lines indicating exons. Arrow heads show the direction of transcription.

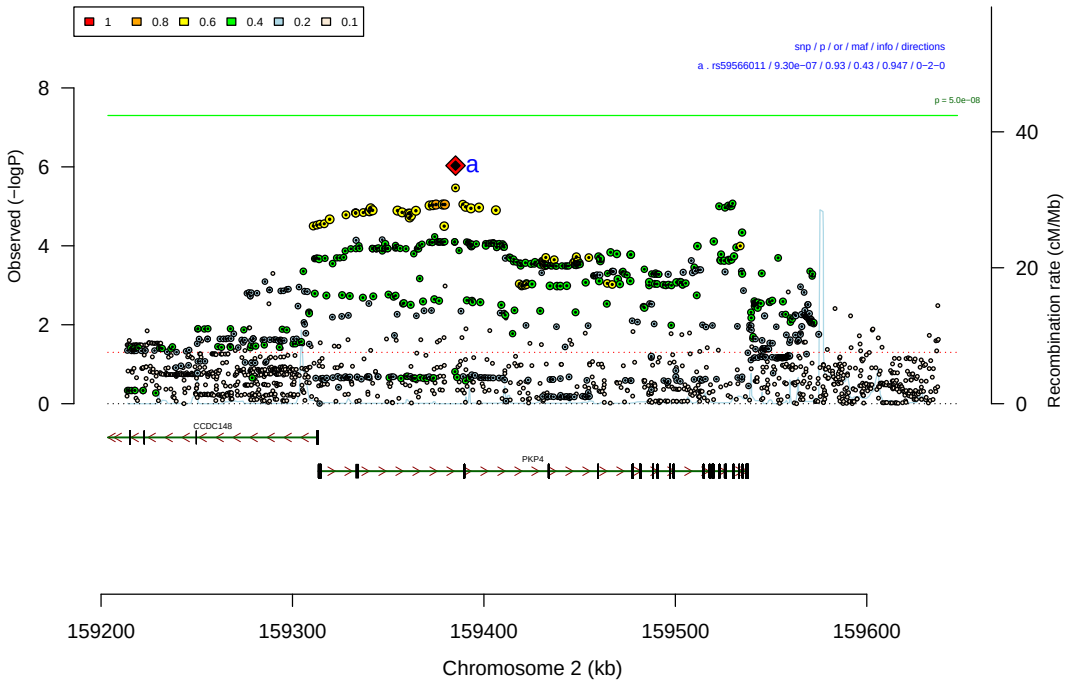

Supplementary Figure 76: Regional plot around *PKP*4 for gene-based MAGMA analysis of iPSYCH-PGC meta (18 381 cases and 27 969 controls). Chromosomal position is on the horizontal axis in kb, The significance of the association expressed as $-\log_{10}(\mathrm{P})$ (from z-test) is plotted vertically (left axis) and the recombination rate from HapMap is shown as light blue curve (right axis). The dot size is proportional to LD between the plotted SNP and the index SNP defining the associated region. Index SNPs are marked by diamonds and labelled with letters. Colouring is based on degree of LD to that SNP as represented by r^2 (legend for r^2 is in the upper left corner). A black centre indicates that the markers is present in the 1000 Genomes Project but not in HapMap3. The green line shows the genome-wide significance level ($5 \cdot 10^{-8}$). The upper right corner show details of the index SNPs (marker name/association p-value/odds ratio for the minor allele/minor allele frequency/imputation quality/direction of effect in the two studies (N one direction - N other direction- N missing)). The green lines in the lower half show genes (based on UCSC) with black vertical lines indicating exons. Arrow heads show the direction of transcription.

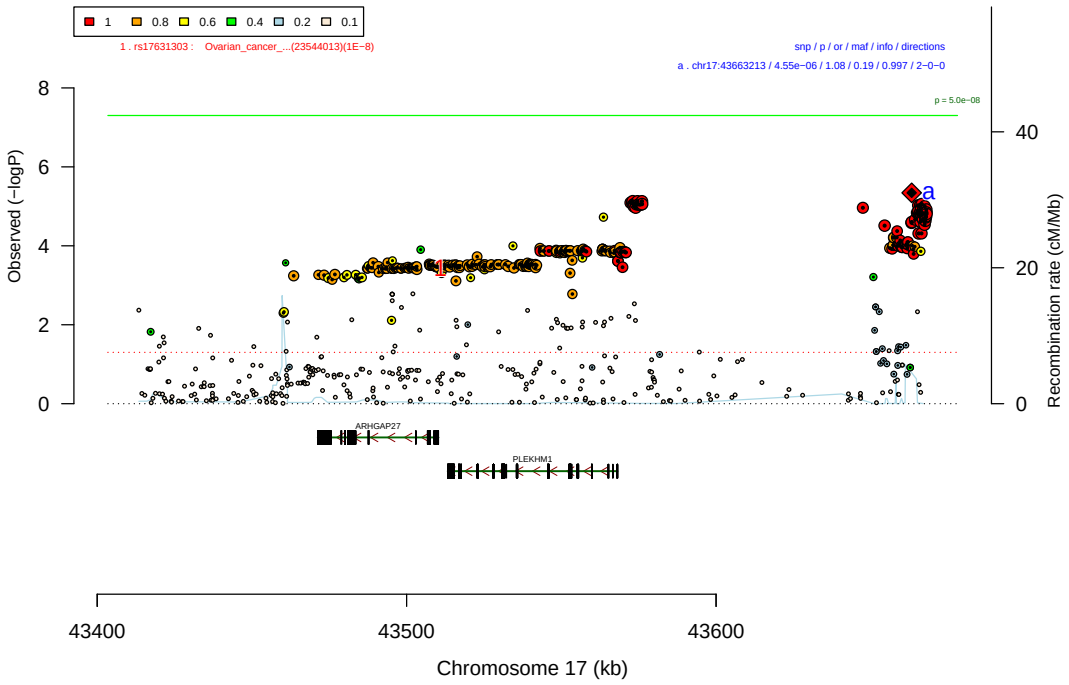

Supplementary Figure 77: Regional plot around *PLEKHM1* for gene-based MAGMA analysis of iPSYCH-PGC meta (18 381 cases and 27 969 controls). Chromosomal position is on the horizontal axis in kb, The significance of the association expressed as $-\log_{10}(P)$ (from z-test) is plotted vertically (left axis) and the recombination rate from HapMap is shown as light blue curve (right axis). The dot size is proportional to LD between the plotted SNP and the index SNP defining the associated region. Index SNPs are marked by diamonds and labelled with letters. Colouring is based on degree of LD to that SNP as represented by r^2 (legend for r^2 is in the upper left corner). A black centre indicates that the markers is present in the 1000 Genomes Project but not in HapMap3. The green line shows the genome-wide significance level ($5 \cdot 10^{-8}$). The upper right corner show details of the index SNPs (marker name/association p-value/odds ratio for the minor allele/minor allele frequency/imputation quality/direction of effect in the two studies (N one direction - N other direction- N missing)). Loci listed in the GWAS Catalogue for other phenotypes are shown in the upper left corner (capped at 10). The green lines in the lower half show genes (based on UCSC) with black vertical lines indicating exons. Arrow heads show the direction of transcription.

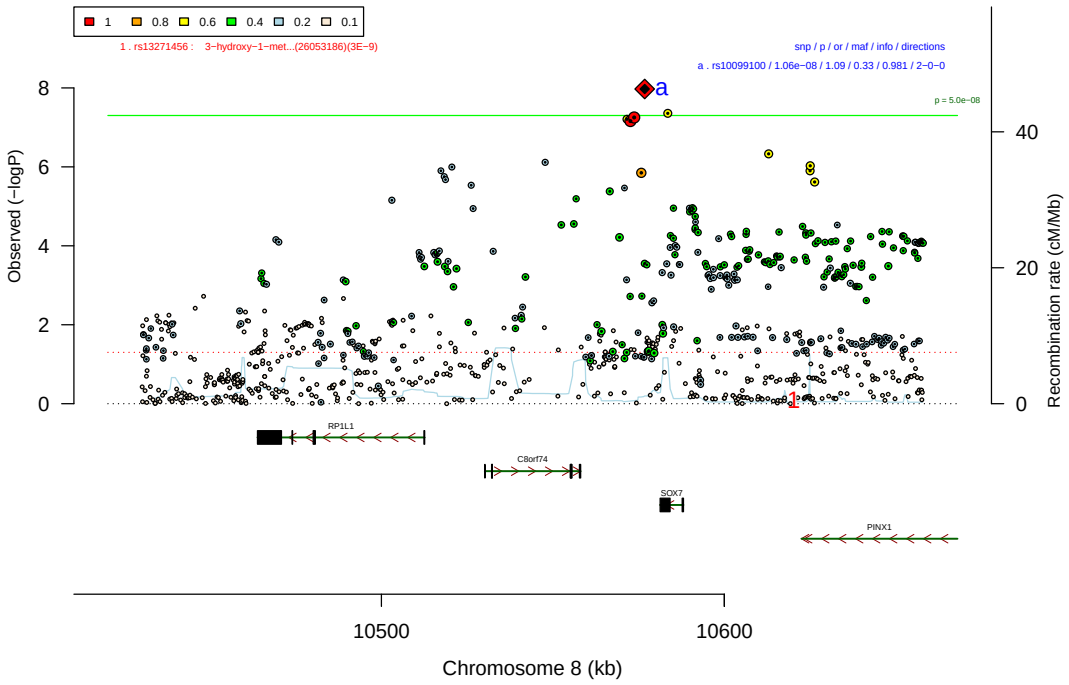

Supplementary Figure 78: Regional plot around *C8orf74* for gene-based MAGMA analysis of iPSYCH-PGC meta (18 381 cases and 27 969 controls). Chromosomal position is on the horizontal axis in kb, The significance of the association expressed as $-\log_{10}(P)$ (from z-test) is plotted vertically (left axis) and the recombination rate from HapMap is shown as light blue curve (right axis). The dot size is proportional to LD between the plotted SNP and the index SNP defining the associated region. Index SNPs are marked by diamonds and labelled with letters. Colouring is based on degree of LD to that SNP as represented by r^2 (legend for r^2 is in the upper left corner). A black centre indicates that the markers is present in the 1000 Genomes Project but not in HapMap3. The green line shows the genome-wide significance level ($5 \cdot 10^{-8}$). The upper right corner show details of the index SNPs (marker name/association p-value/odds ratio for the minor allele/minor allele frequency/imputation quality/direction of effect in the two studies (N one direction - N other direction- N missing)). Loci listed in the GWAS Catalogue for other phenotypes are shown in the upper left corner (capped at 10). The green lines in the lower half show genes (based on UCSC) with black vertical lines indicating exons. Arrow heads show the direction of transcription.

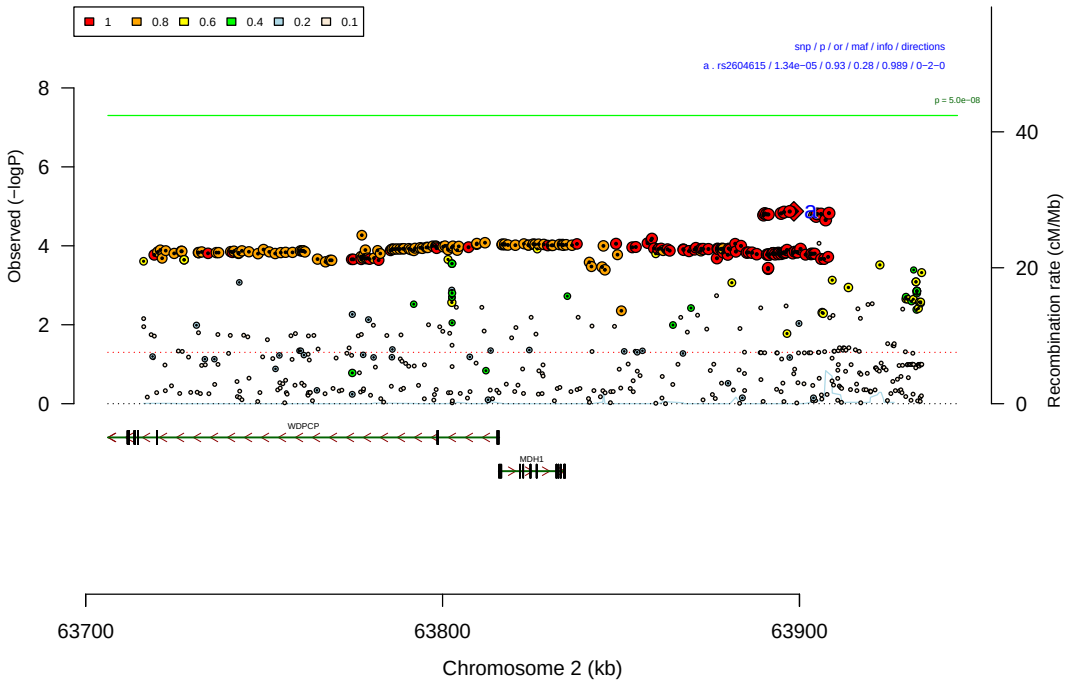

Supplementary Figure 79: Regional plot around *MDH1* for gene-based MAGMA analysis of iPSYCH-PGC meta (18 381 cases and 27 969 controls). Chromosomal position is on the horizontal axis in kb, The significance of the association expressed as $-\log_{10}(P)$ (from z-test) is plotted vertically (left axis) and the recombination rate from HapMap is shown as light blue curve (right axis). The dot size is proportional to LD between the plotted SNP and the index SNP defining the associated region. Index SNPs are marked by diamonds and labelled with letters. Colouring is based on degree of LD to that SNP as represented by r^2 (legend for r^2 is in the upper left corner). A black centre indicates that the markers is present in the 1000 Genomes Project but not in HapMap3. The green line shows the genome-wide significance level ($5 \cdot 10^{-8}$). The upper right corner show details of the index SNPs (marker name/association p-value/odds ratio for the minor allele/minor allele frequency/imputation quality/direction of effect in the two studies (N one direction - N other direction- N missing)). The green lines in the lower half show genes (based on UCSC) with black vertical lines indicating exons. Arrow heads show the direction of transcription.

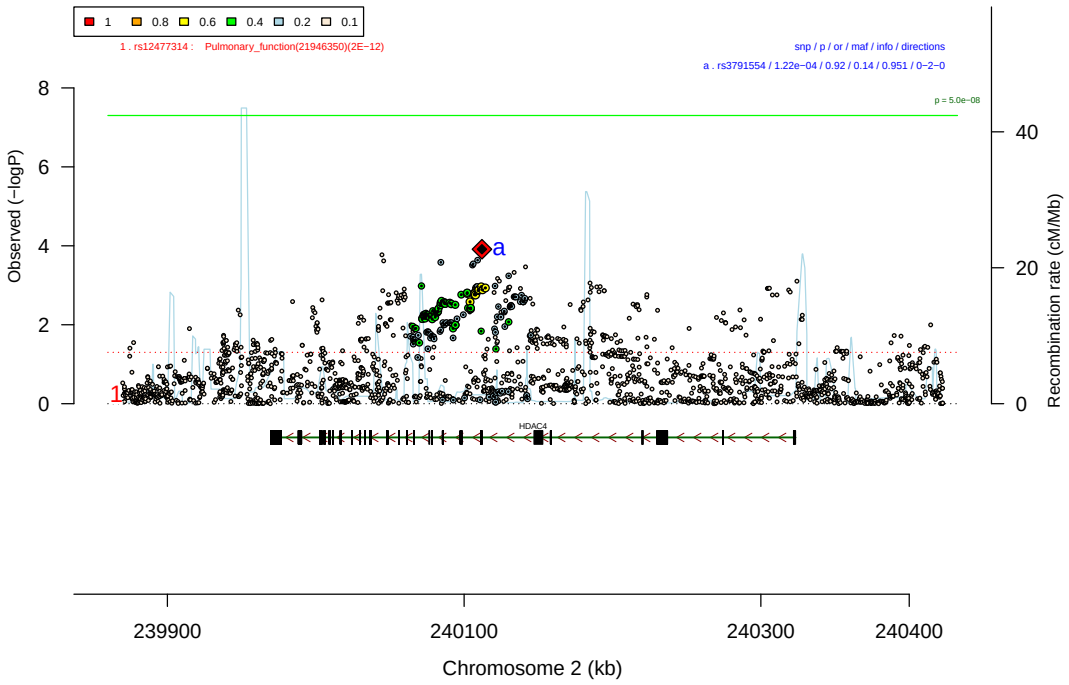

Supplementary Figure 80: Regional plot around *HDAC*4 for gene-based MAGMA analysis of iPSYCH-PGC meta (18 381 cases and 27 969 controls). Chromosomal position is on the horizontal axis in kb, The significance of the association expressed as $-\log_{10}(P)$ (from z-test) is plotted vertically (left axis) and the recombination rate from HapMap is shown as light blue curve (right axis). The dot size is proportional to LD between the plotted SNP and the index SNP defining the associated region. Index SNPs are marked by diamonds and labelled with letters. Colouring is based on degree of LD to that SNP as represented by r^2 (legend for r^2 is in the upper left corner). A black centre indicates that the markers is present in the 1000 Genomes Project but not in HapMap3. The green line shows the genome-wide significance level ($5 \cdot 10^{-8}$). The upper right corner show details of the index SNPs (marker name/association p-value/odds ratio for the minor allele/minor allele frequency/imputation quality/direction of effect in the two studies (N one direction - N other direction- N missing)). Loci listed in the GWAS Catalogue for other phenotypes are shown in the upper left corner (capped at 10). The green lines in the lower half show genes (based on UCSC) with black vertical lines indicating exons. Arrow heads show the direction of transcription.

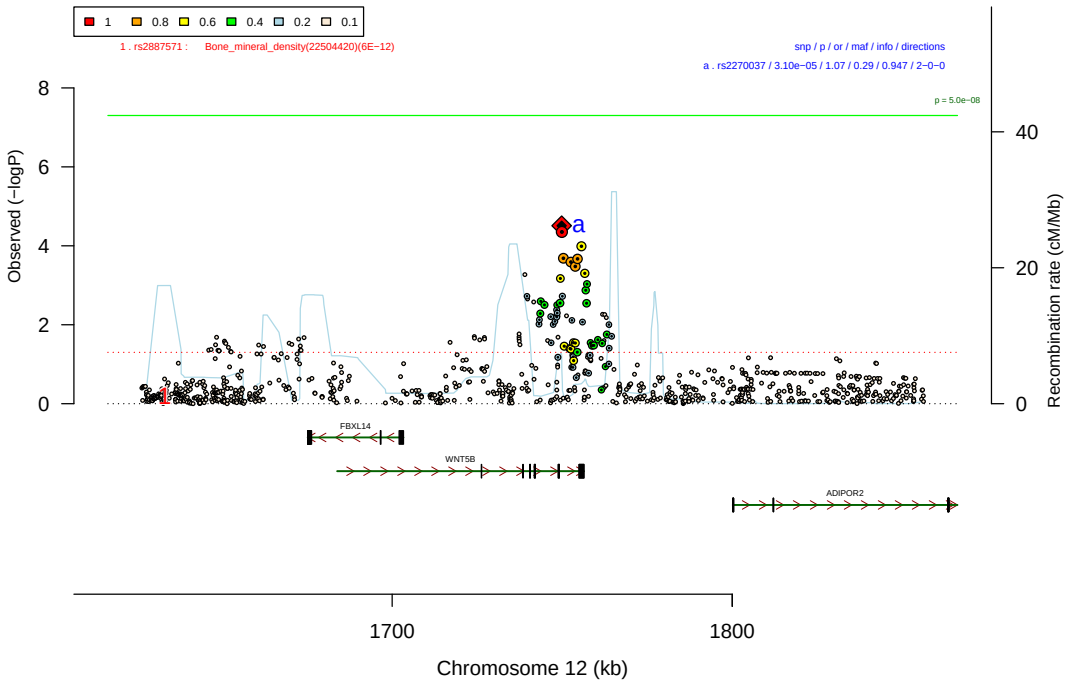

Supplementary Figure 81: Regional plot around *WNT5B* for gene-based MAGMA analysis of iPSYCH-PGC meta (18 381 cases and 27 969 controls). Chromosomal position is on the horizontal axis in kb, The significance of the association expressed as $-\log_{10}(P)$ (from z-test) is plotted vertically (left axis) and the recombination rate from HapMap is shown as light blue curve (right axis). The dot size is proportional to LD between the plotted SNP and the index SNP defining the associated region. Index SNPs are marked by diamonds and labelled with letters. Colouring is based on degree of LD to that SNP as represented by r^2 (legend for r^2 is in the upper left corner). A black centre indicates that the markers is present in the 1000 Genomes Project but not in HapMap3. The green line shows the genome-wide significance level ($5 \cdot 10^{-8}$). The upper right corner show details of the index SNPs (marker name/association p-value/odds ratio for the minor allele/minor allele frequency/imputation quality/direction of effect in the two studies (N one direction - N other direction- N missing)). Loci listed in the GWAS Catalogue for other phenotypes are shown in the upper left corner (capped at 10). The green lines in the lower half show genes (based on UCSC) with black vertical lines indicating exons. Arrow heads show the direction of transcription.

4.2 Polygenic qualities of ASD and its subtypes

4.2.1 Heritability and genetic correlation across subtypes

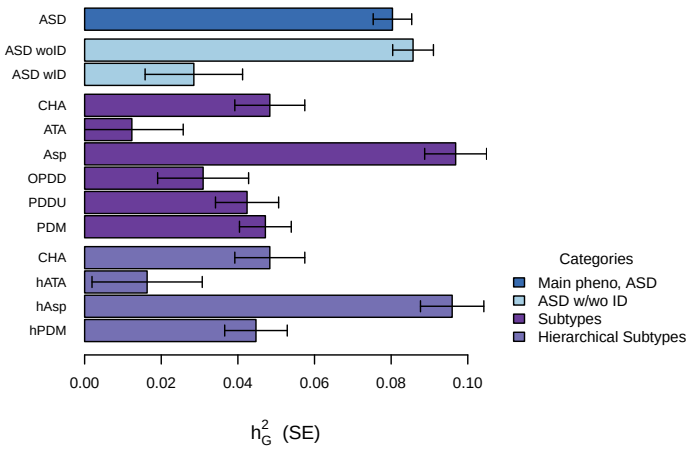

Supplementary Figure 82: Heritability estimates on the liability scale for subtypes and substrata of ASD as estimated by GCTA. Error bars show standard errors. The number of samples are: ASD 13 076, ASD wID 1 873, ASD woID 11 203, CHA and hCHA 3 310, ATA 1 607, Asp 4 622, OPDD 2 042, PDDU 3 753, PDM 5 460, hATA 1 494, hAsp 4 417, hPDM 3 855. For tabulated details, look up Table 14.

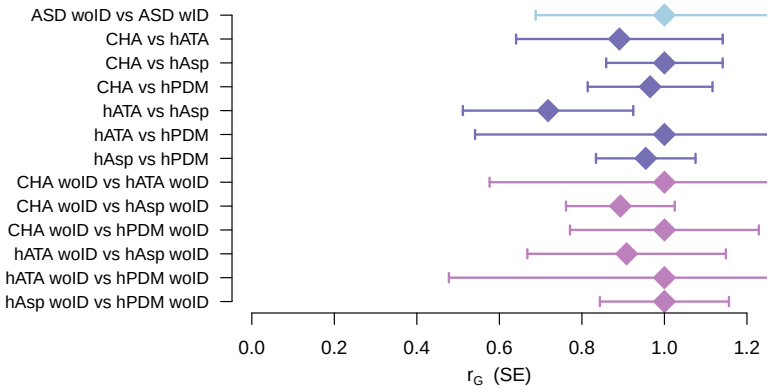

Supplementary Figure 83: GCTA based estimates of genetic correlation, r_G, between ASD subtypes internally in iPSYCH ASD GWAS. Error bars designate standard errors. The number of samples are: ASD 13 076, ASD wID 1 873, ASD woID 11 203, CHA and hCHA 3 310, ATA 1 607, Asp 4 622, OPDD 2 042, PDDU 3 753, PDM 5 460, hATA 1 494, hAsp 4 417, hPDM 3 855. For tabulated details see Table 15.

4.2.2 Multivariate regression

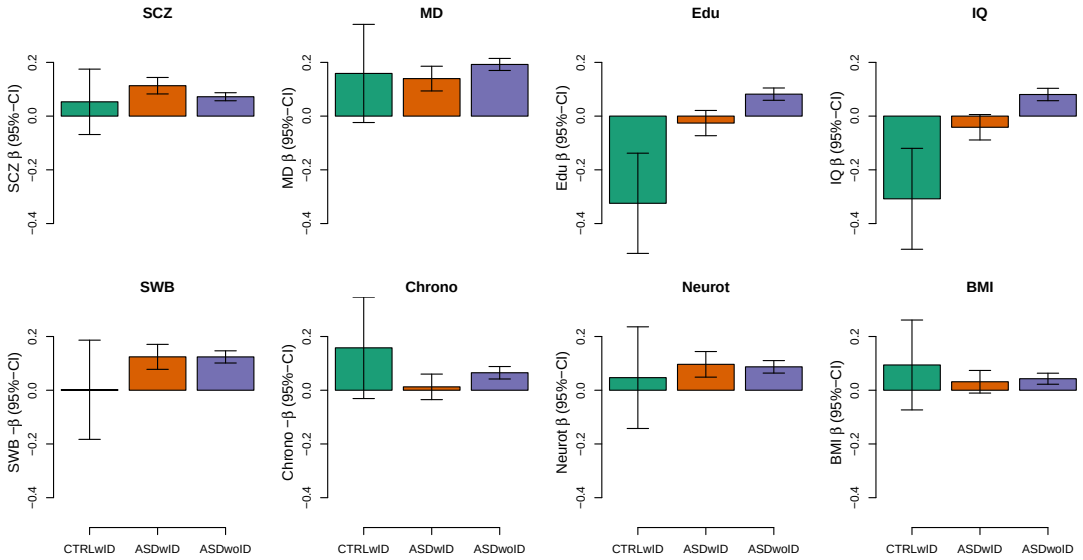

Supplementary Figure 84: Multivariate regression of normalized PRS on ID and ASD subtypes. Controls without ID (22 555) is reference group and the other groups are controls with ID (109), ASD with ID (2 358) and ASD without ID (11 203). The regession is adjusted for waves and relevant PCs, whiskers indicate 95%-CIs). The phenotypes are schizophrenia[8], major depression[48] (both with the Danish samples removed), educational attainment[50], IQ[83], subjective well-being[62] (−1·score), chronotype[63] (−1·score), neuroticism[62], and BMI[236] (−1·score). Beware that the orientation of the scores for subjective well-being, chronotype and BMI have been switched to improve graphical presentation.

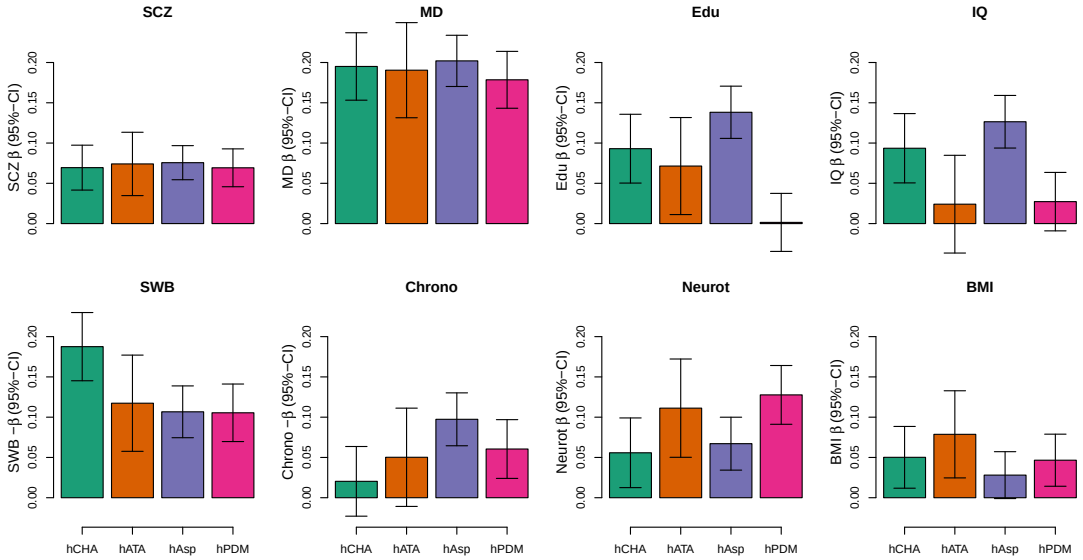

Supplementary Figure 85: Multivariate regression of normalized PRS on hierarchical ASD subtypes without ID (controls is reference group (22 555) and the regession is adjusted for waves and relevant PCs, whiskers indicate 95%-CIs, hCHA 2 358, hATA 1,099, hAsp 4,343, and hPDM 3,403). The plot shows what happens to Figure 3 in the main manuscript when restricting to individuals without ID. Analogous to the analysis including also ID, we find that there is significant heterogeneity across certain subtypes albeit slightly weaker: educational attainment $P = 5.3 \cdot 10^{-8}$, IQ $P = 4.7 \cdot 10^{-5}$, neuroticism $P = 0.017$, chronotype $P = 0.025$ and subjective well-being $P = 0.0064$ (linear hypotheses tested using the Pillai test). The phenotypes are schizophrenia[8], major depression[48] (both with the Danish samples removed), educational attainment[50], IQ[83], subjective well-being[62] (−1·score), chronotype[63] (−1·score), neuroticism[62], and BMI[236] (−1·score). Beware that the orientation of the scores for subjective well-being, chronotype and BMI have been switched to improve graphical presentation.

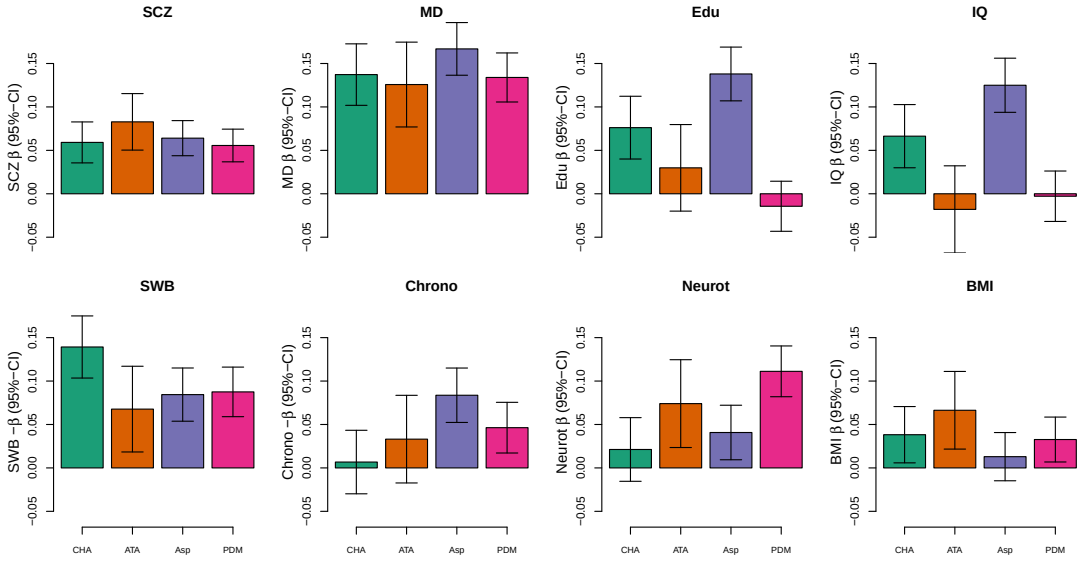

Supplementary Figure 86: Multivariate regression of normalized PRS on the original (non-hierarchical) ASD subtypes. Controls constitute reference group (22 664) and the subtypes are childhood autism (3 310), atypical autism (1 607), Asperger's (4 622), and the two pervasive disorder types comined (5 460). The regession is adjusted for waves and relevant PCs, whiskers indicate 95%-CIs. The plot shows what happens to Figure 3 in the main manuscript when regressing on the original subtypes that includes overlaps. We see that construction of the hierarchical subtypes (and the order in which it is done) does little to change the overall pattern. The phenotypes are schizophrenia[8], major depression[48] (both with the Danish samples removed), educational attainment[50], IQ[83], subjective well-being[62] (−1·score), chronotype[63] (−1·score), neuroticism[62], and BMI[236] (−1·score). Beware that the orientation of the scores for subjective well-being, chronotype and BMI have been switched to improve graphical presentation.

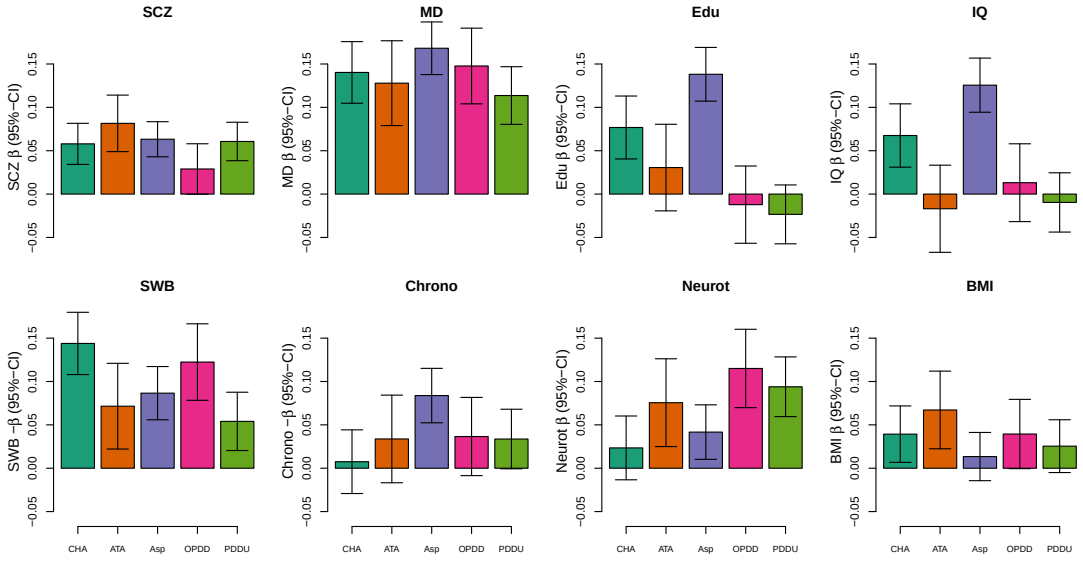

Supplementary Figure 87: Multivariate regression of normalized PRS on the original non-hierarchical ASD subtypes before lumping the two pervasive disorder subtypes Controls constitute reference group (22 664) and the subtypes are childhood autism (3 310), atypical autism (1 607), Asperger's (4 622), other pervasive devopmental disorder (2 042), and pervasive developmental disorder, unspecified (3 753). The regession is adjusted for waves and relevant PCs, whiskers indicate 95%-CIs. The plot shows what happens to Figure 86 when separating the two pervasive disorder subtypes. The overall pattern remains the same, and analogous to the analysis on grouped hierarchical subtypes. The phenotypes are schizophrenia[8], major depression[48] (both with the Danish samples removed), educational attainment[50], IQ[83], subjective well-being[62] (−1·score), chronotype[63] (−1·score), neuroticism[62], and BMI[236] (−1·score). Beware that the orientation of the scores for subjective well-being, chronotype and BMI have been switched to improve graphical presentation.

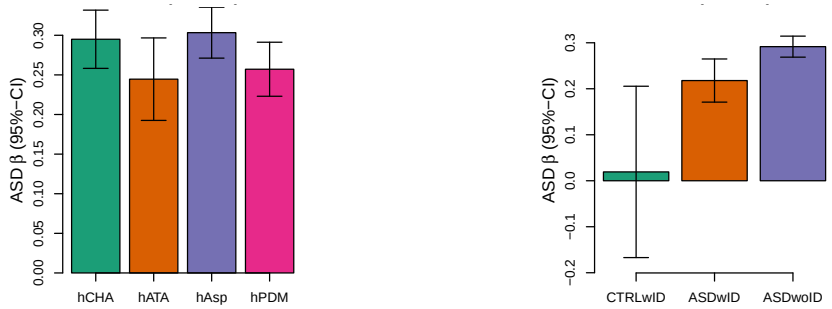

Supplementary Figure 88: Regression of the internally trained ASD PRS on hierarchical subypes (left) and ID/ASD subtypes (right). In both panels the regession is adjusted for waves and relevant PCs, and the whiskers indicate 95%-CIs. In the left panel, the reference group consists of all controls (22,664) and subtypes are the hierarchically defined subtypes for childhood autism (hCHA, N = 3,310), atypical autism (hATA, N = 1,494), Asperger's (hAsp, N = 4,417), and the lumped pervasive disorders developmental group (hPDM, N = 3,855). In the right panel, the reference groups is restricted to controls without ID (22 555), and the subtypes are controls with ID (109), ASD with ID (2 358) and ASD without ID (11 203).

4.2.3 Internally generated PRS

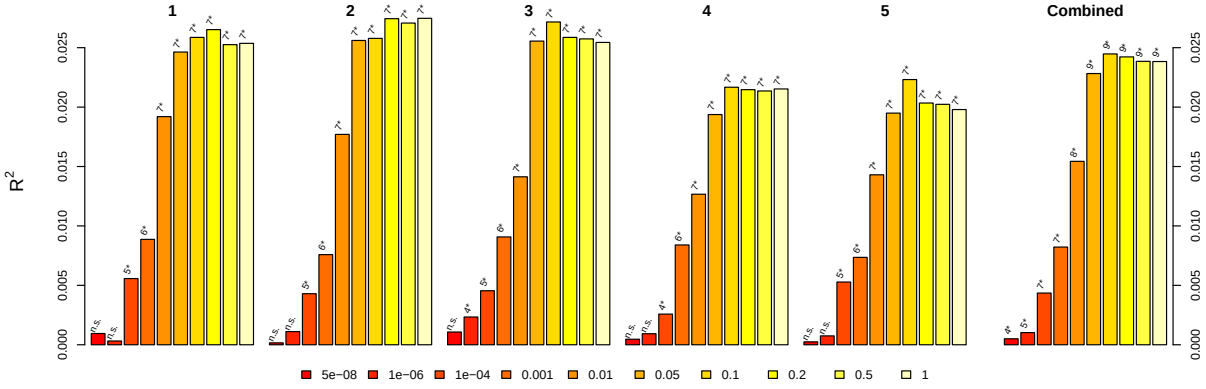

Supplementary Figure 89: Nagelkerke R^2 of PRS trained internally on leave-one-group-out and the PGC ASD shown here when estimated on each of the five groups left out when training as well as on the combined sample (cases/controls in groups 1: 2 624/3 694, 2: 2 622/5 432, 3: 2 611/4 666, 4: 2 583/4 360, 5: 2 636/4 512, and in total 13 076/22 664). Colouring is as shown in the legend signifying the 10 different p-value cut-off in the training set.

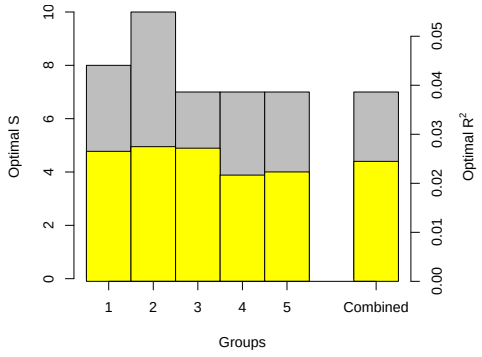

Supplementary Figure 90: Summarizing optimal Nagelkerke R^2 in target set (yellow, right axis) and p-value threshold in training set (grey, left axis) for internally trained leave-one-group-out ASD score across the groups as well as on the combined sample (cases/controls in groups 1: 2 624/3 694, 2: 2 622/5 432, 3: 2 611/4 666, 4: 2 583/4 360, 5: 2 636/4 512, and in total 13 076/22 664). In for most groups as well as for the combined analysis on the full data set, the 7th p-value threshold of 0.1 is the optimal cut point.

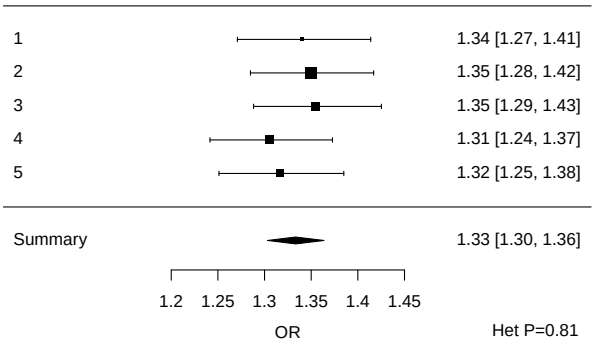

Supplementary Figure 91: Forest plot of effect of the internally trained leave-one-group-out ASD scores as continuous measure with 95%-confidence intervals (cases/controls in groups 1: 2 624/3 694, 2: 2 622/5 432, 3: 2 611/4 666, 4: 2 583/4 360, 5: 2 636/4 512, and in total 13 076/22 664). The score used here are for the p-value threshold S=7, p=0.1.

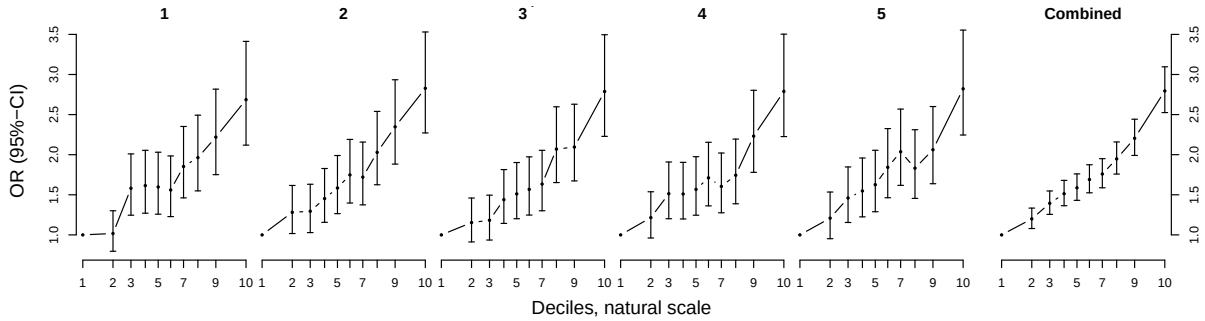

Supplementary Figure 92: Decile plots of internal ASD score over groups. The plot show odds ratio at each score decile relative to the first in the first five panels for the results in each of the 5 groups, and in the last panel the results of regressing the combined score in the full sample (right axis is a identical the left, cases/controls in groups 1: 2 624/3 694, 2: 2 622/5 432, 3: 2 611/4 666, 4: 2 583/4 360, 5: 2 636/4 512, and in total 13 076/22 664). The score used here is for the p-value threshold S=7, p=0.1.

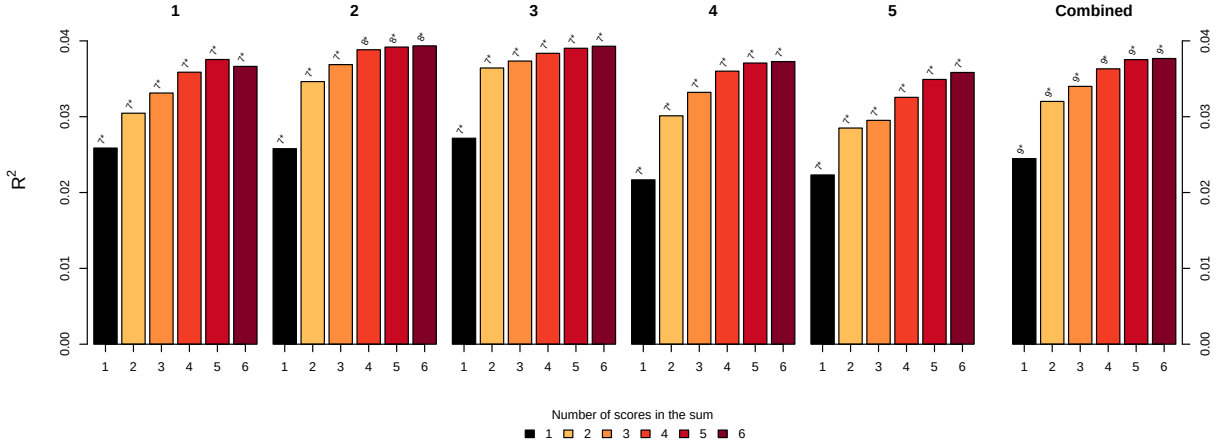

Supplementary Figure 93: Nagelkerke R^2 for multi-phenotype scores presented across leave-out-groups and on the full sample (cases/controls in groups 1: 2 624/3 694, 2: 2 622/5 432, 3: 2 611/4 666, 4: 2 583/4 360, 5: 2 636/4 512, and in total 13 076/22 664). Starting with the internally trained ASD score (S=7,p=0.1) new scores are successively generated by adding terms in a weighted sums of scores for 2 Major depression[48], 3 Subjective Well-Being[62], 4 Schizophrenia[8], 5 Educational attainment[50], 6 Chronotyp[63]. Each colour coded bar give the Nagelkerke R^2 for the weighted sum of that many scores as a predictor for ASD in our sample.

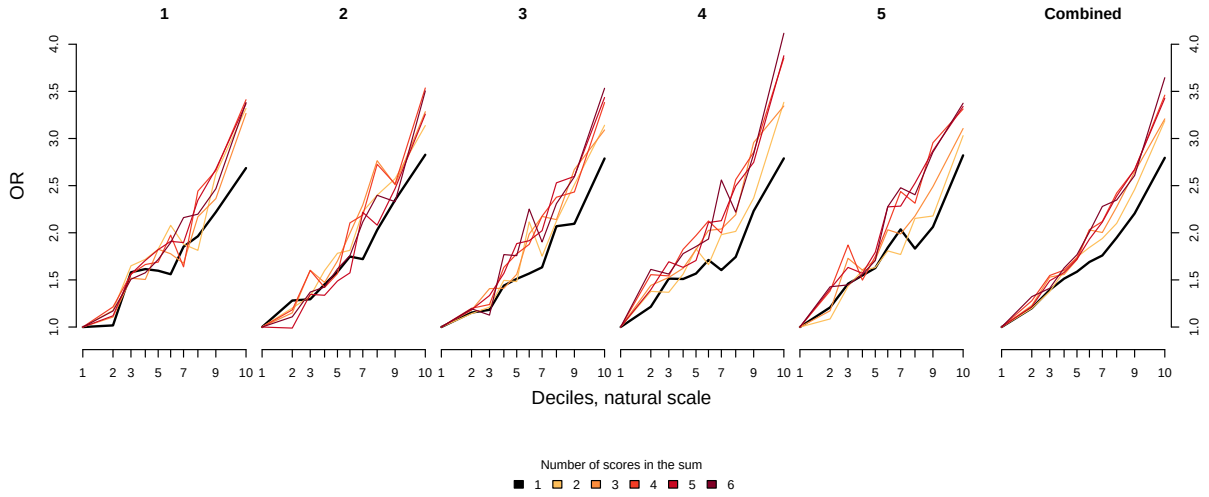

Supplementary Figure 94: Decile plots for multi-phenotype scores over groups on the complete sample (cases/controls in groups 1: 2 624/3 694, 2: 2 622/5 432, 3: 2 611/4 666, 4: 2 583/4 360, 5: 2 636/4 512, and in total 13 076/22 664). The plot show for each group and combined to the full sample, the odds ratio at each score decile relative to the first (right axis is a identical the left). Starting with the internally trained ASD score (S=7,p=0.1) new scores are successively generated by adding terms in a weighted sums of scores for 2 Major depression[48], 3 Subjective Well-Being[62], 4 Schizophrenia[8], 5 Educational attainment[50], 6 Chronotyp[63].

4.2.4 Functional and tissue specific enrichment

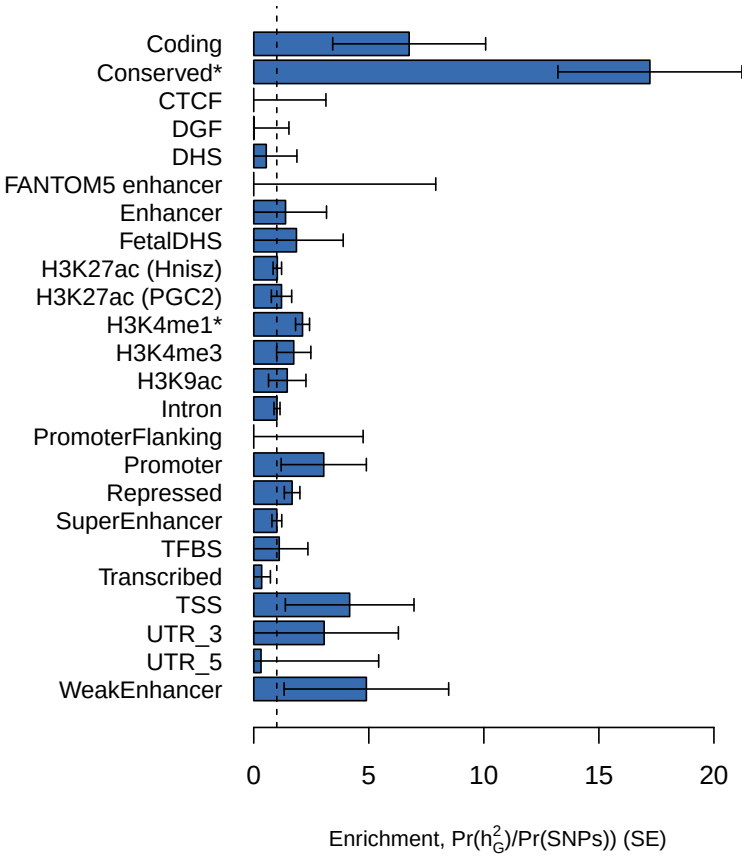

Supplementary Figure 95: Enrichment estimates by LDSC for the 24 main annotations from [58] and based on the main ASD scan of 18 381 cases and 27 969 controls. The error bars represent jackknife standard errors around the estimates of enrichment, the dashed line designate the neutral scenario or no enrichment, and significance (from z-scores as described in [58]) at α-level 0.05 after Bonferroni correction for the 24 hypotheses tested is indicated by an asterisk at the name.

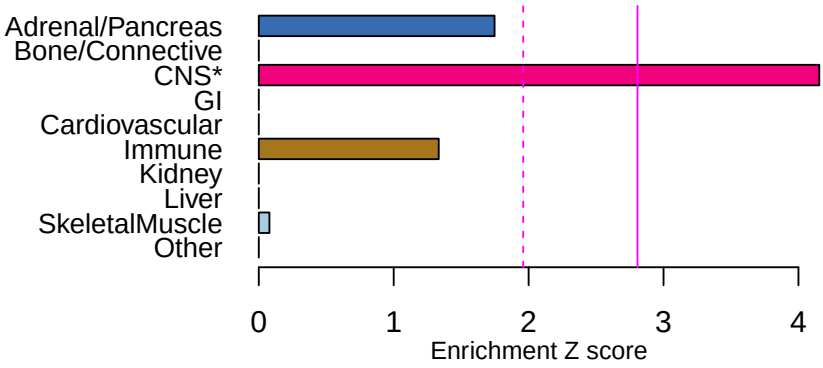

Supplementary Figure 96: Tissue enrichment based on LDSC, using the original cell type annotation of LDSC. The dashed magenta line indicates statistical significance at α-level 0.05 and the solid line significance after Bonferroni correction for the number of tissues tested (significance from z-test). Tissues achieving global statistical significance are marked by an asterisk.

Supplementary Figure 97: Tissue enrichment based on LDSC and roadmap h3k4me1 cell type annotation[59, 60]. The dashed magenta line indicates statistical significance at α-level 0.05 and the solid line significance after Bonferroni correction for the number of tissues tested (significance from z-test). Tissues achieving global statistical significance are marked by an asterisk.

4.3 Hi-C analysis

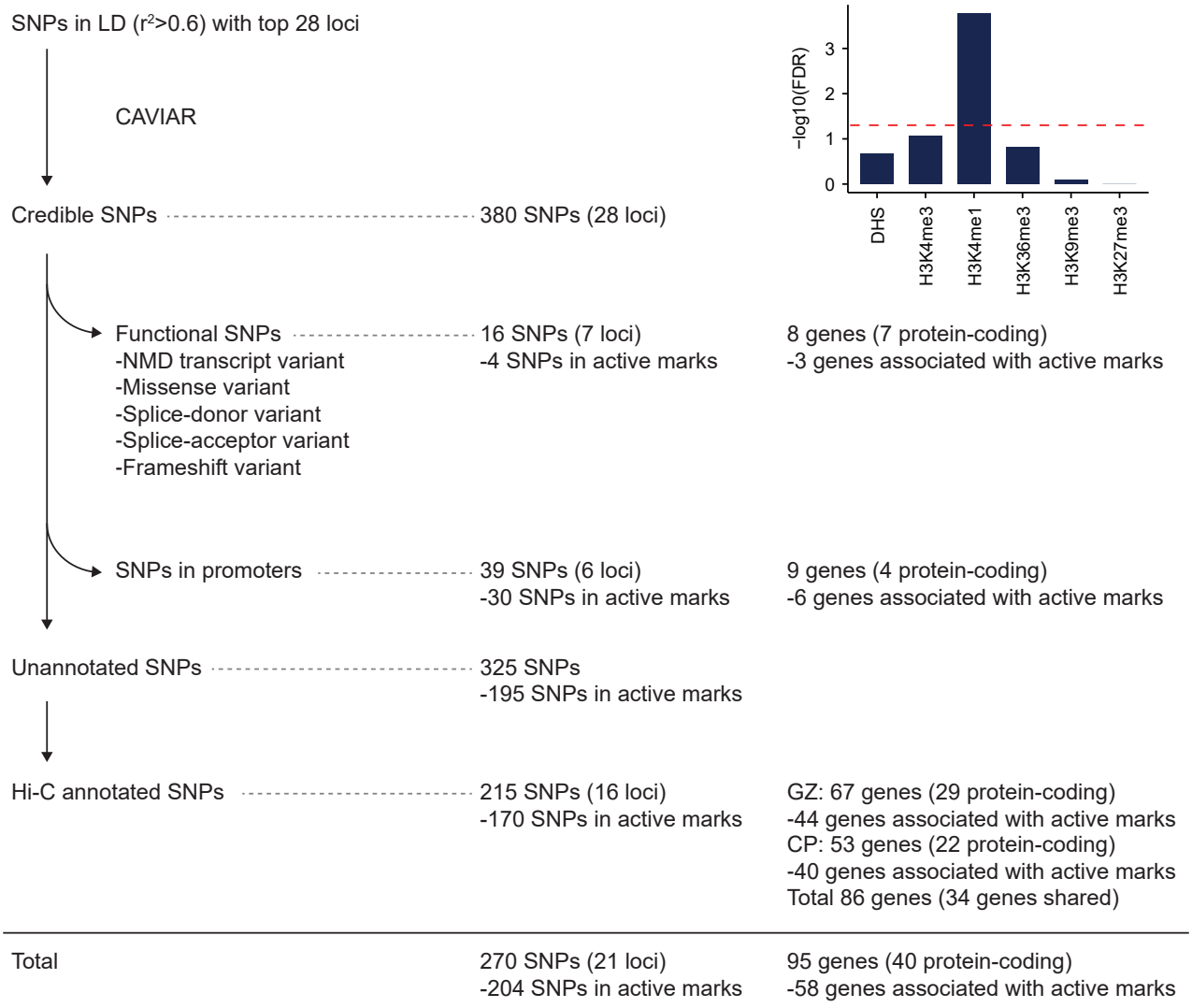

Supplementary Figure 98: Defining putative target genes of ASD loci. Credible SNPs were derived from top 28 ASD loci by CAVIAR, resulting in 380 SNPs that are enriched in H3K4me1 marks in fetal brain. Credible SNPs were subsequently categorized into functional SNPs (SNPs that cause nonsynonymous variants and SNPs located within promoters) and unannotated SNPs. Functional SNPs were directly assigned to their target genes, while unannotated SNPs were assigned to their target genes based on chromatin contact profiles in fetal brain.